MICROSTRUCTURAL CHARACTERIZATION AND MECHANICAL PROPERTIES OF CARBON NANOTUBE REINFORCED NICKEL ALUMINIDE COMPOSITES

BY

MARY AJIMEGOH AWOTUNDE

217093293

ARTICLE BASED THESIS

SUBMITTED IN FULFILLMENT OF THE REQUIREMENTS FOR THE AWARD OF

DOCTORAL DEGREE IN METALLURGY

FACULTY OF ENGINEERING AND BUILT ENVIRONMENT, UNIVERSITY OF

JOHANNESBURG

SUPERVISOR: PROF. PETER A. OLUBAMBI

CO-SUPERVISORS: DR. BRENDON M. SHONGWE, DR. ADEWALE O. ADEGBENJO

JULY 2019

DECLARATION

I, the undersigned, hereby declare that this dissertation is a collection of articles from my doctoral research titled "Microstructural characterization and mechanical properties of carbon nanotube toughened nickel aluminide composites" which I herewith submit for the award of

DOCTORAL DEGREE (PhD) IN METALLURGY

to the University of Johannesburg, Department of Metallurgy, is my own work apart from the recognized assistance of my supervisors, and has not been previously submitted by me to another higher institution to obtain a research degree. I further declare that all sources cited or quoted are acknowledged appropriately by means of a comprehensive list of references.

Signature: …………………...………………
MARY AJIMEGOH AWOTUNDE

Date: ……05..…/…07………./…2019……..................

DEDICATION

This work is dedicated to my Heavenly Father, Almighty God, the Master Planner, the

Extraordinary Strategist, the Sovereign God, the One who has been with me from the beginning

of time, and without Whom I will not be here today.

ACKNOWLEDGEMENT

To the Pacesetters Church, thank you for feeding me with the undiluted word of God, propelling me towards excellence and removing impossibilities from my vocabulary. To Bishop Adelakun and Pastor Ezekiel-my spiritual fathers, who being true fathers, gave me feathers to fly and Rehoboth Cathedral family as a whole, you are highly appreciated.

To my amazing family, my brothers and sisters, who gave me unflinching support throughout the program. They were always ready to hear my long discussions with the twists and challenges, like they did not have challenges of their own. God bless you all abundantly!

And lastly, but definitely not the least, my deep appreciation goes to my husband Oluwaseyi Awotunde and our daughters – Oluwatomisin, Oluwatoni and Mokirafoluwa. To my princesses, thank you for sacrificing so much for this cause. May eternity reward you richly. To my husband, thank you for giving me this one in a million opportunity to pursue my dreams. Your sacrifices were simply invaluable.

ABSTRACT

Toughened nickel aluminides were successfully synthesized by incorporating multi-walled carbon nanotubes (MWCNTs) into nickel aluminide (NiAl) intermetallic matrix. The drive to retain the relative lightweight of NiAl motivated the choice of MWCNTs as the reinforcing agent in this study. Moreover, enhanced mechanical properties were anticipated in the reinforced composites owing to the exceptional properties of the MWCNTs. Elemental powders of nickel and aluminium were blended together with MWCNTs in a novel two stage ball milling for optimum dispersion and preservation of the structural integrity of the MWCNTs. The milled powders were consolidated by Spark Plasma Sintering (model HHPD-25, FCT GmbH, Germany). The milled powders and sintered samples were characterized using Scanning Electron Microscopy, Transmission Electron Microscopy and X-Ray Diffraction. The nano-structural evolution of the MWCNTs during their dispersion via dry ball milling was further evaluated using Raman Spectroscopy. The mechanical properties and fracture behaviours of the reinforced sintered samples were critically evaluated using nanoindentation techniques.

Results show that the integration of MWCNTs into the NiAl matrix led to an enhancement of the fracture toughness. An inverse relationship between the hardness and fracture toughness of the NiAl composites was established. The intergranular fracture morphology of the unreinforced NiAl transited to a dominantly dimpled fracture morphology in the NiAl-1.0 wt% CNTs composites indicating enhanced ductility and fracture toughness.

The improvement of the fracture toughness of the reinforced NiAl is attributed to the uniform dispersion of the MWCNTs within the NiAl matrix, the preservation of MWCNTs aspect ratios and the disordering of the B2 ordered NiAl intermetallic structure.

Table of Contents

UNIVERSITY
OF
JOHANNESBURG

Lists of Figures

Article 1

Article 2

Article 3

Article 4

Article 5

List of Tables

CHAPTER ONE

INTRODUCTION

1.1 Background of research

Nickel aluminide (NiAl) is a remarkable intermetallic compound that has drawn the attention of researchers and engineers alike. The driving force for the extensive studies on this compound is the unique combination of properties it possesses – namely high oxidation resistance (Wu et al., 2011; Sulka and Jozwik, 2011), high strength even at elevated temperatures (Sikka et al., 2000) and high temperature wear resistance (Zhu et al., 2014). These exceptional properties in addition to its lightweight (5.9 g/cm^3) have given them a competitive edge over existing nickel super alloys. Prominent among engineering requirements for aerospace, power plants and automotive industries are advanced materials that can withstand high temperatures without degradation or oxidation. Consequently, intermetallics like nickel aluminides showing such structural integrity at elevated temperatures are of immense interest to engineers (Morsi, 2001).

The unique properties exhibited by nickel aluminides have stimulated intensive investigation especially for high temperature structural applications such as heat shields for combustion chambers and first-row vanes in industrial gas turbines (Morsi, 2001; Scheppe et al., 2002). Additionally, its alloys are being developed earnestly with broad utilizations ranging from furnace rolls and radiant burner tubes for steel production to heat treating fixtures, forging dies, and corrosion-resistant parts for chemical industries (Stollof et al., 2000; Sikka et al., 2000). Nickel aluminides have doubtlessly found use in a number of successful applications, but are still far from wide commercialization. This is owing to the low plasticity and lack of ambient temperature toughness that they exhibit (Jozwik et al., 2015), which has significantly crippled their industrial use.

The poor fracture toughness of nickel aluminides is credited to the deficient slip systems possessed by this intermetallic (Noebe et al., 1993; Povarova et al., 2011). The unavailability of sufficient slip systems in a material prevents the material from deforming plastically before fracturing. This is an undesirable feature in structural materials as it promotes abrupt failures of materials in service. Diverse efforts have therefore been made in the research community to subdue the brittleness of NiAl mostly by introducing an additional element into the dual system to enhance the ductility and toughness. Rare earth metals like rhenium and carbides of refractory metals like tungsten have been incorporated into this intermetallic system in a bid to improve the fracture toughness to the minimum requirement of 20 MPa√m (Bochenek et al., 2018;

1

Gostischev et al., 2017). Very recently, nanomaterials like carbon nanotubes (CNTs) were also introduced into the B2 intermetallic matrix for the singular purpose of alleviating this poor structural quality (Ameri et al., 2016; Groven and Puszynski, 2012).

The motivation for choosing to incorporate CNTs in NiAl in this work is particularly for weight savings in terms of weight reduction, leading to a reduction of fuel consumption and consequently pollution (Miracle and Darolia, 2000; Munir and Wen, 2016). Owing to the ultra-high strength (up to ~100 GPa) and super high Young's modulus (~1 TPa) of CNTs (Popov, 2004), current research interests have shifted focus from particulate ceramic materials to nano-scale materials like CNTs as ideal reinforcements for metallic matrices. Recently, CNTs have proven to be ideal reinforcing candidates owing to the enhanced mechanical properties exhibited by the CNTs reinforced metal matrices (Ogawa et al., 2018). They have been widely incorporated into metallic matrices like copper (Duan et al., 2019), titanium (Adegbenjo et al., 2017), nickel (Aristizabal et al., 2018) and aluminium (Esawi et al., 2010). The composites reinforced with CNTs are of particular interest because of their enhanced properties that make them promising materials in aerospace, automobile and defence industries (Bakshi and Agarwal, 2011; Tjong, 2013).

Despite the intense investigations on CNT reinforced composites, achieving a balanced combination of strength and toughness has been a daunting task for researches till date, as there seem to be a trade-off between the two very essential properties. (Chen et al., 2016; Backshi and Agarwal, 2011). Numerous reports exist in literature of enhanced tensile strength achieved as a result of CNTs reinforcement, but mostly at the expense of significant loss in toughness of the composite or vice versa (Jiang et al., 2012; Yang et al., 2013; Li et al., 2015; Salama et al., 2017, Xu et al., 2017).

Previous studies have shown that key requirements to achieving balanced mechanical properties in CNTs reinforced composites are uniform dispersion of the CNTs in the matrix, preservation of the structural integrity of the CNTs and good interfacial bonding between the reinforcement and the matrix. In the quest to achieve these requirements, different techniques have been developed over the years including, nano-scale dispersion (Kwon et al., 2009), high energy ball milling (Esawi et al., 2009), in-situ grown method (He et al., 2009), flake PM (Jiang et al., 2012), friction stirring (Liu et al., 2013), and solution coating (Chen et al., 2016). Nevertheless, the expected improvements in mechanical properties by incorporating CNTs have not yet been fully realized (Esawi et al., 2010).

The processing techniques for NiAl have evolved progressively over the years as various fabrication routes have been employed in the quest to improve its properties. Combustion synthesis (Groven and Puszynski, 2012), mechanical alloying (Enayati et al., 2008), directional solidification (Guo et al., 2001) and powder metallurgy processes (Bochenek et al., 2018) have all been explored by scholars. Among the powder metallurgy techniques, unconventional techniques such as Spark Plasma Sintering (SPS) of the mechanically milled composite powders have recently been observed as an effective novel sintering technique (Morsi et al., 2010). This is due to the extremely fast cooling rates (500 °C/min) and short holding times at relative low sintering temperatures (Zhang et al., 2014) which have led to significant enhancements in the mechanical properties of the composites fabricated via this route.

Diverse levels of strength improvements have been documented severally by researchers due to the addition of different alloying elements. However, the effects of these alloying elements on the fracture toughness of NiAl have not been as intensively investigated as strength improvements. In addition, CNTs are the lightest alloying element that has been incorporated into the NiAl matrix till date. Thus, any accrued improvements as a result of CNTs reinforcement in NiAl will be effected at no compromise to the lightweight of NiAl.

1.2 Problem Statement

In spite of the exceptional combination of properties of nickel aluminides especially at high temperatures, their low fracture toughness (Geist et al., 2015) has significantly restricted their resourcefulness in the aerospace and automotive industries. In the quest to alleviate this poor mechanical attribute, various alloying elements have been incorporated into the NiAl matrix. However, the strengthening effects of these alloying elements have been intensely investigated, whereas little is available in literature on the toughening effects of these additions. Hence, the low fracture toughness of NiAl persists till date.

Owing to the grain refinement properties of CNTs (Mokdad et al., 2016), they are proposed as an excellent addition to improve the fracture toughness of nickel aluminides. In spite of the recent focus on CNT as an ideal reinforcement for metal matrices, few researchers have been able to successfully incorporate well dispersed CNTs into metal matrices. Traditional and modern routes have been investigated, yet, difficulties such as non-uniform distribution of CNT in metal matrix (Esawi et al., 2010) and agglomeration of CNTs (Peng and Chang, 2015) still exist. This is doubtlessly impeding the full actualization of CNT potential in revolutionizing the composite world as better dispersion of CNTs lead to better mechanical properties of the

resulting composites.

The most prevalent fabrication technique for NiAl synthesis has been mechanical alloying (MA) process which promotes homogenous mixing of the constituent elements of NiAl. However, integrating CNTs into NiAl matrix via the MA route will cause catastrophic damage to the delicate tubular nanostructures as observed in other metals and alloys. This damage could initiate interfacial reactions between the CNTs and aluminium leading to the formation of the brittle carbide phase Al_4C_3 which tends to adversely affect the mechanical properties of the resulting composites (Housaer et al., 2015). This may occur either as mechanical damage during high energy milling of the powders or as thermal damage of the CNTs during conventional sintering, due to the high temperatures involved. These can cause detrimental effects on the mechanical properties of the resulting composite due to the presence of the brittle phase (Simoes et al., 2017).

The risk associated with the thermal damage of CNTs during conventional sintering processes lead to poor mechanical properties of the composites due to the presence of the undesirable brittle aluminium carbide phase. Suitable sintering techniques that will preclude this menace are thus mandatory in order to produce CNTs reinforced NiAl composites with enhanced mechanical properties suitable for aerospace and automotive industry applications.

1.3 Research Questions

This study was embarked upon to answer the following research questions which guided this research:

- What dispersion technique would be best suited for dispersing CNTs in nickel aluminide matrix powders without inflicting catastrophic damage to the nanotubes?
- Would CNTs reinforcement improve the mechanical properties of NiAl, particularly the strength and fracture toughness?
- Will NiAl be successfully formed by reactive sintering via spark plasma sintering without the formation of interfacial reaction product, Al_4C_3?
- How best can milling and sintering parameters be combined to achieve the desired composition of intermetallic during the reactive sintering?

1.4 Aim and Objectives

The aim of this research is to synthesize and characterize toughened NiAl-CNTs composites fabricated by reactive synthesis via spark plasma sintering.

The specific objectives of this research include:

1) To develop an ideal methodology for the uniform dispersion of MWCNTs within nickel aluminide matrix powders without destroying their structural integrity.
2) To understand the interfacial reactions between CNTs and matrix powders with a view to preventing the formation of undesirable interfacial reaction products during the dispersion process.
3) To optimize milling and sintering parameters that would yield the desired NiAl intermetallic phase.
4) To study the interactions between the CNTs reinforcements and dislocations within the intermetallic matrix
5) To investigate the toughening effects and mechanisms of CNTs on the NiAl system.

1.5 Justification

Significant research has been conducted on alleviating the limitations of NiAl, yet only few scholars have reported on the effects of such efforts on the fracture toughness of nickel aluminide. Strengthening effects of alloying elements have been widely investigated; still literature lacks sufficient data on effective toughening of NiAl composites.

The observed gap is due to the unavailability of adequate literature on the major drawback of NiAl composites. Thus, this work seeks to throw more light on the effects of CNTs addition on the fracture toughness of NiAl composites which will produce vital information to serve as a guide for other researchers and engineers alike.

1.6 Scope of the work

The scope of this work comprises a two stage ball milling technique using a low energy ball milling procedure for 7 h at 150 rpm and a high energy ball milling procedure for 1 h at 75 rpm respectively. This was done to ensure a homogenous mix without inflicting significant damage to the nanotubes. Consolidation of the bulk composites was done using the novel spark plasma sintering (SPS) technique to prevent thermal damage of the CNTs. Sintering parameters like pressure and temperature were varied during the optimization studies to determine the best combination of sintering parameters that will yield better mechanical properties. The optimized parameters were then used to fabricate NiAl composites with varying CNTs reinforcement contents namely, 0, 0.5 and 1.0 weight percent. The influence of CNTs on the mechanical

properties of NiAl was evaluated, particularly the strength and fracture toughness. The nano-structural evolution, structural integrity and dispersion characteristics of the CNTs in NiAl matrix powders were assessed using SEM, Raman and TEM extensively. The phase identification was done using XRD techniques. Fracture toughness and strength properties were determined using the nanoindentation techniques.

1.7 Structure of the thesis

Chapter One of this thesis introduces nickel aluminides as potential materials for aerospace applications, their limitations, the motivation for reinforcing NiAl with CNTs, aim, objectives and scope of the research. This study produced five (5) articles that have been published or submitted to reputable DHET approved journals and these are presented in Chapters Two and Three.

Paper 1 is presented in Chapter Two, chronicling and reviewing previous and recent works on NiAl fabrication processes, reinforcement types and recent trends. It provides a robust but concise background on the inter-relationship between the processing route, reinforcement content and resulting mechanical properties. **Paper 2** is presented with an elaborate review on the different dispersion methods that have been utilized over the years till date, in the quest to integrate CNTs into metal matrices - particularly aluminium matrices, aluminium being a major constituent of the NiAl composite. The core of this paper lies in the in-depth review of dispersion methods which provides a sturdy framework on which the rest of the study is hinged. Chapter Three encompasses the totality of three published and submitted papers as they relate to one another in sequential fashion. **Paper 3** is a publication on the optimization of dispersion parameters in ensuring enhanced dispersion of CNTs in milled nickel and aluminium matrix powders. Ball milling routes were varied and compared, while the dispersion characteristics of CNTs were assessed in order to identify the best combination of milling routes and milling parameters like speed, ball to powder ratio and milling time. The effects of these parameters on the properties of the nanotubes were evaluated concisely. **Paper 4** investigated and validated the selected dispersion route identified in **Paper 3**. The nano-structural evolution of the CNTs in the NiAl matrix was investigated in the differently dispersed powders. The powders were consolidated via SPS and their mechanical properties investigated. The feasibility of fabricating NiAl-CNTs composites via reactive sintering was also investigated in this paper. **Paper 5** presents extensive details of the synthesized NiAl-CNTs composites via the optimized

dispersion and sintering parameters and investigated the mechanical properties as it varies across increasing CNTs reinforcement content. The role of CNTs as it influences the hardness and fracture toughness of NiAl were investigated using nanoindentation techniques. Fracture surfaces and porosity levels were examined and the relationship between hardness and densification was established. The toughening mechanism was discussed, and the effect of nanotube additions in the ordered lattice of the NiAl system was also studied.

Chapter Four conclusively links all the papers, forming a seamless narration of the novelty of this investigation and its significant contribution to scientific knowledge. Future work is also recommended therein.

The papers that ensued from this work are outlined as follows:

Paper 1:   Mary A. Awotunde, Olusoji O. Ayodele, Adewale O. Adegbenjo, Avwerosuoghene M. Okoro, Mxolisi B. Shongwe, Peter A. Olubambi. NiAl intermetallic composites—a review of processing methods, reinforcements and mechanical properties *Journal of Advanced Manufacturing Technology (published)* https://doi.org/10.1007/s00170-019-03984-9

Paper 2:   Mary A. Awotunde, Adewale O. Adegbenjo, Babatunde A. Obadele, Moses Okoro, Brendon M. Shongwe, Peter A. Olubambi. Influence of sintering methods on the mechanical properties of aluminium nanocomposites reinforced with carbonaceous compounds: A review. *Journal of Materials and Technology 2019, 8 (2): 2432–2449*

Paper 3:   Mary A. Awotunde, Olusoji O. Ayodele, Adewale O. Adegbenjo, Avwerosuoghene M. Okoro, Mxolisi B. Shongwe, Peter A. Olubambi Influence of ball milling parameters on the dispersion characteristics and structural integrity of MWCNTs in nickel aluminide matrix powders. *Journal of Particulate Science and Technology.* (Submitted and under review)

Paper 4:   Mary A. Awotunde, Adewale O. Adegbenjo, Olusoji O. Ayodele, Avwerosuoghene M. Okoro, Mxolisi B. Shongwe, Peter A. Olubambi. Interdependence of carbon nanotubes agglomerations, its structural integrity and the mechanical properties of reinforced nickel aluminide composites.

Paper 5:   Mary A. Awotunde, Adewale O. Adegbenjo, Olusoji O. Ayodele, Avwerosuoghene M. Okoro, Mxolisi B. Shongwe, Peter A. Olubambi. Reactive synthesis of CNTs reinforced nickel aluminide composites by spark plasma sintering. *Journal of Composites Part B* (submitted and under review)

REFERENCES

ADEGBENJO, A.O., OBADELE, B.A., OLUBAMBI, P. A. 2018. Densification, hardness and tribological characteristics of MWCNTs reinforced Ti6Al4V compacts consolidated by spark plasma sintering, Journal of Alloys and Compounds, 749, 818-833.

AMERI, S., SADEGHIAN, Z. & KAZEMINEZHAD, I. 2016. Effect of CNT addition approach on the microstructure and properties of NiAl-CNT nanocomposites produced by mechanical alloying and spark plasma sintering. *Intermetallics*. 76, 41- 48.

ARISTIZABAL, K., KATZENSTEINER, A., BACHMAIER, A., MÜCKLICH, F. & SUAREZ, S. 2017. Study of the structural defects on carbon nanotubes in metal matrix composites processed by severe plastic deformation. *Carbon*, 125, 156-161

BAKSHI, S. R. & AGARWAL, A. 2011. An analysis of the factors affecting strengthening in Carbon nanotube reinforced aluminium composites. *Carbon,* 49, 533–44.

BOCHENEK, K., WĘGLEWSKI, W., MORGIEL, J. & BASISTA, M. 2018. Influence of rhenium addition on microstructure, mechanical properties and oxidation resistance of NiAl obtained by powder metallurgy, *Materials Science and Engineering: A*, 735, 121-130.

CHEN, B., KONDOH, K., IMAI, H., UMEDA, J. 2016. Simultaneously enhancing strength and ductility of carbon nanotube/aluminium composites by improving bonding conditions. Scr. Mater. 113, 158–162.

DUAN, B., ZHOU, Y., WANG, D. & ZHAO, Y. 2019. Effect of CNTs content on the microstructures and properties of CNTs/Cu composite by microwave sintering, *Journal of Alloys and Compounds.* 771, 498-504.

ENAYATI, M. H., KARIMZADEH, F. & ANVARI, S. Z. 2008. Synthesis of nanocrystalline NiAl by mechanical alloying. Journal of Materials Processing Technology, 200, 312–315.

ESAWI, A. M. K., MORSI, K., SAYED, A., GAWAD, A. A. & BORAH, P. 2009. Fabrication and properties of dispersed carbon nanotube aluminium composites. *Mater. Sci. Eng. A,* 508, 1-2, 167-173.

ESAWI, A. M. K., MORSI, K., SAYED, A., TAHER, M. & LANKA, S. 2010. Effect of carbon nanotube (CNT) content on the mechanical properties of CNT-reinforced aluminium composites. *Composites Science and Technology* 70, 2237–2241.

ESAWI, A., MORSI, K., SAYED, A., TAHER, M. & LANKA, S. 2010. Effect of carbon nanotube (CNT) content on the mechanical properties of CNT-reinforced aluminium composites, Composites Science and Technology, 70, 2237-2241

GEIST, D., GAMMER, C., RENTENBERGER, C., KARNTHALER, H. P. 2015. Sessile dislocations by reactions in NiAl severely deformed at room temperature. *J. Alloys Comp*. 621, 371-377.

GOSTISHCHEV, V. V., ASTAPOV, I. A. & KHIMUKHIN, S. N. 2017. Exothermic Synthesis of Cast Nickel Aluminide Alloys with Tungsten and Molybdenum Carbides. *Inorganic Materials* 53, 2, 160–163.

GROVEN, L. & PUSZYNSKI, J. 2012. Combustion synthesis and characterization of nickel aluminide–carbon nanotube composites, *Chemical Engineering Journal*, 183, 515-525.

GUO, J., CUI, C., CHEN, Y., LI, D. & YE, H. 2001. Microstructure, interface and mechanical property of the DS NiAl/Cr (Mo, Hf) composite, *Intermetallics*, 9, 287-297.

HE, C.N., ZHAO, N.Q., SHI, C. S. & SONG, S. Z. 2009. Mechanical properties and microstructures of carbon nanotube-reinforced Al matrix composite fabricated by in situ chemical vapor deposition. *J. Alloys Compd,* 487, 1-2, 258-262.

HOUSAER, F., BECLIN, F., TOUZINA, M., TINGAUD, D., LEGRIS, A. & ADDAD, A. 2015. Interfacial characterization in carbon nanotube reinforced aluminium matrix composites. *Materials Characterization,* 110, 94–101.

JIANG, L., LI, Z., FAN, G., CAO, L. & ZHANG, D. 2012. The use of flake powder metallurgy to produce carbon nanotube (CNT)/aluminium composites with a homogenous CNT distribution. *Carbon,* 50, 5, 1993-1998.

JOZWIK, P., POLKOWSKI, W. & BOJAR, Z. 2015. Applications of Ni$_3$Al Based Intermetallic Alloys - Current Stage and Potential Perspectives. *Materials,* 8, 2537-2568, doi:10.3390/ma8052537

KWON, H., ESTILI, M., TAKAGI, K., MIYAZAKI, T. & KAWASAKI, A. 2009. Combination of hot extrusion and spark plasma sintering for producing carbon nanotube reinforced aluminium matrix composites. *Carbon*, 47, 3, 570-577.

LI, J. L., XIONG, Y. C., WANG, X. D., YAN, S. J., YANG, C., HE, W. W., CHEN, J. Z., WANG, S. Q., ZHANG, X. Y. & DAI, S. L. 2015. Microstructure and tensile properties of bulk nanostructured aluminium/graphene composites prepared via cryomilling. *Materials Science & Engineering A,* 626, 400–405.

LIU, Z. Y., XIAO, B. L., WANG, W. G. & MA, Z. Y. 2013. Developing high-performance aluminium matrix composites with directionally aligned carbon nanotubes by combining friction stir processing and subsequent rolling. *Carbon*, 62, 35-42.

MIRACLE, D. B & DAROLIA, R. 2000. NiAl and its alloys, *Intermetallic Compounds: Principles and Practice*. 2, 53-72.

MOKDAD, F., CHEN, D. L., LIU, Z.Y., XIAO, B. L., NI, D. R., MA, Z.Y. 2016. Deformation and strengthening mechanisms of a carbon nanotube reinforced aluminium composite. *Carbon*, 104, 64-77

MORSI K. 2001. Review: Reaction Synthesis Processing of Ni-Al Intermetallics. *Mater. Sci. Eng. A*. 299, 1-5.

MORSI, K., ESAWI, A. M. K., BORAH, P., LANKA, S. & EL-SAYED, A. 2010. Characterization and spark plasma sintering of mechanically milled aluminium–carbon nanotube (CNT) composite powders. *J. Compos. Mater.* doi: 10.1177/0021998310361990.

MUNIR, K.S & WEN, C. 2016. Deterioration of the Strong sp2 Carbon Network in Carbon Nanotubes during the Mechanical Dispersion Processing—A Review, *Critical Reviews in Solid State and Materials Sciences*. 41, 347-366.

NOEBE, R. D., BOWMAN, R. R. & NATHAL, M. V. 1993. Physical and mechanical properties of the B2 compound NiAl. *International Materials Reviews*, 4, 193-232.

OGAWA, F., YAMAMOTO, S & MASUDA, C. 2018. Strong, ductile, and thermally

conductive carbon nanotube-reinforced aluminum matrix composites fabricated by ball-milling and hot extrusion of powders encapsulated in aluminum containers, *Materials Science and Engineering: A*, 711, 460-469.

PENG, T AND CHANG, I. 2015. Uniform dispersion of carbon nanotube in aluminium powders by wet shake-mixing approach. *Powder Technology*, 284, 32–39.

POPOV, V.N. 2004. Carbon nanotubes: properties and application. *Mater. Sci. Eng. R Rep*. 43, 3, 61-102.

POVAROVA, K. B., DROZDOV, A. A, KAZANSKAYA, N. K., MOROZOV, A. E. & ANTONOVA, A. V. 2011. Physicochemical approaches to designing NiAl-based alloys for high-temperature operation. *Russian Metallurgy (Metally)* 3, 209-220.

SALAMA, E. I., ABBAS, A. & ESAWI. A. M. K. 2017. Preparation and properties of dual-matrix carbon nanotube-reinforced aluminum composites. *Composites: Part A,* 99, 84–93.

SCHEPPE, F., SAHM, P. R., HERMANN, W., PAUL, U. & PREUHS, J. 2002. Nickel aluminides: a step toward industrial application. *Materials Science and Engineering A*, 329-331, 596-601.

SIKKA, V. K., DEEVI, S. C., VISWANATHAN, S., SWINDEMAN, R. W. & SANTELLA, M. L. 2000. Advances in processing of Ni$_3$Al-based intermetallics and applications. *Intermetallics,* 8, 1329–1337.

SIMÕES, S., VIANA, F., REIS M. A. L. & VIEIRA, M. F. 2017. Aluminium and Nickel Matrix Composites Reinforced by CNTs: Dispersion/Mixture by Ultrasonication. *Metals*, 7, 279; doi: 10. 3390/met7070279

STOLOFF, N. S., LIU, C. T. & DEEVI, S. C. 2000. Emerging applications of intermetallics. *Intermetallics*. 8, 9-11, 1313-20.

SULKA, G. & JÓŹWIK, P. 2011. Electrochemical behaviour of Ni$_3$Al-based intermetallic alloys in NaOH. *Intermetallics*. 19, 974–981.

TJONG, S.C. 2013. Recent progress in the development and properties of novel metal matrix nanocomposites reinforced with carbon nanotubes and graphene nanosheets. *Mater. Sci. Eng. R Rep*, 74, 10 281-350.

WU, L., YAO, J., DONG, H., HE, Y., XU, N., ZOU, J., HUANG, B. & LIU, C.T. 2011. The

corrosion behaviour of porous Ni$_3$Al intermetallic materials in strong alkali solution. *Intermetallics*, 19, 1759–1765.

XU, R., TAN, Z., XIONG, D., FAN, G., GUO, Q., ZHANG, J., SU, Y., LI, Z. & ZHANG, D. 2017. Balanced strength and ductility in CNT/Al composites achieved by flake powder metallurgy via shift-speed ball milling. *Composites: Part A,* 96, 57–66.

YANG, X., LIU, E., SHI, C., HE, C., LI, J., ZHAO, N., KONDOH, K. 2013. Fabrication of carbon nanotube reinforced Al composites with well-balanced strength and ductility. *Journal of Alloys and Compounds,* 563, 216–220.

ZHANG, Z. H., LIU, Z. F., LU, J. F. & SHEN, X. B. 2014. The sintering mechanism in spark plasma sintering – proof of the occurrence of spark discharge. *Scr. Mater*. 81, 56–59.

ZHU, S., BI, Q., YANG, J., QIAO, Z., MA, J., LI, F., YIN, B. & LIU, W. 2014. Tribological behaviour of Ni$_3$Al alloy at dry friction and under sea water environment. *Tribol. Int*. 75, 24–30.

CHAPTER TWO

This chapter presents the review of literatures accessed in the course of this work. This presented a solid background and foundation upon which this study was based. Vital information deduced from available studies guided the directions for this study. The literature review was published in two articles. Article 1 focused on the progression of research done on NiAl composites till date, including the various alloying elements, their effects on mechanical properties and the relationship between these factors and the employed processing routes. The general challenges encountered in the manufacturing of this brittle intermetallic were discussed as well. With each processing technique presenting some limitations, newer processing routes that have been developed to circumvent these shortcomings were also discussed. The effects of the different alloying elements on the microstructure obtained were discussed. This review made evident the shortage of literature available especially for NiAl composites reinforced with CNTs. In addition, the few works that investigated this combination employed similar dispersion route in the fabrication of NiAl-CNTs. This led to the achievements of very modest results as CNTs agglomerations still persisted which limited the expected enhancement of properties. Article 2 therefore, focused on the numerous dispersion routes that have been utilized in dispersing CNTs into aluminium matrices. The lack of relevant literature for NiAl-CNTs composites motivated this review which explored the evolution of various dispersion techniques, their dynamics and technicalities. From literature, no other matrix has been so extensively investigated as aluminium matrices for the incorporation of CNTs. This made it a perfect case study for this purpose in addition to being a major constituent of the compound of choice in this work. The progression of various dispersion techniques over the years were critically reviewed in this work. The focus was on the level of dispersion obtained with each dispersion method and the effect of the dispersion method on the nanotube morphologies. The relationship between the method of dispersion employed and the resulting mechanical properties was established.

These reviews helped identify the various research gaps existing in literature as it pertains to NiAl composites, which formed a comprehensive background on which this work was built.

ORIGINAL ARTICLE

NiAl intermetallic composites—a review of processing methods, reinforcements and mechanical properties

Mary A. Awotunde[1] · Olusoji O. Ayodele[1] · Adewale O. Adegbenjo[1,2] · Avwerosuoghene M. Okoro[1] · Mxolisi B. Shongwe[3] · Peter A. Olubambi[1]

Abstract

Modern day technology demands consistent and frequent advancements in materials for specialized applications. Nickel aluminide is one of such materials with distinctive properties that make them particularly suitable for high temperature applications especially in aerospace industries. However, the lack of ambient temperature ductility of this intermetallic has greatly restricted its applicability in service. In this review, the various efforts of researchers in solving this major limitation of nickel aluminides is evaluated and summarized, with particular emphasis on reinforcement types and processing methods that have been explored over the years.

Keywords Nickel aluminide · Intermetallic · Ductility · Aerospace industries

1 Introduction

The exceptional and attractive high temperature mechanical properties of nickel aluminide (NiAl) has made it a key research focus for about five decades now. Its excellent resistance to oxidation and high thermal conductivity make it a superlative choice for high temperature applications especially in aerospace, automobile and power sectors [1, 2]. With the recent fuel saving expeditions in top gear, the low density of this intermetallic is a huge complementary advantage [3]. The B2 intermetallic structure of NiAl makes it structurally stable even at critical higher temperatures that are of engineering importance. This is made possible due to the singular phase of the B2 structure which persists even to melting point, making it a perfect fit for high temperature structural applications [4]. Unfortunately, the major bottleneck to the diverse

applicability of this intermetallic is its poor room temperature mechanical properties, particularly its ductility and fracture toughness. The shortage of slip systems and the difficulty of slip transmission across grain boundaries have been identified as the sole culprits of the brittleness of NiAl [5].

Through the years and currently, various approaches are being explored to improve the limitation of this intermetallic so as to maximally tap into the multi functionality of this material. Researchers have incorporated ductile phases into the brittle system, employed directional solidification routes, refined grain sizes, explored heat treatment, added rare earth metals and even recently, integrated nanostructures into NiAl matrices [6–10]. The essence of this study is to evaluate the various processing methods that have been explored, including the varied alloying/reinforcement phases considered, as it effects on the mechanical properties of the resulting NiAl composites in a concise overview.

✉ Mary A. Awotunde
  mary.awotunde@uniben.edu

1 Center for Nanoengineering and Tribocorrosion, School of Mining, Metallurgy and Chemical Engineering, University of Johannesburg, Johannesburg, South Africa

2 Mechanical Engineering Department, The Ibarapa Polytechnic, Eruwa, Oyo State 200005, Nigeria

3 Institute for NanoEngineering Research, Tshwane University of Technology, Pretoria, South Africa

2 Processing routes for NiAl

2.1 Self-propagating high temperature synthesis or combustion synthesis

A variety of methods have been used over the years, in quick succession, with each method an improvement over the previous one. The traditional melting and casting have been

🌀 Springer

Review Article 1: NiAl INTERMETALLIC COMPOSITES - A REVIEW OF PROCESSING METHODS, REINFORCEMENTS AND MECHANICAL PROPERTIES

Mary A. Awotunde, Olusoji O. Ayodele, Adewale O. Adegbenjo, Avwerosuoghene M. Okoro, Mxolisi B. Shongwe, Peter A. Olubambi, 2019. Journal of Advanced Manufacturing Technology (published) https://doi.org/10.1007/s00170-019-03984-9

Abstract

Modern day technology demands consistent and frequent advancements in materials for specialized applications. Nickel aluminide is one of such materials with distinctive properties that make them particularly suitable for high temperature applications especially in aerospace industries. However, the lack of ambient temperature ductility of this intermetallic has greatly restricted its applicability in service. In this review, the various efforts of researchers in solving this major limitation of nickel aluminides is evaluated and summarized, with particular emphasis on reinforcement types and processing methods that have been explored over the years.

Keywords: Nickel aluminide, intermetallic, ductility, aerospace industries

1. Introduction

The exceptional and attractive high temperature mechanical properties of nickel aluminide (NiAl) has made it a key research focus for about five decades now. Its excellent resistance to oxidation and high thermal conductivity make it a superlative choice for high temperature applications especially in aerospace, automobile and power sectors [1, 2]. With the recent fuel saving expeditions in top gear, the low density of this intermetallic is a huge complementary advantage [3]. The B2 intermetallic structure of NiAl makes it structurally stable even at critical higher temperatures that are of engineering importance. This is made possible due to the singular phase of the B2 structure which persists even to melting point, making it a perfect fit for high temperature structural applications [4]. Unfortunately, the major bottleneck to the diverse applicability of this intermetallic is its poor room temperature mechanical properties, particularly its ductilityand fracture toughness. The shortage of slip systems and the difficulty of slip transmission across grain boundaries have been identified as the sole culprits of the brittleness of NiAl [5].

Through the years and currently, various approaches are being explored to improve the limitation of this intermetallic so as to maximally tap into the multi functionality of this material. Researchers have incorporated ductile phases into the brittle system, employed

directional solidification routes, refined grain sizes, explored heat treatment, added rare earth metals and even recently, integrated nanostructures into NiAl matrices [6-10]. The essence of this study is to evaluate the various processing methods that have been explored, including the varied alloying/reinforcement phases considered, as it effects on the mechanical properties of the resulting NiAl composites in a concise overview.

2. Processing routes for NiAl

2.1 Self-propagating high temperature synthesis (SHS) or combustion synthesis

A variety of methods have been used over the years, in quick succession, with each method an improvement over the previous one. The traditional melting and casting have been generally used for metals, but casting through orthodox heating is not an economically viable route for the fabrication of nickel aluminides owing to the high melting temperature of NiAl which stands at 1638°C [11]. This leads to huge costs due to energy consumption of the metal casting process, hence other more energy efficient methods of melting have been developed. Moreover, the wide dissimilarity between the melting temperature and densities of nickel and aluminium poses additional difficulties such as evaporation and segregation of the aluminium during casting [12]. The self-propagating high temperature synthesis of NiAl is an established fabrication route of this intermetallic which tends to avoid the bottlenecks of conventional melting and casting processes. This route has been widely used due to the shorter processing times, cost effectiveness and in-situ synthesis of the intermetallic [13-16]. There are two methods of doing this, namely the plane wave propagating method and the thermal explosion method [11]. Using the SHS method, the intermetallic is formed as a result of an exothermic, self-sustained reaction among the starting or elemental powders [14] leading to a spontaneous release of heat in excess of 1912K, causing the mix to melt. The dominant mechanism is the dissolution-precipitation mechanism [17, 18] with the ceramic particulates precipitating out during solidification. The molten metal provides a conducive environment which aids the mass transfer and diffusion of the reinforcement phases and particles. Some disadvantages of this method however, are the high levels of porosity [11], the formation of intermediate phases and presence of raw materials even at the end of the process, as a result of incomplete combustion [19]. These intermediate phases may cause undesirable properties in the performance of composite. A schematic representation of the SHS process is shown in Fig. 1. Shokati et al [15] utilized this route with a focus on mitigating these disadvantages and observed the complete combustion of the starting powders. X-ray Diffraction results confirmed the lack of

intermediate phases and undesirable compounds which they attributed to insignificant heat losses, adequate heating rates and low particle size of raw materials.
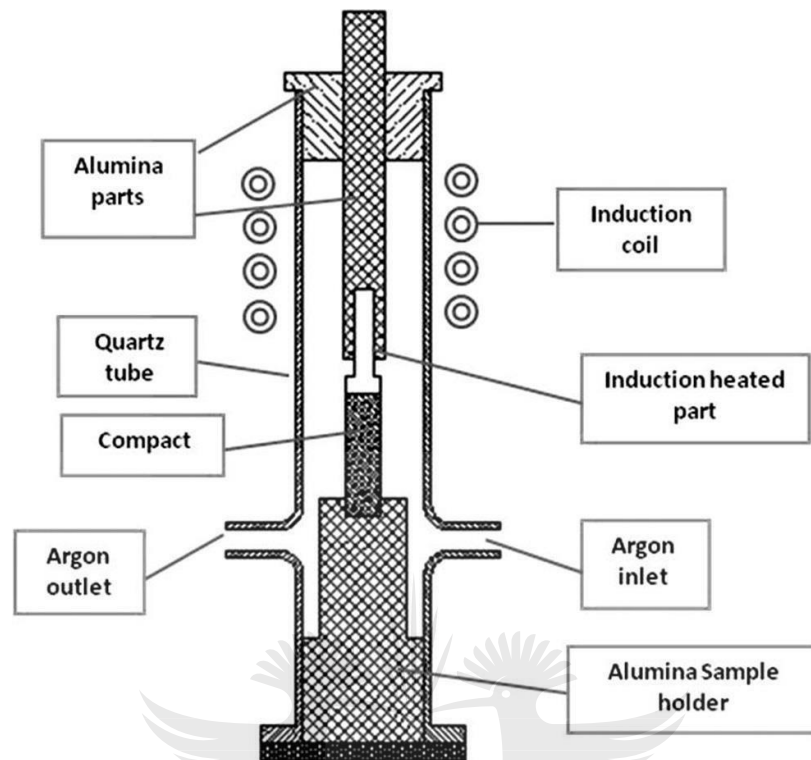
Fig. 1. Schematic representation of experimental setup used for the synthesis of NiAl by SHS process [11].

2.2 Powder metallurgy process (PM)

The advantages of powder metallurgy over other fabrication routes are quite apparent. The ease of process control and elimination of product waste due to near net shaping come top on the list. Azarmi [20] explored this route to improve the mechanical properties of NiAl using conventional sintering after powder blending and compaction. To preclude the major limitation of this route, he employed hot compaction after sintering to reduce the porosity levels to as low as 4.7% in the NiAl-10 vol% SiC composite. As the reinforcement content increased however, porosity was observed to increase as well, leading to a decrease in densification. In spite of the numerous advantages of this route, the low densities observed during this solid state process can be quite daunting. However novel sintering routes like spark plasma sintering have been documented to produce highly dense composites with outstanding mechanical properties [21]. More remarkable is the fact that this high densification is achieved in shorter times than that of other sintering methods [22].

Bochenek et al [23] compared the microstructure and mechanical properties of NiAl-Re (rhenium) composites obtained via hot pressing (HP) and spark plasma sintering (SPS) techniques. The composites fabricated by HP were sintered at 1400 °C, using 30 MPa and 60 min dwell time, while those produced during SPS were sintered at 1400 °C, using 20 MPa and 30 min dwell time. It was observed that the shorter sintering times typical of SPS, led to grain growth inhibition which produced a fine grained microstructure as shown in Fig. 2. They however mentioned that the rhenium did not have sufficient time to diffuse around the grain boundaries in the SPSed samples as was observed in the hot pressed composites which had larger grains and well diffused rhenium particles at the grain boundaries leading to stronger cohesion between them. The probable cause of this was the reduced dwell time experienced by the spark plasma sintered (SPSed) sample. Ideally though, the SPS is an ultra-rapid novel sintering technique which offers higher densification even in shorter sintering times. Results also showed that the rhenium reinforcing phase dissolved into NiAl grains forming a NiAl-Re solid solution while some others precipitated at the NiAl grain boundaries. The combination of these two phenomena produced NiAl-Re composites with improved mechanical properties via the powder metallurgy route. General Electric very recently produced titanium aluminide low pressure turbine blades using the PM route [24]. Therefore expectations are high that the same PM route may be utilized to achieve similar feat in NiAl composites.
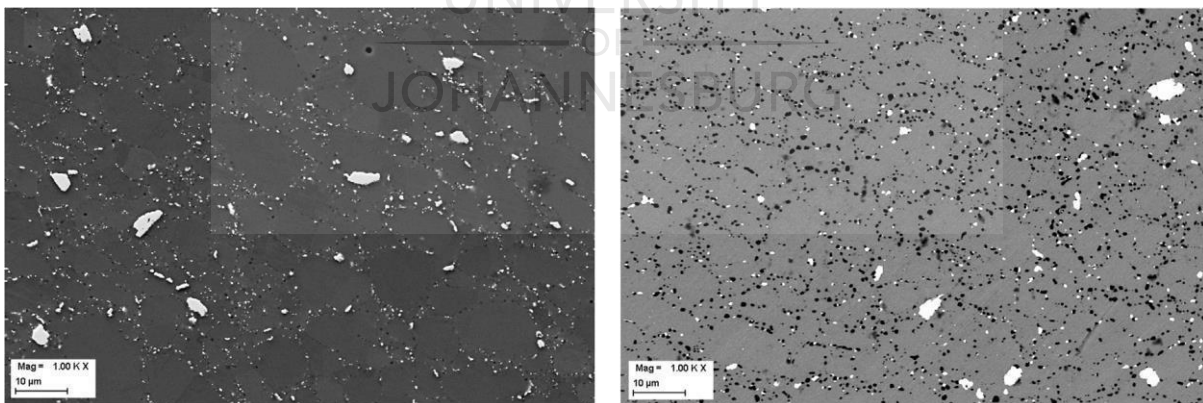
Fig. 2. SEM images of NiAl1.5Re samples produced by HP (left) and SPS (right). The white phase is rhenium, grey NiAl and dark areas are aluminium oxide grains. [23].

Takahashi and Dunand [25] in using the PM route, employed hot isostatic pressing for the consolidation of molybdenum reinforced nickel aluminide. The major disadvantage of this sintering method is the coarsening of the grains and reinforcement which usually lead to the loss of strength of the composite. However minimal coarsening was observed possibly owing to the low solubility of molybdenum in the NiAl intermetallic matrix which prevented rapid coarsening of the molybdenum dispersoids.

2.3 Mechanical alloying (MA)

The nano-structuring of materials using mechanical alloying for effective size reduction has been the most popularly utilized route for the fabrication of NiAl intermetallic composites [26-29]. This popularity was fuelled by the credence that technically brittle systems like nickel aluminide may be altered into ductile materials by nanocystallization [30-32]. MA is a solid-state PM processing technique that is used to obtain fine grained materials with crystallite sizes usually less than 100 nm [33] by employing high energy ball milling processes for a prolonged duration. NiAl is thus obtained through a process of solid state diffusion and someresearchers have documented the occurrence of a self-sustaining exothermic reaction [28]. This explosive release of energy was attributed to the oxidation of the starting aluminium powder particles [34, 35]. The duration of milling have ranged from 30 h to as high as 128 h over the years. Khajersarvi [33] utilized this method and obtained crystallite size of 28 nm after 128 h of milling, having started with pure elemental powders of nickel and aluminium. The NiAl formation was recorded to have commenced after 16 h of milling. Some authors however document the complete formation of the NiAl compound after 16 h of milling [36]. Microhardness values of the mechanically alloyed intermetallic was found to be 350 Hv and this hardness was attributed to the complete formation of a single intermetallic phase ofNiAl.

Using the Williamson-Hall equation [37], the crystallite size can be deduced as follows:

$$\beta_r \cos\theta = \frac{k\lambda}{L} + 2\,\varepsilon \sin\theta \dots\dots\dots(1)$$

Where β_r is the peak width, ε is the internal strain, λ is the wavelength, k is Scherrer constant, θ is the Bragg's diffraction angle and L is the crystallite size.

During MA, high energy ball milling is the desired route of choice, owing to the enormous impactful forces it exerts on the powders resulting in effective size reduction and homogeneity.

The total energy expended during milling can be estimated using equation (2)

$$E_i = \sum_{j=1}^{n} \frac{1}{2Ms} M_b \, v_j^2 \ldots\ldots\ldots (2)$$

Where n indicates the number or frequency of impacts among the milling balls per second, M_b symbolizes the mass of the milling balls, M_s is the mass of the samples and v_j is the relative impact velocity of the milling balls [38]. The dominant mechanisms during the MA process is the cold working of powder particles and fracturing, hence the interplay between these two mechanisms yield the final powder morphology. The cold working, fracturing and re-welding of these powder particles give rise to faster solid state diffusion given the reduced diffusion distance between the welded powder particles [39].

Enayati et al [40] obtained an unprecedented microhardness value of 1035 Hv while employing the MA route exclusively without the addition of alloying elements. They observed a progressive increase in microhardness values with increase in the milling time as indicated in Fig. 3. After 40 h of milling, NiAl was said to form through an unceasing inter-diffusive reaction between nickel and aluminium in between the interfaces without an explosive reaction.
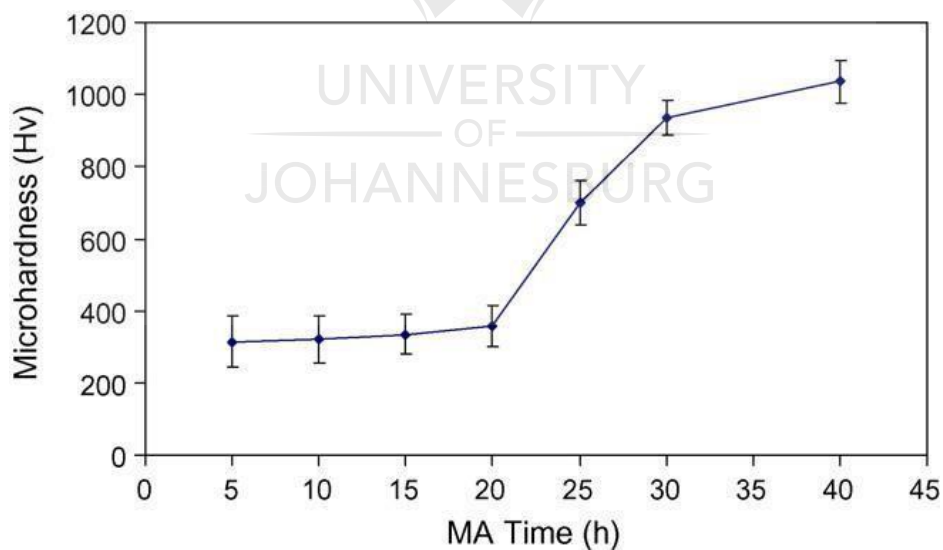
Fig. 3. Microhardness values as a function of milling time for NiAl powder particles. [40].

2.4 Directional solidification (DS)
DS has majorly been used to produce NiAl-Cr-Mo eutectic alloys for almost five decades now [41]. The crux of this method is the substitution of chromium by the molybdenum which

transforms the phase morphology from chromium rods to lamellar plates in the intermetallic matrix. Impressive results in the improvement of fracture toughness of this eutectic have been documented, namely from 6 MPa√m to about 26 MPa√m for various compositions of this eutectic [6, 42]. The in-depth discourse on the mechanism of DS is outside the scope of this work and has been discussed extensively elsewhere by Bochenek and Basista [9].

There are however different compositions of the NiAl-Cr-Mo eutectic alloys with diverse alloying additions. It is being said that the major drawbacks of this eutectic is the low growth rate that needs to be employed to obtain an excellent DS structure with improved fracture toughness, typically as low as 25 mm/h, which may be too slow for economic viability [43]. Moreover, despite the good combination of room temperature and high temperature properties of these eutectics, their creep properties are still lower than that of super-alloys [41]. It was observed that the formation of the heusler phase Ni_2AlHf in hafnium reinforced eutectic alloys NiAl-Cr(Mo)-0.1Hf, improves strength at elevated temperatures, however this strength is enhanced to the detriment of the room temperature ductility of the intermetallic [44]. To improve the ductility of this eutectic, scadium was added and its properties evaluated for its effect on room temperature ductility [45]. It was observed that with increasing scadium addition from 0 to 0.1 wt%, the characteristic inter-lamellar and inter-cellular spacing of this eutectic reduces, as observed in Fig 4. In addition to this modification of the microstructure by scadium, it was also observed that the segregation of this rare earth metal around the grain boundaries, detoxifies the grain boundaries from impurities that adversely affect the cohesive strength [46], hence significantly improving the compressive strength of the reinforced composite.
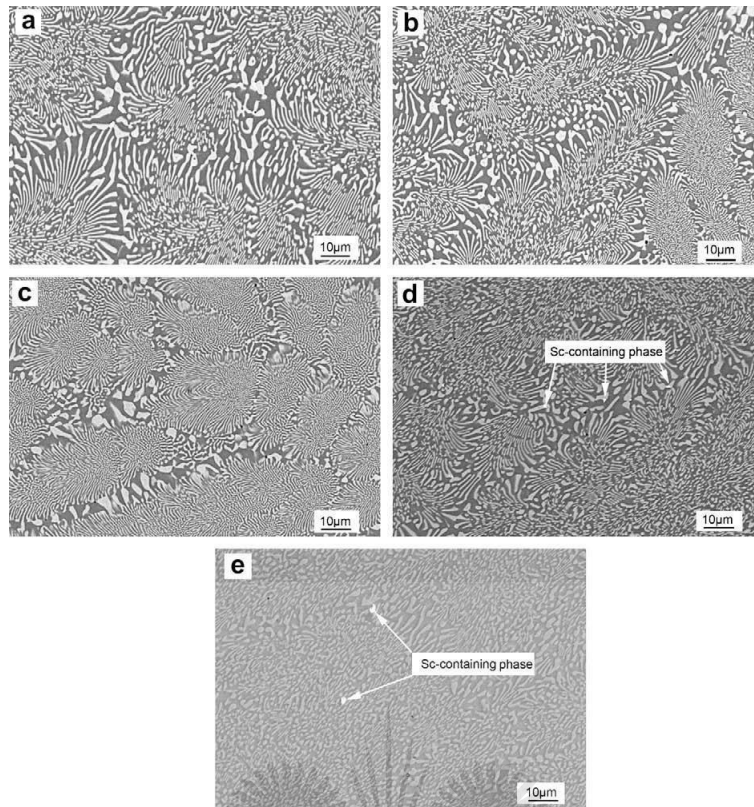
Fig. 4. SEM BSE (back scattered electron) images of NiAl–Cr (Mo)–Hf alloys containing various Sc content (wt%): (a) 0, (b) 0.05, (c) 0.1, (d) 0.2, (e) 0.3. [45].

In the same vein, holmium was added to NiAl–28Cr–6Mo–0.15Hf eutectic alloy [47]. The high temperature yield strength was improved, however the mechanical properties were observed to be reinforcement content sensitive. Compressive strength and ductility increased with increase in holmium content up till 0.1 at%, above which the mechanical properties begin to diminish. Much work has been done on these eutectics with impressive enhancements especially on the fracture toughness. More work still needs to be done however on other properties like creep and oxidation resistance for a full range study in determining its applicability in service.

3. Mechanical properties of various reinforcement phases/alloying elements

It is believed that the mechanical properties of NiAl can be enhanced by micro or macro alloying with diverse elements. The choice of the alloying elements are sometimes dependent on their intrinsic properties (in which case, they are added as ex-situ reinforcement particles) or the solid solutions and precipitates formed with other elements during composite processing (in which case, they are termed as in-situ reinforcements) [48].

22

4. Particulate reinforcement

Several scholars have incorporated various alloying elements into NiAl with a view to improving its mechanical properties. Ceramic particles like ZrB_2, NbC, TiB_2, Al_2O_3 and TiC [15, 17, 49, 50] have all been investigated widely in the NiAl systems due to the ideology that incorporating particles that are harder than the matrix would impart the desired properties into the selected matrix.

4.1 Titanium alloys

Shokati et al, [15] incorporated in-situ formed TiB_2 and TiN in various proportions into the NiAl matrix. They obtained the highest hardness values from the 40 wt% (TiB_2-TiN) reinforced composite of 909±79 Hv over the unreinforced with hardness values of 374±15 Hv. With increase of the hardness being proportional to the increase of the reinforcement, it can be concluded that the enhancement in the hardness was a direct consequence of the presence of the reinforcing phase. Authors also alluded the improvement to the uniform dispersion (Fig. 5) of the reinforcement phases, which is an advantage of in-situ formed reinforcement phases in composites [51, 52].
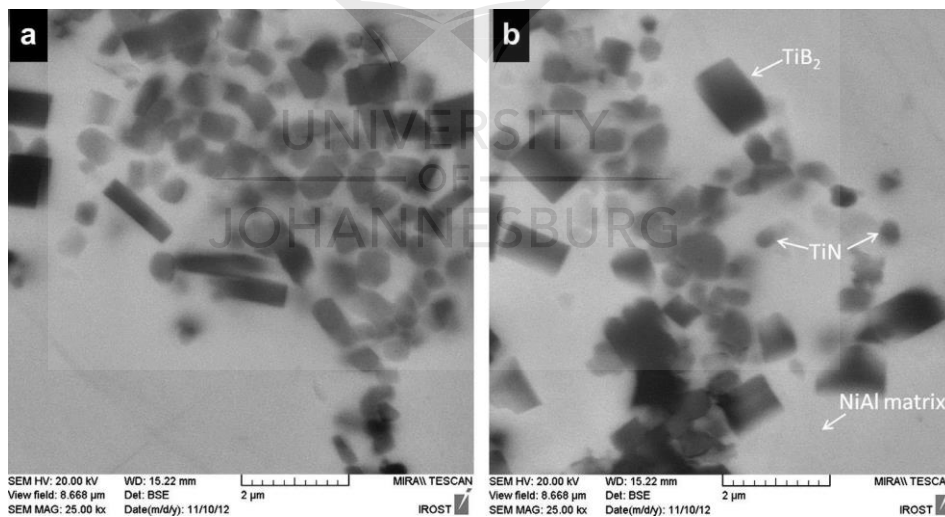
Fig. 5. FESEM images of (a) NiAl-20 wt.% (TiB2–TiN), (b) NiAl-30 wt.% (TiB2–TiN) showing the in-situ formed reinforcement phases after the combustion synthesis of Ni-Al-B-N-Ti. [15].

4.2 Silicon carbide

The consideration of NiAl is particularly for high temperature applications where creep is important. Azarmi [20], studied the effect of SiC particulate reinforcement on NiAl with particular emphasis on its enhancement of the creep properties of the intermetallic (Fig. 6). The SiC particulates content was varied between 0 and 30 vol% with pre-alloyed NiAl powders. The hardness values of the composites were observed to increase up on till 20 vol% (507 Hv) reinforcement, after which a decline commenced in direct correlation with the densification pattern. This was a clear indication of a strong dependence of the hardness on the densification and not solely on the reinforcement content, since higher reinforcement content led to higher porosities and hence lower hardness. Results also showed the formation of nickel rich portions in the resulting microstructure which is believed to improve the strength and plasticity of the NiAl-SiC composite at higher temperatures.
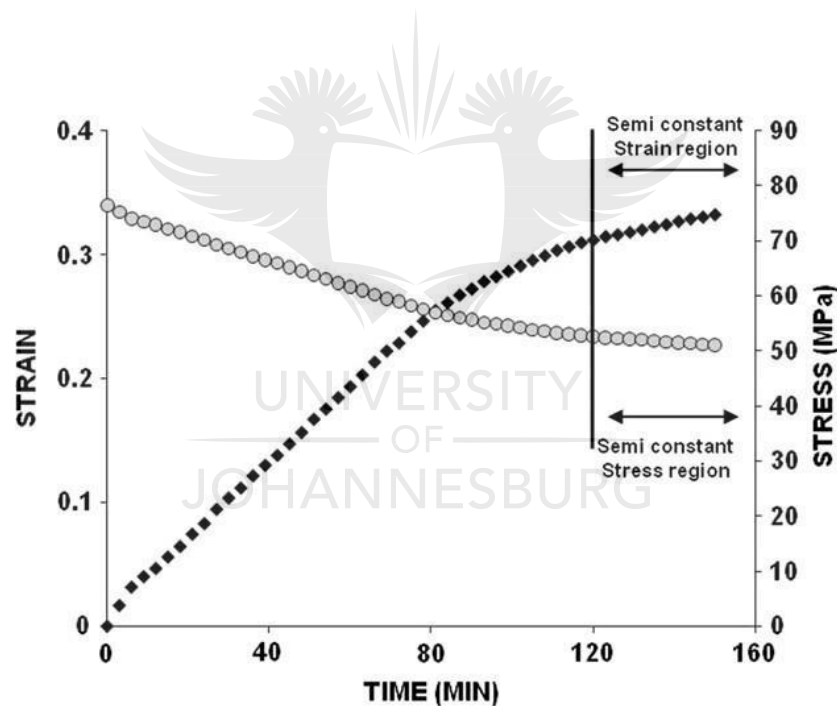
Fig. 6. Creep strain and stress versus time for a typical constant load creep test for NiAl-20 vol% SiC composite. [20]

A reduction in the creep rate was observed as a result of the SiC triggering a complicated triaxial stress state in the intermetallic structure, which led to the reduction of the effective shear stress. Thus, the steady state creep rate, corresponding to the point at which work hardening equals recovery, was observed to be higher in the unreinforced than in the SiC reinforced composite.

This signified that the SiC reinforcement proved effective in restricting dislocation movement during the creep process. The steady state creep rate as it relates to temperature and stress is governed by the following equation:

$$\varepsilon = K\, \sigma^n \exp(-Q/RT) \ldots\ldots\ldots\ldots (3)$$

Where ε is the steady state creep rate, Q is the thermal activation energy, n is the stress exponent, R is the universal gas constant, σ is the applied stress and T is the temperature.

4.3 Tungsten and molybdenum

The high hardness of refractory materials makes them attractive as reinforcement phases for intermetallic matrices like NiAl. Molybdenum and tungsten have been incorporated by various researchers into the NiAl system over the years. Though these refractory materials are not lightweight, their versatility in this intermetallic system is ascribed to their propensity to impart ductility and their high thermal conductivity [25]. Gostishchev et al [53] decided on integrating borides of tungsten and molybdenum into NiAl matrix. They obtained improved hardness of 8.4 GPa for NiAl reinforced with Mo_2B_5 and 9.4 GPa for NiAl reinforced with W_2B_5 and an additional phase of another aluminide-Ni_2Al_3. Since the solubility of tungsten and molybdenum in NiAl matrix is low, the microstructure revealed sequestered inclusions of these refractories in the intermetallic matrix. Hardness values of the boride precipitates were as high as 29.2 GPa for tungsten boride and 24.4 GPa for molybdenum boride.

In a similar study, Takahashi and Dunand [25] also reinforced NiAl intermetallic with molybdenum and tungsten and evaluated the resulting properties. Tungsten proved to be a more effective reinforcement for the NiAl matrix than molybdenum, possibly owing to its intrinsic higher strength and the smaller size of its dispersoids. Though the microhardness values between the two reinforced composites was not significant, given that tungsten is heavier than molybdenum, in terms of density compensated hardness, the molybdenum proved to be a more effective reinforcement. NiAl reinforced with 10 vol% tungsten showed microhardness values of 500 Hv, while 30 vol% reinforced NiAl showed 670 Hv. The molybdenum reinforced composites showed similar trend and followed closely behind at 480 Hv and 660 Hv respectively for the 10 vol% and 30 vol% reinforced NiAl composites respectively. They also observed from the results that these refractory reinforced NiAl composites could be utilized in high temperature environments up until 900 ℃ without being coated, indicating that the tungsten and molybdenum additions did not impair the oxidation resistance of the NiAl

composites. This value was said to be higher than was observed in composites reinforced with the same refractories but fabricated via directional solidification route.

Liu et al [30] incorporated molybdenum carbide also in the NiAl matrix, in varying compositions between 0 and 10 wt%. The NiAl-10 wt% Mo_2C showed the highest hardness of 668.27 Hv over the unalloyed NiAl of 549.69 Hv. The porosity was observed to gradually increase with increasing weight percent of molybdenum carbide additions, but there was a simultaneous increment in the microhardness values as well. This showed that the microhardness values were not dependent solely on densification, but rather on the reinforcement content. This increase was due to homogenously dispersed molybdenum carbide precipitates which formed secondary phase strengthening. This secondary phase strengthening in addition to the ultra-fine grained composite gave rise to more impediments in the way of dislocation movement within the matrix, thus leading to strength improvements in the reinforced composite. The fracture mode of the reinforced composite was observed to be predominantly transgranular cleavage with a minor dimpled structure. NiAl-8 wt% Mo_2C showed the best wear resistance properties with the wear mechanism identified to be by plastic deformation and the worn surfaces protected by a tribofilm. Whereas the worn surface of the unalloyed NiAl showed that the dominant wear mechanism in this sample was by brittle micro-fracture due to the presence of thin and shallow fragments from the worn surface.

4.4 Rhenium

Rhenium is a rare earth metal that has been identified as a good reinforcement element in NiAl matrices [23]. A detailed work on the effect of this rare metal on the fracture toughness of NiAl was done by Bochenek et al [23] by adding it in various compositions. They observed the highest fracture toughness in the NiAl-1.25Re composites with a significant 12.69 MPa√m and flexural strength of 882.6 MPa. This improvement was ascribed to the grain boundary strengthening mechanisms of rhenium. The diffused rhenium around the grain boundaries were seen to act as ductile bridges between the grain boundaries. In addition, the diffusion of rhenium into the NiAl grains led to the strengthening of the grain boundaries. Ultimately these mechanisms improved the grain boundary cohesion which has the propensity to improve the fracture toughness of NiAl [4].

5. Nano-reinforcement

Recently, researchers have intensified investigations on incorporating smartness and multi-

functionalities in the fabrication of new generation composites via the incorporation of nano reinforcements [54, 55]. Researchers have explored size reduction due to the strong gains of improved mechanical properties of nano-reinforced composites as smaller reinforcement size has been documented to alleviate the properties of the resulting composites. This size effect however poses the challenge of agglomeration of the reinforcement phases within the matrix as agglomeration becomes worse with reduction in particle size of reinforcing phases. Among these nano reinforcements, carbon nanotubes have gained popularity due to their versatility in various matrices like polymers [56], ceramics [57] and metals [58].

5.1 Carbon nanotubes (CNTs)

Carbon nanotubes (Fig. 7) [59] have recently been introduced into the NiAl intermetallic matrix with modest results [10, 60]. CNTs possess extraordinary properties like Young's modulus of ~1TPa, tensile strength of ~130 GPa and thermal conductivity of ~3000W/M/K [61]. Considering the exceptional properties of these nanomaterials, the documented results are not a reflection of its outstanding properties as they still fall short in terms of mechanical properties as compared to their particulate reinforced equivalents.
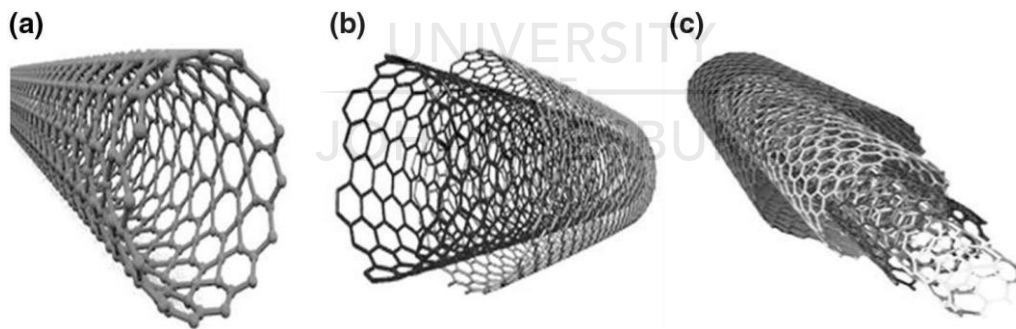
Fig. 7. Illustrates the structures of CNTs: SWCNTs (a), DWCNTs (b), and MWCNTs (c). [59]

Groven and Puszynski [60] incorporated both single walled and multi walled CNTs into NiAl matrix and evaluated the resulting mechanical properties. Results showed that the single walled carbon nanotubes (SWCNTs) imparted better mechanical properties than the multi-walled carbon nanotubes (MWCNTs). There was an improvement in the mechanical properties of

SWCNTs reinforced NiAl from 3.5 GPa to 4.6 GPa for the 1 wt %, above this SWCNTs content, the hardness began to deteriorate. A contrast was observed however for the MWCNTs reinforced NiAl which revealed an outright decrease in mechanical properties for all compositions of the MWCNTs. The incorporation of CNTs into the intermetallic matrix has proven to be a daunting task as it has been for metallic matrices as well. The high length to diameter ratio coupled with the strong Van der waals forces that exist between these tubes keep them tightly bundled together [62], resisting any form of distribution. This introduces the dynamics of effective dispersion into the mix to alleviate the properties of NiAl. From the works of Groven and Puszynski [60], a very high sensitivity was detected between dispersion methods of single walled CNTs and microhardness values of the resulting composites. The more rigorous dispersion directly translated to higher microhardness values. For instance, with ultrasonication alone as the dispersion method, microhardness value of 2.92±0.51 GPa was recorded. When mechanical mixing was used in addition to ultrasonication, microhardness values increased to 3.48±0.17 GPa. From Fig. 8, mats and patches of CNTs can be observed from the micrographs, strongly indicating that the utilized combined dispersion route was still not sufficient in effectively dispersing the nanotubes.
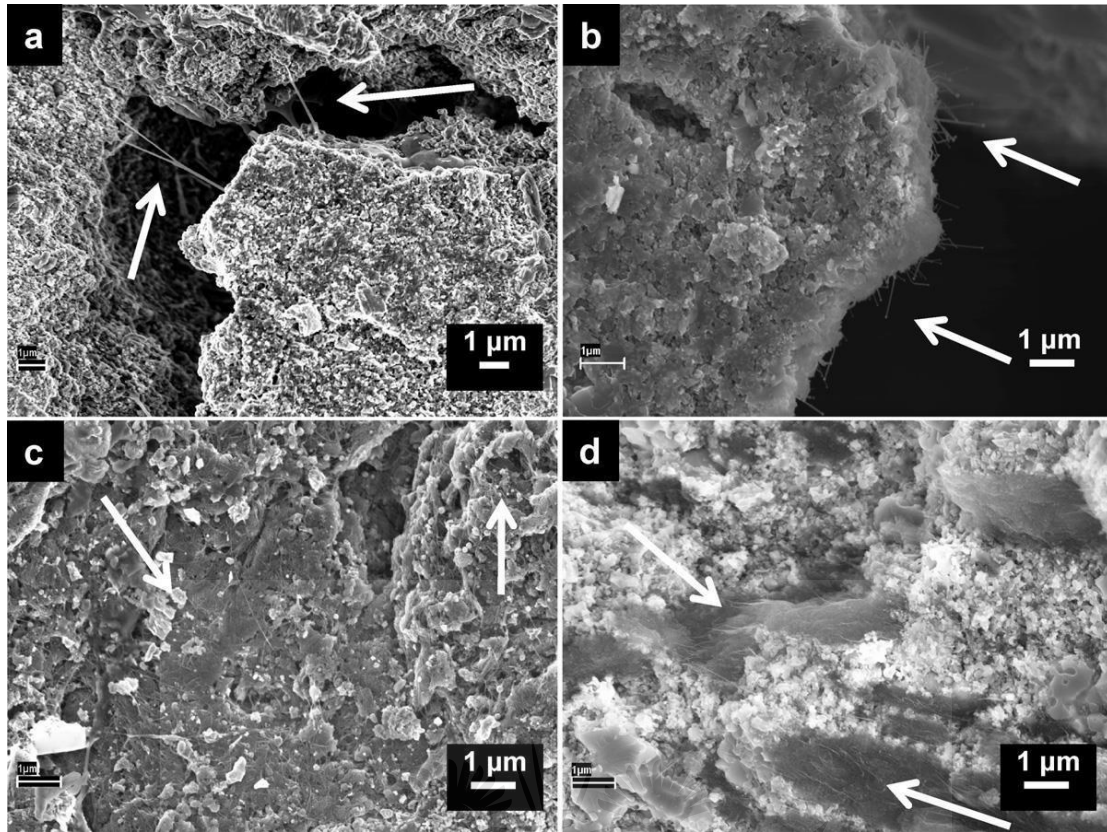
Fig. 8- SEM images of fractured surfaces of x wt% SWCNTs–NiAl composites. (a and b) 1.0 wt.%, (c) 2.5 wt.% and (d) 5.0 wt.%. Arrows indicate regions of SWCNTs for images a, c, and d. Alumina whiskers were also observed as shown in image (b). Scale bars are 1 μm. [60].

In a similar work by Ameri et al [10], CNTs were dispersed into NiAl matrix using mechanical alloying. From the results summarized in Table 1, it can be inferred that the microhardness and fracture toughness values were strongly dependent upon the densification, and in turn, the densification values obtained were a direct reflection of the dispersion method and CNTs content. The best combination of properties was achieved from the sample with 0.5 wt% CNTs where the nanotubes were added to the mix 15 h after MA had commenced. Fracture toughness values obtained was greater than 5.83 MPa√m with microhardness values of 5.6 GPa. NiAl was observed to appear at 15 h into MA and its formation was completed after 40 h of MA.

Table 1- Properties of spark plasma sintered NiAl and NiAl-CNTs samples. [10]

Specimen code	Density gcm^{-3}	Relative density %	Porosity %	Hardness GPa	Toughness, MPam$^{1/2}$
NiAl(50 h)	5.49	92.8	7.2	5.49	5.67 ± 0.03
NiAl(45 h)-0.5%CNT	5.28	89.3	10.7	4.61	5.07 ± 0.03
NiAl(45 h)-1%CNT	5.05	85.6	14.4	4.16	4.60 ± 0.05
NiAl(20 h)	5.51	93.2	6.8	5.41	5.48 ± 0.02
NiAl(15 h)-0.5%CNT	5.63	95.4	4.6	5.60	>5.83
NiAl(15 h)-1%CNT	4.49	76.1	23.9	2.94	3.07 ± 0.07

From Fig. 9, a phenomenon known as crack bridging can be observed from the micrographs, which has been identified as an operative toughening mechanism [63]. The CNTs bridging the crack between particles can help to keep the composites together to prevent premature failure.
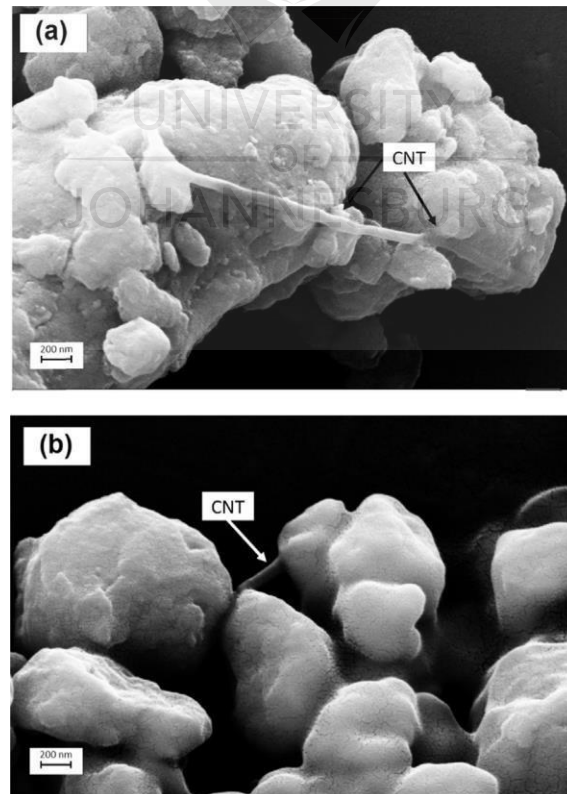
Fig. 9. Secondary electron micrographs of nanocomposite powders a) NiAl (45 h)-0.5% CNT and b) NiAl (45 h)-1% CNT. [10]

It is believed that CNTs have the potential to greatly improve the mechanical properties of nickel aluminide. Though only moderate improvements have been documented, these few works have helped to blaze the trail in the assertion that these nanotubes can be effectively integrated into an intermetallic structure like NiAl. Of all the alloying additions proposed and explored for the improvement of the plasticity of NiAl, CNTs have the added advantage of being the lightest, consequently leading to a much lighter nickel aluminide composite. Recently the authors of this review evaluated three different ball milling approaches to disperse CNTs in NiAl matrix in an attempt to improve dispersion and by extension, the mechanical properties. The best dispersion was obtained from a two stage milling comprising of both low and high energy milling processes. This route was then developed to produce dense compacts of CNTs reinforced composites with full details to be published soon. In the preliminary studies, micrographs obtained from the fracture surfaces of the reinforced composite are shown in Fig. 10, with the unalloyed NiAl revealing a purely intergranular fracture mode (which is very consistent with literature as shown in Fig. 11), while the CNTs reinforced NiAl revealed a mixed fracture mode of both intergranular and dimpled microstructure. This is significantly different from the fractography micrographs documented in literature for work done on NiAl-CNTs. More work is being done by the authors to improve on this promising result and obtain a predominantly dimpled microstructure on the carbon nanotube reinforced intermetallic composite.
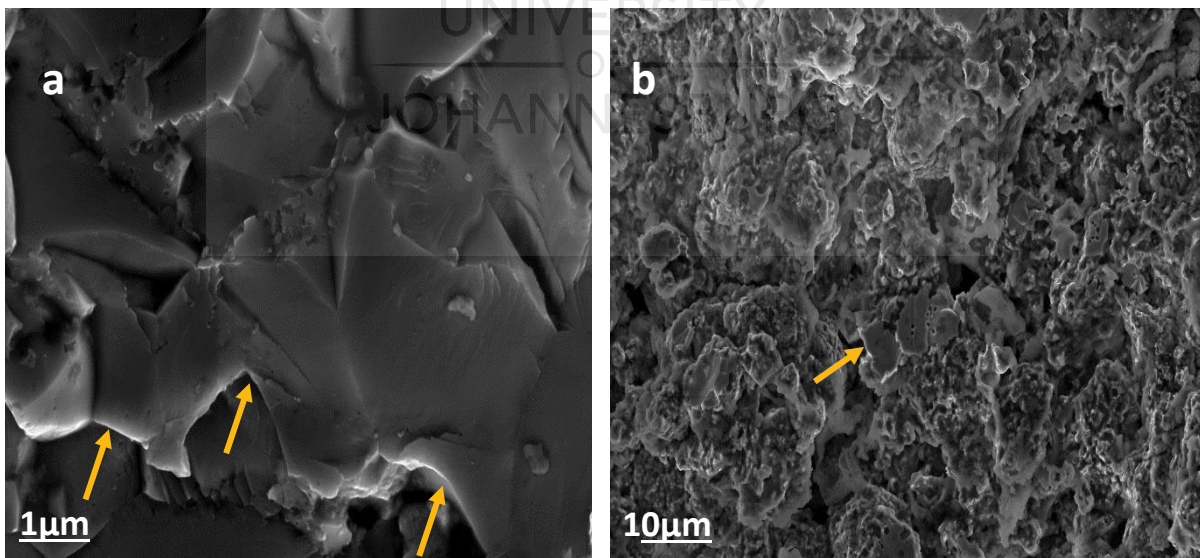
Fig. 10. Micrographs showing the fracture morphology of a) Pure NiAl and b) NiAl-0.5 wt% CNTs by authors
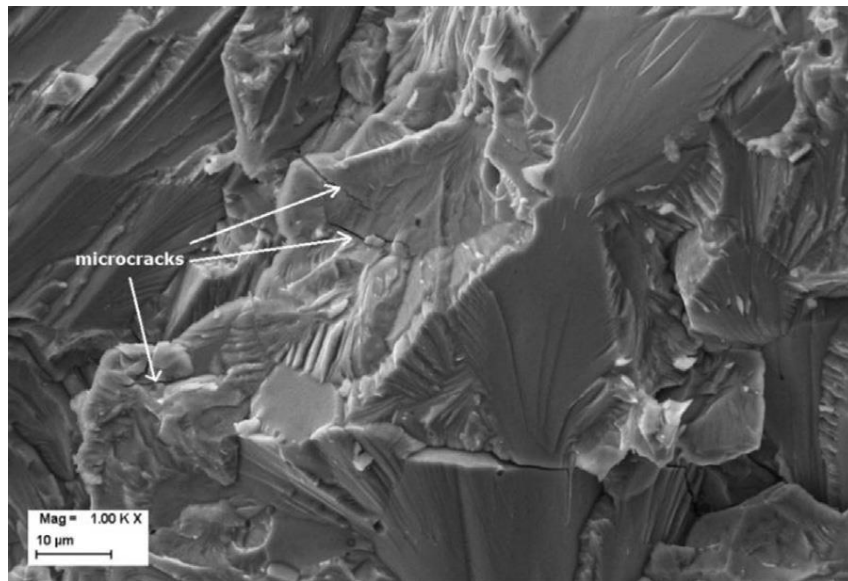
Fig. 11. Fracture surface of NiAl specimen without rhenium addition after four point bending test (SEVNB); microcracks in NiAl grains are marked by arrows. [23]

6. NiAl coatings

The inherent excellent oxidation resistance of NiAl has incited its use as a choice material for thermal barrier coatings. This thermal advantage has been ascribed to the formation of a thin, tenacious layer of Al_2O_3, which acts as protection against diverse corrosive environments [64]. Though bulk composites of NiAl are still being intensively investigated for diverse applications, NiAl coatings are already being utilized effectively in service as protective coatings on expensive super-alloys due to their resistance even in hyper corrosive environments [65]. Though there exists many coating techniques, thermal spray techniques are the most commonly used method of fabricating these NiAl coatings [15]. The powder mixtures are mainly produced by mechanical alloying processes for homogeneity. Movahedi [66] utilized mechanical alloying for the preparation of powder compacts that was later applied viathermal spraying. They reinforced the NiAl with 15 wt% (Al_2O_3-13TiO_2) reinforcement and compared between two spraying techniques-namely air plasma spraying (APS) and high velocity oxy fuel (HVOF). Results showed that the HVOF produced a coating with dense microstructure having only few pores as shown in Fig. 12. Whereas the microstructure of the APS coating showed an in-homogenous structure with heavy pores as observed in Fig. 13. The heavy porosity was attributed to the growth of confined air on impacting particles in liquefied state. The success of the HVOF however was ascribed to lower coating oxidation as a result of high particle velocities and low particle temperatures employed, leading to a reduction in volume fraction of molten phase. The alloyed NiAl coating was also compared to the unalloyed NiAl coating

and was found to possess higher fracture toughness of 7.12 MPa√m over the 4.28 MPa√m of the unalloyed [67]. This was made possible by the pinning effect of the reinforcement particles in limiting the crack promulgation during the indentation testing.
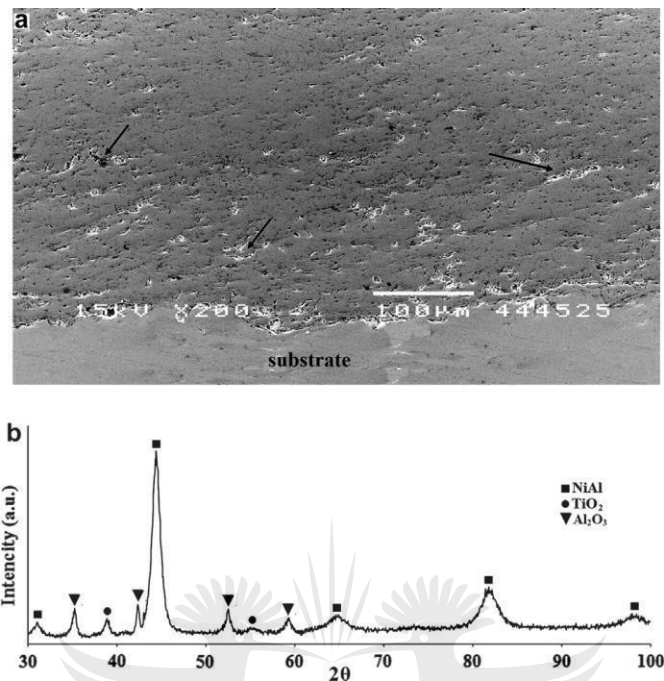
Fig. 12. (a) Cross-sectional microstructure and (b) XRD pattern of as-sprayed NiAl-15 wt% (Al₂O₃–13% TiO₂) HVOF coating. [66]
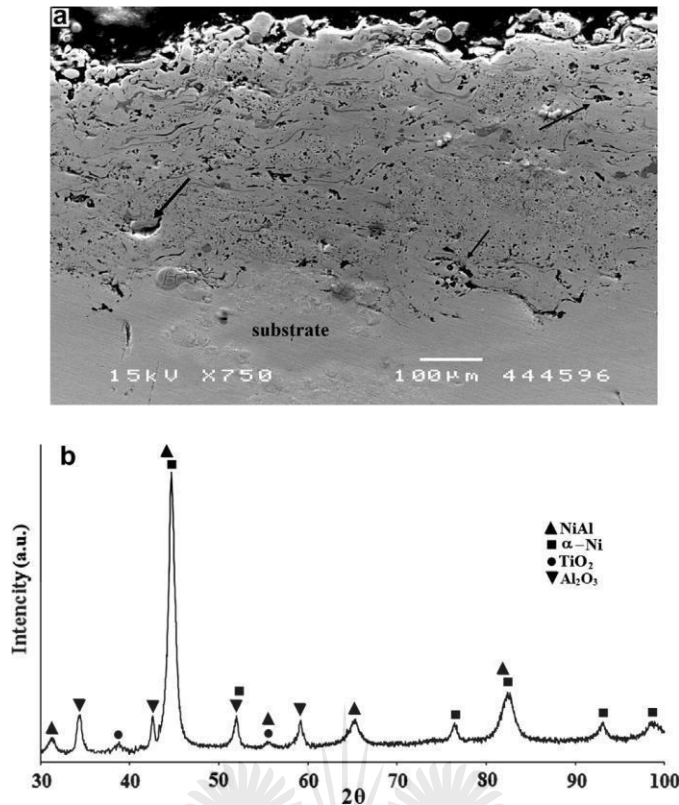
Fig. 13. (a) Cross-sectional microstructure and (b) XRD pattern of as-sprayed NiAl-15 wt% (Al_2O_3–13% TiO_2) APS coating. [66]

As a worthy substitute for expensive nickel based superalloys, nickel aluminide coatings have been established to alleviate molten salt corrosion. In a study by Audigie, [68] they evaluated the behaviour of nickel aluminide coatings in static molten nitrate salt. Results showed that there was very minimal inter-diffusion between the substrate and the intermetallic coating and after 1000 h at 580 ℃, the nickel aluminide coatings still retained their original microstructure without showing any signs of material degradation which validated the excellent corrosion resistance of the aluminide coating. They alluded this resistance to the presence of the two oxides - $NiAl_2O_4$ and Al_2O_3 which served as effective barriers against the corrosion. Interestingly even when this Al_2O_3 layer experiences a local breakdown or spalling, the aluminium 'reservoir' underneath undergoes selective oxidation in a process similar to self-healing thereby healing the continuous oxide scale [65].

Researchers have documented that at temperatures above 1100 ℃, nickel aluminides form a very stable layer of Al_2O_3, however, below this temperature variations of metastable alumina scales form during oxidation [69]. Some alloying additions have the propensity to change the growth of alumina from the metastable (θ-Al_2O_3) to the thermodynamically stable one (γ-Al_2O_3). Khan et al [70] introduced chromium oxide nanoparticles into the aluminide coating

34

which not only slowed down the oxidation rate but also led to the formation of a more adherent scale. The chromium oxide was said to act as a catalyst in speeding up the transformation and growth rate of the metastable alumina phase to the stable alumina phase.

7. Future trends in NiAl manufacturing

The structure-property relationship in composites is crucial in the manufacturing and processing of nickel aluminides. The difficulties associated with some complexities of manufacturing nickel aluminide are strong indicators determining the choice of fabrication routes. For this reason, traditional methods like investment casting and ingot metallurgy gradually gave way to powder metallurgy techniques. Additive manufacturing (AM) is a recent and innovative manufacturing technology that may be well suited for the manufacturing of complex intermetallics like NiAl, which may likely preclude some commonly observed difficulties in NiAl manufacturing. The technology behind AM manufacturing goes by several names like rapid prototyping [71], rapid manufacturing [72], solid free-form fabrication [73] and 3D printing [74, 75]. Typically, the process entails the translation of a computerized 3 dimensional model into a finished product by successively printing materials by gradual material accumulation [76], without employing cutting tools [77] or moulds [76]. Medical and aerospace sectors have both benefited extensively from the novelty and flexibility of AM processes [78]. Though the economic viability of AM processes still need to be ascertained on some levels due to limitations in material availability [74], surface imperfections [79], costs and porosity defects [80], nevertheless the potentials for this process are enormously huge. This bottom-up [81], layer by layer approach has the advantages of high geometric precision, freedom from manufacturing constraints and proficient use of materials which eliminates wastage [82]. Investigations have led to improvements on different methods of additive manufacturing processes namely fused deposition modelling, inkjet printing, stereolithography and powder bed fusion [80] amongst others. AM processing has progressively carved out a niche by revolutionizing the manufacturing sector, and the products are becoming increasingly prevalent [83]. Further investigations and research advances are presently focused on increasing the range of materials usable for these processes, especially amorphous metals, high entropy alloys, high strength alloys and composite metals [84, 85]. With this continuing trend, intermetallic composites like NiAl can readily benefit from the flexibilities and novelties offered by AM, possibly leading to the desired enhancement of this intermetallic compound.

8. Conclusion

The development and improvement of NiAl intermetallics have taken different twists and turns over the years. The diverse fabrication methods have stimulated an equally diverse range of mechanical properties in this intermetallic. Intense research is still on-going to bring this intermetallic into wide commercialized usage and expectations are high that breakthrough is imminent. This paper reviewed the various fabrication methods of nickel aluminide composites with emphasis on the mechanical properties obtained as a function of their processing method and alloying additions.

The highlights are as follows:

- The microstructure and mechanical properties of the various nickel aluminide composites have been successfully modified and enhanced via various fabrication routes and varied alloying elements.
- The strength properties have been significantly enhanced, whereas the major drawback of poor fracture toughness in NiAl intermetallic systems have not been as aggressively reported as the strength values.
- The most impressive enhancements in fracture toughness have been achieved by DS of NiAl-Cr-Mo alloys. However other high temperature mechanical properties of this eutectic need to be evaluated to assess its suitability in actual service conditions.
- Reinforcement of NiAl intermetallic systems with CNTs have proven to be a feasible feat, showing promising results. Though the improvements have been modest, owing to the agglomerations and clustering of the nanotubes, it is expected that with better levels of dispersion, significant improvements will be made in NiAl-CNTs composites.

References

[1] D. Wu, K. Dahl, T. Christiansen, M. Montgomery, J. Hald, Corrosion behaviour of Ni and nickel aluminide coatings exposed in a biomass fired power plant for two years, Surface and Coatings Technology, (2019).

[2] G. Dey, Physical metallurgy of nickel aluminides, Sadhana, 28 (2003) 247-262.

[3] D.B. Miracle, R. Darolia, NiAl and its alloys, Intermetallic Compounds: Principles and Practice, 2 (2000) 53-72.

[4] Ş. Talaş, Nickel aluminides, Intermetallic Matrix Composites, Elsevier2018, pp. 37-69.

[5] I. Baker, P. Munroe, Improving intermetallic ductility and toughness, JOM, 40 (1988) 28-31.

[6] Z. Shang, J. Shen, L. Wang, Y. Du, Y. Xiong, H. Fu, Investigations on the microstructure and room temperature fracture toughness of directionally solidified NiAl–Cr (Mo) eutectic alloy, Intermetallics, 57 (2015) 25-33.

[7] N.S. Stoloff, C. Koch, C.T. Liu, O. Izumi, High-temperature ordered intermetallic alloys II; Proceedings of the Second Symposium, Boston, MA, Dec. 2-4, 1986,(1987).

[8] A. Ponomareva, Y.K. Vekilov, I. Abrikosov, Effect of Re content on elastic properties of B2 NiAl from ab initio calculations, Journal of Alloys and Compounds, 586 (2014) S274-S278.

[9] K. Bochenek, M. Basista, Advances in processing of NiAl intermetallic alloys and composites for high temperature aerospace applications, Progress in Aerospace Sciences, 79 (2015) 136-146.

[10] S. Ameri, Z. Sadeghian, I. Kazeminezhad, Effect of CNT addition approach on the microstructure and properties of NiAl-CNT nanocomposites produced by mechanical alloying and spark plasma sintering, Intermetallics, 76 (2016) 41-48.

[11] M. Shekari, M. Adeli, A. Khobzi, M. Kobashi, N. Kanetake, Induction-activated self-propagating, high-temperature synthesis of nickel aluminide, Advanced Powder Technology, 28 (2017) 2974-2979.

[12] K.S. Mohammed, H.T. Naeem, Effect of milling parameters on the synthesis of Al–Ni intermetallic compound prepared by mechanical alloying, The Physics of Metals and Metallography, 116 (2015) 859-868.

[13] C. Biffi, P. Bassani, Z. Sajedi, P. Giuliani, A. Tuissi, Laser ignition in self-propagating high temperature synthesis of porous NiTinol shape memory alloy, Materials Letters, 193 (2017) 54-57.

[14] R. Rosa, P. Veronesi, A. Casagrande, C. Leonelli, Microwave ignition of the combustion synthesis of aluminides and field-related effects, Journal of Alloys and Compounds, 657 (2016) 59-67.

[15] A.A. Shokati, N. Parvin, M. Shokati, Combustion synthesis of NiAl matrix composite powder reinforced by TiB2 and TiN particulates from Ni–Al–Ti–BN reaction system, Journal of Alloys and Compounds, 585 (2014) 637-643.

[16] T. Talako, M. Sharafutdinov, T. Grigor'eva, I. Vorsina, A. Barinova, N. Lyakhov, Production of Ni x Al y/Al 2 O 3 composites using a combination of mechanical activation and self-propagating high-temperature synthesis, Combustion, Explosion, and Shock Waves, 45 (2009) 662.

[17] H.E. Camurlu, F. Maglia, Self-propagating high-temperature synthesis of ZrB2 or TiB2 reinforced Ni–Al composite powder, Journal of Alloys and Compounds, 478 (2009) 721-725.

[18] A.A. Shokati, N. Parvin, N. Sabzianpour, M. Shokati, A. Hemmati, In situ synthesis of NiAl–NbB2 composite powder through combustion synthesis, Journal of Alloys and Compounds, 549 (2013) 141-146.

[19] A. Biswas, S. Roy, K. Gurumurthy, N. Prabhu, S. Banerjee, A study of self-propagating high-temperature synthesis of NiAl in thermal explosion mode, Acta Materialia, 50 (2002) 757-773.

[20] F. Azarmi, Creep properties of nickel aluminide composite materials reinforced with SiC particulates, Composites Part B: Engineering, 42 (2011) 1779-1785.

[21] O.E. Falodun, B.A. Obadele, S.R. Oke, A.M. Okoro, P.A. Olubambi, Titanium-based matrix composites reinforced with particulate, microstructure, and mechanical properties using spark plasma sintering technique: a review, The International Journal of Advanced Manufacturing Technology, (2019) 1-13.

[22] A. Bisht, M. Srivastava, R.M. Kumar, I. Lahiri, D. Lahiri, Strengthening mechanism in graphene nanoplatelets reinforced aluminum composite fabricated through spark plasma sintering, Materials Science and Engineering: A, 695 (2017) 20-28.

[23] K. Bochenek, W. Węglewski, J. Morgiel, M. Basista, Influence of rhenium addition on microstructure, mechanical properties and oxidation resistance of NiAl obtained by powder metallurgy, Materials Science and Engineering: A, 735 (2018) 121-130.

[24] B. Bewlay, M. Weimer, T. Kelly, A. Suzuki, P. Subramanian, The science, technology, and implementation of TiAl alloys in commercial aircraft engines, MRS Online Proceedings Library Archive, 1516 (2013) 49-58.

[25] T. Takahashi, D. Dunand, Nickel aluminide containing refractory-metal dispersoids 2: Microstructure and properties, Materials Science and Engineering: A, 192 (1995) 195-203.

[26] A. Mashreghi, M. Moshksar, Partial martensitic transformation of nanocrystalline NiAl intermetallic during mechanical alloying, Journal of Alloys and Compounds, 482 (2009) 196-198.

[27] E. Kubaski, O. Cintho, J. Capocchi, Effect of milling variables on the synthesis of NiAl intermetallic compound by mechanical alloying, Powder technology, 214 (2011) 77-82.

[28] E. Liu, J. Jia, Y. Bai, W. Wang, Y. Gao, Study on preparation and mechanical property of nanocrystalline NiAl intermetallic, Materials & Design, 53 (2014) 596-601.

[29] E. Zelaya, M. Esquivel, D. Schryvers, Evolution of the phase stability of Ni–Al under low energy ball milling, Advanced Powder Technology, 24 (2013) 1063-1069.

[30] E. Liu, Y. Gao, J. Jia, Y. Bai, W. Wang, Microstructure and mechanical properties of in situ NiAl–Mo2C nanocomposites prepared by hot-pressing sintering, Materials Science and Engineering: A, 592 (2014) 201-206.

[31] M. Khodaei, M. Enayati, F. Karimzadeh, Mechanochemical behavior of Fe 2 O 3–Al–Fe powder mixtures to produce Fe 3 Al–Al 2 O 3 nanocomposite powder, Journal of materials science, 43 (2008) 132-138.

[32] K.S. Mohammed, H.T. Naeem, S.N. Iskak, Study of the feasibility of producing Al–Ni intermetallic compounds by mechanical alloying, The Physics of Metals and Metallography, 117 (2016) 795-804.

[33] A. Khajesarvi, G. Akbari, Properties evaluation and studying production mechanism of nanocrystalline NiAl intermetallic compound by mechanical alloying, Metallurgical and Materials Transactions A, 47 (2016) 1881-1888.

[34] M. Atzmon, Characterization of AlNi formed by a self-sustaining reaction during mechanical alloying, Materials Science and Engineering: A, 134 (1991) 1326-1329.

[35] R. Maric, K. Ishihara, P. Shingu, Structural changes during low energy ball milling in the Al-Ni system, Journal of materials science letters, 15 (1996) 1180-1183.

[36] M. Alizadeh, G. Mohammadi, G.-H.A. Fakhrabadi, M.M. Aliabadi, Investigation of chromium effect on synthesis behavior of nickel aluminide during mechanical alloying process, Journal of Alloys and Compounds, 505 (2010) 64-69.

[37] J.I. Langford, A. Wilson, Scherrer after sixty years: a survey and some new results in the determination of crystallite size, Journal of Applied Crystallography, 11 (1978) 102-113.

[38] H. Mio, J. Kano, F. Saito, K. Kaneko, Optimum revolution and rotational directions and their speeds in planetary ball milling, International Journal of Mineral Processing, 74 (2004) S85-S92.

[39] C. Suryanarayana, Mechanical alloying and milling, Progress in materials science, 46 (2001) 1-184.

[40] M. Enayati, F. Karimzadeh, S. Anvari, Synthesis of nanocrystalline NiAl by mechanical alloying, journal of materials processing technology, 200 (2008) 312-315.

[41] H. Cline, J. Walter, E. Lifshin, R. Russell, Structures, faults, and the rod-plate transition in eutectics, Metallurgical Transactions, 2 (1971) 189-194.

[42] M.B. Rahaei, D. Jia, Processing behavior of nanocrystalline NiAl during milling, sintering and mechanical loading and interpretation of its intergranular fracture, Engineering Fracture Mechanics, 132 (2014) 136-146.

[43] J.D. Whittenberger, S. Raj, I.E. Locci, J.A. Salem, Elevated temperature strength and room-temperature toughness of directionally solidified Ni-33Al-33Cr-1Mo, Metallurgical and Materials Transactions A, 33 (2002) 1385-1397.

[44] J. Guo, C. Cui, Y. Chen, D. Li, H. Ye, Microstructure, interface and mechanical property of the DS NiAl/Cr (Mo, Hf) composite, Intermetallics, 9 (2001) 287-297.

[45] Y. Xie, J. Guo, Y. Liang, L. Zhou, H. Ye, Modification of NiAl–Cr (Mo)–0.15 Hf alloy by Sc addition, Intermetallics, 17 (2009) 400-403.

[46] J. Guo, K. Huai, Q. Gao, W. Ren, G. Li, Effects of rare earth elements on the microstructure and mechanical properties of NiAl-based eutectic alloy, Intermetallics, 15 (2007) 727-733.

[47] J. Guo, L. Sheng, Y. Tian, L. Zhou, H. Ye, Effect of Ho on the microstructure and compressive properties of NiAl-based eutectic alloy, Materials Letters, 62 (2008) 3910-3912.

[48] T. Chen, J. Hampikian, N. Thadhani, Synthesis and characterization of mechanically alloyed and shock-consolidated nanocrystalline NiAl intermetallic, Acta materialia, 47 (1999) 2567-2579.

[49] L. Sheng, F. Yang, T. Xi, J. Guo, Investigation on microstructure and wear behavior of the NiAl–TiC–Al2O3 composite fabricated by self-propagation high-temperature synthesis with extrusion, Journal of Alloys and Compounds, 554 (2013) 182-188.

[50] H. Zhao, F. Qiu, S. Jin, Q. Jiang, High room-temperature plastic and work-hardening effect of the NiAl-matrix composites reinforced by particulates, Intermetallics, 19 (2011) 376-381.

[51] S.C. Tjong, Z. Ma, Microstructural and mechanical characteristics of in situ metal matrix composites, Materials Science and Engineering: R: Reports, 29 (2000) 49-113.

[52] A.E. Steinman, S. Corthay, K.L. Firestein, D.G. Kvashnin, A.M. Kovalskii, A.T. Matveev, P.B. Sorokin, D.V. Golberg, D.V. Shtansky, Al-based composites reinforced with AlB2, AlN and BN phases: Experimental and theoretical studies, Materials & Design, 141 (2018) 88-98.

[53] V. Gostishchev, I. Astapov, S. Khimukhin, Fabrication of nickel–aluminum alloys with tungsten and molybdenum borides by the method of self-propagating high-temperature synthesis, Inorganic Materials: Applied Research, 8 (2017) 546-550.

[54] B. Han, S. Sun, S. Ding, L. Zhang, X. Yu, J. Ou, Review of nanocarbon-engineered multifunctional cementitious composites, Composites Part A: Applied Science and Manufacturing, 70 (2015) 69-81.

[55] P. Alafogianni, K. Dassios, C. Tsakiroglou, T. Matikas, N. Barkoula, Effect of CNT addition and dispersive agents on the transport properties and microstructure of cement mortars, Construction and Building Materials, 197 (2019) 251-261.

[56] R. Haggenmueller, H. Gommans, A. Rinzler, J.E. Fischer, K. Winey, Aligned single-wall carbon nanotubes in composites by melt processing methods, Chemical physics letters, 330 (2000) 219-225.

[57] A. Peigney, E. Flahaut, C. Laurent, F. Chastel, A. Rousset, Aligned carbon nanotubes in ceramic-matrix nanocomposites prepared by high-temperature extrusion, Chemical Physics Letters, 352 (2002) 20-25.

[58] S. Suarez, F. Lasserre, F. Mücklich, Mechanical properties of MWNT/Ni bulk composites: Influence of the microstructural refinement on the hardness, Materials Science and Engineering: A, 587 (2013) 381-386.

[59] A. Okoro, M. Awotunde, O. Ajiteru, S. Lephuthing, P. Olubambi, R. Machaka, Effects of carbon nanotubes on the mechanical properties of spark plasma sintered titanium matrix composites—A review, 2018 IEEE 9th International Conference on Mechanical and Intelligent Manufacturing Technologies (ICMIMT), IEEE, 2018, pp. 54-59.

[60] L. Groven, J. Puszynski, Combustion synthesis and characterization of nickel aluminide–carbon nanotube composites, Chemical Engineering Journal, 183 (2012) 515-525.

[61] P. Kim, L. Shi, A. Majumdar, P. McEuen, Thermal transport measurements of individual multiwalled nanotubes, Physical review letters, 87 (2001) 215502.

[62] S. Yazdani, R. Tima, F. Mahboubi, Investigation of wear behavior of as-plated and plasma-nitrided Ni-B-CNT electroless having different CNTs concentration, Applied Surface Science, 457 (2018) 942-955.

[63] Z. Xia, L. Riester, W. Curtin, H. Li, B. Sheldon, J. Liang, B. Chang, J. Xu, Direct observation of toughening mechanisms in carbon nanotube ceramic matrix composites, Acta Materialia, 52 (2004) 931-944.

[64] R. Mitra, R. Wanhill, Structural intermetallics, Aerospace Materials and Material Technologies, Springer2017, pp. 229-245.

[65] B. Grégoire, G. Bonnet, F. Pedraza, Mechanisms of formation of slurry aluminide coatings from Al and Cr microparticles, Surface and Coatings Technology, 359 (2019) 323-333.

[66] B. Movahedi, Microstructural evolutions of nickel-aluminide nanocomposites during powder synthesis and thermal spray processes, Advanced Powder Technology, 25 (2014) 871-878.

[67] B. Movahedi, Fracture toughness and wear behavior of NiAl-based nanocomposite HVOF coatings, Surface and Coatings Technology, 235 (2013) 212-219.

[68] P. Audigié, V. Encinas-Sánchez, M. Juez-Lorenzo, S. Rodríguez, M. Gutiérrez, F. Pérez, A. Agüero, High temperature molten salt corrosion behavior of aluminide and nickel-aluminide coatings for heat storage in concentrated solar power plants, Surface and Coatings Technology, 349 (2018) 1148-1157.

[69] Y. Huang, X. Peng, The promoted formation of an α-Al2O3 scale on a nickel aluminide with surface Cr2O3 particles, Corrosion Science, 112 (2016) 226-232.

[70] A. Khan, Y. Huang, Z. Dong, X. Peng, Effect of Cr2O3 nanoparticle dispersions on oxidation kinetics and phase transformation of thermally grown alumina on a nickel aluminide coating, Corrosion Science, (2019).

[71] R. Noorani, Rapid prototyping: principles and applications, (2006).

[72] G.N. Levy, R. Schindel, J.-P. Kruth, Rapid manufacturing and rapid tooling with layer manufacturing (LM) technologies, state of the art and future perspectives, CIRP annals, 52 (2003) 589-609.

[73] R. Xu, Rapid prototyping technology and rapid prototyping manufacturing, Beijing: Atomic Energy Press, 2004.

[74] K.V. Wong, A. Hernandez, A review of additive manufacturing, ISRN Mechanical Engineering, 2012 (2012).

[75] S.J. Ford, L. Mortara, T.H. Minshall, The emergence of additive manufacturing: introduction to the special issue, (2015).

[76] L. Chen, Y. He, Y. Yang, S. Niu, H. Ren, The research status and development trend of additive manufacturing technology, The International Journal of Advanced Manufacturing Technology, 89 (2017) 3651-3660.

[77] T.D. Ngo, A. Kashani, G. Imbalzano, K.T. Nguyen, D. Hui, Additive manufacturing (3D printing): A review of materials, methods, applications and challenges, Composites Part B: Engineering, 143 (2018) 172-196.

[78] W.K. Liu, Y.C. Shin, Special issue on Additive manufacturing: progress in modeling and simulation with experimental validations in additive manufacturing, Computational Mechanics, 61 (2018) 519-520.

[79] S.H. Huang, P. Liu, A. Mokasdar, L. Hou, Additive manufacturing and its societal impact: a literature review, The International Journal of Advanced Manufacturing Technology, 67 (2013) 1191-1203.

[80] X. Wang, M. Jiang, Z. Zhou, J. Gou, D. Hui, 3D printing of polymer matrix composites: A review and prospective, Composites Part B: Engineering, 110 (2017) 442-458.

[81] G. Chryssolouris, P. Stavropoulos, G. Tsoukantas, K. Salonitis, A. Stournaras, Nanomanufacturing processes: a critical review, International Journal of Materials and Product Technology, 21 (2004) 331-348.

[82] J.-P. Kruth, M.-C. Leu, T. Nakagawa, Progress in additive manufacturing and rapid prototyping, Cirp Annals, 47 (1998) 525-540.

[83] S.A. Tofail, E.P. Koumoulos, A. Bandyopadhyay, S. Bose, L. O'Donoghue, C. Charitidis, Additive manufacturing: scientific and technological challenges, market uptake and opportunities, Materials today, 21 (2018) 22-37.

[84] D. Wu, W. Gao, D. Hui, K. Gao, K. Li, Stochastic static analysis of Euler-Bernoulli type functionally graded structures, Composites Part B: Engineering, 134 (2018) 69-80.

[85] A.C. Kandemir, S.N. Ramakrishna, D. Erdem, D. Courty, R. Spolenak, Gradient nanocomposite printing by dip pen nanolithography, Composites Science and Technology, 138 (2017) 186-200.

Review Article

Influence of sintering methods on the mechanical properties of aluminium nanocomposites reinforced with carbonaceous compounds: A review

Mary A. Awotunde[a,*], Adewale O. Adegbenjo[a], Babatunde A. Obadele[a], Moses Okoro[a], Brendon M. Shongwe[b], Peter A. Olubambi[c]

[a] Centre for Nanoengineering and Tribocorrosion, School of Mining, Metallurgy and Chemical Engineering, University of Johannesburg, Johannesburg, South Africa
[b] Institute for NanoEngineering Research, Tshwanhe University of Technology, Pretoria, South Africa
[c] Head of School of Mining, Metallurgy and Chemical Engineering, University of Johannesburg, Johannesburg, South Africa

ARTICLE INFO

ABSTRACT

This paper succinctly reviews from the corpus of literature the reinforcement of aluminium with carbonaceous nanocompounds (CNTs, GNPs, graphenes etc.), with particular emphasis on the strength and ductility of the resulting composites based on the utilized fabrication routes. Owing to the unique intrinsic properties of these carbonaceous nanocompounds, they have been widely reported as ideal reinforcement materials for aluminium and its compounds. Significant amount of work has been published on the use of solid-state sintering as a novel route for the incorporation of these nanocompounds in aluminium matrices. This paper therefore aims to review some relevant aspects of the fabrication processes of these aluminium based composites such as (i) effects of the sintering routes and parameters on the resulting properties of the composites; (ii) the effect of dispersion techniques on the resulting properties of the composites; (iii) the strength–ductility trade-off in the reinforced composites; and (iv) the intermetallics formed between the carbonaceous nanocompounds and aluminium.

1. Introduction

Recent technological demands require a wide (and sometimes conflicting) range of properties unachievable in single traditional materials. This birthed the evolution of reinforcing traditional materials with various elements such that the resulting composite material would benefit from the synergistic effect of both the reinforcement and the matrix. The rudimentary principles of composite materials dates back in time, from vintage buildings with straw reinforced clay to present day structures using reinforced concrete [1]. This makes it possible for the different constituents to work in synergy in such a complementary manner as to subdue the limitations of each constituent [2]. Aluminium and its alloys

41

Review Article 2: INFLUENCE OF SINTERING METHODS ON THE MECHANICAL PROPERTIES OF ALUMINIUM NANOCOMPOSITES REINFORCED WITH CARBONACEOUS COMPOUNDS: A REVIEW

Mary A. Awotunde, Adewale O. Adegbenjo, Babatunde A. Obadele, Moses Okoro, Brendon M. Shongwe, Peter A. Olubambi, 2019. Journal of Materials Research and Technology, pp. 2432–2449

Abstract

This paper succinctly reviews from the corpus of literature the reinforcement of aluminium with carbonaceous nanocompounds (CNTs, GNPs, graphenes etc), with particular emphasis on the strength and ductility of the resulting composites based on the utilized fabrication routes. Owing to the unique intrinsic properties of these carbonaceous nanocompounds, they have been widely reported as ideal reinforcement materials for aluminium and its compounds. Significant amount of work has been published on the use of solid-state sintering as a novel route for the incorporation of these nanocompounds in aluminium matrices. This paper therefore aims to review some relevant aspects of the fabrication processes of these aluminium based composites such as (i) effects of the sintering routes and parameters on the resulting properties of the composites; (ii) the effect of dispersion techniques on the resulting properties of the composites; (iii) the strength-ductility trade-off in the reinforced composites; and (iv) the intermetallics formed between the carbonaceous nanocompounds and aluminium.

Keywords – aluminium; nanocomposites; sintering; carbonaceous compounds; intermetallics

1. Introduction

Recent technological demands require a wide (and sometimes conflicting) range of properties unachievable in single traditional materials. This birthed the evolution of reinforcing traditional materials with various elements such that the resulting composite material would benefit from the synergistic effect of both the reinforcement and the matrix. The rudimentary principles of composite materials dates back in time, from vintage buildings with straw reinforced clay to present day structures using reinforced concrete [1]. This makes it possible for the different constituents to work in synergy in such a complementary manner as to subdue the limitations of each constituent [2]. Aluminium and its alloys have been extensively investigated owing to their light weight [3], high specific strength [4], good corrosion resistance [5], good thermal conductivity [6], low electrical resistivity [7], high damping capacity [8] and low cost [9].

These unique properties make them ideal choices for automotive, aerospace and marine industries [10]. However, despite these excellent properties, the low strength of aluminium restricts its use especially for structural applications [11].

To overcome the strength limitation of aluminium and its alloys, the addition of silicon carbide [12], alumina [13, 14], aluminium nitride [15], tungsten carbide [16], silicon nitride [17], titanium carbide [18], silica [19], boron carbide [20, 21], titanium dioxide [22], graphite [23-25], zirconium boride [26], tantalum carbide [27] have been reported. Superior properties of these materials such as refractoriness, high hardness, high compressive strength and wear resistance, make them appropriate reinforcements in aluminium matrices [28-30]. The high cost of some of these ceramics especially in developed countries led to the incorporation of industrial and agro waste [31] such as fly ash, coconut ash, bagasse ash, rice husk ash [32-34], that have shown huge promise as alternative reinforcements. Though they seem to possess inferior properties compared to the reinforcements offered by conventional ceramics [35, 36] they have been successfully used as hybrid reinforcements alongside conventional ceramics.

2. Carbonaceous compounds

Recent advances in nanotechnology have emerged with numerous novel nanomaterials possessing extraordinary properties. Owing to the success of carbon nanotubes (CNTs) additions in polymer and ceramic matrices [37], CNTs and other carbon allotropes have been regarded as ideal reinforcements for aluminium matrices and recent research on this has grown enormously. Efforts have been largely focused on investigating their contribution to the enhancement of the mechanical performance of the composites. The excellent strength, wear properties and thermal conductivities of CNTs, graphene nanoplatelets, graphene oxides, graphene nano fibers and graphene nanosheets are obvious reasons for the incorporation of these nanomaterials in different matrices [38, 39].

Carbon based reinforcements are ideal reinforcement candidates due to the remarkable combination of their properties. Carbon reinforcements present morphologically and dimensionally in different reinforcing phases - carbon nanotubes (CNT) (1D), graphene (Gr) (2D), and carbon fibre (3D) [40]. These graphitic structured materials have recently been among the more widely researched materials [41], due to their exceptional mechanical [42], thermal, [43-45], electrical [46] and tribological behaviours [41]. Their versatility extends to multidisciplinary applications like energy conversions, super capacitors and photocatalysis [47]. Moreover, improved manufacturing techniques have made these materials more

43

economically friendly [48].

With Young's modulus of ~1TPa, tensile strength of ~130 GPa and thermal conductivity of ~3000W/M/K [49], these carbon allotropes make excellent reinforcements in composites [50]. Furthermore, these materials have the added advantage of undergoing plastic deformation under severe bending stress conditions without failing prematurely [51].

Discovery of exceptional materials are however, not sufficient in itself, as appropriate processing routes also have to be developed to incorporate these 'super' reinforcements in various matrices for the realization of the expected enhanced mechanical properties of the composites. Fabrication processes may be mostly categorised into solid and liquid state processes [52]. Some solid state fabrication methods include: diffusion bonding [53], electroplating [54], spray deposition [55], immersion plating [56], chemical vapour deposition [57], physical vapour deposition [58]. While some of the liquid state processes are: stir casting [59] squeeze casting [60], compo-casting [61], pressureless infiltration [62], ultrasound assisted solidification [63], vortex process [64], sol-gel synthesis [65], laser deposition [66] and powder metallurgy [67].

3. Powder metallurgy (PM)

Powder metallurgy can be described simply as the manufacture of components from powder materials. The process starts with powder mixing and or milling, followed by compaction and sintering of the compacted powders to achieve the least possible porosities or the highest possible density. PM through solid-state sintering is particularly suitable for composites fabrication due to its flexibility to synthesize a wide variety of compositions and to produce intricate shapes with near net accuracy [68]. This simplicity places it clearly ahead of many other manufacturing processes with more complicated processes. In literature, a considerable amount of work has been devoted to producing aluminium matrix composites by using powder metallurgy [69] [41]. In addition to the low temperatures employed, the solid-state mixing techniques lend themselves easily to the incorporation of these nano reinforcements in metal matrices [3]. Moreover, the interaction between matrix and reinforcements can be avoided because of lower processing temperatures usually associated with PM methods [70]. PM produces a better interface and more uniform distribution of reinforcement materials within the matrix, leading to improved mechanical properties [9]. It also simplifies the production of complex engineering components [71] and provides excellent control over microstructure, including size, morphology and volume fraction of matrix and reinforcement [72], [73]. PM

routes have proven their mettle as they offer several advantages over traditional casting processes, hence they have been the preferred route for most researchers especially for the incorporation of these carbon allotropes [3], [74], [75], [76].

3.1 Sintering techniques

In simple terms, sintering can be described as the application of heat and pressure. The major focus during sintering processes is to achieve full or maximum densification, hence sintering parameters like temperature, pressure and holding time are varied till this is achieved. Extensive efforts have been carried out on the development of sintering methods for full densification of bulk composites. Since the pores in the material significantly affect the mechanical properties, the reduction of porosity can and will improve the performances of the resulting composites [77]. Owing to variations in the sintering techniques available, differing properties are subsequently imparted in the resulting bulk composites.

3.1.1 Conventional Sintering

This is the simplest and most traditional method for producing metal matrix CNT composite compacts. Conventional sintering was one of the earliest techniques utilized to synthesize metal composites, but limited success was achieved due to the poor densities of the resulting structures. In cases where nanomaterials like CNTs are incorporated into the metal matrices, post-sintering operations like hot pressing or extrusion of the product might be necessary to enhance densification. In the conventional heating method, slow heating rates and long dwell times during a sintering cycle usually result in exaggerated grain growth phenomenon [9]. In this method, the specimen is heated using heating elements like silicon rods and the heat is then transferred to the specimen either by conduction, convection or radiation. This poses the risk of non-uniform heating and creation of thermal gradients, which in turn results in internal stresses in the specimen. This is because part of the volumetric heat energy is lost by dissipation from surfaces, leaving the centre of the specimen slightly hotter than the surfaces [78]. In Gao et al [79] graphene oxide and aluminium powders were sintered at 600°C for 1h under a pressure of 25 MPa to prepare Gr/Al composites. At 0.3 wt % CNT, the ultimate tensile strength (UTS) of the composite reaches the maximum which is about 30% higher than that of pure Al prepared with the same process. The remarkable strengthening was attributed to the homogeneous dispersion of graphene in Al matrix. The enhanced tensile properties of the Gr/Al

composites were explained by the efficient load transfer of graphene in Al matrix. During electrostatic self-assembly, the large sizes of the graphene are protected, so the contact areas between graphene and Al matrix were enhanced, resulting in the increase of load transfer sites.

3.1.2 Microwave Sintering

Microwave sintering with volumetric heating mechanism offers a number of advantages over conventional sintering. These advantages include enhanced diffusion process, high heating rates, shorter processing times, and improvement of microstructures. Microwave sintering utilizes only a fraction of the time required in conventional sintering. In microwave heating, the rate of grain growth is reduced, due to a decrease in sintering time. Therefore, samples sintered in a microwave process obtain a uniform microstructure with smaller grains and consequently, a higher mechanical strength as compared to conventional sintering [80].

Initially there were misconceptions that metals reflect microwaves, resulting in sparks, and this constrained the use of microwave sintering to ceramics and their composites [78]. However, it was shown by Walkiewicz et al [81] that the sparking phenomena applied to only bulk metals. In powder form, metals tend to absorb microwaves and can thus be heated significantly [82].

Saheb [83] compared microwave sintering to spark plasma sintering of aluminium alloys Al 2124 and 6061 at same sintering temperatures and holding times. Microstructures obtained from the SPSed samples showed that increase of sintering temperature from 450°C to 500°C improved the densification, and dramatically reduced the size and the number of pores. Higher sintering temperatures to 550°C did not show any further improvement on densification. The complete densification - total elimination of pores however, was not achieved in the microwave sintered alloys as achieved in the SPSed samples as can be seen from Figs. 1 & 2. Apparently, obtaining similar results using microwave energy even under similar processing conditions was not possible, due to the differing mechanisms of sintering. For spark plasma and microwave sintering, increasing the sintering temperature from 400 to 450°C increases the microhardness from 56.81 to 66.31 HV and 40.23 to 45.75 HV, respectively, while a further increase of temperature to 500°C increases the microhardness to 70.16 HV for spark plasma sintering and decreases the microhardness to 32.27 HV for microwave sintering. The same trend was observed for the Al 2124. The increase of microhardness with the increase of sintering temperature followed the same trend as the increase of density. This was due to the elimination of pores during sintering and possibly precipitation of fine particles [84]. The observed decrease in microhardness with further increase in sintering temperature to 500°C for the microwave

sintering was however believed to be as a result of grain growth of the α-aluminium phase.
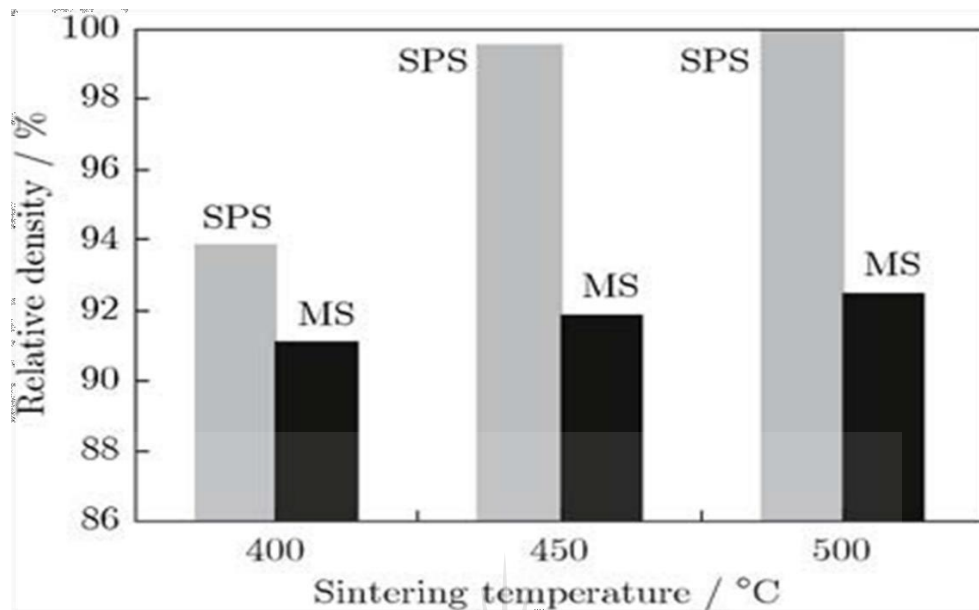
Fig. 1 - Relative density of spark plasma and microwave sintered Al2124 alloy - Saheb et al [83].

3.1.3 Hot Pressing (HP) technique

In hot pressing, powder mixtures or the pressed compact are subjected to high temperature while being pressed in a die. The applied temperature and pressure result in easy deformation through creep and material transfer, and these help in achieving high densities. The heating could be done by electrical resistance heating, induction heating, or radiation. The holding time is critical since grain coarsening would occur for long heating periods. A hot press can also be used for near net shape manufacturing of components by low-pressure forging. Hot pressing has the advantage of producing high density composites due to the concurrent action of temperature and pressure. To prevent oxidation of the composites, the operation has to be carried out in vacuum and this can be expensive due to the need for insulation at high temperatures. The time required during hot pressing to attain useful densities is approximately 1 h in most studies [85], [86].
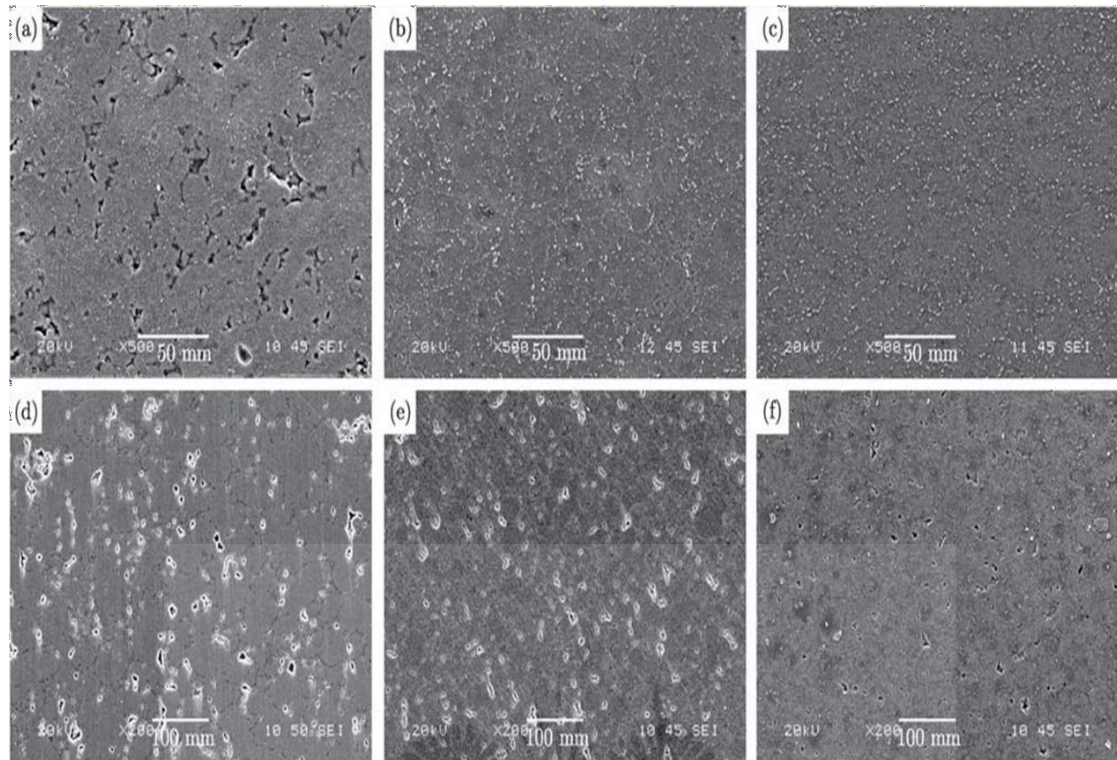
Fig. 2 - SEM micrographs of Al2124 alloy: (a) SPS, 400°C; (b) SPS, 450°C; (c) SPS, 500°C; (d) MS, 400°C; (e) MS, 450°C; (f) MS, 500°C. – Saheb et al [83].

Kim et al [87] compared the hot pressing method to the SPS method in aluminiumcomposites with CNT contents of 1, 3 and 5 wt %. Results show that the SPS method produced a greater hardness than the HP method. It was suggested that the composites fabricated with the HP method were exposed to a high temperature for a longer duration of dwell time that grain growth occurred. In contrast, the SPS method did not produce composites with particle growth because of the rapid temperature rise and fast sintering by self-generation of heat [88]. Maximum stress was also found to be greater in the SPSed samples as compared to the HPed composites. Maximum stress indicates the stress point at which crack initiates. In terms of the amount of wear, composites fabricated by the SPS method had also exhibited reduced wear properties than fabricated composite by the HP method.

Long sintering times are most likely to stimulate thermally activated diffusion-controlled grain growth. If occurring, this phenomenon adversely affects the mechanical properties and renders the achievement of superior characteristics impossible [89]. On the other hand, high sintering temperatures can cause thermal damage of the CNTs and thus promote undesirable interfacial

48

reaction between the Al matrix and the CNTs [90]. Houasaer et al [91] in his work comparing the hot press (HP) technique with the spark plasma sintering (SPS), showed that there was interfacial reaction between the aluminium matrix and the CNTs during the HP method which was not observed in the SPS method. The authors explained that the duration of heating in the sintering process plays a major role in interfacial reactions and growth of intermetallics between the matrix and reinforcement.

3.1.4 Hot Isostatic Pressing

In case of HIP, the pressure is applied uniformly from all directions by using a gaseous or molten salt medium. This leads to uniform densification in all directions and ensures isotropic properties.

Yan et al [92] combined graphene nanoflakes (GNFs) in aluminium alloy containing 1.5% Cu and 3.9% Mg elements. Hot isostatic pressing (HIP) was carried out at 480°C and 110 MPa for 2h. Afterwards, the 40mm diameter billet was preheated at 450°C for 1h in a stainless steel mold and then hot extruded into 12mm diameter rods. Results show that with the addition of only 0.5 wt% GNFs, the yield strength was increased by nearly 50%, from 214 to 319 MPa and the tensile strength increased from 373 MPa to 467MPa. More remarkable was the fact that this increase in strength was achieved without causing a loss of ductility in the resulting composite. These results demonstrate that graphene nanoflakes (GNFs) have a great potential as an ideal reinforcement for aluminium matrix composites. They attributed the excellent ductility properties to the multiple wrinkled structures of GNFs.

3.1.5 Spark Plasma Sintering

Spark plasma sintering (SPS), also known as electric field assisted sintering (EFAS), plasma assisted sintering (PAS), and pulsed electric current sintering (PECS), is a variation of hot pressing in which the heat source is a pulsed DC current that is passed through the die or the powders (depending on whether the powder is electrically conducting) during consolidation. Spark discharges at the particle interfaces are believed to produce rapid heating, which enhances the sintering rate. The heating rates are quite high compared to hot pressing and can be up to 1000 Ks^{-1}. Efficient densification of powder can be achieved in this process through spark impact pressure, joule heating, and electrical field diffusion [93], [94]. This method is, generally, suitable for consolidation of nano powders, without allowing sufficient time for grain

growth. Compared to conventional sintering and hot pressing, SPS definitely is a promising method for obtaining high-density MM-Carbon compound compacts. The short sintering time is also favourable in ensuring minimal or no reaction between CNT and metal matrix. Spark plasma sintering over the past decade has been extensively used in consolidating a wide range of materials including metallic alloy powders. This novel, non-conventional sintering method has proven to be advantageous offering full densification of materials owing to high heating rates, low sintering temperatures, and short sintering cycles over conventional sintering methods [1].

There is no general consensus on what mechanisms are activated during the sintering of initial powders in SPS, but some researchers have striven to propose theories based on their experimental results or assumptions. It is predicted that three mechanisms are active: (i) activation by pulsed current, (ii) resistance sintering (heating through electrical current passage) and (iii) pressure application [95], [96], [97]. However, overheating on the particles surface which leads to localized melting in particle contacts has been the popularly believed mechanism [98]. SPS features energy saving and low power consumption in comparison to the conventional sintering techniques and is also reported that this process can lead to near full densification [99], [100]. In this method, the starting powders are poured into a graphite mold and the sintering process is performed simultaneously with applied external pressure and electrical current [89], [101].
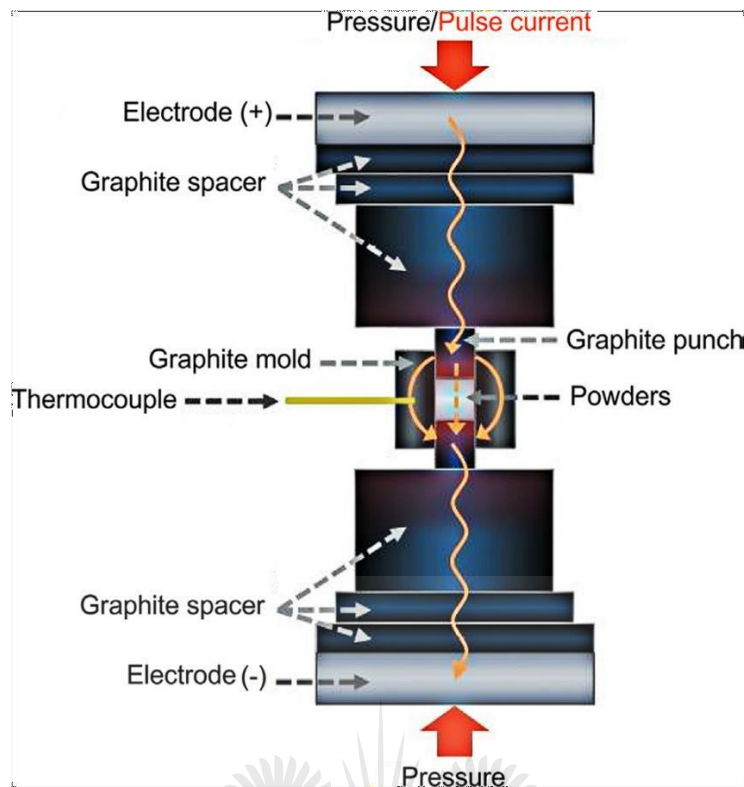
Fig. 3 – A schematic view of the SPS apparatus and its components - Nishikata et al [101].

However, high costs and limited sample geometries are the main disadvantages of SPS and HP [102] and they are practically inappropriate for manufacturing nanocomposites for large scale production of various geometries having satisfactory performance at affordable prices [103].

Bisht et al [104] successfully synthesized Al-GNP (graphene nanoplatelets) composite, with 21.4% improvement in strength and hardness, by spark plasma sintering route (SPS). He observed that SPS yielded high relative density of the structures, without affecting the intrinsic structure of GNPs [105]. Authors recorded relative density of 99.8% in the Al-1wt% composite which yielded the best mechanical properties. Dense and clean interface between GNP and Al, without interfacial reaction product. Authors attributed this to the short sintering time availed by the SPS technique.

Table 1 – Summary of merits and demerits of different sintering methods

Sintering methods	Method Description	Merits	Demerits
Conventional sintering [9, 76]	Heating is through conduction, convection or radiation. Slow heating rates and long dwell times.	Simplicity of operation	Poor density of bulk compacts, coarse grains due to grain growth. Non-uniform heating resulting in thermal gradients across the composite.
Microwave sintering [78]	Volumetric heating mechanism	Higher heating rates and shorter sintering times as compared to conventional sintering, leading to better mechanical properties	Poor densification as compared to novel sintering techniques like spark plasma sintering
Hot press sintering [85]	Heating is done by electrical resistance, induction or radiation	Simultaneous application of heat and pressure leading to better densification	Long dwell times which poses the risk of grain coarsening and interfacial reactions which may be undesirable
Hot isostatic pressing	Simultaneous application of heat	Uniform densification of the	Long dwell times

[90]	and uniform pressure from all directions	composite resulting in isotropic properties	
Spark plasma sintering [102]	Active mechanisms are: activation by pulsed current, resistance heating and applied Pressure	Highest heating rates and lowest sintering times. Grain growth is prevented resulting in highly dense, fine grained structures yielding excellent mechanical properties.	High cost

3.2 Effect of sintering temperature

Guo et al [90] investigated the effect of SPS sintering temperature on the mechanical properties of AMCs using two different sintering temperatures ($590^{o}C$ and $630^{o}C$) and CNT content (0.75 and 1.0 wt %). Results showed that the composite which contained 0.75 % CNTs and sintered at $590^{o}C$ had the lesser yield strength (YS), ultimate tensile strength (UTS) and elongation (EL). No matter the content of the CNTs, the mechanical properties of the composites were significantly improved by increasing the sintering temperature from 590°C to 630°C, including the strength and ductility. Thus indicating that the SPS sintering temperature plays a significant role in enhancing the mechanical properties of the composites. Higher sintering temperature contributes to the creation of the electric field generated among the particles and excites high-temperature plasmas under the action of pulse current, which facilitates a cleaning effect on the surface of particles, leading to the elimination of the barriers of atom diffusion. With externally applied pressure, the positive effects generated by higher temperature can accelerate the rearrangement of particles and lead to a higher density. The composite with low content of the CNTs indicates less Al-CNTs interface and Al atom diffusion barriers, so Al atoms can diffuse readily and fill the interstices between the adjacent particles during the sintering process.

Clustered CNTs act as a diffusion barrier during sintering process [106], and consequently reducing the sinterability of the powders.
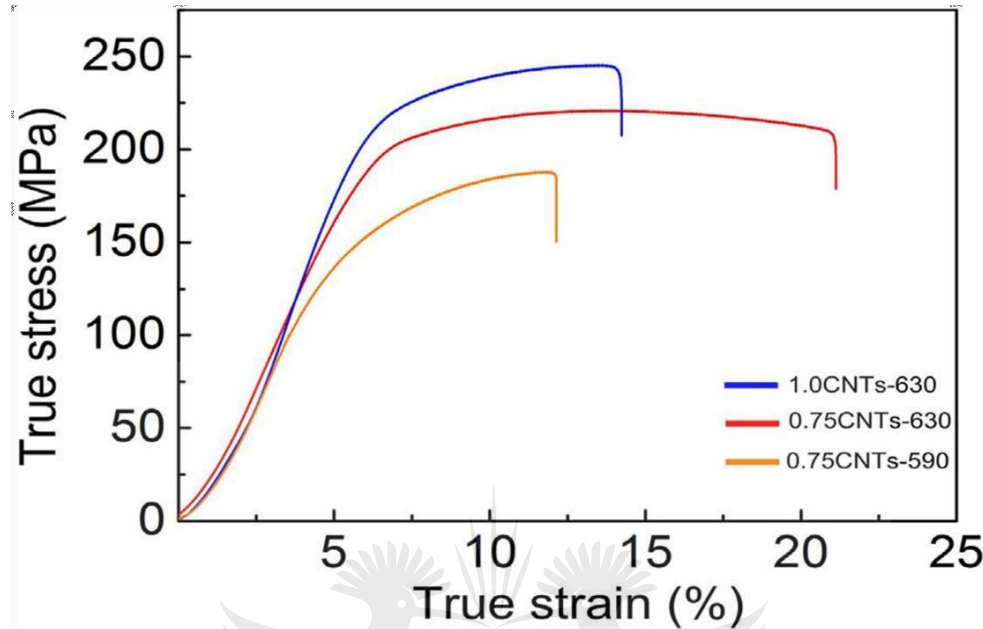
Fig. 4 – The effect of sintering temperature on mechanical properties. The tensile stress-strain curves of the rolled composites - Guo et al, 2017 [90].

Saheb et al [83] observed that at constant sintering time of 20 min, the sintering temperature had an important influence on the densification of samples, due to the fact that sintering is a thermally activated process controlled mainly by diffusion [84]. Therefore, the higher the sintering temperature, the higher the diffusion rate, and consequently the less the pores in the bulk composite. The yield strength (YS), ultimate tensile strength (UTS) and elongation of the CNT/Al composite sintered at 800 K were measured to be 127 MPa, 186 MPa and 11.2%, respectively. As temperature is increased to 850 and 900 K respectively, both strength and ductility of CNT/Al composites improved progressively. YS, UTS and elongation of the composite sintered at 900 K were respectively 150 MPa, 212 MPa and 20.4%, translating to 18%, 14% and 82% improvement respectively in comparison with those of the composite sintered at 800 K.

3.3 Post sintering operations

Post deformation of sintered compacts can further enhance the density of the bulk composites [107], [108]. This approach has been used mainly for Al-based composites. Hot extrusion, equal channel angular extrusion (ECAE), and hot/cold rolling have been widely employed as deformation techniques. Hot extrusion is the most commonly used process and perhaps, most preferred [109] for deformation processing of metal matrix (MM) - CNT composites [85] [92]. In hot extrusion, the sintered or pressed compact is heated to the required temperature and then forced through a die typically conical in shape maintained at the high temperature. Inside the die, the compact undergoes a gradual reduction in area in the conical portion due to the application of shear stresses. The ratio of the area of the material at the entry to the exit is known as the extrusion ratio. Yan et al [92] employed hot extrusion to achieve GNF alignment in the Al matrix. ECAE is a recently developed technique in which a material is extruded through a die in which the extrusion ratio is 1. However, the material has to pass through a bent region. A lot of shear deformation is induced in the material. There is a considerable grain refinement due to this thermo-mechanical treatment. Hot rolling is believed to improve the properties by improving the density and dispersion of CNTs by breaking CNT clusters.

For example, Chen et al [110] used hot extrusion as a post-sintering measure to enhance the bonding strength between the Al powder particles and the dispersion uniformity of the CNTs in the Al matrix. The traditional trade-off tendency between strength and ductility in metal based composites was evaded in Al/CNTs composites owing to concurrent improvement of Al–Al grains and CNT–Al interfacial bonding by hot extrusion. Zare et al, [107], [108] applied equal channel angular pressing (ECAP) as the post-sintering processing to consolidate the fabricated materials. The well-densified composites with only 2 vol% CNTs after eight ECAP passes exhibited an approximately 30% increase in the yield strength compared to the pure Al samples. In general, ECAP process has two channels with the same cross - sectional area. Samples are usually circular or square according to the dimensions of the channels. After applying the appropriate lubricants, the sample is placed in the inlet channel and extruded through the outlet channel using a punch under pressure. The deformation mode in the ECAP process is a simple shear.

Rashad et al [111] did not observe significant difference in experimental densities before and after extrusion, which they attributed to the low extrusion ratio (5:1). Though not much significant difference was observed in the densities, the hardness values increased with increase in GNPs weight contents in aluminium matrix. The increased hardness of composite materials

could be due to presence of reinforcement particles possessing high strength which offered high constraint during indentations. Furthermore, the hardness of pure aluminium and its composites increased after extrusion process. This confirmed that the extrusion process played a vital role by minimizing the voids and cavities in sintered materials, and this led to increase in mechanical properties of composites. Expectedly, a reduction of voids and cavities ought to lead to an increased densification of the composites which was not observed here.

In particular, it was found that a combination of spark plasma sintering (SPS) and hot-extrusion [110], [112], [113] was effective in fabricating high-performance composites because of the high density, fine grains and good CNT alignment [114].

Generally, for SPSed AMCs, it is difficult to obtain a strong bonding strength between the Al powder particles and completely eliminate the residual pores due to the short diffusion time. Hence, it may be necessary to strengthen the interfacial bonding and enhance the densification by post deformation [90]. Guo et al [90] followed up with hot rolling process with 5 passes after spark plasma sintering to enhance densification and hardness as can be seen in Fig. 5. Results showed that hot rolling can further densify the composites sintered at 630°C, since the residual pores were almost eliminated after the hot rolling process. It can be seen that the hot rolling can significantly improve the density of all the fabricated composites and the difference in density among the three composites is significantly decreased, due to the reduction of residual pores by the plastic deformation during hot rolling.
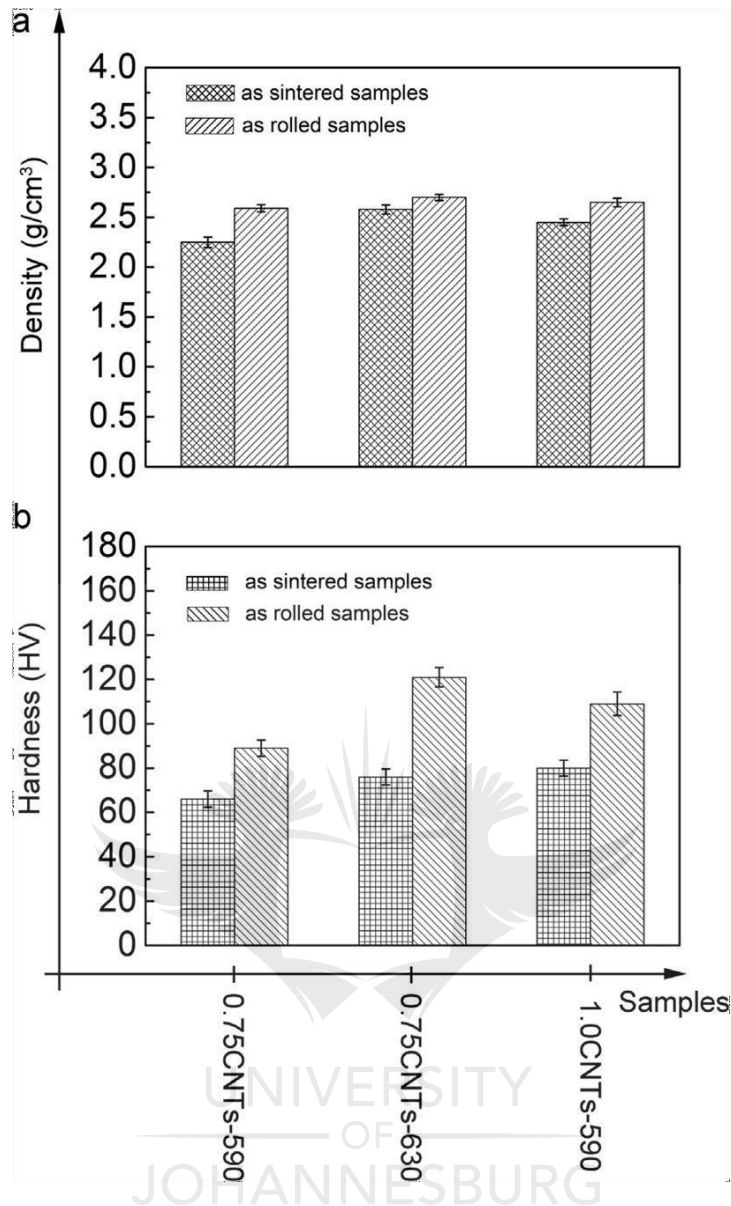
Fig. 5 - The effect of post sintering operations on the density and hardness of AMCs (a) The density and (b) hardness of the fabricated composites – Guo et al [90].

By combination of SPS and hot-extrusion, authors have achieved high densities over 99% [110]. A large extrusion ratio of 37 was applied which was helpful to improve the bonding conditions. It is because a large extrusion ratio brings a higher degree of material deformation. Larger deformation leads to better physical contact between grain boundaries and between CNT and Al, which are beneficial to improve the bonding conditions and mechanical properties of CNT/Al composites. The results suggest that high-energy consolidation conditions may be favourable to achieve optimal composite structures and excellent mechanical performances of

CNT-reinforced MMCs by powder metallurgy.

4. Effects of dispersion methods

To successfully achieve the improvement in metal composites reinforced with these carbonaceous compounds, uniform dispersion is undoubtedly the singular most important requirement in AMCs. Different dispersion methods lead to differing degrees of dispersion even with the same combination of matrix and reinforcements hence, reports from literature show differing results even with similar reinforcement and matrix combinations. Ahmad et al [86] and Bocanegra-Bernala [102] both incorporated CNTs in an Al_2O_3 matrix but achieved different results. While Ahmad et al [86] reported improvement in fracture toughness of 94% over monolithic Al_2O_3, Bocanegra-Bernala [102] reported a 40% decrease in his study. Bartolucci et al [115] also reported a decrease in mechanical properties with additions of 1 wt % of GNPs and CNTs respectively. These may be attributed to the differing processing routes, hence the intrinsic attributes of the reinforcements are not sufficient in determining the resulting mechanical properties of AMCs as processing routes obviously play a crucial role as well.

The final performance of a metal matrix composite depend upon three key factors consisting the matrix, the reinforcement, and the matrix/reinforcement interface [68] with the interface strongly dependent on the 'dispersibility' of the reinforcement in the matrix. In the past, the role of matrices was only associated with holding reinforcements securely. It is important to understand the roles of the matrix, the properties of the reinforcement and the ensuing interaction between the matrix and the reinforcement. The interface or the region between the matrix and the reinforcement actually plays a key role in stress transfer between the matrix and the reinforcement. If the bonding between the two is weak; which can occur due to poor wettability issues or lack of interaction in-between (and this is consistent with carbon allotrope additions and metal matrices); the final composite will have poor mechanical properties [2].

The dispersion of CNTs in the powder mixture is so crucial because subsequent processing stages like compaction and sintering will not improve the dispersion. Outstanding CNT clusters remaining in the powder mixture will ultimately still be present in the final component [1].

Achieving uniform dispersion of these carbonaceous compounds in the metal matrix has been the major challenge for researchers till date. Few researchers have been able to successfully disperse these allotropes owing to their high aspect ratio and strong van der waals forces that keep them entangled in clusters. To solve this agglomeration problem, traditional and novel techniques such as nano-scale dispersion [116], high energy ball milling [117], in-situ grown method [118], flake PM [119], solution coating [110], molecular level mixing [120], and cryomilling [121] have all been developed in the past decade.

4.1 Ball milling

So far, the ball-milling process has been the most widely used method of dispersing carbon allotropes in metallic matrices [3], [11], [92]. Usually, CNTs would remain to be clustered in the early stage of ball milling and this short term milling is inadequate for good interfacial bonding [122] whereas, the morphology and structural integrity of these nanomaterials are often damaged with prolonged ball milling and this triggers interfacial reactions during milling, which may cause a negative strengthening effect in the reinforced nanocomposites. Poirier et al [123] and Chen et al [112] however, reiterate that severe CNT structure damage, such as CNT shortening and crystal-structure change, are good sacrifices to make in exchange for the rewards of homogenous CNT dispersion.

Alrasheedi [72] reinforced Aluminium with 2.5 and 5% volume fractions of Graphene Nano Sheets (GNS) by mixing using a milling machine at a constant speed of 250 rpm for 15 minutes which seemed to be inadequate for uniform dispersion of the reinforcement in the aluminium matrix. Results showed that the addition of GNSs to aluminium decreased the relative density of the specimens, confirming the presence of GNSs promoted the porosity formation if still in clustered state.

Bastwros et al [41] incorporated graphene in an Al6061 matrix after ball milling of the powders. Results show that as milling time increased from 60 to 90 minutes, flexural strengths increased significantly to 760 MPa and 800 MPa, respectively with strength increase of 47% and 34%. The increase in the UTS of the composites milled for 90 minutes was attributed to more dispersion of the graphenes in the matrix. Esawi et al [117] observed that the milling parameters are strong indicators to the mechanical properties of the resulting composites. Longer milling times of 3hours yielded higher strength values due to apparently better dispersion, as compared to values obtained after 30mins of milling. However, high energy ball milling apparently causes

unavoidable damage on the delicate structures of these nano materials.

4.2 Nano scale dispersion

Noguchi et al [116] developed the Nano scale Dispersion route for improvement of CNT dispersion. A sevenfold increase in compressive yield strength was reported with the addition of just 1.6 vol % CNTs. This remarkable strength was attributed to the uniform dispersion of the nanotubes using the NSD process. Though this process was quite complicated, the results were well worth it. The authors attribute the remarkable improvement to the novel dispersion method which improved the wettability between the aluminium and CNTs.

4.3 Flake powder metallurgy

Jiang et al [119] explored the flake powder metallurgy (flake PM) route in order to overcome the challenge of non-uniform distribution of carbon nanotubes (CNTs) in CNT/Al composites. This route solved the poor wettabillity issue between CNTs and aluminium powders by using slurry blending. By changing spherical Al powders to nanoflakes and surface modifying them with a polyvinyl alcohol hydrosol, flake PM produced homogenously distributed CNTs on the aluminium. This route also preserved the structural integrity of the CNTs as they were protected from impact forces of milling balls as compared to ball milling processes. Hence, a composite with high tensile strength of 435 MPa and good combination of properties was produced and authors attribute these to the minimally damaged and uniformly distributed CNTs in the aluminium matrix.

5. Effect of reinforcement content

At higher sintering temperatures, the diffusion between the matrix and reinforcement particle is easier, resulting in better sinterability of materials [90], [111]. However, Bisht et al [104] reported an optimum volume fraction of 1.0 wt % GNPs above which the mechanical properties were not enhanced owing to less sinterability of the composites due to the difficulty in dispersing higher volume fraction of GNPs.

Gao et al [79] observed a limiting volume fraction of graphene in his study at 0.3 wt % which yielded UTS of ~110 MPa, which was about 30% higher than that of unreinforced Al ~86 MPa. Results showed that in the 0.5 wt. % Gr/Al composite, a lot of graphene was located at the boundaries of the Al grains, making cracks to form preferentially in graphene and extend to the Al matrix during tension, decreasing the tensile properties of the Gr/Al composite. A shift in the fracture mechanism was also observed from a typical dimpled fracture surface for pure Al to flat and not so dimpled surface as the graphene content increased as can be seen in Fig. 6.
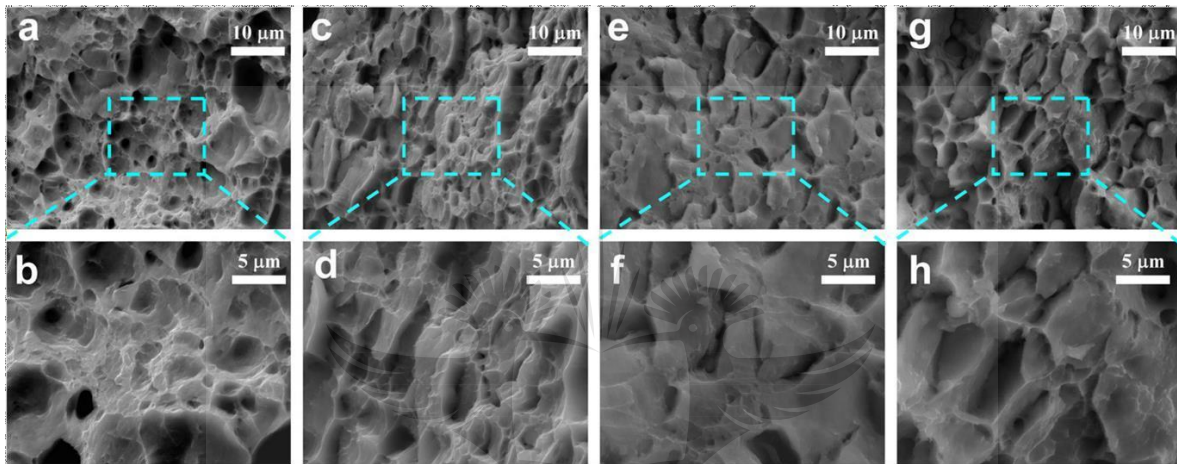
Fig. 6 –Tensile fractographs of the Gr/Al composites with different graphene contents. (a and b) pure Al, (c and d) 0.1 wt.% Gr/Al, (e and f) 0.3 wt.% Gr/Al, and (g and h) 0.5 wt.% Gr/Al - Gao et al, 2016 [79].

Both Clegg [124] and Wang et al [125] explained that with a little CNT content, the hardness of the composite increases because the CNTs fill the microvoids of the aluminium particles. However, with addition of high CNT, the excess CNTs that remain after filling the microvoids form agglomerates with the aluminium particles. This conglomeration interrupts the sintering and causes defects. The effects of this could be as bad as porosity effects [109], [126]. Apoint is therefore reached where, as the CNT content increases, irrespective of the intrinsic strengthening properties of the reinforcement, the composite strength begins to decrease as shown in Fig. 7.
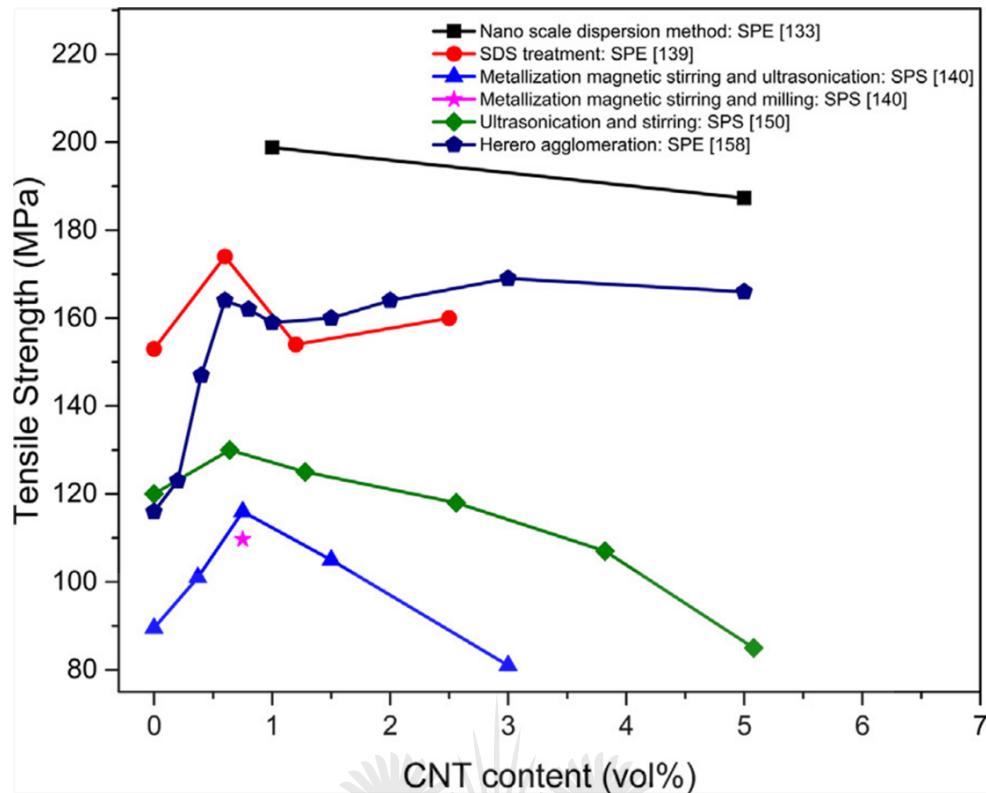
Fig. 7 – The variation of tensile strength as a function of CNT content for SPSed CNT-Al nanocomposites processed by different mixing methods - Kwon and Kawasaki [127].

Esawi et al [3] investigated the mechanical properties of CNT reinforced Al composites. They observed that dispersion of CNT became progressively difficult above 2% volume fraction addition. Mechanical properties were observed to improve significantly with CNT addition with the most significant obtained at 2% CNT addition (tensile strength of ~260MPa). Higher additions did not yield further enhancements as expected. This is owing to the agglomeration of CNTs at such high additions [121].

Guo et al [90] observed an agglomeration of CNTs with increasing content from 0.75 – 1.0 wt % and this led to a reduction in the mechanical properties of the AMCs. This shows that the agglomeration of the CNTs in the 1.0CNTs-630 composite weakens the bonding between the Al powder particles and thus decreases the ductility of the AMCs as seen in Fig. 5.

Rashad et al [111] observed an enhancement in the UTS and failure strain of aluminium composites with 0.25wt% additions. But in contrast, the effect of higher additions of 0.5 and 1.0 wt % was detrimental to the mechanical properties. Both tensile strength and failure strain decreased with the increase in GNPs additions. This is due to overlapping of GNPs with each other and due to strong pi–pi attractions between graphene sheets.

6. The ductility/strength trade-off

The improvements in the strength properties seem to be achieved at the expense of ductility and fracture toughness of reinforced AMCs. Numerous reports exist in literature of enhanced tensile strength achieved by the reinforcement of aluminium with CNT accompanied by a reduction in ductility of AMCs [119], [122], [11], [79], [128]. Despite intense investigations of aluminium matrix composites (AMCs), achieving a balanced combination of strength and toughness has been a daunting task for researches till date, as there seem to be a trade-off between the two very essential properties [110], [129]. This is obviously a hindrance to their practical applications as these are crucial requirements since ductility is needed for formability while adequate fracture toughness is required for the prevention of catastrophic brittle failures in service. Key requirements to achieving balanced mechanical properties of AMCs are also hinged on uniform dispersion of the CNTs in the matrix and good interfacial bonding between the reinforcement and the matrix [110], [109].

Though it has been reported that these nanomaterials could be incorporated into brittle materials to generate toughened composites that would be suitable for advanced engineering applications [99]. However, a strength-ductility trade-off has been severally reported in these composites. Saheb et al [83] displayed this trade-off tendency. In their work, with the elongation of pure Al increasing from 21.1 to 24.1% came the reduction of UTS from 172 to 166 MPa as sintering temperature is increased from 800 to 900 K. The trade-off tendency in pure metals is due to the fact that both strength and ductility are mainly determined by one factor-the level of difficulty in dislocation movement [130].

He et al [118] fabricated high strength CNT/Al composites using the in-situ grown CNT method. Nevertheless, while the strength increased up to more than 200MPa (216–398 MPa), the ductility decreased significantly with fracture elongation of 0.7–4.7%. Najimi and Shahverdi [128] using a two stage milling method, achieved a remarkable tensile strength of 538MPa with only 1.5 wt % CNT addition but with a ductility of ~0.05.

Aggressive dispersion methods like high energy ball milling tend to yield high strength values but are usually accompanied by very little ductility owing to the severe damage of the nano-reinforcements. Morsi and Esawi [131] reported that prolonged ball milling improved the disentanglement and dispersion of CNTs, but also compromised their structures.

6.1 Two stage milling

To overcome this balance dilemma, Xu et al [129] employed a two stage milling process, precisely an 8 h low energy ball milling at 135 rpm followed by a 1 h high energy ball milling process at 270 rpm. Results showed that with 1.5 wt. % CNT reinforcement, the AMCs exhibited a yield strength of 326 MPa, an ultimate tensile strength of 376 MPa and a total elongation of 12.4%. The enhanced properties could be explained by the dispersion method which utilized flake powder mechanism and then a short term high speed ball milling (HSBM), to obtain cold welded particles with good CNT/Al bonding, without too much structural damage to CNTs. Owing to this balance between the uniform dispersion, interfacial bonding and structural integrity of CNTs, the desired balance between strength and ductility was achieved.

6.2 Dual matrix approach

Salama et al [132] experimented with a dual matrix approach. Typical single matrix (SM) was produced via dispersing CNTs in a pure aluminium matrix using HEBM of 400rpm for 2 h. Then the novel dual matrix (DM) was obtained by embedding the pre-processed SM powders into a secondary matrix of pure aluminium using HEBM for 30 minutes and 60 minutes, while keeping the total CNT content strictly to 1 wt % and 2.5 wt % for both matrices. Results show surprisingly that the dual matrices with secondary milling showed higher ductility values as compared to single matrices though accompanied by a loss in strength. This, the authors attributed to the fact that secondary milling resulted in a stronger bond between the two phases due to continuous impact of the milling media and this led to an efficient load transfer. The best combination of properties was achieved in the DM with 50% mixed powder ratio, with tensile strength of 298.3 MPa and 11.6 % ductility and 348.3 MPa and 7.15 % respectively for both 1 and 2.5 wt % respectively. Increased strength was attributed to the work hardening effect associated with the milling process.

6.3 Boundary modification

Chen et al [110] focused on improving the boundary conditions between aluminium and CNTs to obtain a good balance of strength and ductility by varying sintering temperatures. He observed that higher sintering temperatures enhanced the CNT-Al interface, promoting good interfacial bonding, thus yielding better mechanical properties. The CNT–Al interface in the

composite sintered at 800K becomes indistinct in the composite sintered at 900K, reasonably resulting from enhanced diffusions of atoms near the interface. For the specimens sintered at 800 K, debonding phenomenon of local micro cracks produced at grain boundaries are suggestive of insufficient grain boundary conditions. As sintering temperature is increased to 900 K however, the fracture surface exhibits a ductile failure mode with numerous dimples and plastically deformed grain boundaries (GBs), suggesting good bonding conditions of Al matrix with the CNT reinforcement.

6.4 In-situ grown method

This is a method in which CNTs are directly 'grown' on aluminium powder particles using a catalyst such as cobalt or nickel while the aluminium particles act as substrate. This direct growth of CNTs is able to facilitate the uniform dispersion of undamaged CNTs within the aluminium matrix, leading to a significant enhancement of mechanical properties. One of the major challenges of this method however, is the cultivation or growth of high quality CNTs. In their work, Tang et al [133] shows that by a careful control of parameters especially synthesis temperature, high quality CNTs with good crystallinity can be grown.

Yang et al [122] explored an in-situ chemical vapour deposition method where CNT was grown on Al using Cobalt as a catalyst to synthesize 2.5 wt % CNT. The Al/CNT were then dispersed using short term high energy ball milling at 500rpm to improve interfacial bonding between CNT and Al. They obtained UTS of 334MPa with ductility of 17.9%. This significant increase can be attributed to the homogenously dispersed CNTs as a result of the growth of CNTs on the aluminium particles. This led to efficient stress transfer during tensile deformation, thereby improving the strength of the composite [134].
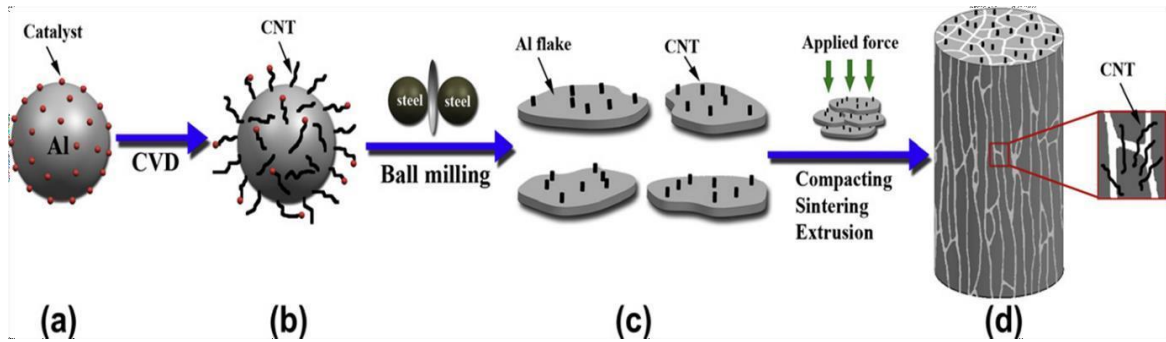
Fig. 8 – A schematic illustration of the procedure to fabricate CNT/Al composites. (a) Preparation of Co catalyst spread homogeneously on the surface of Al powder, (b) in-situ synthesis of CNTs in Al powder by CVD, (c) ball milling of the in-situ synthesized CNT/Al powders, and (d) fabrication of CNT/Al composites by compacting, sintering and hot extrusion – Yang et al [122]

6.5 Cryogenic milling

Cryogenic milling (or cryomilling) is a mechanical mixing process whereby the starting powders are milled at extremely low temperatures using liquid nitrogen. At these low temperatures, usually in the range of (~100 K) recovery and recrystallization processes become exceptionally slow while the dispersion of reinforcements in the matrix occurs. As a result, composites sintered with the admixed powders processed by this method have considerably high strength [135].

He et al [121] utilized a cryogenic milling process to disperse varying compositions of carbon nanotubes in Al 2009 matrix. CNTs/2009 powders were cryogenically milled under liquid nitrogen using ball-to-powder weight ratio of 39:1, milling time of 2 h and rotation speed of 180 rpm respectively. They achieved a good balance of high strength with yield strength of 443.3 MPa and elongation of 10.2 %, proving that CNTs could be dispersed in such a short time under cryogenic conditions. This balance of strength and ductility was attributed to the excellent dispersion and relatively low damage of the CNTs during cryogenic milling. Carbon nanotubes effectively transferred stress to the matrix and reflected cracks under loading. Fractographic images revealed CNT pull-out and bridging with a dimpled fracture surface.

Table 2 – Summary of main dispersion methods

Dispersion method	Method Description	Advantages	Disadvantages	Results
Ball milling [126]	Low energy ball milling (LEBM) leads to partial declustering of CNT agglomerates. High energy ball milling (HEBM) is effective in detangling a Higher proportion of CNTs from their Clusters	LEBM preserves the structural integrity of the CNTs. HEBM is more effective in dispersing the CNTs	Difficult to achieve uniform dispersion with LEBM only. Damage of CNT unique structures which is detrimental to Mechanical properties of Resulting Composites	UTS: 429 MPa Elongation: 0.035
Nanoscale dispersion [114]	Wettability between the Aluminium matrix and CNT reinforcement is Enhanced	Good interfacial bonding leading to remarkable increase in mechanical properties with little CNT content	Very complicated Procedure	Compressive strength: 280MPa Elongation: 15%
Flake powder metallurgy [117]	Poor wettability is improved by conversion of aluminium to thin flakes and slurry blending	Interfacial bonding is enhanced and CNT integrity is preserved	Slightly Complicated	UTS: 435MPa Elongation:6%

Two stage milling [127]	Prolonged LEBM at low speed followed by a short term HEBM at high speed	Good combination of strength and ductility due to and good interfacial bonding	Careful selection of parameters during HEBM is important to prevent CNT damage	UTS: 376MPa Elongation: 12.4%
Dual matrix approach [130]	Comprises of embedding pre-processed CNT-Al admixed powders into pure Al matrix using HEBM	Good combination of properties	Two stages of HEBM which may lead to higher CNT damage	UTS: 348.3 MPa Elongation: 7.15%
In-situ grown method [120]	CNTs are grown on Al powder particles using Co or Ni as catalyst	High CNT content can be incorporated into Al matrix. Clustering and agglomerations are significantly reduced or eliminated	High quality CNTs are seldom obtained	UTS: 334 MPa Elongation: 17.9%
Cryogenic milling or cryomilling [119]	Milling at cryogenic temperatures under liquid Nitrogen	Prolonged milling is not required	Due to shorter milling times, CNT structure is preserved	UTS: 560 MPa Elongation: 10.2%

7. Intermetallics of aluminium formed during sintering

It has been established from literature that intermetallics are formed due to damage of the carbon allotropes during milling or sintering of Al-based composites. Structural damage (during milling) and (or) thermal damage (during sintering) seem to trigger interfacial reactions which lead to the formation of the Al_4C_3 intermetallic phase [74]. It has been established that sites of structural disorders, defects in the graphitic planes, amorphous carbon layers, nanodefects, and open tube ends of MWCNTs, selectively favour the production of this intermetallic phase [136], [137]. Usually, highly stable defect-free graphitic planes of the carbon nanotube or graphene tend not to react with aluminium to form aluminium carbide even at very high temperatures. What has not been established however, is the actual role of these intermetallics in the mechanical behaviour and properties of the resulting composites.

In Zhang et al [85], it was observed that some of the GNPs were embedded in the Al matrix, but others reacted with Al and formed Al_4C_3 phase. Bastwros et al [41], Wu et al [138], Esawi et al [3] also speculated the same effect of aluminium carbide on the composites. Ci et al [137], in line with this, observed Al_4C_3 at the open ends of nanotubes and the amorphous surface layers at annealing temperatures as low as 500ºC. It is reported that such carbides could enhance the Al–CNT bonding and hinder CNT pull-out, therefore their presence in this regard, would not be considered as detrimental from the mechanical point of view. Gao et al [79], Bartolucci et al [115], Hassan et al [28] Liu et al [139], however seem to have a contrary view as they believe that this interfacial reaction product has a negative strengthening effect on the resulting composite. They observed carbide formation between defective graphene nanoplatelets and aluminium due to the employed processing route via thermal exfoliation of graphite oxide. Previous results that have reported the presence of Al_4C_3 in the composite utilized processing temperatures that were above 500ºC showing that thermal damage can trigger the formation of this carbide phase.

Dispersion methods like ultrasonication and low energy ball milling tend to prevent mechanical damage of CNTs while SPS seem to prevent thermal damage of the CNT due to the short sintering times. However, there have been reported cases in literature where Al_4C_3 detection was observed after SPS but this is mostly attributed to the mechanical damage of the carbon allotropes during the dispersion of the nanoparticles, especially high energy ball milling. Hence the formation of this intermetallic phase is largely sensitive to processing routes. Ju et al [105] observed that the formation of Al_4C_3 could be detrimental to the composites owing to its brittleness but Kwon et al [140] suggests that if this brittle phase is homogenously dispersed in

the composite, it could lead to higher strengthening effects.

Housaer et al [91] compared hot pressing and spark plasma sintering for the fabrication of the CNT/Al composites. Al_4C_3 was found to be present in the hot pressed samples but there was no evidence of formation of same in the SPSed samples, proving that the sintering method and particularly the duration of sintering plays a major role in the initiation and growth of the Al_4C_3 particles. It was observed that the duration of the sintering stage in SPS was six times shorter than that of the hot pressing process and as such, too short to encourage the formation and growth of Al_4C_3. SPS technique proved to be an effective route for controlling the CNT-Al interface while completing the sintering process.

As a novel and rapid powder consolidation process, SPS offers several advantages over the conventional sintering process such as much faster heating and cooling rates [141]. Such characteristics can avoid damage of the delicate structures of these nanocompounds and possible adverse chemical interfacial reactions, thus obtaining a fine grain sized metal matrix. Kwon et al [142] showed that Al_4C_3 produced during the fabrication of MWCNT/Al composites led to an increase of the UTS from 85 MPa to 194 MPa owing to the improved wettability between the matrix and reinforcement. In addition to this, the Al_4C_3 – Al interface is said to possess superior strength in comparison to the Al – CNT interface [44]. On the contrary, other researchers claimed that Al_4C_3 was very brittle and thermodynamically unstable, and thus its formation at the interface would lower the strength of MWCNT/Al composites [143]. Li et al [144] reported that the UTS of 1.0 vol. % MWCNT/Al composite decreased by 24.4% after forming an Al_4C_3 layer between the MWCNTs and the Al matrix.

Park et al [145] observed that the Al_4C_3 reaction on the surface of the CNTs improves the wettability between the Al matrix and CNTs [121], [146]. Consequently, the formation of Al_4C_3 at the interface between Al and the CNTs improves interfacial bonding and facilitates effective load transfer, thereby improving mechanical properties of the composite. The role of this intermetallic on the interface is a critical issue as the interfacial strength is a determining factor of the composite performance [147]. The extraordinary properties of these carbon allotropes would be inconsequential if the applied load on the composites cannot be successfully transferred from the aluminium matrix to the reinforcements due to a weakened interface [148] [149].

In Najimi et al [128] it was further validated that the CNT being not fully transformed into Al_4C_3, allows the strong interior portion of the CNTs coupled with the formation of Al_4C_3 at the interface between Al and the CNTs for effective load transfer, improving mechanical

properties of the composite [150]. The generated aluminium carbide during the sintering process was implanted into the aluminium matrix in the extrusion process. Such implanted aluminium carbides would adhere to the Al matrix and the CNTs more strongly [140].

Zhou et al [151] clarified in their study that the yield strength (YS) increased with increase in the Al_4C_3 amount, reaching to a maximum value of 116.4 MPa at 11% Al_4C_3, that is, formation of a small quantity of Al_4C_3 (~11%) produced at the MWCNT-Al interface could be effective to improve the load transfer in the MWCNT/Al composites [152]. They produced Al_4C_3 nanostructures at the end of the MWCNTs, incorporated in the Al matrix, by appropriate heat treatment. The stress contrast seen around the Al_4C_3 in the HRTEM image revealed the evidence of a trace of friction, which may lead to the improvement of the anchor effect from the Al matrix. This anchor effect of Al_4C_3 may restrict local interfacial slipping and increase the resistance of the Al matrix to deformation. They concluded that the formation of Al_4C_3 could effectively enhance the load transfer in MWCNT/Al composites as this stress contrast is a proof of strong interfacial bonding [151]. (Fig. 9).

The control of the size, amount and geometry of interfacial Al_4C_3 compounds reacted from CNTs and Al matrix seem to be crucial to clarifying the role of this intermetallic compound [153]. The Al_4C_3 precipitate is identified to either occur as individual nanoparticles formed from partially reacted CNTs with Al [142] or nanorod crystals evolved from completely reacted CNTs [152], [154]. Chen et al [114] showed a preference for the nanoparticles by showing that at medium temperatures (800-875 K), the quantity of Al_4C_3 nanoparticles increased at the interface between partially reacted CNTs and Al matrix. This had a positive effect on the interface strength and load transfer efficiency as both increased significantly compared to the low temperature sintered composites, proving that this intermetallic in nanoparticle dimensions can improve the mechanical properties. At high temperatures of 900 K, however, some mono-crystal Al_4C_3 phases with rod shapes were formed in Al matrix, and these resulted in decreased strengthening effect.
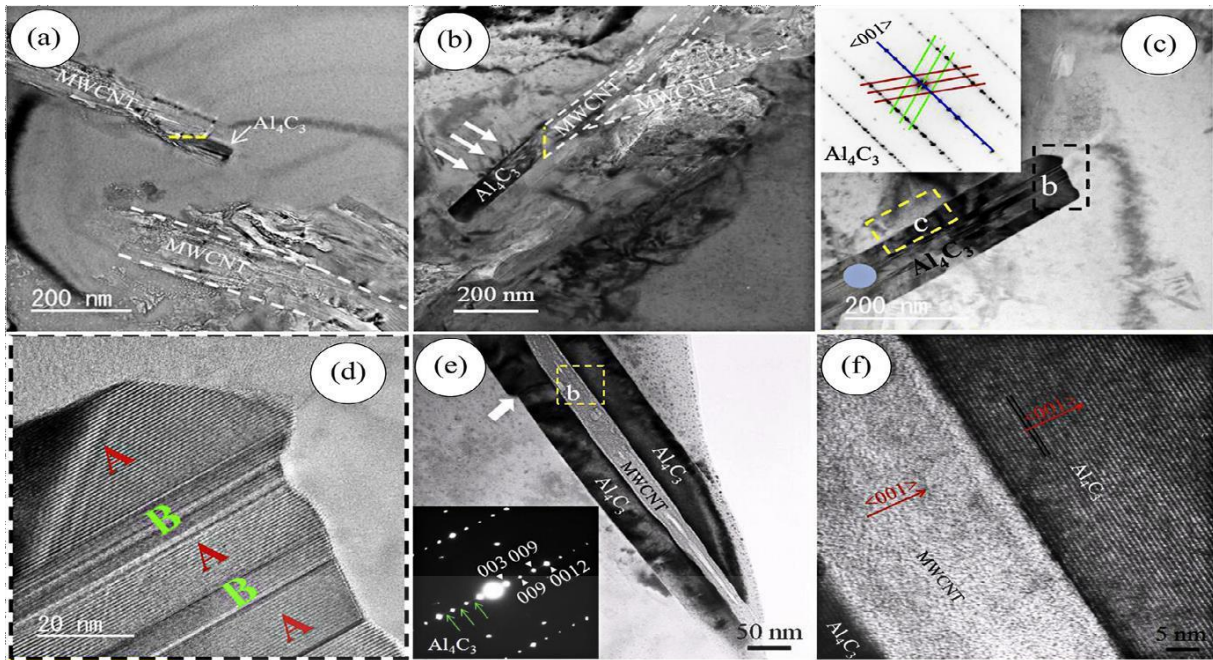
Inset Fig. 9 – HRTEM images of a SPSed CNT-dispersed Al nanocomposite after heat treatment (a) at 600°C for 0.1 h and (b) at 610°C for 1 h. These images shows the formation of Al_4C_3 precipitates at CNT ends where they tend to grow along the nanotubes. (c) HRTEM image of twinned Al_4C_3 in a SPSed CNT-dispersed Al nanocomposite after heat treatment at 640°C for 2 h with SAED pattern, (d) magnified picture of insert b in (c). (e) HRTEM image of a SPSed 5 vol% CNT dispersed Al nanocomposite after heat treatment at 610°C for 1 h with SAED pattern, and (f) the high magnification image of insert b in (e). These images indicate the formation of Al_4C_3 dispersoids at the outer walls of defective CNTs and their epitaxial growth parallel to sidewalls of nanotubes - Zhou et al [151].

Guo et al [155] corroborated this by extensively evaluating the size effect of this intermetallic by its precipitation during heat treatment. It was observed that the higher the heat treatment temperature, the larger the size of the precipitated Al_4C_3. This led to the deterioration of both strength and ductility of the composite for two reasons. First, the production of high quantity and large sized Al_4C_3 consumed a high quantity of CNTs available for load bearing functions. Secondly, the inherent brittleness of large sized Al_4C_3 significantly reduces the efficacy of the load transfer mechanism. It was thus concluded that few smaller sized Al_4C_3 are beneficial for the enhancement of the mechanical properties of the composites, while a high amount of larger sized Al_4C_3 would be detrimental to the composite properties.

8. Conclusion

The significance of effective processing routes to facilitate the incorporation of these 'super' reinforcements to bring about the desired properties, has been established. Among the discussed sintering techniques, SPS has emerged as a novel route owing to the short sintering times which effectively prevents grain growth and preserves the integrity of the delicate structures of the carbon allotrope reinforcements. Other sintering techniques which favour grain growth tend to produce composites with inferior properties to that produced by SPS. However, there is a need to develop this process economically to aid commercialization of spark plasma sintered composites.

Achieving homogenous dispersion of these carbonaceous compounds in aluminium matrices has remained a major challenge for researchers till date. Traditional and sophisticated methods have been explored with varying degrees of success. To effectively exploit the full potential of these carbon allotropes, the challenge to homogenously disperse undamaged nanostructures have to be fully overcome. Moreover, more fabrication methods yielding composites with good combination of both high strength and good ductility are required to mitigate the strength-ductility trade-off usually observed in reinforced composites. Also, effective, economical and uncomplicated methods of dispersion have to be developed and adapted for large scale production.

More work is required in clarifying the actual role of the intermetallic compound-Al_4C_3 in the carbon allotrope reinforced composites. It has been a major controversial subject within the research community. Three schools of thought have been established – some observe that it is detrimental and has negative strength effects, some others document that it has positive strengthening effects while some yet believe that it is beneficial in small amounts but detrimental in large amounts, that is, the role of the intermetallic is size, amount and geometry dependent.

Acknowledgement

Conflict of interest

Authors declare no conflict of interest.

References

[1] A. Agarwal, S.R. Bakshi, D. Lahiri, Carbon nanotubes: reinforced metal matrix composites, CRC press2016.

[2] K. Shirvanimoghaddam, S.U. Hamim, M.K. Akbari, S.M. Fakhrhoseini, H. Khayyam, A.H. Pakseresht, E. Ghasali, M. Zabet, K.S. Munir, S. Jia, Carbon fiber reinforced metal matrix composites: Fabrication processes and properties, Composites Part A: Applied Science and Manufacturing, 92 (2017) 70-96.

[3] A. Esawi, K. Morsi, A. Sayed, M. Taher, S. Lanka, Effect of carbon nanotube (CNT) content on the mechanical properties of CNT-reinforced aluminium composites, Composites Science and Technology, 70 (2010) 2237-2241.

[4] S.P. Rawal, Metal-matrix composites for space applications, Jom, 53 (2001) 14-17.

[5] M. Reboul, B. Baroux, Metallurgical aspects of corrosion resistance of aluminium alloys, Materials and Corrosion, 62 (2011) 215-233.

[6] J.-M. Molina, M. Rhême, J. Carron, L. Weber, Thermal conductivity of aluminum matrix composites reinforced with mixtures of diamond and SiC particles, Scripta Materialia, 58 (2008) 393-396.

[7] V. Recoules, P. Renaudin, J. Clérouin, P. Noiret, G. Zérah, Electrical conductivity of hot expanded aluminum: Experimental measurements and ab initio calculations, Physical Review E, 66 (2002) 056412.

[8] G.-c. LI, M. Yue, X.-l. He, L. Wei, P.-y. LI, Damping capacity of high strength-damping aluminum alloys prepared by rapid solidification and powder metallurgy process, Transactions of Nonferrous Metals Society of China, 22 (2012) 1112-1117.

[9] E. Ghasali, A. Pakseresht, F. Safari-Kooshali, M. Agheli, T. Ebadzadeh, Investigation on microstructure and mechanical behavior of Al–ZrB2 composite prepared by microwave and spark plasma sintering, Materials Science and Engineering: A, 627 (2015) 27-30.

[10] E. Omrani, A.D. Moghadam, P.L. Menezes, P.K. Rohatgi, Influences of graphite reinforcement on the tribological properties of self-lubricating aluminum matrix composites for green tribology, sustainability, and energy efficiency—a review, The International Journal of Advanced Manufacturing Technology, 83 (2016) 325-346.

[11] J. Li, Y. Xiong, X. Wang, S. Yan, C. Yang, W. He, J. Chen, S. Wang, X. Zhang, S. Dai, Microstructure and tensile properties of bulk nanostructured aluminum/graphene composites prepared via cryomilling, Materials Science and Engineering: A, 626 (2015) 400-405.

[12] M.H. Rahman, H.M. Al Rashed, Characterization of silicon carbide reinforced aluminum matrix composites, Procedia Engineering, 90 (2014) 103-109.

[13] B. Park, A. Crosky, A. Hellier, Fracture toughness of microsphere Al2O3–Al particulate metal matrix composites, Composites Part B: Engineering, 39 (2008) 1270-1279.

[14] K.K. Alaneme, K.O. Sanusi, Microstructural characteristics, mechanical and wear behaviour of aluminium matrix hybrid composites reinforced with alumina, rice husk ash and graphite, Engineering Science and Technology, an International Journal, 18 (2015) 416-422.

[15] L. Jia, K. Kondoh, H. Imai, M. Onishi, B. Chen, S.-f. Li, Nano-scale AlN powders and AlN/Al composites by full and partial direct nitridation of aluminum in solid-state, Journal of Alloys and Compounds, 629 (2015) 184-187.

[16] A. Lekatou, A. Karantzalis, A. Evangelou, V. Gousia, G. Kaptay, Z. Gácsi, P. Baumli, A. Simon, Aluminium reinforced by WC and TiC nanoparticles (ex-situ) and aluminide particles (in-situ): Microstructure, wear and corrosion behaviour, Materials & Design (1980-2015), 65 (2015) 1121-1135.

[17] P. Sharma, S. Sharma, D. Khanduja, Production and some properties of Si3N4 reinforced aluminium alloy composites, Journal of Asian Ceramic Societies, 3 (2015) 352-359.

[18] M. Krasnowski, S. Gierlotka, T. Kulik, TiC–Al composites with nanocrystalline matrix produced by consolidation of milled powders, Advanced Powder Technology, 26 (2015) 1269-1272.

[19] A. Dixit, K. Kumar, Optimization of mechanical properties of silica gel reinforced aluminium MMC by using Taguchi method, Materials Today: Proceedings, 2 (2015) 2359-2366.

[20] B. Previtali, D. Pocci, C. Taccardo, Application of traditional investment casting process to aluminium matrix composites, Composites Part A: Applied Science and Manufacturing, 39 (2008) 1606-1617.

[21] A. Alizadeh, A. Abdollahi, H. Biukani, Creep behavior and wear resistance of Al 5083 based hybrid composites reinforced with carbon nanotubes (CNTs) and boron carbide (B4C), Journal of Alloys and Compounds, 650 (2015) 783-793.

[22] J. Shin, H. Choi, D. Bae, The structure and properties of 2024 aluminum composites reinforced with TiO2 nanoparticles, Materials Science and Engineering: A, 607 (2014) 605-610.

[23] P. Ravindran, K. Manisekar, P. Narayanasamy, N. Selvakumar, R. Narayanasamy, Application of factorial techniques to study the wear of Al hybrid composites with graphite addition, Materials & Design, 39 (2012) 42-54.

[24] P. Ravindran, K. Manisekar, R. Narayanasamy, P. Narayanasamy, Tribological behaviour of powder metallurgy-processed aluminium hybrid composites with the addition of graphite solid lubricant, Ceramics International, 39 (2013) 1169-1182.

[25] A. Baradeswaran, A.E. Perumal, Wear and mechanical characteristics of Al 7075/graphite composites, Composites Part B: Engineering, 56 (2014) 472-476.

[26] I. Dinaharan, N. Murugan, S. Parameswaran, Influence of in situ formed ZrB2 particles on microstructure and mechanical properties of AA6061 metal matrix composites, Materials Science and Engineering: A, 528 (2011) 5733-5740.

[27] E. Ghasali, K. Shirvanimoghaddam, A.H. Pakseresht, M. Alizadeh, T. Ebadzadeh, Evaluation of microstructure and mechanical properties of Al-TaC composites prepared by spark plasma sintering process, Journal of Alloys and Compounds, 705 (2017) 283-289.

[28] S. Hassan, O. Aponbiede, V. Aigbodion, Precipitation hardening characteristics of Al–Si–Fe/SiC particulate composites, Journal of alloys and Compounds, 466 (2008) 268-272.

[29] S.-L. Zhang, Y.-T. Zhao, G. Chen, X.-N. Cheng, C.-J. She, X.-Y. Wang, D.-N. Wu, Effects of in situ TiB2 particle on microstructures and mechanical properties of AZ91 alloy, Journal of Alloys and Compounds, 494 (2010) 94-97.

[30] M.A. Baghchesara, H. Abdizadeh, Microstructural and mechanical properties of nanometric magnesium oxide particulate-reinforced aluminum matrix composites produced by powder metallurgy method, Journal of mechanical science and technology, 26 (2012) 367-372.

[31] M.O. Bodunrin, K.K. Alaneme, L.H. Chown, Aluminium matrix hybrid composites: a review of reinforcement philosophies; mechanical, corrosion and tribological characteristics, journal of materials research and technology, 4 (2015) 434-445.

[32] Y. Loh, D. Sujan, M. Rahman, C. Das, Sugarcane bagasse—The future composite material: A literature review, Resources, Conservation and Recycling, 75 (2013) 14-22.

[33] H. Anilkumar, H. Hebbar, K. Ravishankar, Mechanical properties of fly ash reinforced aluminium alloy (Al6061) composites, International journal of mechanical and materials engineering, 6 (2011) 41-45.

[34] V. Aigbodion, S. Hassan, E. Dauda, R. Mohammed, The development of mathematical model for the prediction of ageing behaviour for Al-Cu-Mg/bagasse ash particulate composites, Journal of Minerals and Materials Characterization and Engineering, 9 (2010) 907.

[35] D.S. Prasad, A.R. Krishna, Production and mechanical properties of A356. 2/RHA composites, International journal of advanced science and technology, 33 (2011) 51-58.

[36] K.K. Alaneme, I.B. Akintunde, P.A. Olubambi, T.M. Adewale, Fabrication characteristics and mechanical behaviour of rice husk ash–Alumina reinforced Al-Mg-Si alloy matrix hybrid composites, journal of Materials Research and Technology, 2 (2013) 60-67.

[37] W.A. Curtin, B.W. Sheldon, CNT-reinforced ceramics and metals, Materials Today, 7 (2004) 44-49.

[38] S.-I. Oh, J.-Y. Lim, Y.-C. Kim, J. Yoon, G.-H. Kim, J. Lee, Y.-M. Sung, J.-H. Han, Fabrication of carbon nanofiber reinforced aluminum alloy nanocomposites by a liquid process, Journal of Alloys and Compounds, 542 (2012) 111-117.

[39] A.D. Moghadam, B.F. Schultz, J. Ferguson, E. Omrani, P.K. Rohatgi, N. Gupta, Functional metal matrix composites: self-lubricating, self-healing, and nanocomposites-an outlook, Jom, 66 (2014) 872-881.

[40] Y. Huang, Q. Ouyang, D. Zhang, J. Zhu, R. Li, H. Yu, Carbon materials reinforced aluminum composites: a review, Acta Metallurgica Sinica (English Letters), 27 (2014) 775-786.

[41] M.M. Bastwros, A.M. Esawi, A. Wifi, Friction and wear behavior of Al–CNT composites, Wear, 307 (2013) 164-173.

[42] B. Peng, M. Locascio, P. Zapol, S. Li, S.L. Mielke, G.C. Schatz, H.D. Espinosa, Measurements of near-ultimate strength for multiwalled carbon nanotubes and irradiation-induced crosslinking improvements, Nature nanotechnology, 3 (2008) 626.

[43] F. Gardea, D.C. Lagoudas, Characterization of electrical and thermal properties of carbon nanotube/epoxy composites, Composites Part B: Engineering, 56 (2014) 611-620.

[44] B. Chen, L. Jia, S. Li, H. Imai, M. Takahashi, K. Kondoh, In situ synthesized Al4C3 nanorods with excellent strengthening effect in aluminum matrix composites, Advanced Engineering Materials, 16 (2014) 972-975.

[45] J. Chen, I. Huang, Thermal properties of aluminum–graphite composites by powder metallurgy, Composites Part B: Engineering, 44 (2013) 698-703.

[46] C. Balázsi, B. Fényi, N. Hegman, Z. Kövér, F. Wéber, Z. Vértesy, Z. Kónya, I. Kiricsi, L.P. Biró, P. Arató, Development of CNT/Si3N4 composites with improved mechanical and electrical properties, Composites Part B: Engineering, 37 (2006) 418-424.

[47] X. Wang, Y. Liu, H. Pang, S. Yu, Y. Ai, X. Ma, G. Song, T. Hayat, A. Alsaedi, X. Wang, Effect of graphene oxide surface modification on the elimination of Co (II) from aqueous solutions, Chemical Engineering Journal, 344 (2018) 380-390.

[48] R. Pérez-Bustamante, F. Pérez-Bustamante, I. Estrada-Guel, L. Licea-Jiménez, M. Miki-Yoshida, R. Martínez-Sánchez, Effect of milling time and CNT concentration on hardness of CNT/Al2024 composites produced by mechanical alloying, Materials characterization, 75 (2013) 13-19.

[49] P. Kim, L. Shi, A. Majumdar, P. McEuen, Thermal transport measurements of individual multiwalled nanotubes, Physical review letters, 87 (2001) 215502.

[50] C. Lee, X. Wei, J.W. Kysar, J. Hone, Measurement of the elastic properties and intrinsic strength of monolayer graphene, science, 321 (2008) 385-388.

[51] J.-P. Salvetat, J.-M. Bonard, N. Thomson, A. Kulik, L. Forro, W. Benoit, L. Zuppiroli, Mechanical properties of carbon nanotubes, Applied Physics A, 69 (1999) 255-260.

[52] A.P. Reddy, P.V. Krishna, R.N. Rao, N. Murthy, Silicon Carbide Reinforced Aluminium Metal Matrix Nano Composites-A Review, Materials Today: Proceedings, 4 (2017) 3959-3971.

[53] R.G.R. Nimal, M. Sivakumar, S.G. Raj, S.A. Vendan, G. Esakkimuthu, Microstructural, mechanical and metallurgical analysis of Al interlayer coating on Mg-Al alloy using diffusion bonding, Materials Today: Proceedings, 5 (2018) 5886-5890.

[54] J. Zhang, B.-h. Wang, G.-h. Chen, R.-m. Wang, C.-h. Miao, Z.-x. Zheng, W.-m. Tang, Formation and growth of Cu–Al IMCs and their effect on electrical property of electroplated Cu/Al laminar composites, Transactions of Nonferrous Metals Society of China, 26 (2016) 3283-3291.

[55] D. Woo, F. Heer, L. Brewer, J. Hooper, S. Osswald, Synthesis of nanodiamond-reinforced aluminum metal matrix composites using cold-spray deposition, Carbon, 86 (2015) 15-25.

[56] J.-l. Zhao, J.-c. Jie, C. Fei, C. Hang, T.-j. Li, Z.-q. Cao, Effect of immersion Ni plating on interface microstructure and mechanical properties of Al/Cu bimetal, Transactions of Nonferrous Metals Society of China, 24 (2014) 1659-1665.

[57] S. Altmannshofer, B. Miller, A.W. Holleitner, J. Boudaden, I. Eisele, C. Kutter, Deposition of micro crystalline silicon films using microwave plasma enhanced chemical vapor deposition, Thin Solid Films, 645 (2018) 180-186.

[58] L. Ulmer, F. Pitard, D. Poncet, O. Demolliens, Formation of Al3Ti during physical vapour deposition of titanium on aluminium, Microelectronic engineering, 37 (1997) 381-387.

[59] B.C. Kandpal, J. Kumar, H. Singh, Manufacturing and technological challenges in Stir casting of metal matrix composites–A Review, Materials Today: Proceedings, 5 (2018) 5-10.

[60] J. Maj, M. Basista, W. Węglewski, K. Bochenek, A. Strojny-Nędza, K. Naplocha, T. Panzner, M. Tatarková, F. Fiori, Effect of microstructure on mechanical properties and residual stresses in

interpenetrating aluminum-alumina composites fabricated by squeeze casting, Materials Science and Engineering: A, (2017).

[61] S.A. Sajjadi, H. Ezatpour, M.T. Parizi, Comparison of microstructure and mechanical properties of A356 aluminum alloy/Al2O3 composites fabricated by stir and compo-casting processes, Materials & Design, 34 (2012) 106-111.

[62] D. Wang, Z. Zheng, J. Lv, G. Xu, S. Zhou, W. Tang, Y. Wu, Interface Design in 3D-SiC/Al-Si-Mg Interpenetrating Composite Fabricated by Pressureless Infiltration, Ceramics International, (2018).

[63] N. Srivastava, G. Chaudhari, Strengthening in Al alloy nano composites fabricated by ultrasound assisted solidification technique, Materials Science and Engineering: A, 651 (2016) 241-247.

[64] M.K. Akbari, O. Mirzaee, H. Baharvandi, Fabrication and study on mechanical properties and fracture behavior of nanometric Al2O3 particle-reinforced A356 composites focusing on the parameters of vortex method, Materials & Design, 46 (2013) 199-205.

[65] S. Khorramie, M. Baghchesara, D. Gohari, Fabrication of aluminum matrix composites reinforced with Al2ZrO5 nano particulates synthesized by sol-gel auto-combustion method, Transactions of Nonferrous Metals Society of China, 23 (2013) 1556-1562.

[66] F. Chang, D. Gu, D. Dai, P. Yuan, Selective laser melting of in-situ Al4SiC4+ SiC hybrid reinforced Al matrix composites: Influence of starting SiC particle size, Surface and Coatings Technology, 272 (2015) 15-24.

[67] Y.X. Gan, J. Dong, J.B. Gan, Carbon network/aluminum composite made by powder metallurgy and its corrosion behavior in seawater, Materials Chemistry and Physics, 202 (2017) 190-196.

[68] E. Ghasali, M. Alizadeh, T. Ebadzadeh, Mechanical and microstructure comparison between microwave and spark plasma sintering of Al–B4C composite, Journal of Alloys and Compounds, 655 (2016) 93-98.

[69] B. Yao, C. Hofmeister, T. Patterson, Y.-h. Sohn, M. van den Bergh, T. Delahanty, K. Cho, Microstructural features influencing the strength of trimodal aluminum metal-matrix-composites, Composites Part A: Applied Science and Manufacturing, 41 (2010) 933-941.

[70] J.d. Torralba, C. Da Costa, F. Velasco, P/M aluminum matrix composites: an overview, Journal of Materials Processing Technology, 133 (2003) 203-206.

[71] M. Yildirim, D. Özyürek, M. Gürü, The effects of precipitate size on the hardness and wear behaviors of aged 7075 aluminum alloys produced by powder metallurgy route, Arabian Journal for Science and Engineering, 41 (2016) 4273-4281.

[72] A. Liang, X. Jiang, X. Hong, Y. Jiang, Z. Shao, D. Zhu, Recent Developments Concerning the Dispersion Methods and Mechanisms of Graphene, Coatings, 8 (2018) 33.

[73] W.C. Harrigan Jr, Commercial processing of metal matrix composites, Materials Science and Engineering: A, 244 (1998) 75-79.

[74] C. Deng, D. Wang, X. Zhang, A. Li, Processing and properties of carbon nanotubes reinforced aluminum composites, Materials Science and engineering: A, 444 (2007) 138-145.

[75] R. George, K. Kashyap, R. Rahul, S. Yamdagni, Strengthening in carbon nanotube/aluminium (CNT/Al) composites, Scripta Materialia, 53 (2005) 1159-1163.

[76] R. Perez-Bustamante, I. Estrada-Guel, W. Antúnez-Flores, M. Miki-Yoshida, P. Ferreira, R. Martínez-Sánchez, Novel Al-matrix nanocomposites reinforced with multi-walled carbon nanotubes, Journal of Alloys and compounds, 450 (2008) 323-326.

[77] R. Abedinzadeh, S.M. Safavi, F. Karimzadeh, A study of pressureless microwave sintering, microwave-assisted hot press sintering and conventional hot pressing on properties of aluminium/alumina nanocomposite, Journal of Mechanical Science and Technology, 30 (2016) 1967-1972.

[78] P.R. Matli, R.A. Shakoor, A.M. Amer Mohamed, M. Gupta, Microwave rapid sintering of Al-metal matrix composites: a review on the effect of reinforcements, microstructure and mechanical properties, Metals, 6 (2016) 143.

[79] X. Gao, H. Yue, E. Guo, H. Zhang, X. Lin, L. Yao, B. Wang, Preparation and tensile properties of homogeneously dispersed graphene reinforced aluminum matrix composites, Materials & Design, 94 (2016) 54-60.

[80] S. Takayama, Y. Saiton, M. Sato, T. Nagasaka, T. Muroga, Y. Ninomiya, Microwave sintering for metal powders in the air by non-thermal effect, Proceedings of the 9th Conference on Microwave and High Frequency Heating, 2003, pp. 369-372.

[81] J. Walkiewicz, G. Kazonich, S. McGill, Microwave heating characteristics of selected minerals and compounds, Minerals and Metallurgical Processing, 5 (1988) 39-42.

[82] D. Agrawal, Microwave sintering of ceramics, composites and metallic materials, and melting of glasses, Transactions of the Indian ceramic society, 65 (2006) 129-144.

[83] N. Saheb, Spark plasma and microwave sintering of Al6061 and Al2124 alloys, International Journal of Minerals, Metallurgy, and Materials, 20 (2013) 152-159.

[84] R.M. German, Sintering theory and practice, Solar-Terrestrial Physics (Solnechno-zemnaya fizika), (1996) 568.

[85] H. Zhang, C. Xu, W. Xiao, K. Ameyama, C. Ma, Enhanced mechanical properties of Al5083 alloy with graphene nanoplates prepared by ball milling and hot extrusion, Materials Science and Engineering: A, 658 (2016) 8-15.

[86] I. Ahmad, H. Cao, H. Chen, H. Zhao, A. Kennedy, Y.Q. Zhu, Carbon nanotube toughened aluminium oxide nanocomposite, Journal of the European Ceramic Society, 30 (2010) 865-873.

[87] I.-Y. Kim, J.-H. Lee, G.-S. Lee, S.-H. Baik, Y.-J. Kim, Y.-Z. Lee, Friction and wear characteristics of the carbon nanotube–aluminum composites with different manufacturing conditions, Wear, 267 (2009) 593-598.

[88] S. Kishimoto, N. Shinya, Compressive behavior of micro-metallic closed cellular materials fabricated by spark-plasma sintering, Materials Science and Engineering: A, 483 (2008) 679-682.

[89] A. Azarniya, A. Azarniya, S. Sovizi, H.R.M. Hosseini, T. Varol, A. Kawasaki, S. Ramakrishna, Physicomechanical properties of spark plasma sintered carbon nanotube-reinforced metal matrix nanocomposites, Progress in Materials Science, 90 (2017) 276-324.

[90] B. Guo, S. Ni, J. Yi, R. Shen, Z. Tang, Y. Du, M. Song, Microstructures and mechanical properties of carbon nanotubes reinforced pure aluminum composites synthesized by spark plasma sintering and hot rolling, Materials Science and Engineering: A, 698 (2017) 282-288.

[91] F. Housaer, F. Beclin, M. Touzin, D. Tingaud, A. Legris, A. Addad, Interfacial characterization in carbon nanotube reinforced aluminum matrix composites, Materials Characterization, 110 (2015) 94-101.

[92] S. Yan, S. Dai, X. Zhang, C. Yang, Q. Hong, J. Chen, Z. Lin, Investigating aluminum alloy reinforced by graphene nanoflakes, Materials Science and Engineering: A, 612 (2014) 440-444.

[93] V. Viswanathan, T. Laha, K. Balani, A. Agarwal, S. Seal, Challenges and advances in nanocomposite processing techniques, Materials Science and Engineering: R: Reports, 54 (2006) 121-285.

[94] J. Adachi, K. Kurosaki, M. Uno, S. Yamanaka, Porosity influence on the mechanical properties of polycrystalline zirconium nitride ceramics, Journal of nuclear materials, 358 (2006) 106-110.

[95] D. Tiwari, B. Basu, K. Biswas, Simulation of thermal and electric field evolution during spark plasma sintering, Ceramics International, 35 (2009) 699-708.

[96] W. Chen, U. Anselmi-Tamburini, J. Garay, J. Groza, Z.A. Munir, Fundamental investigations on the spark plasma sintering/synthesis process: I. Effect of dc pulsing on reactivity, Materials Science and Engineering: A, 394 (2005) 132-138.

[97] U. Anselmi-Tamburini, J. Garay, Z. Munir, Fundamental investigations on the spark plasma sintering/synthesis process: III. Current effect on reactivity, Materials Science and Engineering: A, 407 (2005) 24-30.

[98] A. Pakdel, A. Witecka, G. Rydzek, D.N.A. Shri, A comprehensive microstructural analysis of Al–WC micro-and nano-composites prepared by spark plasma sintering, Materials & Design, 119 (2017) 225-234.

[99] I. Ahmad, B. Yazdani, Y. Zhu, Recent advances on carbon nanotubes and graphene reinforced ceramics nanocomposites, Nanomaterials, 5 (2015) 90-114.

[100] A. Kasperski, A. Weibel, C. Estournès, C. Laurent, A. Peigney, Preparation-microstructure-property relationships in double-walled carbon nanotubes/alumina composites, Carbon, 53 (2013) 62-72.

[101] K. Nishikata, A. Kimura, T. Shiina, A. Ota, M. Tanase, K. Tsuchiya, Fabrication and characterization of high-density MoO3 pellets, 2012 Powder Metallurgy World Congress & Exhibition (PM2012), 2012, pp. 14-18.

[102] M. Bocanegra-Bernal, C. Dominguez-Rios, J. Echeberria, A. Reyes-Rojas, A. Garcia-Reyes, A. Aguilar-Elguezabal, Spark plasma sintering of multi-, single/double-and single-walled carbon nanotube-reinforced alumina composites: Is it justifiable the effort to reinforce them?, Ceramics International, 42 (2016) 2054-2062.

[103] H. Ghobadi, A. Nemati, T. Ebadzadeh, Z. Sadeghian, H. Barzegar-Bafrooei, Improving CNT distribution and mechanical properties of MWCNT reinforced alumina matrix, Materials Science and Engineering: A, 617 (2014) 110-114.

[104] A. Bisht, M. Srivastava, R.M. Kumar, I. Lahiri, D. Lahiri, Strengthening mechanism in graphene nanoplatelets reinforced aluminum composite fabricated through spark plasma sintering, Materials Science and Engineering: A, 695 (2017) 20-28.

[105] J.-M. Ju, G. Wang, K.-H. Sim, Facile synthesis of graphene reinforced Al matrix composites with improved dispersion of graphene and enhanced mechanical properties, Journal of Alloys and Compounds, 704 (2017) 585-592.

[106] M.H. Wichmann, K. Schulte, H.D. Wagner, On nanocomposite toughness, Composites Science and Technology, 68 (2008) 329-331.

[107] H. Zare, M. Jahedi, M.R. Toroghinejad, M. Meratian, M. Knezevic, Microstructure and mechanical properties of carbon nanotubes reinforced aluminum matrix composites synthesized via equal-channel angular pressing, Materials Science and Engineering: A, 670 (2016) 205-216.

[108] H. Zare, M. Jahedi, M.R. Toroghinejad, M. Meratian, M. Knezevic, Compressive, shear, and fracture behavior of CNT reinforced Al matrix composites manufactured by severe plastic deformation, Materials & Design, 106 (2016) 112-119.

[109] S.R. Bakshi, A. Agarwal, An analysis of the factors affecting strengthening in carbon nanotube reinforced aluminum composites, Carbon, 49 (2011) 533-544.

[110] B. Chen, K. Kondoh, H. Imai, J. Umeda, M. Takahashi, Simultaneously enhancing strength and ductility of carbon nanotube/aluminum composites by improving bonding conditions, Scripta Materialia, 113 (2016) 158-162.

[111] M. Rashad, F. Pan, Z. Yu, M. Asif, H. Lin, R. Pan, Investigation on microstructural, mechanical and electrochemical properties of aluminum composites reinforced with graphene nanoplatelets, Progress in natural science: materials international, 25 (2015) 460-470.

[112] B. Chen, S. Li, H. Imai, L. Jia, J. Umeda, M. Takahashi, K. Kondoh, Load transfer strengthening in carbon nanotubes reinforced metal matrix composites via in-situ tensile tests, Composites Science and Technology, 113 (2015) 1-8.

[113] H. Kurita, M. Estili, H. Kwon, T. Miyazaki, W. Zhou, J.-F. Silvain, A. Kawasaki, Load-bearing contribution of multi-walled carbon nanotubes on tensile response of aluminum, Composites Part A: Applied Science and Manufacturing, 68 (2015) 133-139.

[114] B. Chen, J. Shen, X. Ye, H. Imai, J. Umeda, M. Takahashi, K. Kondoh, Solid-state interfacial reaction and load transfer efficiency in carbon nanotubes (CNTs)-reinforced aluminum matrix composites, Carbon, 114 (2017) 198-208.

[115] S.F. Bartolucci, J. Paras, M.A. Rafiee, J. Rafiee, S. Lee, D. Kapoor, N. Koratkar, Graphene–aluminum nanocomposites, Materials Science and Engineering: A, 528 (2011) 7933-7937.

[116] T. Noguchi, A. Magario, S. Fukazawa, S. Shimizu, J. Beppu, M. Seki, Carbon nanotube/aluminium composites with uniform dispersion, Materials Transactions, 45 (2004) 602-604.

[117] A.M. Esawi, K. Morsi, A. Sayed, A.A. Gawad, P. Borah, Fabrication and properties of dispersed carbon nanotube–aluminum composites, Materials Science and Engineering: A, 508 (2009) 167-173.

[118] C. He, N. Zhao, C. Shi, S. Song, Mechanical properties and microstructures of carbon nanotube-reinforced Al matrix composite fabricated by in situ chemical vapor deposition, Journal of Alloys and Compounds, 487 (2009) 258-262.

[119] L. Jiang, Z. Li, G. Fan, L. Cao, D. Zhang, The use of flake powder metallurgy to produce carbon nanotube (CNT)/aluminum composites with a homogenous CNT distribution, Carbon, 50 (2012) 1993-1998.

[120] S.I. Cha, K.T. Kim, S.N. Arshad, C.B. Mo, S.H. Hong, Extraordinary strengthening effect of carbon nanotubes in metal-matrix nanocomposites processed by molecular-level mixing, Advanced Materials, 17 (2005) 1377-1381.

[121] T. He, X. He, P. Tang, D. Chu, X. Wang, P. Li, The use of cryogenic milling to prepare high performance Al2009 matrix composites with dispersive carbon nanotubes, Materials & Design, 114 (2017) 373-382.

[122] X. Yang, E. Liu, C. Shi, C. He, J. Li, N. Zhao, K. Kondoh, Fabrication of carbon nanotube reinforced Al composites with well-balanced strength and ductility, Journal of Alloys and Compounds, 563 (2013) 216-220.

[123] D. Poirier, R. Gauvin, R.A. Drew, Structural characterization of a mechanically milled carbon nanotube/aluminum mixture, Composites Part A: Applied Science and Manufacturing, 40 (2009) 1482-1489.

[124] W.J. Clegg, Role of Carbon in the Sintering of Boron-Doped Silicon Carbide, Journal of the American Ceramic Society, 83 (2000) 1039-1043.

[125] L.Y. Wang, J. Tu, W. Chen, Y. Wang, X. Liu, C. Olk, D. Cheng, X. Zhang, Friction and wear behavior of electroless Ni-based CNT composite coatings, Wear, 254 (2003) 1289-1293.

[126] S.R. Bakshi, Plasma and cold sprayed aluminum carbon nanotube composites: Quantification of nanotube distribution and multi-scale mechanical properties, Florida International University, 2009.

[127] H. Kwon, A. Kawasaki, Effect of Spark Plasma Sintering in Fabricating Carbon Nanotube Reinforced Aluminum Matrix Composite Materials, Advances in Composite Materials for Medicine and Nanotechnology, InTech2011.

[128] A. Najimi, H. Shahverdi, Effect of milling methods on microstructures and mechanical properties of Al6061-CNT composite fabricated by spark plasma sintering, Materials Science and Engineering: A, 702 (2017) 87-95.

[129] R. Xu, Z. Tan, D. Xiong, G. Fan, Q. Guo, J. Zhang, Y. Su, Z. Li, D. Zhang, Balanced strength and ductility in CNT/Al composites achieved by flake powder metallurgy via shift-speed ball milling, Composites Part A: Applied Science and Manufacturing, 96 (2017) 57-66.

[130] W. Callister, D. Rethwisch, The structure of crystalline solids, Materials Science and Engineering: An Introduction, (2007) 38-63.

[131] K. Morsi, A. Esawi, Effect of mechanical alloying time and carbon nanotube (CNT) content on the evolution of aluminum (Al)–CNT composite powders, Journal of Materials Science, 42 (2007) 4954-4959.

[132] E.I. Salama, A. Abbas, A.M. Esawi, Preparation and properties of dual-matrix carbon nanotube-reinforced aluminum composites, Composites Part A: Applied Science and Manufacturing, 99 (2017) 84-93.

[133] J. Tang, G. Fan, Z. Li, X. Li, R. Xu, Y. Li, D. Zhang, W.-J. Moon, S.D. Kaloshkin, M. Churyukanova, Synthesis of carbon nanotube/aluminium composite powders by polymer pyrolysis chemical vapor deposition, Carbon, 55 (2013) 202-208.

[134] C. He, N. Zhao, C. Shi, X. Du, J. Li, H. Li, Q. Cui, An approach to obtaining homogeneously dispersed carbon nanotubes in Al Powders for preparing reinforced Al-matrix composites, Advanced Materials, 19 (2007) 1128-1132.

[135] D. Witkin, E.J. Lavernia, Synthesis and mechanical behavior of nanostructured materials via cryomilling, Progress in Materials Science, 51 (2006) 1-60.

[136] W. Zhou, S. Sasaki, A. Kawasaki, Effective control of nanodefects in multiwalled carbon nanotubes by acid treatment, Carbon, 78 (2014) 121-129.

[137] L. Ci, Z. Ryu, N.Y. Jin-Phillipp, M. Rühle, Investigation of the interfacial reaction between multi-walled carbon nanotubes and aluminum, Acta Materialia, 54 (2006) 5367-5375.

[138] Y. Wu, G.-Y. Kim, A.M. Russell, Effects of mechanical alloying on an Al6061–CNT composite fabricated by semi-solid powder processing, Materials Science and Engineering: A, 538 (2012) 164-172.

[139] Z. Liu, S. Xu, B. Xiao, P. Xue, W. Wang, Z. Ma, Effect of ball-milling time on mechanical properties of carbon nanotubes reinforced aluminum matrix composites, Composites Part A: Applied Science and Manufacturing, 43 (2012) 2161-2168.

[140] H. Kwon, D.H. Park, J.F. Silvain, A. Kawasaki, Investigation of carbon nanotube reinforced aluminum matrix composite materials, Composites Science and Technology, 70 (2010) 546-550.

[141] H.-C. Oh, S.-H. Lee, S.-C. Choi, The reaction mechanism for the low temperature synthesis of Cr2AlC under electronic field, Journal of Alloys and Compounds, 587 (2014) 296-302.

[142] H. Kwon, M. Estili, K. Takagi, T. Miyazaki, A. Kawasaki, Combination of hot extrusion and spark plasma sintering for producing carbon nanotube reinforced aluminum matrix composites, Carbon, 47 (2009) 570-577.

[143] Z. Liu, B. Xiao, W. Wang, Z. Ma, Developing high-performance aluminum matrix composites with directionally aligned carbon nanotubes by combining friction stir processing and subsequent rolling, Carbon, 62 (2013) 35-42.

[144] H. Li, J. Kang, C. He, N. Zhao, C. Liang, B. Li, Mechanical properties and interfacial analysis of aluminum matrix composites reinforced by carbon nanotubes with diverse structures, Materials Science and Engineering: A, 577 (2013) 120-124.

[145] J.G. Park, D.H. Keum, Y.H. Lee, Strengthening mechanisms in carbon nanotube-reinforced aluminum composites, Carbon, 95 (2015) 690-698.

[146] B. Sarina, T. Kai, A. Kvithyld, E. Thorvald, M. Tangstad, Wetting of pure aluminium on graphite, SiC and Al2O3 in aluminium filtration, Transactions of nonferrous metals society of China, 22 (2012) 1930-1938.

[147] B. Guo, X. Zhang, X. Cen, X. Wang, M. Song, S. Ni, J. Yi, T. Shen, Y. Du, Ameliorated mechanical and thermal properties of SiC reinforced Al matrix composites through hybridizing carbon nanotubes, Materials Characterization, 136 (2018) 272-280.

[148] B. Guo, M. Song, J. Yi, S. Ni, T. Shen, Y. Du, Improving the mechanical properties of carbon nanotubes reinforced pure aluminum matrix composites by achieving non-equilibrium interface, Materials & Design, 120 (2017) 56-65.

[149] B. Guo, X. Zhang, X. Cen, B. Chen, X. Wang, M. Song, S. Ni, J. Yi, T. Shen, Y. Du, Enhanced mechanical properties of aluminum based composites reinforced by chemically oxidized carbon nanotubes, Carbon, 139 (2018) 459-471.

[150] H. Kwon, M. Leparoux, Hot extruded carbon nanotube reinforced aluminum matrix composite materials, Nanotechnology, 23 (2012) 415701.

[151] W. Zhou, T. Yamaguchi, K. Kikuchi, N. Nomura, A. Kawasaki, Effectively enhanced load transfer by interfacial reactions in multi-walled carbon nanotube reinforced Al matrix composites, Acta Materialia, 125 (2017) 369-376.

[152] W. Chen, Y. Liu, C. Yang, D. Zhu, Y. Li, (SiCp+ Ti)/7075Al hybrid composites with high strength and large plasticity fabricated by squeeze casting, Materials Science and Engineering: A, 609 (2014) 250-254.

[153] E. Neubauer, M. Kitzmantel, M. Hulman, P. Angerer, Potential and challenges of metal-matrix-composites reinforced with carbon nanofibers and carbon nanotubes, Composites Science and Technology, 70 (2010) 2228-2236.

[154] W. Zhou, S. Bang, H. Kurita, T. Miyazaki, Y. Fan, A. Kawasaki, Interface and interfacial reactions in multi-walled carbon nanotube-reinforced aluminum matrix composites, Carbon, 96 (2016) 919-928.

[155] B. Guo, B. Chen, X. Zhang, X. Cen, X. Wang, M. Song, S. Ni, J. Yi, T. Shen, Y. Du, Exploring the size effects of Al4C3 on the mechanical properties and thermal behaviors of Al based composites reinforced by SiC and carbon nanotubes, Carbon, 135 (2018) 224-235.

CHAPTER THREE

INVESTIGATIONS PUBLISHED FROM THIS STUDY

3.1 Synopsis

CNTs reinforcement of the nickel aluminide (NiAl) intermetallic matrix was investigated in this study. For the fabrication of the NiAl-CNTs composites, reactive sintering was carefully navigated using the spark plasma sintering technique. Dispersion routes were varied, evaluated and compared to determine the best technique of dispersing CNTs in an intermetallic matrix. Dispersion parameters of the selected dispersion route were still further optimized to achieve homogeneous dispersion of the nanotubes. Sintering parameters were also varied, particularly the temperature and pressure, to prevent the melting out of aluminium during the sintering process due to the melting temperature variance between nickel and aluminium. Characterization techniques like SEM, TEM, XRD, EDS, SAED, HR-TEM and Raman Spectroscopy were employed to study the microstructure-property relationship of the fabricated composites. Finally, the strength and fracture toughness properties were assessed via nanoindentation techniques.

Three (3) papers were produced from this work, all of which are currently under review, been accepted or already published in reputable ISI peer reviewed journals. All the articles are sequentially presented herein, with a view to achieving the specific objectives of this research. Each article embodies the introduction or background, raw materials used, comprehensive experimental procedure, results, thorough analyses and discussion of the results and a concise conclusion based on the findings. Funding organizations were appropriately acknowledged and the consulted literatures cited accordingly at the end of each article.

3.2 THE PUBLISHED ARTICLES:

This work produced three articles which have been published and (or) under review. These articles are herein presented without any modifications.

RESEARCH PAPER 1: INFLUENCE OF BALL MILLING PARAMETERS ON THE DISPERSION AND STRUCTURAL INTEGRITY OF MWCNTs IN NICKEL ALUMINIDE MATRIX POWDERS

Abstract

The novelty of incorporating carbon nanotubes (CNTs) in various matrices is becoming increasingly significant for the development of various composites to match the rising technological demands in industry. However, for the potentials of CNTs to be fully realized, the mandatory requirement to uniformly disperse them must be achieved. To effectively disperse these nanotubes in metallic matrices, ball milling has emerged as an effective method, but concerns still persist as to the ability of this method to achieve uniform dispersion without significant damage to the CNTs. In this work, multi-walled carbon nanotubes (MWCNTs) were dispersed in a nickel aluminide matrix via three different milling methods, using both low and high energy milling regimes. The admixed powders were characterized using X-ray diffraction, Raman spectroscopy, scanning electron microscopy, energy-dispersive x-ray spectrometry and transmission electron microscopy techniques. Results show that a two stage milling, comprised of a 6 h low energy milling with a short term follow up of a low 2 h high energy milling achieved the best MWCNTs dispersion and retained their structural integrity.

Keywords: Ball milling, carbon nanotubes, dispersion, structural integrity, nickel aluminide, two stage milling

1. Introduction

For almost three decades now, carbon nanotubes (CNTs) have drawn researchers' attention in a progressive fashion. The reason is not far-fetched, as they possess exceptional qualities that transcend the qualities of traditional materials. With Young's Modulus of 1TPa, density of 2.1g/cm^3, tensile strength of ~130 GPa and thermal conductivity of ~3000W/M/K, these nanomaterials stand a clear shoulder ahead of their particulate and fibre counterparts [1].

However, despite these exceptional properties, effective dispersion of these nanomaterials in metal matrices is a crucial factor [2], which has remained a daunting task for researchers till date [3]. This is owing to the strong van der waals forces [4] and poor wettability between metal matrices and carbon nanotubes [5]. Overcoming these challenges mandated researchers to explore and develop various dispersion techniques such as the ultrasonic-assisted solvent dispersion [6], high energy ball milling [7, 8], in-situ synthesis [9, 10], molecule level mixing [11], melt infiltration [12], cryomilling [1] and nano scale dispersion [13] with variable levels of success.

Of these processes, ball milling is fast becoming one of the most popular methods owing to the simplicity of its operation, flexibility for bulk processing and low cost [1, 14, 15]. The high energy ball milling process has been identified as a viable route to achieving homogenously dispersed CNTs in reinforced composites [7]. Due to the distinctive procedure of high energy ball milling, which comprises of continual disintegration and fracturing of powder particles, a uniform dispersion of reinforcements can be attained in the powder matrix [16]. However, the repetitive collision forces of the milling balls on the CNTs, poses the risk of unavoidable damage to these delicate nanomaterials. The damages caused by harsh milling conditions may occur via vacancies in the carbon-carbon structure of CNTs, open edges and side wall sp^3 disorders [17]. The production of flattened CNTs with distorted or open end tips, and deformation of side walls are all structural defects that are indicative of aggressive ball milling conditions which destroy the morphology of the CNTs and adversely affect their unique characteristics [18]. To this end, ball-milling parameters must be carefully selected and controlled appropriately in order to achieve uniform dispersion while minimizing damage to the CNTs.

The superior characteristics of CNTs reinforced composites as compared to their unreinforced counterparts are not only dependent on the degree of dispersion, but also on the preserved crystallinity of the CNTs in the system [17]. Of utmost importance also, is the fact that the load bearing capacities of CNTs are extremely contingent on their cylindrical nature and structural integrity [19]. Thus, the challenge remains to preserve the structural integrity, and by extension, the unique properties of CNTs, while still ensuring their uniform dispersion in the matrix materials [20, 21]. This balance is extremely crucial in obtaining good mechanical properties in the resulting composites as it has been widely established that effective dispersion of CNTs is a mandatory requirement before any substantial benefit can be realized in the composites [2]. In-homogenous dispersion of CNTs due to clustering and agglomeration in metal matrices have led

to a deterioration in strength of the resulting composites owing to the generation of micro-cracks at the interface, leading to deteriorating mechanical properties which is counterproductive [5]. The CNTs clusters acting as crack nucleation sites in the composites, lead to sudden failure of the composites under loading [22].

The dispersion of CNTs in powder matrices is quite critical, as successive processing stages like compaction and sintering will not enhance the dispersion. Any residual CNTs agglomerates in the admixed powders will unarguably still be present in the finished component [5]. In addition, it is inferred that pre-agglomerated CNTs before sintering results in a higher concentration of defects in CNTs due to friction experienced by discrete CNTs from the neighbouring CNTs and adjacent metal matrix powders [23]. Thus, it is becoming more pertinent to establish a simple and effective dispersion method as a basis for composite synthesis.

CNTs have been incorporated into ceramic [3], polymer [24, 25] and metal [26, 27] matrices. However, very few researchers have incorporated these nanomaterials into intermetallic matrices like nickel aluminides. In this work, MWCNTs were dispersed in a nickel aluminide matrix using three different ball milling regimes, with varying times and speeds in a bid to do a detailed study of what transpires at each stage of milling during dispersion. Furthermore, a combination of low energy ball milling and high energy ball milling [22, 28] was utilized in some of the regimes, with a view to optimizing a good balance between the two milling processes and analysing the level of dispersion at each milling stage. Previous studies have opined that processing techniques utilized in dispersing CNTs in metal matrices dictate the resulting dispersion and structural integrity of CNTs [23]. Hence, to fully actualize the reinforcing outcome of CNTs in metal matrix composites (MMCs), emphasis should be placed on the dispersion stage, with parameters painstakingly selected and optimized.

The motivation for this study was targeted at surmounting the difficulties encountered during the dispersion of CNTs in metallic powder matrices as there is a need to focus on improving the dispersion of CNTs especially during pre-sintering stages. Uniform distribution of CNTs in the metal matrix and preservation of the structural integrity of CNTs are the major determinants on which the mechanical characteristics of CNTs reinforced MMCs are hinged [29, 30], therefore the need to strike a balance between these highlighted factors during dispersion. This present work investigated quantitatively the MWCNTs evolution during their dispersion in NiAl matrix powders via three milling regimes. The emphasis of this study is to determine the best method of CNTs dispersion in nickel aluminide matrix powders by extensive

characterization of the admixed powders after the selected ball milling regimes. It is anticipated that the results obtained will form a valuable ground work and contribute to the synthesis of MWCNTs reinforced NiAl composites suitable for high temperature use in aerospace and automobile applications.

2. Materials and Method

2.1 Raw materials

The MWCNTs dispersed in the powder matrix were obtained from Nanocyl Belgium, with the following specifications - average diameter of 9.5 nm and l.5 µm average length. 99.8 % pure spherical aluminium powder with average particle size of 25µm was obtained from TLS Technik GmbH & Co., Germany and commercially available nickel, supplied by Weartech Limited with particle size of 0.5 - 3.0 µm and 99.5 % purity were used as starting powders in this study.

2.2 Ball milling processes of Ni-Al-CNTs

Planetary ball mills, Retsch PM 100 MA (for low energy ball milling - LEBM) and Retsch PM 400 MA (for high energy ball milling - HEBM) were employed for dispersing MWCNTs in NiAl metal matrix powders. Constant weight fraction of MWCNTs (1 wt %) was employed for effective evaluation and comparison across all samples. The elemental powders and the 1 wt % MWCNTs powders were poured into stainless steel milling jar of 250 ml capacity. Two different sizes of milling balls were used with diameters 5 and 10 mm respectively. The essence of combining the different ball sizes was to preclude the cold welding of the powders and to increase the impact energy available to the powders [31]. The ball-to-powder ratio (BPR) for this investigation was set at 10:1 with the ball milling machine pre-set to 10 min break after each 10 min interval of milling on both the high and low energy milling machines. This was done to ensure that the powders do not get excessively charged up due to impact forces arising from the ball to powder collisions [32]. Powder mixtures with composition Ni:Al = 1:1 with 1 wt % MWCNTs were milled together using different ball milling regimes namely:

(i) 250 rpm for 4 h (HEBM)

(ii) 150 rpm for 6 h (LEBM) followed by secondary milling at 75rpm for 2h (HEBM)

(iii) 100 rpm for 6 h (LEBM) followed by secondary milling at 150rpm for 1h (HEBM)

8 h was chosen as the total maximum ball milling threshold for this work as Liu et al, [33] documented that when ball-milling duration extended further than 8 h, enhancement in the dispersion was not so evident, whereas the damage to CNTs became more severe. A process control agent (PCA) was not used in the course of this work as it was assumed that the hydrophobic fibrous structure of MWCNTs will enable them act as lubrication during ball milling [34] and consequently reduce cold welding while increasing the deformation rate of the powder particles [35, 36]. Moreover, PCA was left out in order to exclude the likelihood of contamination regularly encountered when PCA decomposes into its basic elements during milling which could eventually promote cold welding over fracturing of powders [37, 38]. MWCNTs were used for this work as they have larger diameters as compared to SWCNTs with decreased specific surface area. This reduction in the specific surface area is known to enhance the dispersion capabilities of MWCNTs in matrices [39, 40].

2.3 Materials Characterization

The morphology of the MWCNTs in the admixed powder samples was studied by using transmission electron microscopy (TEM, Philips CM200 and JEOL JEM - 2100). TEM analyses of the powder samples were carried out at 150 keV. The morphology of the powder samples were also examined using scanning electron microscopy (SEM) Zeiss Sigma and JEOL JSM–7600F coupled with energy dispersive X-ray spectrometry (EDX). Identification of phases present in the admixed powder samples were characterized via X-ray diffractometer (XRD, PANalytical Empyrean model) with Cu-Kα radiation (λ=0.154 nm) at a scanning rate of 1°/ min. Raman spectroscopy (T6400 Jobin–Yvon, HORIBA, Japan) was performed on both the pure MWCNTs and the admixed powder samples from the three different milling regimes with a 514.5 nm laser employing a 20x objective lens. A spectral range of 200 - 2300 cm^{-1} was employed for all the powder mixtures to quantitatively determine the level of damage on the MWCNTs based on their process history.

3. Results and Discussion

3.1 SEM morphology of admixed NiAl-CNTs powders

Fig. 1 reveals the morphology of the starting powders. Fig. 1a shows the morphology of the pure MWCNTs consisting of cylindrical tubes bounded tightly by van der waals forces, making them highly agglomerated together. These van der waals forces, in addition to the high aspect ratios of the nanotubes make dispersing them in metallic matrices a challenging task [23]. The spherical powders of the as-received aluminium powder particles are displayed in Fig. 1b. While Fig. 1c reveals the uniquely textured nickel powder particles consisting of spiky, needle-like structures. Fig. 1d shows the TEM image of the highly agglomerated MWCNTs in corroboration with the SEM image in Fig. 1a. Fig. 1e displays the interlayer spacing between the pristine CNTs walls, corroborated by the Fast Fourier Transform (FFT) image in Fig. 1f estimating the distance apart to be 0.3507 nm.
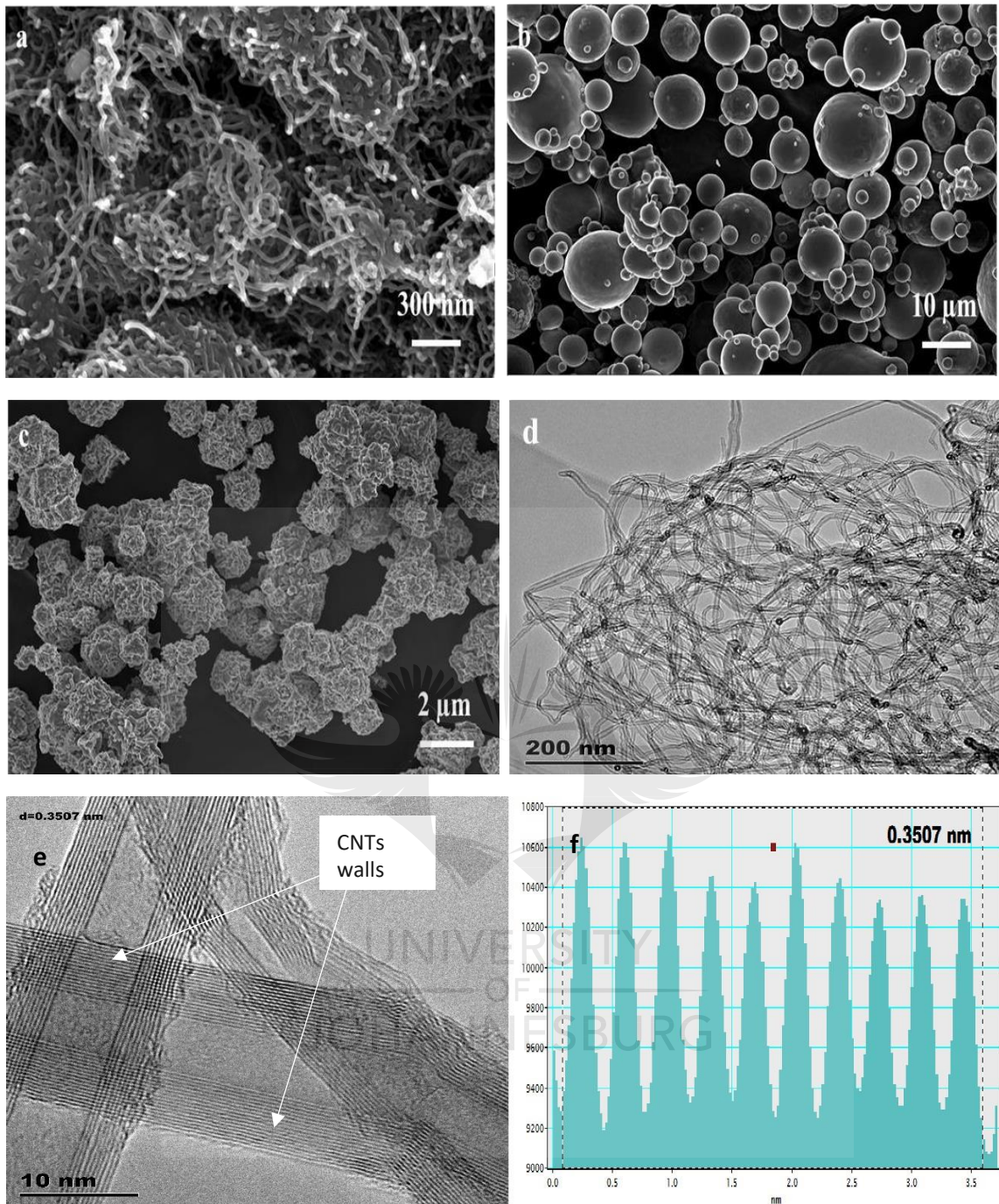
Fig. 1: micrographs of starting powders (a) MWCNTs (b) aluminium (c) nickel (d) TEM micrograph of MWCNTs (e) HR-TEM image revealing the individual CNTs walls and (f) FFT image of pristine MWCNTs

The MWCNTs were added to the nickel and aluminium powder particles from the beginning of each milling regime. Sample A was milled using HEBM at 250 rpm for 4 h. The microstructural evolution of this sample could not be investigated after the first 2 h unlike in the other samples because the powder yield was extremely low, taking out of this amount would

have jeopardized the remaining two hours of milling in this regime. Hence, the absence of micrographs after 2 h of milling for this milling regime. The observed microstructural image of sample A in Figs. 2a and b is consistent with the microstructural evolution observed in Xu et al. [28] after 9 h of HEBM at 270 rpm with no apparent trace of CNTs in these images. This may be attributed to the similarity in the high milling speed of these two regimes. This may be the plausible reason for the apparent absence of observable MWCNTs as the MWCNTs may have been significantly destroyed in this high energy regime. Though this sample experienced the shortest duration of milling, the micrographs indicate that the milling speed is also very crucial and hence a short term milling at extremely high speeds can be as destructive as prolonged milling.
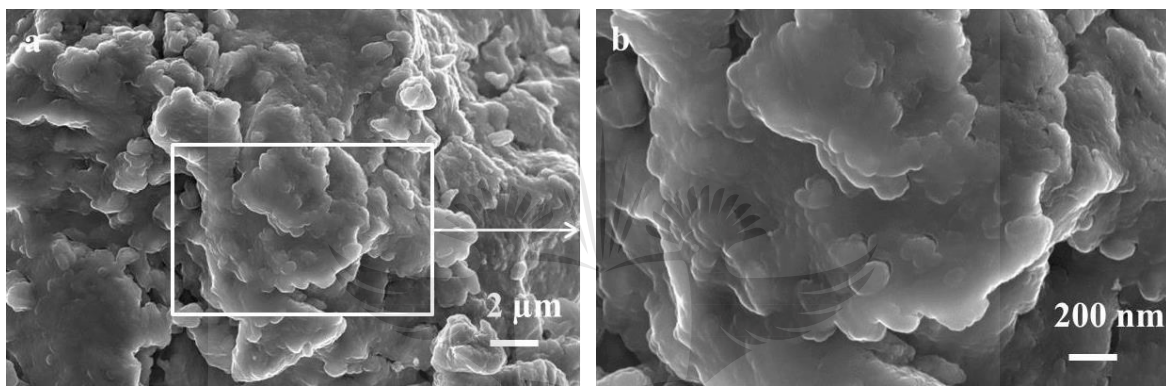
Fig. 2: SEM images of Sample A after 4 h of HEBM at 250 rpm (a) at lower magnification (b) at higher magnification

Fig. 3 depicts the morphology of sample B after every two hours for the full duration of the milling. This sample was subjected to a 6 h low energy milling at 150 rpm in the primary stage which was followed up with a 2 h high energy milling at 75 rpm for the secondary stage. After the first 2 h, MWCNTs clusters were still seen (Fig 3a) but dispersion had commenced as a layer of MWCNTs can be observed across the mid-section of the fractured nickel and aluminium powders demonstrating that the speed was sufficient for the gradual debundling of the MWCNTs. This debundling process progressed uniformly as observed in Figs. 3b and c, with the MWCNTs being dispersed over larger surface areas as the milling time progressed. Fig. 3d (after the secondary stage milling) reveals a uniform microstructure of embedded and well dispersed MWCNTs within the powder matrix. Fig. 3e is a higher magnification of Fig. 3d revealing the MWCNTs clearly dispersed within the matrix powders.
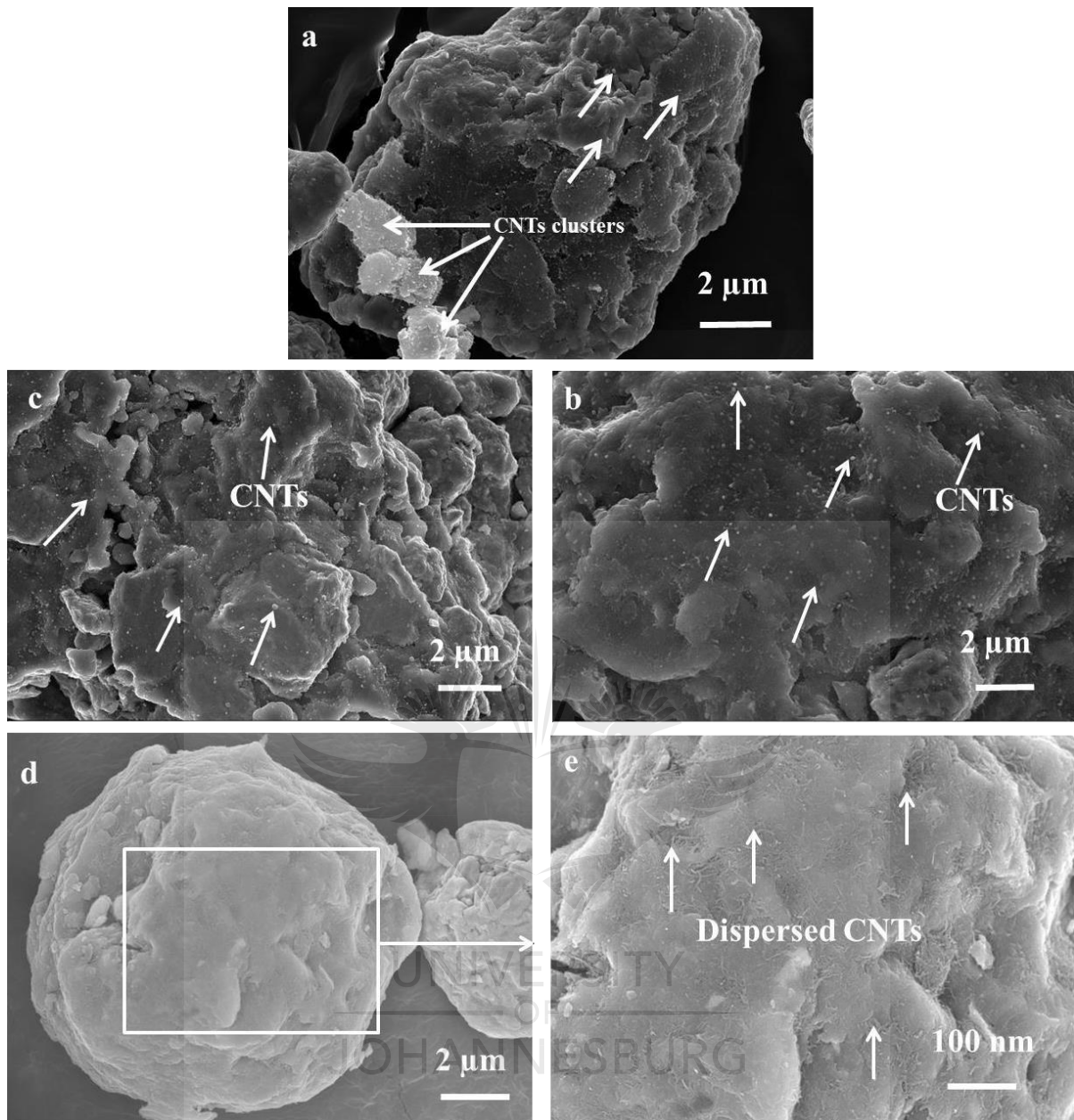
Fig. 3: Sample B (a) after 2 h (b) after 4 h (c) after 6 h (d) after 6h LEBM and 2 h HEBM
(e) high magnification of (d)

As observed in Fig. 4a, after the first 2 h of milling, micrographs still revealed distinct morphologies of the starting powders without any sign of deformation or fracturing. Physically, the powder particles at this stage still settled out owing to the different densities of the mixture. This was an indication that the speed employed at this stage was not sufficient to commence the debundling process for the MWCNTs, nor the deformation of the nickel or aluminium powder particles. This continued even after 4 h of milling in this regime as depicted in Fig. 4b. The debundling of the MWCNTs for this sample can be estimated to have eventually commenced at the final stages of the primary milling as Fig. 4c reveals the attachment of

MWCNTs cluster to a distinct nickel particle powder. During the second stage however, in Fig. 4d, the MWCNTs were seen to be dispersed within the short high energy ball milling duration of only 1 h. It is significant to note that the speed employed during this stage was higher (150 rpm) than that employed during the primary milling (100 rpm) stage. Hence the efficacy of this stage in dispersing the MWCNTs clusters that were still present in the powders after the completion of the primary stage. Fig. 4e shows the MWCNTs dispersed in the matrix at higher magnifications. Comparing Figs. 3e and 4e, it can be observed that the carbon nanotubes in Fig. 3e are well embedded within the fractured powder particles as compared to the MWCNTs in Fig. 4e which seem to be evidently more dispersed over the fractured powder particles and not embedded within the powder particles. This is ascribed to the sufficient milling speed employed in sample B which facilitated debundling and embedding of the nanotubes gently into the powder particles which was not achieved in sample C owing to the insufficient speed of the low energy regime employed. The high speed employed in the HEBM for sample C favoured dispersion of the nanotubes over embedding, hence the significant presence of the nanotubes over the powder particle surface as observed in Fig. 4e.
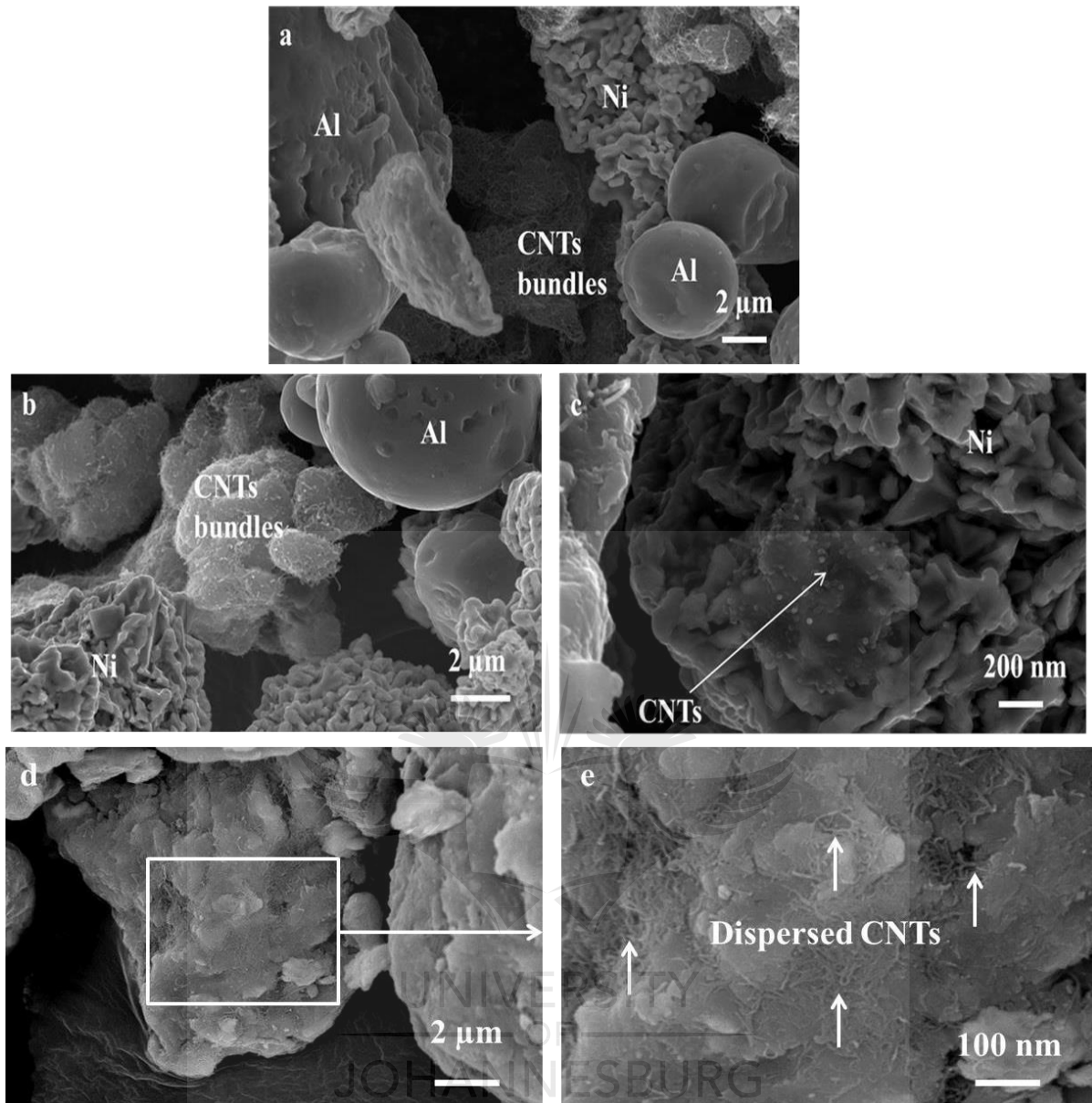
Fig. 4: Sample C (a) after 2 h (b) after 4 h (c) after 6h (d) after 6h LEBM and 1 h HEBM

Fig. 5 depicts the surface morphology of the admixed powders in sample A after the completion of the milling regime. The admixed powder particles are seen to be of near-equal sizes due to the amount of energy transferred to them during the high energy ball milling. Hence, large clusters of powder particles are absent in this image. Back scattered electron images are usually used to distinguish contrasts between areas h94aving differing chemical compositions [41]. The contrasts in sample A are evidenced in Fig. 5b from the back scattered electron images. Since nickel is the heaviest of all the elements present in this matrix, it scatters electrons stronger than the other elements, hence it appears brightest in the image. Fig. 5c depicts the EDS micrograph revealing the presence of carbon, nickel and aluminium in the region highlighted.

94
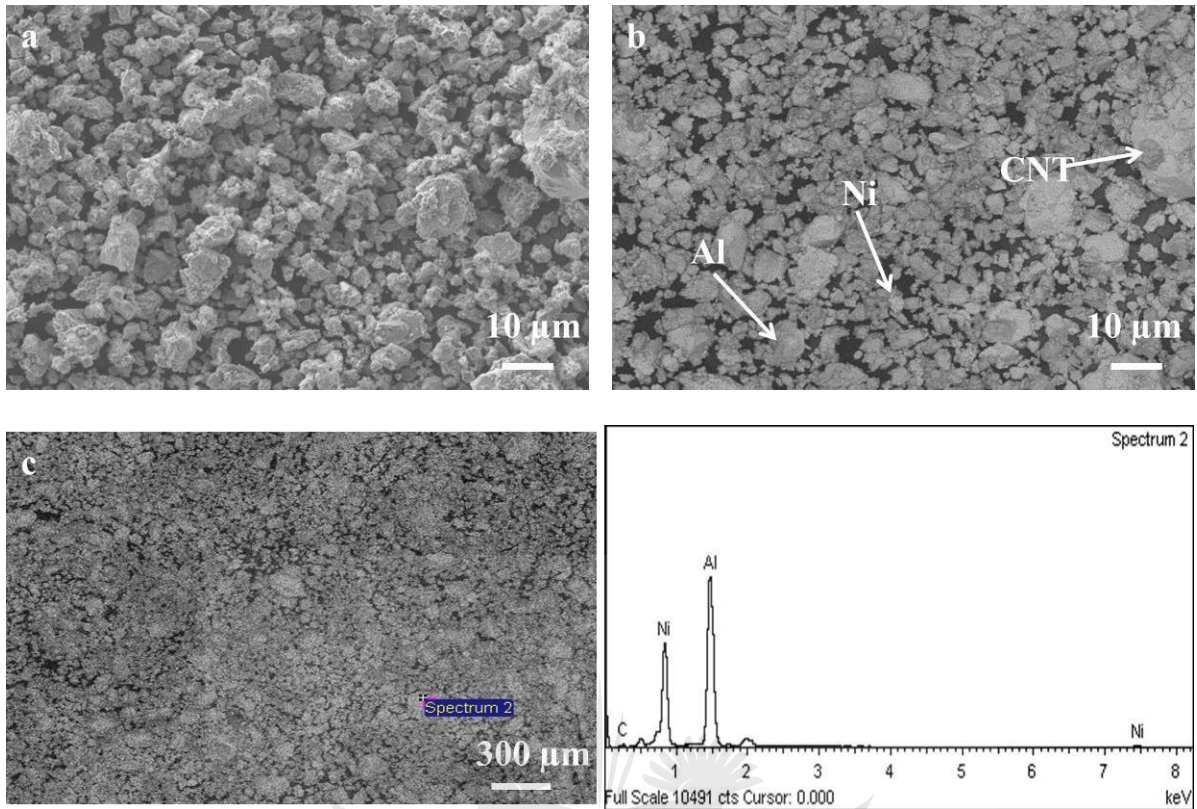
Fig. 5: Sample A (a) Secondary electron images (b) back scattered images (c) EDS

Sample B in Fig. 6a reveals a more coarse powder particle structure with some large clusters observed amidst the smaller powder particles. This is possibly due to the very low speed employed during the high energy milling stage which mayhave led to the accumulation of the admixed powder particles. Fig. 6c shows a region in sample B with the corresponding EDS image revealing the presence of all three elements in the highlighted region.
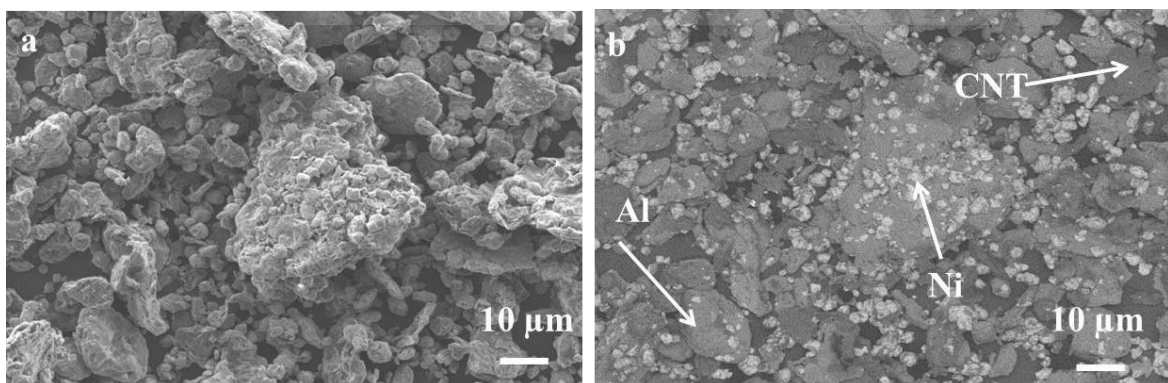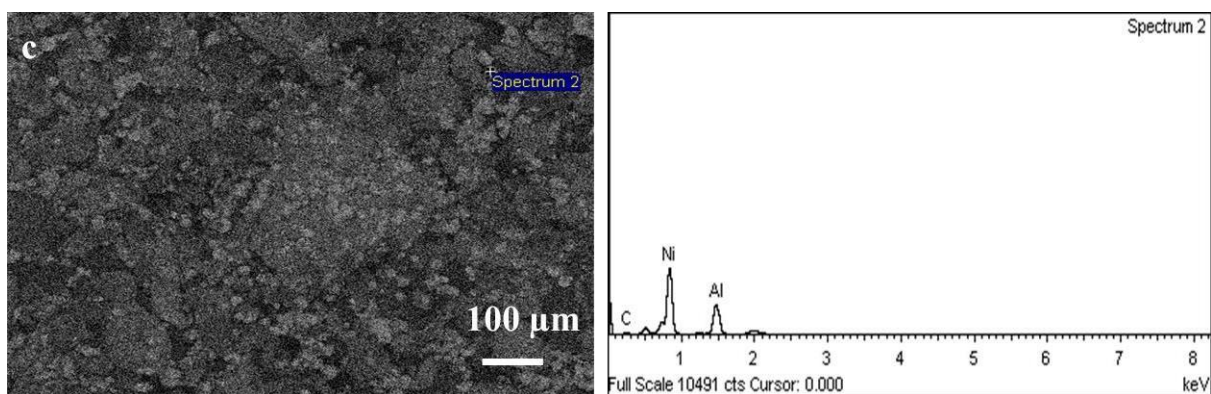
Fig. 6: Sample B (a) Secondary electron images (b) back scattered images (c) EDS

Fig. 7a shows the surface morphology of the admixed powders in sample C. The clusters of the admixed powders here are observed to be less coarse than that which was observed in sample B but not as fine as that which was observed in sample A. The observed morphology therefore seem to be a mid-point between the previous two surface morphologies. Clear contrasts between the nickel, aluminium and MWCNTs in this sample are observed in Fig. 7b while Fig. 7c shows the EDS revealing the presence of these elements in the highlighted region.
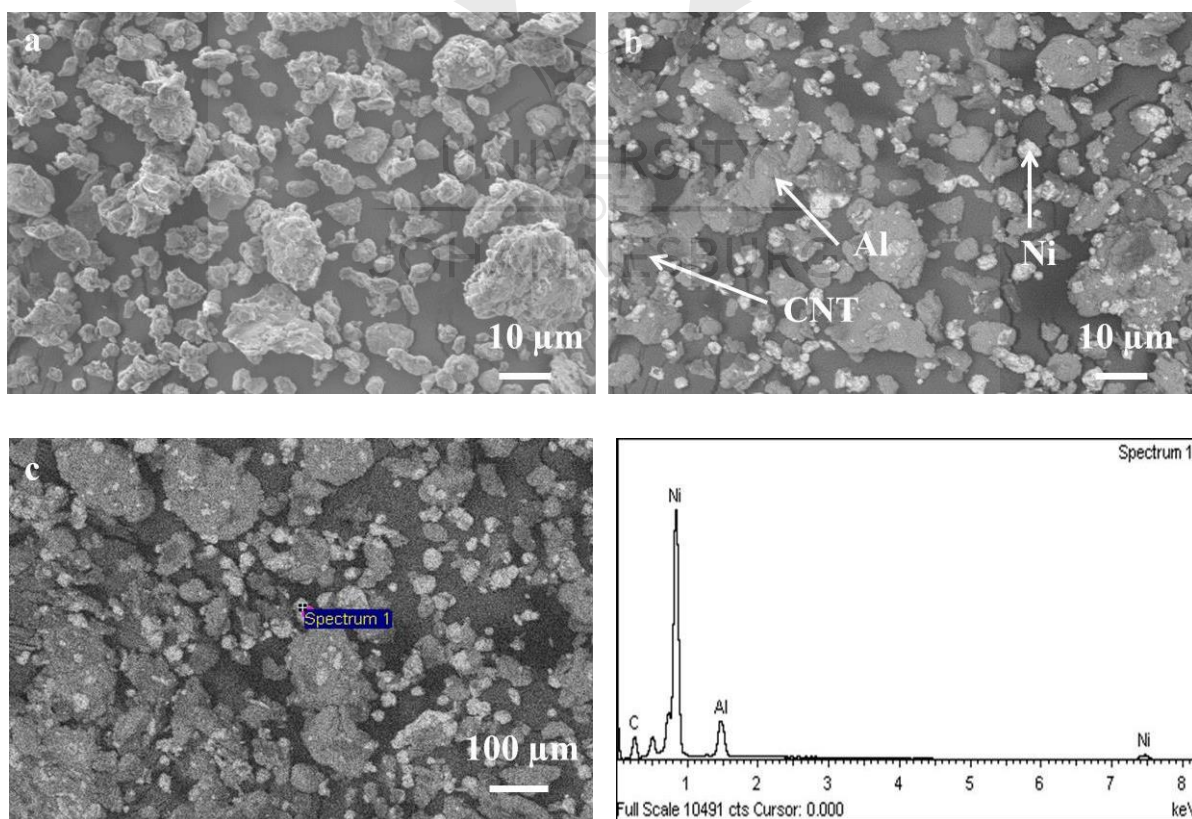
Fig. 7: Sample C (a) Secondary electron images (b) back scattered images (c) EDS

3.2 XRD analyses of admixed powders

Phase identification in the admixed powder samples was done using X-ray diffraction analyses. Fig. 8 shows the XRD spectra of the Ni-Al-CNTs admixed powders processed by the various milling regimes. Distinctive peaks consistent with the formation of nickel aluminide intermetallic compound can be detected in all the samples indicating that mechanochemical reactions took place during the milling regimes facilitating inter-diffusion between the nickel and aluminium. Peaks corresponding to aluminium carbides are also observed across all the samples. This may be a consequence of the HEBM regimes experienced by all the samples at some point in their processing.
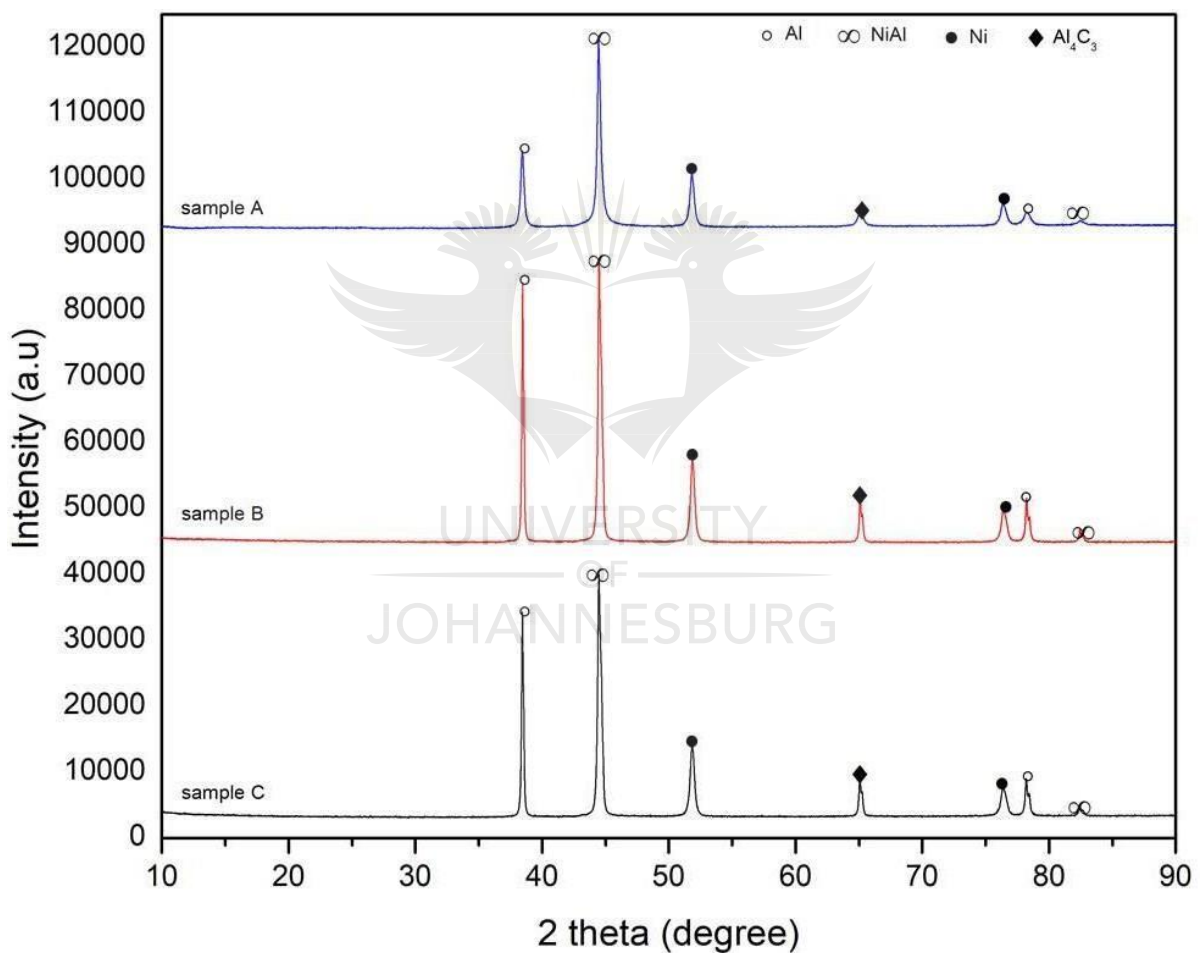
Fig. 8: X-Ray Diffraction patterns of the milled powder samples

Also, no sign of MWCNTs can be seen in Fig. 8, which might be attributed to the small quantity of MWCNTs in the powder samples and the wide variance in the scattering length of carbon atoms as compared to the nickel and aluminium atoms [42]. The XRD limit of low detection

which may be insufficient in identifying low levels of CNTs present within the metal atoms [32]. Distinctive peaks corresponding to the presence of nickel, aluminium, nickel aluminide and aluminium carbide (Al_4C_3) are observed in Fig. 8 for all the milled powder samples. The formation of Al_4C_3 is usually triggered as a result of interfacial reaction between defective CNTs sites and aluminium [43].

3.3 Raman Spectroscopy

Raman spectroscopy was used to evaluate the damage done on the MWCNTs during the various regimes of ball milling. Fig. 9 reveals the Raman spectra of the pure MWCNTs and the NiAl-CNTs admixed powders. It can be observed that the major features of this spectra are the two distinctive peaks namely the D and G peaks which occur at about 1350 cm^{-1} and 1600 cm^{-1} respectively. The D-peak is due to diamond mode (sp^3-bonds), relating to the presence of disorder, defects, vacancies or amorphous carbon in the CNTs structures [44], so that it will heighten and broaden as the concentration of defects increases in the nanotubes [45, 46]. The G-band on the other hand, is due to the graphite mode (sp^2-bonds), corresponding to the degree of crystallinity and graphitic ordering of the C-C atoms and will thus broaden and reduce with increase in the concentration of defects or disordering in the nanotubes [47, 48].
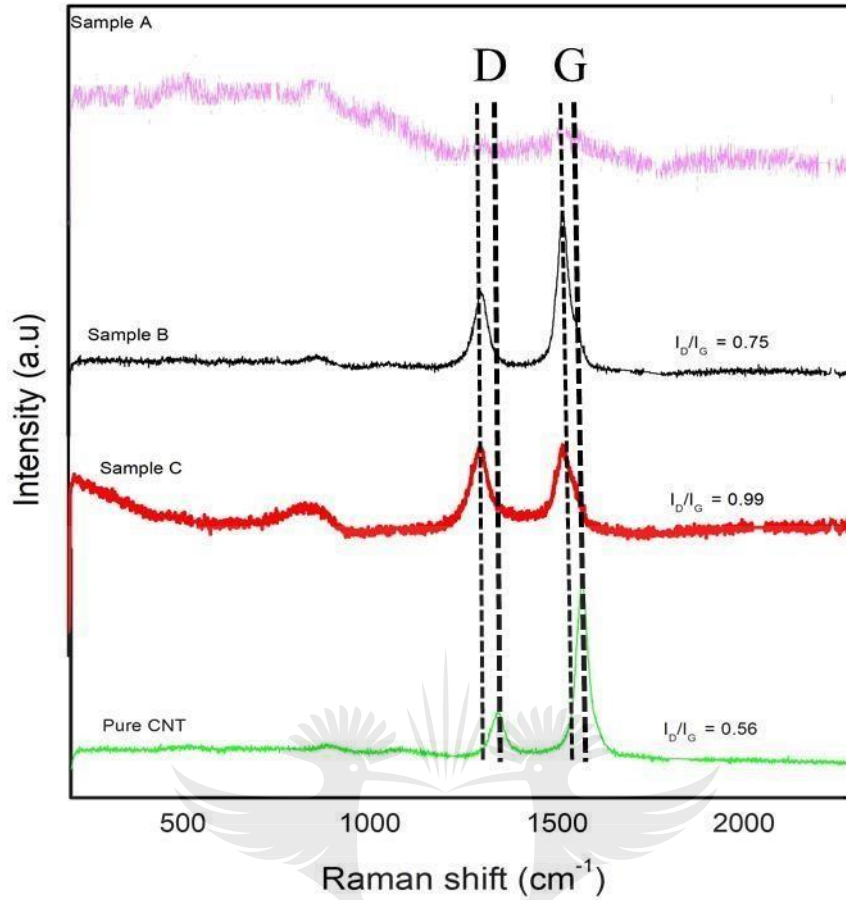
Fig. 9: Raman spectra for the pure MWCNTs and the milled composite powders

Consequently, the I_D/I_G ratio (non sp^2/sp^2 ratio or sp^3/sp^2 ratio) relates to the ratio of the structural defects induced during the dispersion process to the degree of crystallinity in CNTs [49]. Hence, the severity of damage to the CNTs is quantitatively assessed by the average I_D/I_G ratio [50, 51]. It is widely accepted as a valuable quantitative and qualitative means of assessing the structural damage done to CNTs as a result of the dispersion process [52]. The calculated I_D/I_G values are shown in Table 1.

Table 1 - Raman ratios of the admixed powders

Sample Code	I_D/I_G ratio	% increase
As received MWCNTs	0.56	-
Sample A	-	-
Sample B	0.75	34
Sample C	0.99	77

The I_D/I_G ratio of the pure MWCNTs powder was 0.56, showing the dominance of sp^2 C–C bonds over non-sp^2 or sp^3 disorders [50]. Generally, all the samples with the exception of sample A show a Raman ratio less than 1, which indicates the dominance of crystallinity over amorphization.

The degree of disorder, (D band) in the Raman spectra of CNTs increases with intense dispersion conditions. The increase in the D band corresponds to the increase in sp^3 defects in milled CNTs consistent with defects induced on the side walls of the MWCNTs during prolonged milling or with high milling speeds. Once the induced damage becomes significant during the milling processes, the crystallinity of the CNTs invariably reduces [17]. It is essential to maintain the tubular structure of CNTs during dispersion since all the superior properties of the nanotubes can be attributed to this structural uniqueness. Consequently, any impairment done to their structure would undeniably affect their performance as reinforcements [43, 53].

From Fig. 9 it can be observed that the G-band peaks in the milled powders shifted from 1600 cm^{-1} to 1500 cm^{-1} relative to the as received MWCNTs, which may be credited to the permeation of the nickel and aluminium atoms into the MWCNTs, resulting in an adjustment in their sp^2 bonding structure [54]. The I_D/I_G ratios given in Table 1 reveal the different impacts the dispersion methods had on the integrity of the MWCNTs. Unarguably, the I_D/I_G ratios have generally increased compared to that of the as received MWCNTs. Particularly, the intensity of the milling regimes can be quantitatively evaluated by these ratios. Sample A received the harshest milling regime of high energy ball milling throughout the milling process. As shown, no observable D and G peaks can be seen in its Raman spectra. This is due to amorphization of the carbon atoms as a result of the complete loss of crystallinity because of the processing parameters. Since the milling time for this sample A was significantly shorter (4 h) than that of the other routes, the extensive loss of crystallinity observed can therefore be attributed to the high milling speed employed for its dispersion processing. As revealed from these ratios, all the dispersion routes induced some level of damage or disordering in the samples but the degree

of damage is seen to increase significantly with increase in milling speed as Raman ratios got higher with higher milling speeds. The ratio for sample B was 34% higher than for the as received MWCNTs which was the lowest Raman ratio corresponding to the least intensity of damage induced in this study. The sample C however, shows a 77% increase over the ratio of the as received indicating a much higher level of damage in this route than its counterpart route (sample B). Though sample C experienced a low energy regime in the first phase of milling at 100 rpm, Raman results for this sample show that the higher energy regime conducted at 150 rpm was too energetic for the CNTs as much damage is observed to have been induced during this stage with a Raman ratio of almost double that of the as received MWCNTs. Though the high energy milling regime was conducted for just 1 h, significant damage was seen to have been induced at this stage. At the higher milling speed of the secondary stage milling, dispersion was rapid as observed in Figs. 4d and 4e, but so was the damage done to the delicate cylindrical structures of the nanotubes. This is significant because damaged CNTs are potential sites for interfacial reaction leading to carbide formation [50]. Studies have shown that defective CNTs are a necessary pre-requisite for carbide formation but not the only condition to be met, as other parameters such as milling speeds and duration also contribute to triggering this interfacial reaction.

3.4 TEM analyses

Fig. 10 depicts the TEM images of sample A which is dominated by damaged and flattened MWCNTs. Some level of amorphization was evident in this sample as observed in Fig. 10a with what resembles a clustering of damaged nanotubes with the MWCNTs not so visible or even distinct. This is owing to the highly energetic milling regime it experienced as compared to all the other samples. It can be observed that the milling regime of this sample adversely affected the morphology of the MWCNTs. Clearer images of the MWCNTs can be observed in Fig. 10b which reveals the flattened MWCNTs with the powder matrix. Highly deformed and damaged nanotubes are observed in Figs. 10c and d respectively. Due to the extreme damage of the walls of the MWCNTs in this sample which led to the collapse and flattening of their walls, the inter-layer distance between them could not be measured during the high resolution TEM analyses.
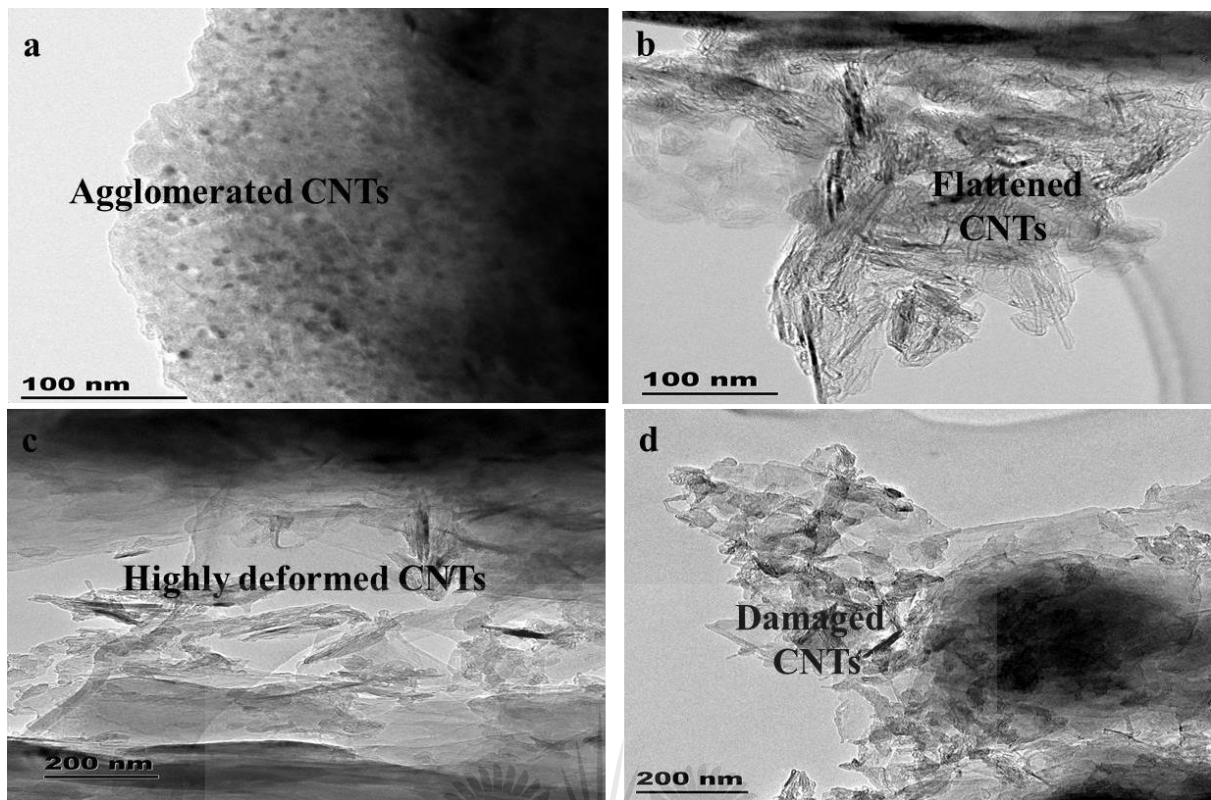
Fig. 10 (a – d): TEM images for sample A milled at 250 rpm for 4 h

However, Fig. 11 reveals a relative uniform dispersion of the MWCNTs within the matrix powders. Fig. 11a shows dispersed MWCNTs in the powder matrix for sample B which experienced a two stage milling with a lower speed during the HEBM. Individual strands of well dispersed nanotubes can be clearly seen in Fig. 11b as well. Fig. 11c shows uniform dispersion of the detangled MWCNTs within the matrix powders. The HR-TEM image of the MWCNTs within this sample is depicted in Fig. 11d revealing the inter-layerspacing between the walls to be 0.355 nm. From Fig. 1d, the interlayer spacing of the pristine MWCNTs was measured to be 0.3507 nm indicating that the milled MWCNTs in sample B differed slightly from the pristine with a marginal 0.0043 nm. This is proof of some slight level of strain induced in the nanotubes during the milling process which was not significant enough to cause colossal damage to them as corroborated by Figs. 9 and 11 on raman spectroscopy and TEM analyses respectively. The nanotubes are also observed to be embedded in the powder particles depicting good interaction between the nanotubes and the matrix powder particles. The images are devoid of any significant damage done to the nanotubes showing that this regime preserved the tubular structure and structural integrity of the MWCNTs. Moreover, the peaks of the fast fourier transform images in the inset of Fig. 11d displays the sharp peaks of the milled CNTs in this sample representing the highly crystalline nature of the CNTs. This indicates that the

crystallinity of the CNTs in this regime was well retained [55].
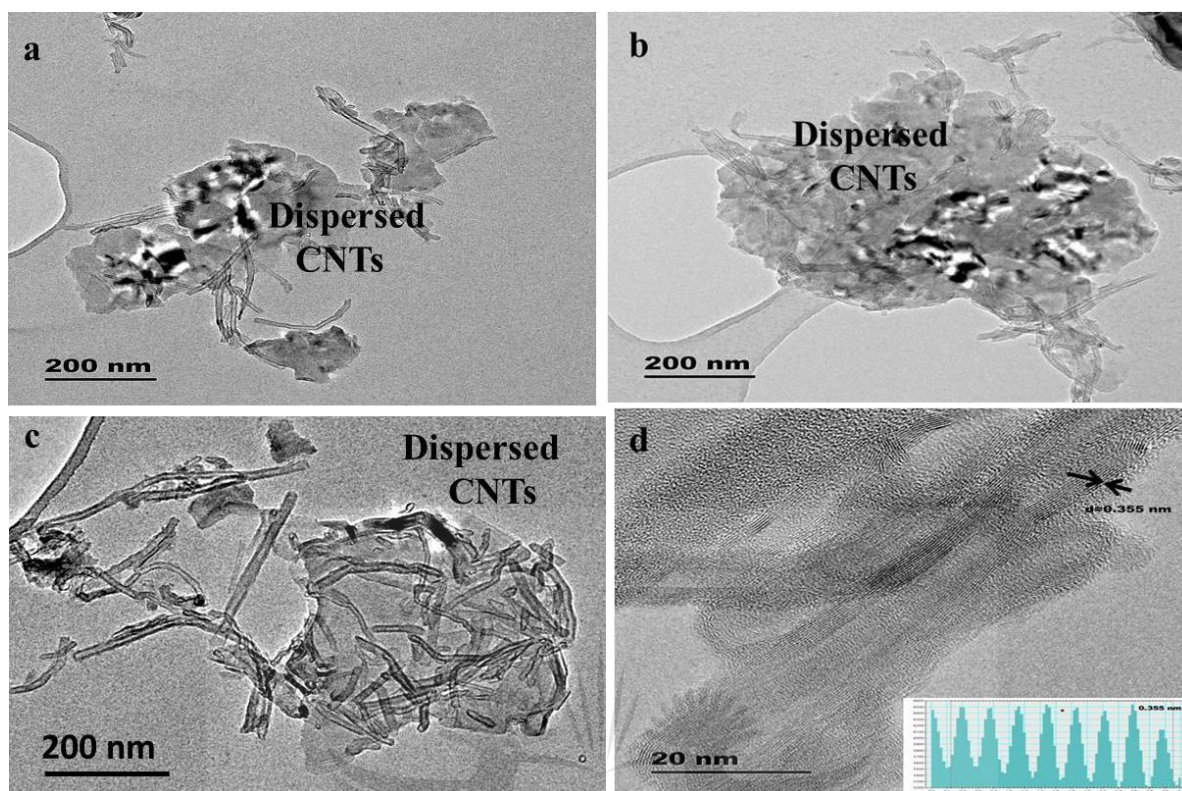
Fig. 11 (a –d): TEM images of sample B milled at 150 rpm for 6 h (LEBM) with additional 2 h milling at 75 rpm (HEBM)

Fig. 12a shows some MWCNTs still loosely clustered together isolated from the matrix powder particles, depicting poor interaction between the nanotubes and the matrix powders. Some individual nanotubes are observed in Fig. 12b detangled within the powder matrix. Fig. 12c reveals some damaged MWCNTs, revealing damage done to the nanotubes owing to the high speed employed during the HEBM regime of this sample. The HR-TEM image in Fig. 12d shows the inter-layer spacing between the walls as 0.340 nm which differs from the pristine inter-layer spacing with a more significant value of 0.0107 nm, indicative of a higher level of damage done to the MWCNTs as compared to the nanotubes in sample B. The plausible reason for this damage is the high speed employed during the secondary stage milling as the primary milling was lower than that employed in sample B and too mild to even cause a detangling of the nanotubes, hence could not have been responsible for this damage. Contrary to sample B, the fast Fourier transform image in Fig. 12d does not display sharp peaks but rather blunt and well-rounded peaks which is an indication of a loss of crystallinity in the milled CNTs in sample C [55].

103
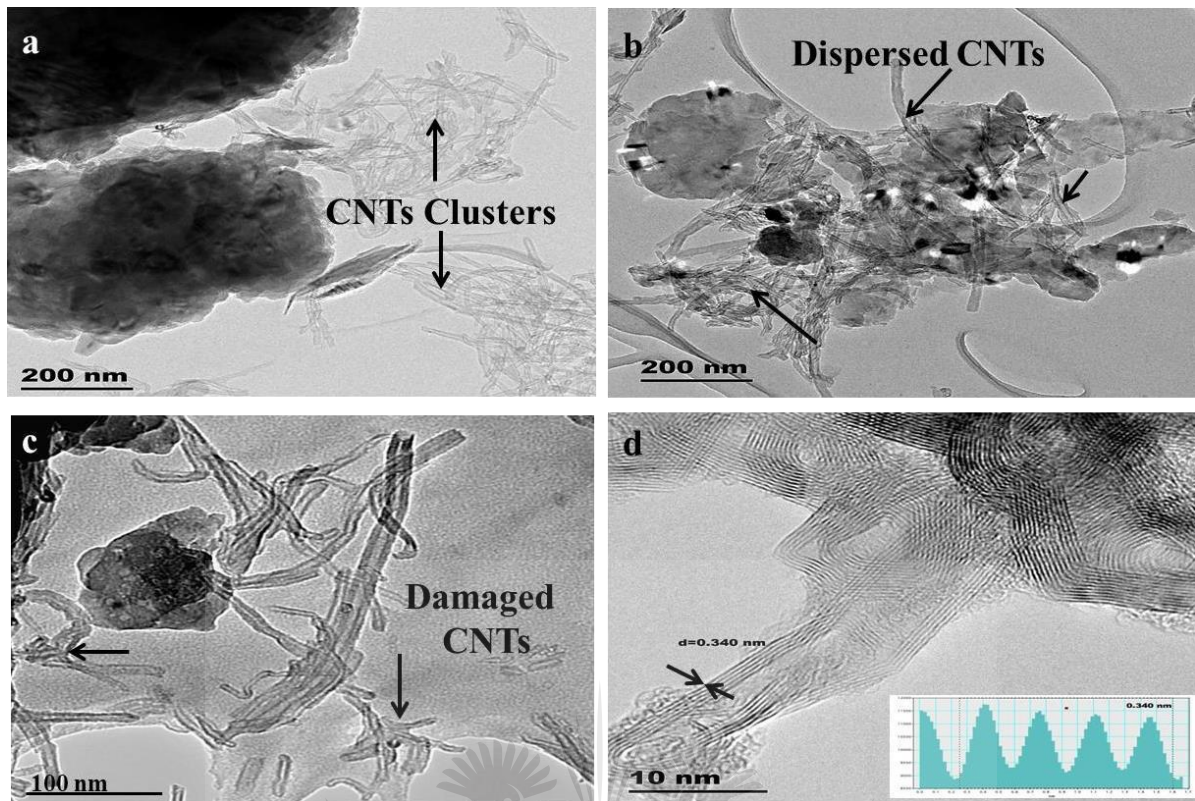
Fig. 12 (a – d): TEM images of sample C milled for 100 rpm for 6 h LEBM and 150 rpm for 1 h HEBM

In the two stage milling regime for sample B, the primary milling comprised of LEBM for the debundling and embedding of MWCNTs in the soft aluminium and nickel powders followed by short term HEBM, for 2 h to achieve better distribution of the MWCNTs and enhanced bonding between the reinforcement and matrix powders. The ductile aluminium and nickel powders apparently protected the embedded MWCNTs during the high energy milling process. Hence the effectiveness of the HEBM in dispersing the CNTs in the matrix powders without inducing substantial damage to the CNTs. Also, the HEBM facilitated the de-agglomeration of the few MWCNTs clusters remaining in the matrix after the completion of the LEBM stage. The novelty of the milling regime in sample B, is the lower milling speed employed during the HEBM. This is a major departure from what is obtainable in literature where the short term follow up HEBM is usually conducted at higher speeds compared to that of the speed during the LEBM stages [22, 28].

104

Low energy ball milling is gentle on the CNT structure, but from reported works, good interfacial bonding is not achieved using this milling method exclusively [28]. A key factor in guaranteeing an efficient load transfer from the reinforcement to the matrix is excellent interfacial bonding [53]. However, poor interfacial bonding has been reported [56, 57] between CNTs and metal matrices and this prevents efficient load transfer mechanism in MMCs. This is undesirable in composites as it tends to defeat the purpose of reinforcement. Composites components synergize by combining the load bearing capacity of the reinforcement with the support system of the matrix. Good interfacial bonding is therefore required for optimum performance of a metal matrix composite.

From the Raman analysis results in Fig. 9, sample B showed the least I_D/I_G ratio of all the three samples depicting the least damage done to the MWCNTs and indicating the highest retention and preservation of the MWCNT structural integrity in this regime. Since lower intensity ratio of D- and G-bands (I_D/I_G) of the CNTs designates higher degree of graphitization and reduced damage [28]. Complementing this with the SEM results in Fig. 3e and TEM results in Fig. 11, which revealed the best dispersion of the MWCNTs, sample B showed the best combination of the two crucial highlighted factors discussed earlier - uniform dispersion and preserved structural integrity. This is perceived to be due to the milling regime which utilized LEBM to disperse and embed MWCNTs in the soft and ductile nickel and aluminium powders, followed by a short term HEBM which did not cause significant damage because the MWCNTs were protected by the surrounding matrix powder particles. Furthermore, a low milling speed was used during the secondary stage milling so as not to induce significant damage to the MWCNTs. From Fig. 11, it can be observed that the MWCNTs in this route retained their unique tubular structures significantly better than in the other regimes as evidenced in Figs. 10b and 12c. Defects like vacancies, open edges and collapsed walls are indicative of harsh milling conditions due to high impact forces from the milling balls, leading to loss of structural integrity and consequently, poor mechanical properties in sintered composites [23, 42]. Undoubtedly, the flattening or collapsing of CNTs walls causes a decline in structural integrity due to the damages in the side walls of the CNTs during milling from the effect of intense collision with milling balls [1] during the harsh milling regime. Minimizing the damage on the reinforcement is a crucial factor for composite preparation. Strengthening effect of the CNTs is predominantly dependent on the implemented processing technique of dispersion, and their inherent properties such as aspect ratio, size, shape and geometry. During processing, as these properties are affected, their load bearing capacity is adversely affected and this prevents efficient stress transfer, leading to composite failing by matrix tensile failure [53].

Comparing Figs. 10, 11 and 12, sample B (Fig. 11) reveals better dispersion and higher retention of original properties of the MWCNTs as against Fig. 12 even though they both went through similar two stage milling procedures. The significant difference between the two was the speed at the second stage high energy milling. The lower speed for sample B prevented much damage and hence preserved the structural integrity of the MWCNTs as corroborated by the Raman ratios in Table 1. Though the first stage low energy milling for sample B was conducted at a higher speed than in sample C, much damage was still not induced at such low energy processes. Furthermore, during the HEBM process of this sample, a very low speed was employed, leading to higher dispersion but reduced damage of the MWCNTs, which was the uniqueness of this milling regime. Sample B therefore shows the best combination of both uniform dispersion and preserved structural integrity of the MWCNTs by careful control of milling parameters.

Conclusion

- This study has shown that the daunting problem of in-homogenous dispersion (due to low milling speeds or inadequate milling time) and excessive milling (due to high milling speeds or prolonged milling), can be solved by a careful choice of processing parameters.

- The two stage milling in sample B showed the best dispersion of CNTs and the highest retention of their structural integrity owing to the careful selection of milling parameters adopted for the dispersion processing. This is a significant deviation from what is usually observed in literature where uniform dispersion is achieved at the expense of CNTs damage or damage is prevented at the expense of significant CNTs agglomerates left undispersed in the matrix. In addition, the lower speed employed during the HEBM secondary milling helped to further preserve the structural integrity of the nanotubes.

- The uniform dispersion achieved in the two stage milling in sample B can be attributed to the long term LEBM which helped to gently debundle and embed the MWCNTs in the fractured powder particles. The follow-up low speed, short term HEBM helped to further disperse the few agglomerates still left within the matrix, hence leading to a homogenous dispersion of the nanotubes without significant damage.

- Severe ball milling conditions lead to damage of the CNTs, loss of their crystallinity and consequently, loss of their structural integrity.

- Optimization of the duration of ball milling and the milling speed during the dispersion processing of CNTs into Ni-Al matrices are crucial to preserving their structural integrity.

Acknowledgement

Conflict of interest

Authors declare no conflict of interest.

References

[1] T. He, X. He, P. Tang, D. Chu, X. Wang, P. Li, The use of cryogenic milling to prepare high performance Al2009 matrix composites with dispersive carbon nanotubes, Materials & Design, 114 (2017) 373-382.

[2] S. Ameri, Z. Sadeghian, I. Kazeminezhad, Effect of CNT addition approach on the microstructure and properties of NiAl-CNT nanocomposites produced by mechanical alloying and spark plasma sintering, Intermetallics, 76 (2016) 41-48.

[3] M. Bocanegra-Bernal, C. Dominguez-Rios, J. Echeberria, A. Reyes-Rojas, A. Garcia-Reyes, A. Aguilar-Elguezabal, Spark plasma sintering of multi-, single/double-and single-walled carbon nanotube-reinforced alumina composites: Is it justifiable the effort to reinforce them?, Ceramics International, 42 (2016) 2054-2062.

[4] K. Aristizabal, A. Katzensteiner, A. Bachmaier, F. Mücklich, S. Suárez, On the reinforcement homogenization in CNT/metal matrix composites during severe plastic deformation, Materials Characterization, (2018).

[5] S.R. Bakshi, A. Agarwal, An analysis of the factors affecting strengthening in carbon nanotube reinforced aluminum composites, Carbon, 49 (2011) 533-544.

[6] J.-z. Liao, M.-J. Tan, I. Sridhar, Spark plasma sintered multi-wall carbon nanotube reinforced aluminum matrix composites, Materials & Design, 31 (2010) S96-S100.

[7] M.R. Basariya, V. Srivastava, N. Mukhopadhyay, Microstructural characteristics and mechanical properties of carbon nanotube reinforced aluminum alloy composites produced by ball milling, Materials & Design, 64 (2014) 542-549.

[8] F. Rikhtegar, S. Shabestari, H. Saghafian, The homogenizing of carbon nanotube dispersion in aluminium matrix nanocomposite using flake powder metallurgy and ball milling methods, Powder Technology, 280 (2015) 26-34.

[9] S. Li, Y. Su, Q. Ouyang, D. Zhang, In-situ carbon nanotube-covered silicon carbide particle reinforced aluminum matrix composites fabricated by powder metallurgy, Materials Letters, 167 (2016) 118-121.

[10] X. Yang, T. Zou, C. Shi, E. Liu, C. He, N. Zhao, Effect of carbon nanotube (CNT) content on the properties of in-situ synthesis CNT reinforced Al composites, Materials Science and Engineering: A, 660 (2016) 11-18.

[11] D.H. Nam, J.H. Kim, S.I. Cha, S.I. Jung, J.K. Lee, H.M. Park, H.D. Park, S.H. Hong, Hardness and wear resistance of carbon nanotube reinforced aluminum-copper matrix composites, Journal of nanoscience and nanotechnology, 14 (2014) 9134-9138.

[12] H. Uozumi, K. Kobayashi, K. Nakanishi, T. Matsunaga, K. Shinozaki, H. Sakamoto, T. Tsukada, C. Masuda, M. Yoshida, Fabrication process of carbon nanotube/light metal matrix composites by squeeze casting, Materials Science and Engineering: A, 495 (2008) 282-287.

[13] T. Noguchi, A. Magario, S. Fukazawa, S. Shimizu, J. Beppu, M. Seki, Carbon nanotube/aluminium composites with uniform dispersion, Materials Transactions, 45 (2004) 602-604.

[14] A. Esawi, K. Morsi, A. Sayed, M. Taher, S. Lanka, Effect of carbon nanotube (CNT) content on the mechanical properties of CNT-reinforced aluminium composites, Composites Science and Technology, 70 (2010) 2237-2241.

[15] J. Li, Y. Xiong, X. Wang, S. Yan, C. Yang, W. He, J. Chen, S. Wang, X. Zhang, S. Dai, Microstructure and tensile properties of bulk nanostructured aluminum/graphene composites prepared via cryomilling, Materials Science and Engineering: A, 626 (2015) 400-405.

[16] A.M. Esawi, K. Morsi, A. Sayed, A.A. Gawad, P. Borah, Fabrication and properties of dispersed carbon nanotube–aluminum composites, Materials Science and Engineering: A, 508 (2009) 167-173.

[17] K.S. Munir, C. Wen, Deterioration of the Strong sp2 Carbon Network in Carbon Nanotubes during the Mechanical Dispersion Processing—A Review, Critical Reviews in Solid State and Materials Sciences, 41 (2016) 347-366.

[18] N.G. Chopra, F. Ross, A. Zettl, Collapsing carbon nanotubes with an electron beam, Chemical physics letters, 256 (1996) 241-245.

[19] O. Lourie, D. Cox, H. Wagner, Buckling and collapse of embedded carbon nanotubes, Physical Review Letters, 81 (1998) 1638.

[20] E. Neubauer, M. Kitzmantel, M. Hulman, P. Angerer, Potential and challenges of metal-matrix-composites reinforced with carbon nanofibers and carbon nanotubes, Composites Science and Technology, 70 (2010) 2228-2236.

[21] A. Agarwal, S.R. Bakshi, D. Lahiri, Carbon nanotubes: reinforced metal matrix composites, CRC press2016.

[22] A. Najimi, H. Shahverdi, Effect of milling methods on microstructures and mechanical properties of Al6061-CNT composite fabricated by spark plasma sintering, Materials Science and Engineering: A, 702 (2017) 87-95.

[23] K.S. Munir, Y. Zheng, D. Zhang, J. Lin, Y. Li, C. Wen, Microstructure and mechanical properties of carbon nanotubes reinforced titanium matrix composites fabricated via spark plasma sintering, Materials Science and Engineering: A, 688 (2017) 505-523.

[24] Y. Hou, J. Tang, H. Zhang, C. Qian, Y. Feng, J. Liu, Functionalized few-walled carbon nanotubes for mechanical reinforcement of polymeric composites, ACS nano, 3 (2009) 1057-1062.

[25] J.N. Coleman, U. Khan, W.J. Blau, Y.K. Gun'ko, Small but strong: a review of the mechanical properties of carbon nanotube–polymer composites, Carbon, 44 (2006) 1624-1652.

[26] F. Banhart, Interactions between metals and carbon nanotubes: at the interface between old and new materials, Nanoscale, 1 (2009) 201-213.

[27] S.C. Tjong, Recent progress in the development and properties of novel metal matrix nanocomposites reinforced with carbon nanotubes and graphene nanosheets, Materials Science and Engineering: R: Reports, 74 (2013) 281-350.

[28] R. Xu, Z. Tan, D. Xiong, G. Fan, Q. Guo, J. Zhang, Y. Su, Z. Li, D. Zhang, Balanced strength and ductility in CNT/Al composites achieved by flake powder metallurgy via shift-speed ball milling, Composites Part A: Applied Science and Manufacturing, 96 (2017) 57-66.

[29] Y. Wu, G.-Y. Kim, A.M. Russell, Effects of mechanical alloying on an Al6061–CNT composite fabricated by semi-solid powder processing, Materials Science and Engineering: A, 538 (2012) 164-172.

[30] H. Kurita, M. Estili, H. Kwon, T. Miyazaki, W. Zhou, J.-F. Silvain, A. Kawasaki, Load-bearing contribution of multi-walled carbon nanotubes on tensile response of aluminum, Composites Part A: Applied Science and Manufacturing, 68 (2015) 133-139.

[31] C. Suryanarayana, Mechanical alloying and milling, Progress in materials science, 46 (2001) 1-184.

[32] A. Adegbenjo, P. Olubambi, J. Potgieter, M. Shongwe, M. Ramakokovhu, Spark plasma sintering of graphitized multi-walled carbon nanotube reinforced Ti6Al4V, Materials & Design, 128 (2017) 119-129.

[33] Z. Liu, S. Xu, B. Xiao, P. Xue, W. Wang, Z. Ma, Effect of ball-milling time on mechanical properties of carbon nanotubes reinforced aluminum matrix composites, Composites Part A: Applied Science and Manufacturing, 43 (2012) 2161-2168.

[34] H. Kwon, M. Leparoux, A. Kawasaki, Functionally graded dual-nanoparticulate-reinforced aluminium matrix bulk materials fabricated by spark plasma sintering, Journal of Materials Science & Technology, 30 (2014) 736-742.

[35] S. Azadehranjbar, F. Karimzadeh, M. Enayati, Development of NiFe-CNT and Ni3Fe-CNT nanocomposites by mechanical alloying, Advanced Powder Technology, 23 (2012) 338-342.

[36] M.B. Vishlaghi, A. Ataie, Investigation on solid solubility and physical properties of Cu–Fe/CNT nano-composite prepared via mechanical alloying route, Powder Technology, 268 (2014) 102-109.

[37] A. Nouri, C. Wen, Surfactants in mechanical alloying/milling: a catch-22 situation, Critical Reviews in Solid State and Materials Sciences, 39 (2014) 81-108.

[38] A. Adegbenjo, P. Olubambi, J. Potgieter, E. Nsiah-Baafi, M. Shongwe, Interfacial Reaction During High Energy Ball Milling Dispersion of Carbon Nanotubes into Ti6Al4V, Journal of Materials Engineering and Performance, 26 (2017) 6047-6056.

[39] F.H. Gojny, M.H. Wichmann, B. Fiedler, K. Schulte, Influence of different carbon nanotubes on the mechanical properties of epoxy matrix composites–a comparative study, Composites Science and Technology, 65 (2005) 2300-2313.

[40] A. Esawi, K. Morsi, A. Sayed, M. Taher, S. Lanka, The influence of carbon nanotube (CNT) morphology and diameter on the processing and properties of CNT-reinforced aluminium composites, Composites Part A: Applied Science and Manufacturing, 42 (2011) 234-243.

[41] J.I. Goldstein, D.E. Newbury, J.R. Michael, N.W. Ritchie, J.H.J. Scott, D.C. Joy, Scanning electron microscopy and X-ray microanalysis, Springer2017.

[42] B. Chen, S. Li, H. Imai, L. Jia, J. Umeda, M. Takahashi, K. Kondoh, Load transfer strengthening in carbon nanotubes reinforced metal matrix composites via in-situ tensile tests, Composites Science and Technology, 113 (2015) 1-8.

[43] S. Khorasani, S. Heshmati-Manesh, H. Abdizadeh, Improvement of mechanical properties in aluminum/CNTs nanocomposites by addition of mechanically activated graphite, Composites Part A: Applied Science and Manufacturing, 68 (2015) 177-183.

[44] H. Choi, J. Shin, D. Bae, The effect of milling conditions on microstructures and mechanical properties of Al/MWCNT composites, Composites Part A: Applied Science and Manufacturing, 43 (2012) 1061-1072.

[45] S. Yoo, S. Han, W. Kim, Strength and strain hardening of aluminum matrix composites with randomly dispersed nanometer-length fragmented carbon nanotubes, Scripta Materialia, 68 (2013) 711-714.

[46] T. Peng, I. Chang, Uniformly dispersion of carbon nanotube in aluminum powders by wet shake-mixing approach, Powder Technology, 284 (2015) 32-39.

[47] A.C. Ferrari, Raman spectroscopy of graphene and graphite: disorder, electron–phonon coupling, doping and nonadiabatic effects, Solid state communications, 143 (2007) 47-57.

[48] H. Choi, J. Shin, D. Bae, Grain size effect on the strengthening behavior of aluminum-based composites containing multi-walled carbon nanotubes, Composites Science and Technology, 71 (2011) 1699-1705.

[49] G. Xu, Q. Zhang, W. Zhou, J. Huang, F. Wei, The feasibility of producing MWCNT paper and strong MWCNT film from VACNT array, Applied Physics A, 92 (2008) 531-539.

[50] K.S. Munir, M. Qian, Y. Li, D.T. Oldfield, P. Kingshott, D.M. Zhu, C. Wen, Quantitative Analyses of MWCNT-Ti Powder Mixtures using Raman Spectroscopy: The Influence of Milling Parameters on Nanostructural Evolution, Advanced Engineering Materials, 17 (2015) 1660-1669.

[51] F. Mokdad, D. Chen, Z. Liu, B. Xiao, D. Ni, Z. Ma, Deformation and strengthening mechanisms of a carbon nanotube reinforced aluminum composite, Carbon, 104 (2016) 64-77.

[52] M.S. Dresselhaus, A. Jorio, M. Hofmann, G. Dresselhaus, R. Saito, Perspectives on carbon nanotubes and graphene Raman spectroscopy, Nano letters, 10 (2010) 751-758.

[53] Z. Baig, O. Mamat, M. Mustapha, Recent Progress on the Dispersion and the Strengthening Effect of Carbon Nanotubes and Graphene-Reinforced Metal Nanocomposites: A Review, Critical Reviews in Solid State and Materials Sciences, (2016) 1-46.

[54] H. Choi, J. Shin, B. Min, J. Park, D. Bae, Reinforcing effects of carbon nanotubes in structural aluminum matrix nanocomposites, Journal of Materials Research, 24 (2009) 2610-2616.

[55] A.M. Okoro, R. Machaka, S.S. Lephuthing, M.A. Awotunde, S.R. Oke, O.E. Falodun, P.A. Olubambi, Dispersion characteristics, interfacial bonding and nanostructural evolution of MWCNT in Ti6Al4V powders prepared by shift speed ball milling technique, Journal of Alloys and Compounds, 785 (2019) 356-366.

[56] E.I. Salama, A. Abbas, A.M. Esawi, Preparation and properties of dual-matrix carbon nanotube-reinforced aluminum composites, Composites Part A: Applied Science and Manufacturing, 99 (2017) 84-93.

[57] A. Bisht, M. Srivastava, R.M. Kumar, I. Lahiri, D. Lahiri, Strengthening mechanism in graphene nanoplatelets reinforced aluminum composite fabricated through spark plasma sintering, Materials Science and Engineering: A, 695 (2017) 20-28.
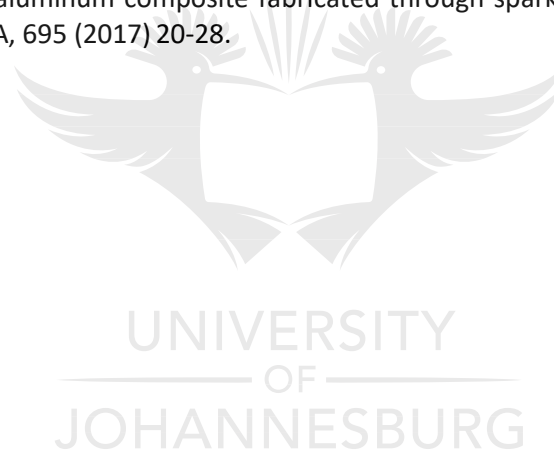
Interdependence of carbon nanotubes agglomerations, its structural integrity and the mechanical properties of reinforced nickel aluminide composites

Mary A. Awotunde [a, *], Adewale O. Adegbenjo [a, c], Olusoji O. Ayodele [a], Avwerosuoghene M. Okoro [a], Mxolisi B. Shongwe [b], Peter A. Olubambi [a]

[a] Center for Nanoengineering and Tribocorrosion, School of Mining, Metallurgy and Chemical Engineering, University of Johannesburg, South Africa
[b] Institute for NanoEngineering Research, Tshwane University of Technology, Pretoria, South Africa
[c] Mechanical Engineering Department, The Ibarapa Polytechnic, Eruwa, Oyo State, 200005, Nigeria

ABSTRACT

Spark plasma sintered NiAl-CNTs intermetallic composites were fabricated via two different ball milling processes. One comprising of an exclusive low energy ball milling (LEBM), and the other comprising of a two-stage milling, typically a prolonged LEBM with a short term high energy ball milling (HEBM). The differently milled powders were consolidated, and the resulting composites characterized. This was done to determine the individual effects of agglomerations vis-à-vis the structural integrity of the nanotubes. The composites were extensively characterized using X-ray diffraction (XRD), transmission electron microscopy (TEM), Raman spectroscopy (RS), scanning electron microscopy (SEM) and nanoindentation techniques. The uniform dispersion of slightly impaired CNTs led to better mechanical properties as compared to the in-homogenous dispersion of higher structural integrity CNTs in the NiAl intermetallic matrices. Results showed that the sample with a two-stage milling exhibited superior mechanical properties in terms of hardness, elastic modulus and fracture toughness with 422.79 Hv, 50.5 GPa and 9 MPa$\sqrt{m}$ respectively.

© 2019 Elsevier B.V. All rights reserved.

1. Introduction

In the recent nano-technological expedition, carbon nanotubes (CNTs) explicitly hold an unrivalled position in the ardent pursuit of the next generation of smart materials. This spot was effortlessly attained for none other reason asides the unique combination of the invincible properties domiciled in these exceptional nano-structures. Their astronomical elastic modulus in the tetra pascal range makes them ten times stronger than steel, coupled with their extreme light weight of ~2.1 g/cm^3 which makes them six times lighter than steel. In addition to these, they also possess excellent electrical and thermal conductivities in excess of 3000 W/mK akin to that of in-plane graphite sheets and diamond crystals [1—3]. These properties have made CNTs a delight to researchers, as their successful integration in diverse matrices is bound to enhance the mechanical properties of the reinforced composites.

To capitalize on the outstanding properties of CNTs however, the key pre-requisite of homogenously dispersing them into metallic matrices have to be achieved. Through the years, diverse dispersion methods have been extensively explored, yet, the conversant contest of inhomogeneous dispersion is not alien to researchers [4—7]. Regardless of the unparalleled properties of CNTs which holds tremendous possibilities for transforming the material world, realization of the transformation seems bleak in the face of this continual struggle for uniform dispersion [8,9]. Of the various dispersion techniques explored, high energy ball milling is the most prevalent route due to its widespread use [10], ostensibly owing to its simplistic operations and low cost [11]. Regrettably, the major drawback of this technique is the extensive damage done to the morphology and structural integrity of the nanotubes, which indisputably affects their mechanical properties adversely [12,13].

The damage done to the delicate nanostructures during high energy ball milling is due to the impact of the characteristic large dose of energy imparted on the powder particles to promote powder particle fracturing and homogenous mixing [14]. This

RESEARCH PAPER 2: INTERDEPENDENCE OF CARBON NANOTUBES AGGLOMERATIONS, ITS STRUCTURAL INTEGRITY AND THE MECHANICAL PROPERTIES OF REINFORCED NICKEL ALUMINIDE COMPOSITES

Abstract

Spark plasma sintered NiAl-CNTs intermetallic composites were fabricated via two different ball milling processes. One comprising of an exclusive low energy ball milling (LEBM), and the other comprising of a two-stage milling, typically a prolonged LEBM with a short term high energy ball milling (HEBM). The differently milled powders were consolidated, and the resulting composites characterized. This was done to determine the individual effects of agglomerations vis-a-vis the structural integrity of the nanotubes. The composites were extensively characterized using X-ray diffraction (XRD), transmission electron microscopy (TEM), Raman spectroscopy (RS), scanning electron microscopy (SEM) and nanoindentation techniques. The uniform dispersion of slightly impaired CNTs led to better mechanical properties as compared to the in-homogenous dispersion of higher structural integrity CNTs in the NiAl intermetallic matrices. Results showed that the sample with a two stage milling exhibited superior mechanical properties in terms of hardness, elastic modulus and fracture toughness with 422.79 Hv, 50.5 GPa and 9 MPa√m respectively.

Keywords: carbon nanotubes, nickel aluminide, agglomerations, structural integrity, nanoindentation

1. Introduction

In the recent nano-technological expedition, carbon nanotubes (CNTs) explicitly hold an unrivalled position in the ardent pursuit of the next generation of smart materials. This spot was effortlessly attained for none other reason asides the unique combination of the invincible properties domiciled in these exceptional nanostructures. Their astronomical elastic modulus in the tetra pascal range makes them ten times stronger than steel, coupled with their extreme light weight of ~ 2.1 g/cm^3 which makes them six times lighter than steel. In addition to these, they also possess excellent electrical and thermal conductivities in excess of 3000 W/mK akin to that of in-plane graphite sheets and diamond crystals [1-3]. These properties have made CNTs

a delight to researchers, as their successful integration in diverse matrices is bound to enhance the mechanical properties of the reinforced composites.

To capitalize on the outstanding properties of CNTs however, the key pre-requisite of homogenously dispersing them into metallic matrices have to be achieved. Through the years, diverse dispersion methods have been extensively explored, yet, the conversant contest of inhomogeneous dispersion is not alien to researchers [4, 5]. Regardless of the unparalleled properties of CNTs which holds tremendous possibilities for transforming the material world, realization of the transformation seems bleak in the face of this continual struggle for uniform dispersion [6, 7]. Of the various dispersion techniques explored, high energy ball milling is the most prevalent route due to its widespread use [8], ostensibly owing to its simplistic operations and low cost [9]. Regrettably, the major drawback of this technique is the extensive damage done to the morphology and structural integrity of the nanotubes, which indisputably affects their mechanical properties adversely [10, 11].

The damage done to the delicate nanostructures during high energy ball milling is due to the impact of the characteristic large dose of energy applied to the powder particles to promote powder particle fracturing and homogenous mixing [12]. This causes calamitous damage to the seamless conical morphology of the nanostructures leading to the loss of their unique properties [11]. To keep this damage at a minimum in order to preserve the structural integrity of the nanotubes, ball milling times are often reduced, which leaves the CNTs heavily clustered in the metal powder matrix. Conversely, some other studies rather employed longer milling times at the risk of damage to the CNTs in order to attain uniform dispersion [6, 11, 13]. A dilemma is therefore brewing in the research community between uniform dispersion and preservation of the structural integrity of the carbon nanotubes. Should dispersion be sacrificed for structural integrity (thereby leaving undamaged but agglomerated CNTs within the matrix) or structural integrity sacrificed for the purpose of uniform dispersion (thereby dispersing 'damaged' CNTs within the matrix)?

To study the agglomeration effects vis-à-vis the structural integrity effects, the two highlighted scenarios will be investigated in this work. One milling regime consisting of 6 h low energy ball milling at 120 rpm, and a second milling regime consisting of a 6 h low energy regime with an additional 1 h of high energy ball milling at 50 rpm were employed. The former milling regime parameter was chosen to simulate the first highlighted effect of sacrificing dispersion for structural integrity. Low energy ball milling has the advantage of preserving the structural ntegrity of the CNTs but lacks the ability to successfully achieve uniform dispersion when used

exclusively [14]. The latter milling regime parameter was chosen to simulate the second highlighted effect of sacrificing structural integrity for the purpose of uniform dispersion. This is as a result of the additional high energy ball milling process which will effectively disperse the CNTs clusters still remaining after the low energy milling procedure. It was expected that some form of damage will occur alongside the higher dispersion achieved via this second route as majority of the processes aimed at enhancing the dispersion of CNTs come with an associated price of some level of damage. However, the purpose is not to cause catastrophic damage which will translate into loss of the nanotube properties, hence the careful selection of ball milling parameters particularly the low speed of the secondary milling.

The matrix of choice for this study is a nickel aluminide (NiAl) intermetallic matrix. CNTs have been extensively incorporated in polymer and metal matrices [15, 16], however, very few researchers have incorporated these nanostructures into intermetallic matrices like NiAl [17]. Nickel aluminides are light intermetallics that can potentially replace expensive nickel base super alloys in service provided the prime constraint of low fracture toughness can be overcome [18, 19]. It is the aim of the authors to evaluate the mechanical properties of the composites obtained from the two processes to effectively assess which regime translates to better properties.

2. Experimental Procedure

2.1 Raw materials

Commercially available nickel, supplied by Weartech Limited with particle size of 0.5-3.0μm and 99.5 % purity, spherical aluminium powder with average particle size of 25 μm supplied by TLS Technik GmbH & Co., and MWCNTs supplied by Nanocyl, Belgium with average diameter of 9.5 nm and average length of l.5 μm were used as starting powders in this study.

2.2 Ball Milling

Nickel and aluminium in equi-atomic weight proportions of ratio 1:1 were placed in 250 ml stainless steel milling jar with 0.5 wt % MWCNTs as reinforcement. Stainless steel milling balls of two different diameters (ø 10 and 5mm) were added to the powder mix to give a ball-to-powder weight ratio of 10:1. The dissimilar sizes of milling balls were used in order to impede the likelihood of cold welding and also guarantee the transfer of sufficient impact

energy to the powders [12]. The powder mix and the milling balls were agitated using a low energy planetary ball mill, Retsch PM 100 at 150 rpm for 6 h during regime I. Regime II comprised of the aforementioned procedure in addition to a high energy ball mill using Retsch PM 400 at 50 rpm for 1 h at the same ball-to-powder weight ratio. Process control agent (PCA) was left out due to the lubricating effect of CNTs which enables them to act as PCA under dry milling conditions [20]. The milling parameters were selected to prevent excessive cold welding with a pre-determined break of 10 min for every 10 min of milling.

2.3 Materials characterization

The morphologies of the as-received and milled powder samples were examined using a field emission scanning electron microscopy (FE-SEM) Carl Zeiss Sigma coupled with energy dispersive X-ray spectrometry (EDX). The morphology of the MWCNTs in the milled powder samples was studied using transmission electron microscopy JEOL JEM - 2100. TEM analyses of the powder samples were carried out at 150 keV. Identification of phases present in the milled powder samples were characterized via X-ray diffractometer (XRD, PANalytical Empyrean model) with Cu-Kα radiation (λ=0.154 nm) at a scanning rate of 1°/ min. Raman spectroscopy (T6400 Jobin–Yvon, HORIBA, Japan) was performed on both the pure MWCNTs and the milled powder samples from the two different milling regimes with a 514.5 nm laser employing a 20x objective lens. A spectral range of 500 - 2500 cm^{-1} was employed for all the powder mixtures to quantitatively assess the level of damage on the MWCNTs based on their milling history.

2.4 Consolidation of bulk composites

The milled powders were compressed in a graphite die and the whole die assembly was placed in the SPS system (model HHPD-25, FCT Germany). 20 mm diameter discs with 5 mm height were sintered at 1000 ºC and 32 MPa with holding time of 7 min and heating rate set at 100 ºC/min.

2.5 Density and hardness measurements

Density measurements of the sintered discs were carried out using the Archimedes' principle according to ASTM standards. Nanoindentation technique was used to obtain the hardness and the elastic modulus of the samples. Indentations were made on the mirror-like surfaces of the

samples and they were loaded with a force of 100 mN. The nanoindentation curves were obtained as the samples were loaded and unloaded, while elastic modulus values extracted from the nanoindentation data was used to calculate the fracture toughness of the samples using the Palmqvist equation [21, 22]. The fracture toughness values obtained are the mean values of four successive measurements repeatedly conducted for accuracy.

2.6 Fractographic examination

The ⌀20mm sintered samples were each cut three-quarter way through with a precision cutting machine to obtain fractographic samples for SEM analyses. The one-quarter portion of the partly cut discs were then gently knocked off to completely severe the sintered discs. Fractographic examinations were performed on these fractured pieces using a High Resolution Scanning Electron Microscope.

3. Results and Discussion

Fig. 1 shows the different morphologies of the starting powders. Fig. 1a depicts the SEM image of the strongly knotted and agglomerated pristine CNTs. With such characteristically large aspect ratios [23] and concurrent strong van der Waals forces in the order of -100 eV/mm [24], the CNTs unsurprisingly exist in clustered state. Fig. 1b illustrates the pure aluminium powders presenting a spherical morphology with varying particle sizes and an average particle size of 25μm. Fig. 1c shows the distinctively spiky-textured morphology of the as-received nickel powders, while Fig. 1d in agreement with Fig. 1a exposes the highly intertwined cylindrical tubes of the pristine nanotubes in a TEM image.
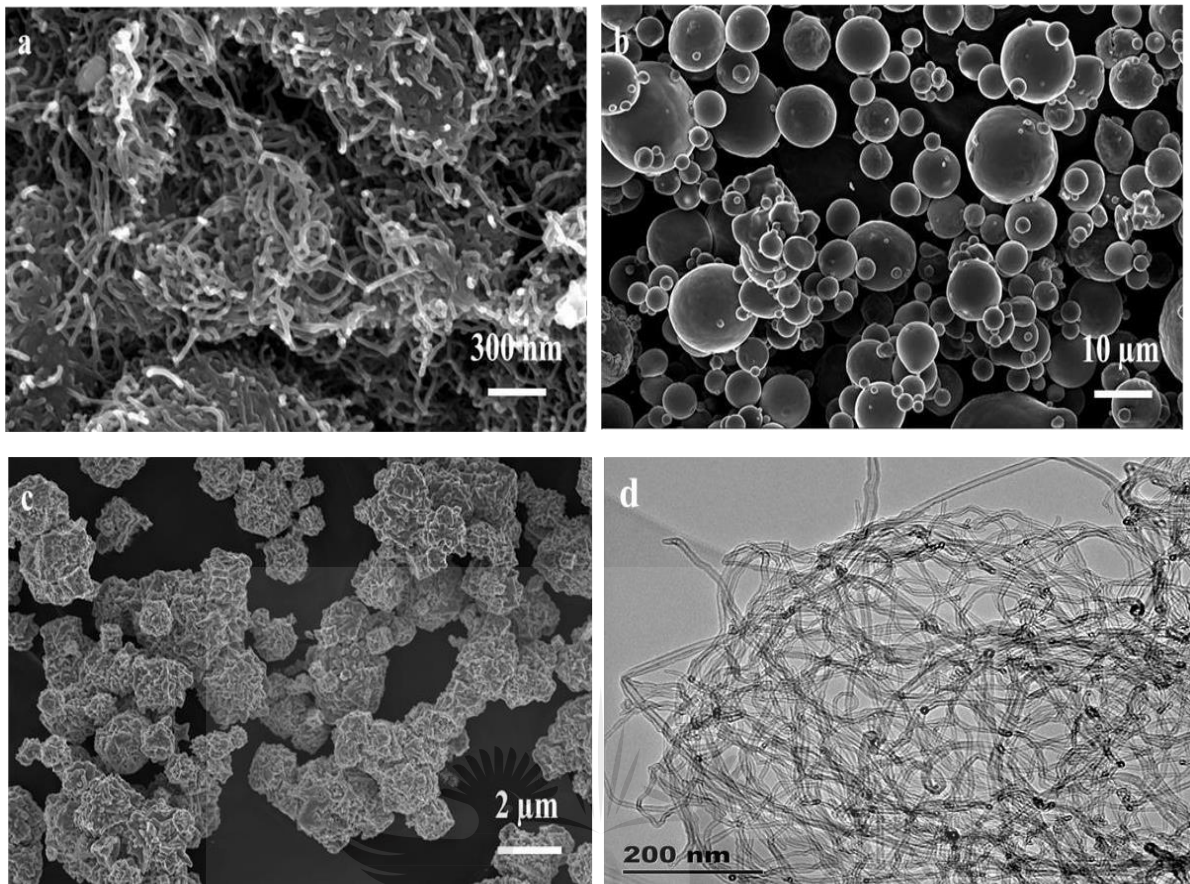
Fig. 1-Showing the SEM morphologies of the starting materials (a) MWCNTs (b) aluminium powders (c) nickel powders and (d) TEM micrograph of the MWCNTs

3.1 Microstructural characterization of ball milled powders

Fig. 2 displays the microstructural evolution of the CNTs in the milled powders using TEM and SEM analyses. Fig. 2a exposes the CNTs clusters still retained undispersed within the matrix powders and some minor strands that have been dispersed in the course of the milling for Sample A (with exclusive LEBM). Fig. 2b shows a well dispersed network of CNTs indicating that at the end of the LEBM, some nanotubes were well dispersed, though some heavy clusters were still retained as observed in Fig. 2a. These retained clusters are also evident in the SEM image as depicted in Fig. 2c (within the dotted white line region), which reveals a colony of CNTs clusters within the fractured and cold welded powder particles.
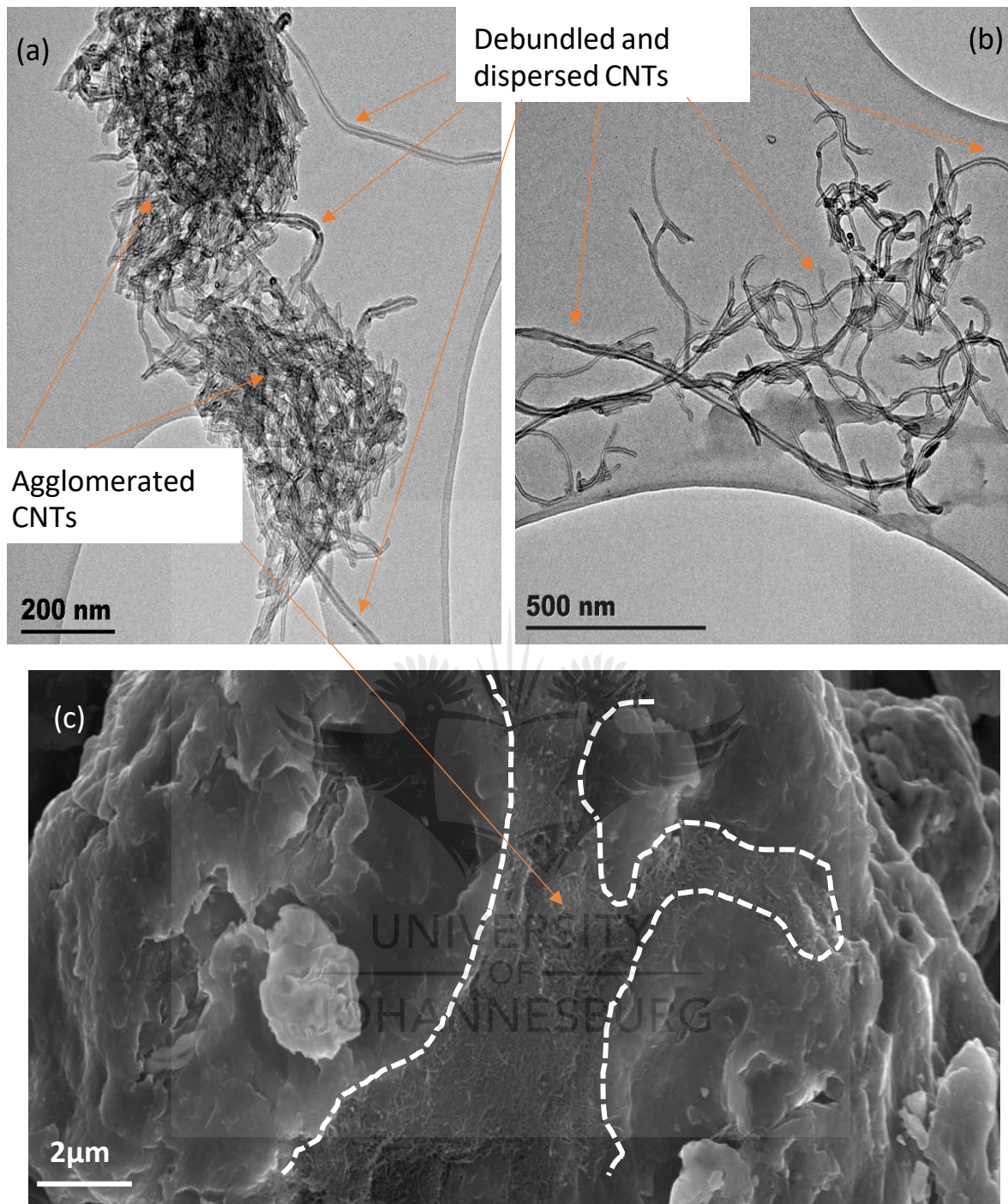
Fig. 2-Micrographs of sample A with one stage milling (a) TEM image of agglomerated CNTs within the powder matrix (b) TEM image of well dispersed CNTs within the powder matrix (c) SEM image showing the agglomerated CNTs within the matrix powders

Fig. 3a shows the SEM images of Sample B (with the two stage milling) after the completion of the two milling stages, with CNTs tips protruding from the cold welded and fractured powder particles. Fig. 3b shows the CNTs tips at higher magnification verifying the efficacy of the two stage milling regime in successfully embedding and dispersing the CNTs in the milled matrix powders. Corroborating this fact is Fig. 3c which depicts the TEM image of Sample B with the

CNTs homogeneously dispersed in the matrix powders. The yellow arrows show some of the slightly damaged sections in the nanotube structures. As earlier projected, a secondary milling stage particularly HEBM has a higher propensity to inflict damage on the nanotubes. However, the damage here is appreciably low due to the extremely low speed of the HEBM which favours dispersion over damage.
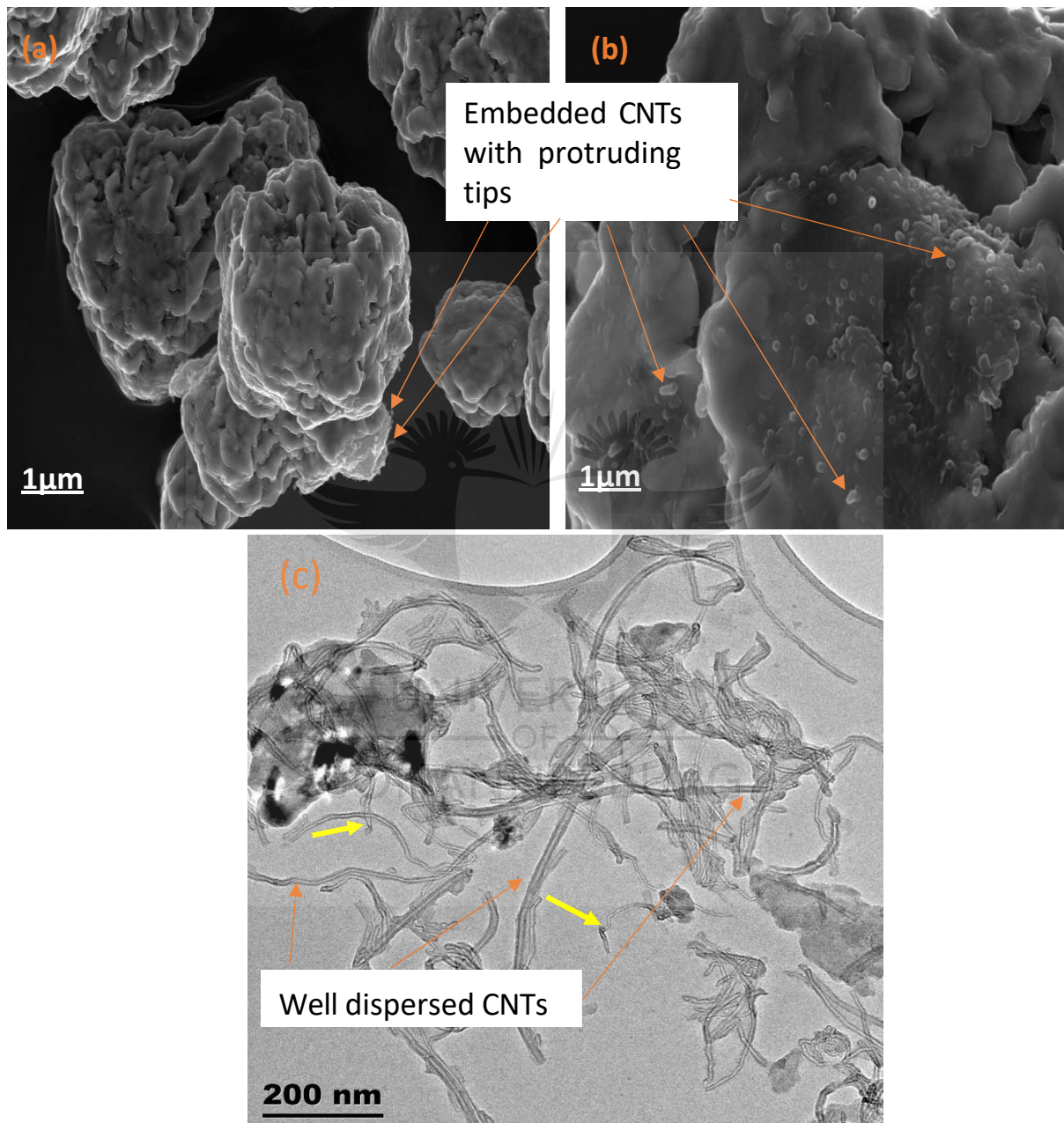
Fig. 3-SEM micrographs of Sample B with two stages of milling showing (a) CNTs well embedded into the matrix powder particles (b) the CNTs tips at higher magnification and (c) TEM micrographs showing well dispersed CNTs with the yellow arrows showing some damaged sections in the CNTs

High resolution (HR) TEM images in Fig. 4a elucidate the distinct graphitic layers of the pristine CNTs walls with an interlayer spacing of 0.3507 nm between two adjacent lattice fringes. The selected area electron diffraction (SAED) pattern in Fig. 4b reveals the characteristic graphitic planes of the CNTs namely (002) and (100) which is in agreement with the lattice fringe spacing of graphite (002) [25]. Furthermore, the halo and coaxial rings are evidently intact at these planes and strictly concentric. The fast fourier transform (FFT) image in Fig.4c confirms the interlayer spacing and reveals the narrow peaks, indicating the highly crystalline nature of the pristine CNTs.
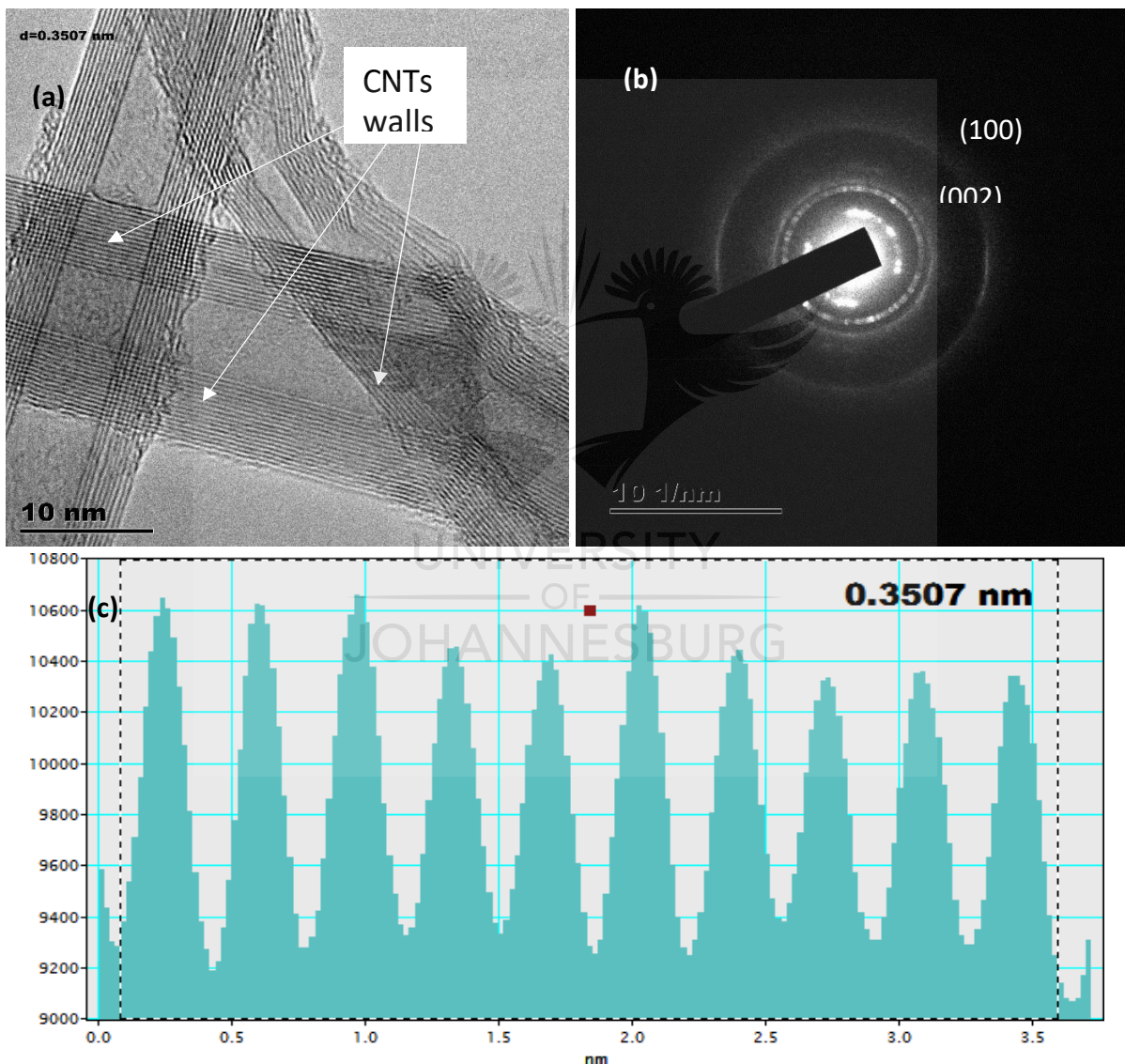
Fig. 4- HR-TEM images of the pristine MWCNTs revealing (a) CNTs walls (b) SAED pattern and (c) FFT image of the pristine CNTs

Fig. 5a reveals the nano-structural evolution of the CNTs dispersed in the NiAl matrix powders through the exclusive LEBM route. It is observed that clusters of CNTs are apparent within the milled powders in the micrographs as seen in Fig. 5a. The impact forces employed in the LEBM are quite insufficient in completely overpowering the resilient van der Waals forces that keep the CNTs intertwined together [26]. Thus, after the completion of the milling regime for Sample A, bundles of agglomerations could still be seen in the powder matrix. The SAED pattern in Fig. 5b depicts an analogous image to that observed for the pristine CNTs in Fig. 4b. Obviously, the milling process did not compromise the structural integrity of the nanotubes. One way of evaluating and assessing the extent of induced strain on the nanotubes is by measuring the interlayer spacing between the walls of the nanotubes. To confirm the impact and effect of LEBM process on the CNTs, the FFT images were obtained under HR-TEM in Fig. 5d. A spacing of 0.3541 nm was ascertained by the measurement which differed from the interlayer spacing of the pristine CNTs by a narrow 0.0034 nm, confirming the slight impact of the milling regime in exerting strain or inducing morphological damage to the tubular structures. The sharp peaks of the FFT image also confirm the highly crystalline nature of the CNTs even after the milling regime, indicating that no amorphous compounds were formed in the course of the milling.
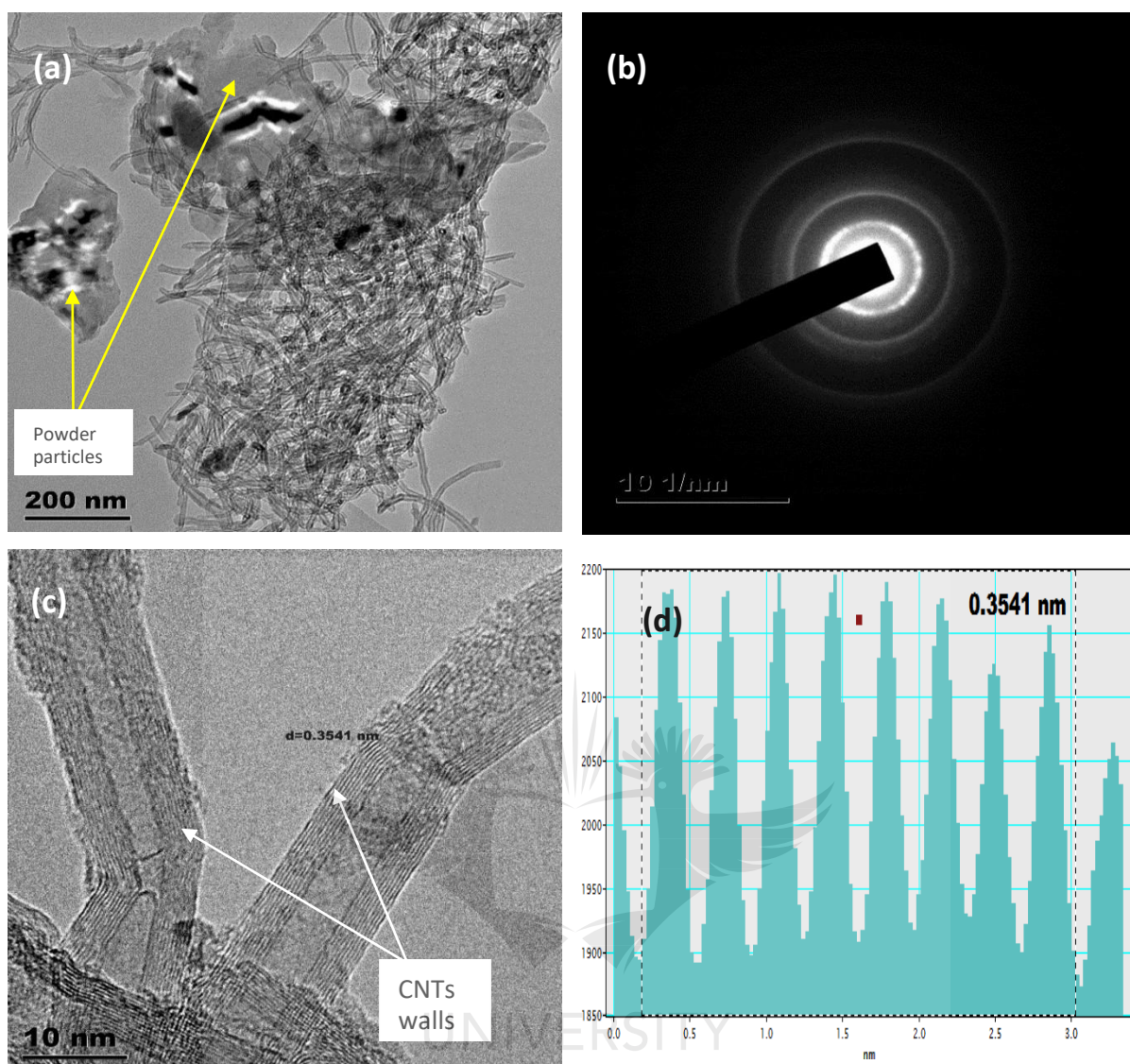
Fig. 5- HR-TEM micrographs of Sample A showing the (a) MWCNTs highly agglomerated in NiAl powder particles (b) SAED pattern (c) CNTs walls and (d) FFT image revealing interlayer spacing between the CNTs walls

The nano-structural evolution of the CNTs in NiAl matrix powders via the two stage milling regime can be observed in Fig. 6a. Well dispersed and embedded CNTs are observed in this micrograph due to the effectiveness of the two stage milling employed in Sample B. The HEBM is typically aimed at exerting highly energetic and impactful forces on the powders to promote homogeneity by subduing the van der Waals forces between the nanotubes [27]. The combination of the mild LEBM and the rigorous HEBM in this milling regime successfully led to the eventual untangling of the knotted nanotubes. Though the HEBM typically exerts more energy, the preceding LEBM process for this regime had effectively embedded both dispersed and clustered CNTs into the powder particles, such that subjecting the admixed powders to

HEBM did not inflict significant damage on the nanostructures because the powder particles were shielding them. Fig. 6b displays the SAED pattern for Sample B where the halo and coaxial rings are however not as intact as those observed in Fig. 5b. In addition, the rings are not strictly concentric, but slightly eccentric with indiscriminate extra spots indicative of some structural damage in the nanotubes. Consequently, the interlayer spacing of Sample B was observed to be 0.3658 nm as shown in Figs. 6 c and d, translating to a higher discrepancy of 0.0151 nm than that observed in the pristine and 0.0117 nm more than that observed for even Sample A. This agrees with the SAED patterns corroborating the effect of a more intense milling regime in Sample B. These results prove that the two stage milling endured by Sample B induced a more significant strain on the nano-structural morphologies of the CNTs, however, it did not amount to significant damage or accumulation of sp^3 defects. This is proven by the apparent lack of stripes on the SAED pattern which is indicative of crystal defects in the graphitic lattice structure [3]. Moreover, the narrow tips of the FFT image as displayed in Fig. 6d is also a strong indication of the retained and preserved crystallinity of Sample B[28].
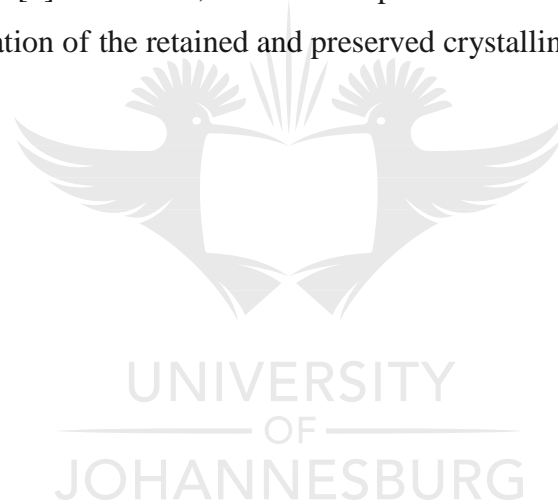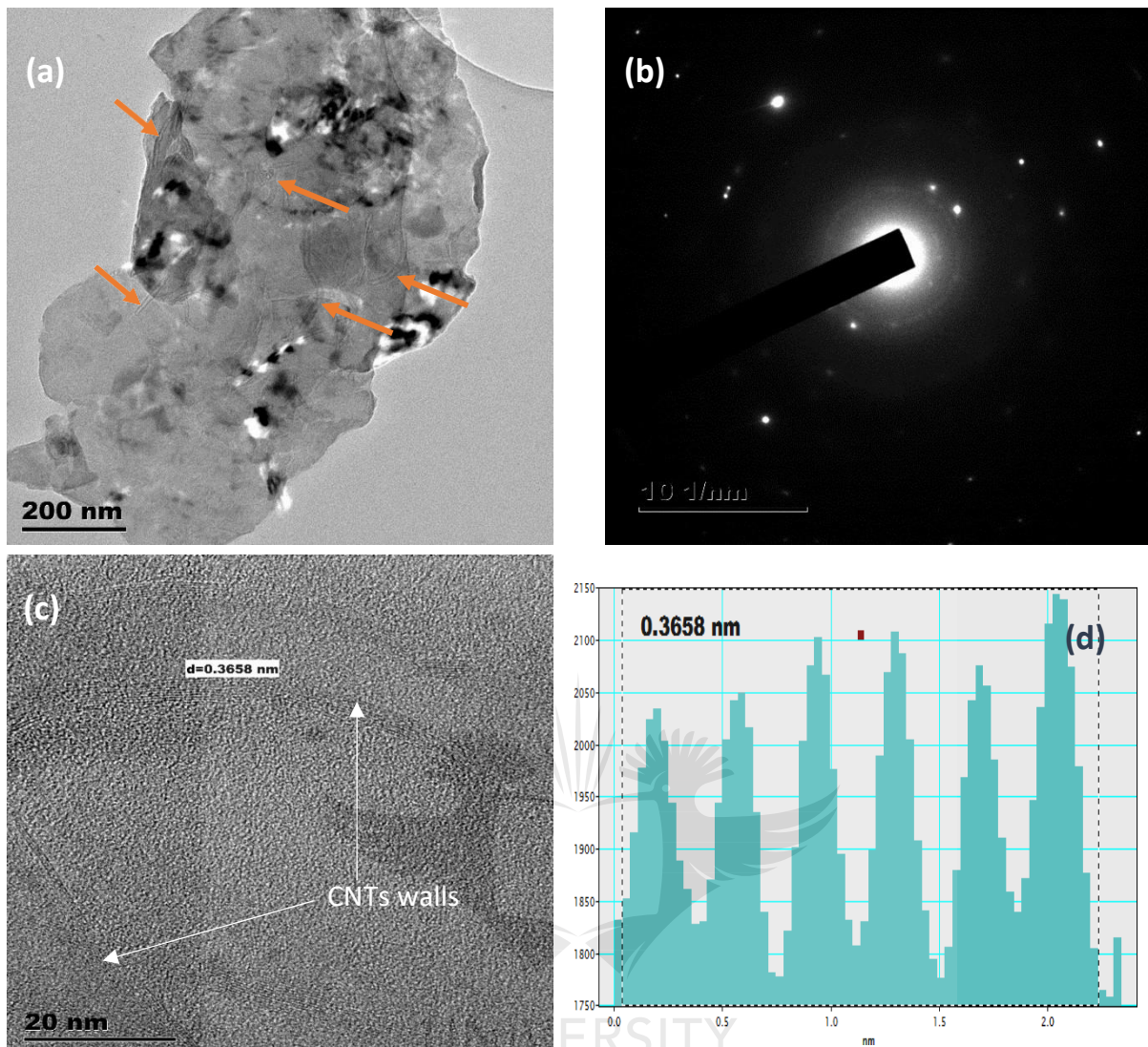
Fig. 6- HR-TEM micrographs of Sample B showing the (a) MWCNTs evenly dispersed in NiAl powder particles (b) SAED pattern (c) CNTs walls and (d) FFT image revealing interlayer spacing between the CNTs walls

3.2 X-ray diffraction (XRD) analyses

XRD was employed for effective phase identification in the milled powder samples after the different milling regimes. Fig. 7 illustrates the XRD spectrums generated from Samples A and B. Individual peaks of nickel, aluminium and nickel aluminide can be observed from the two spectra. The similarity of the spectra indicates similar phases were formed during the ball milling regimes of the samples. NiAl peaks are observed at $2\theta = 44.67$ º which corresponds to the (110) plane. The spectrums are devoid of any peaks corresponding to aluminium carbide (Al_4C_3) even in Sample B, demonstrating that the damage imparted on the nanotubes during the combined milling was not significant or sufficient enough to trigger interfacial reactions

between aluminium and CNTs during milling [29]. This is in agreement with the SAED patterns discussed in the previous section which suggests that some damage was incurred, but not significant due to the absence of streaks and bands on the diffraction patterns [3]. Significant damage ultimately results into vacancies and damaged walls which are natural prospective sites for interfacial reactions leading to carbide formations [30].
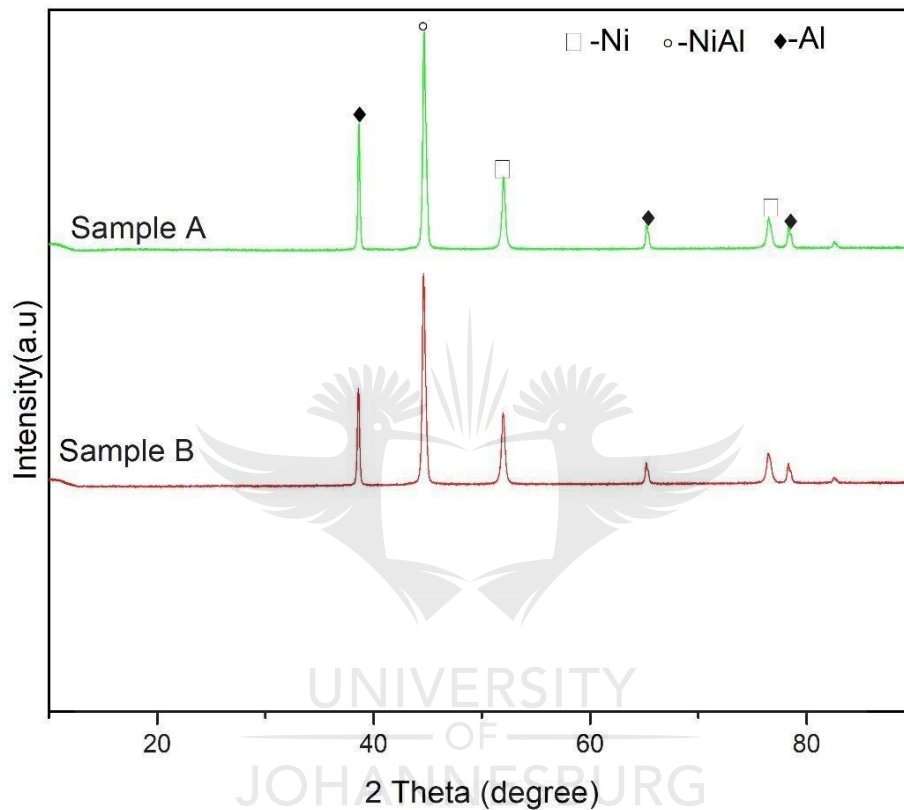
Fig. 7-XRD patterns for the milled powders of Samples A and B

3.3 Raman spectroscopy

Fig. 8 reveals the Raman peaks of the pristine MWCNTs powders with the D band peak at 1340 cm^{-1} and the G band's characteristic peak at approximately 1580 cm^{-1}. The D band is ascribed to the intensity of lattice defects, reflecting the damage of the 2D symmetrical bonds present in the CNTs. Conversely, the G band denotes the level of crystallinity, the nearness of the carbon nanotube structure to perfect hexagonal graphitic structure, and thus will appear narrower and higher for highly crystalline carbon nanotubes [31, 32]. The structural integrity of the nanotubes can be assessed and quantified by their characteristic I_D/I_G ratios where a higher ratio depicts

an increase in structural defects and a corresponding decrease in crystallinity.
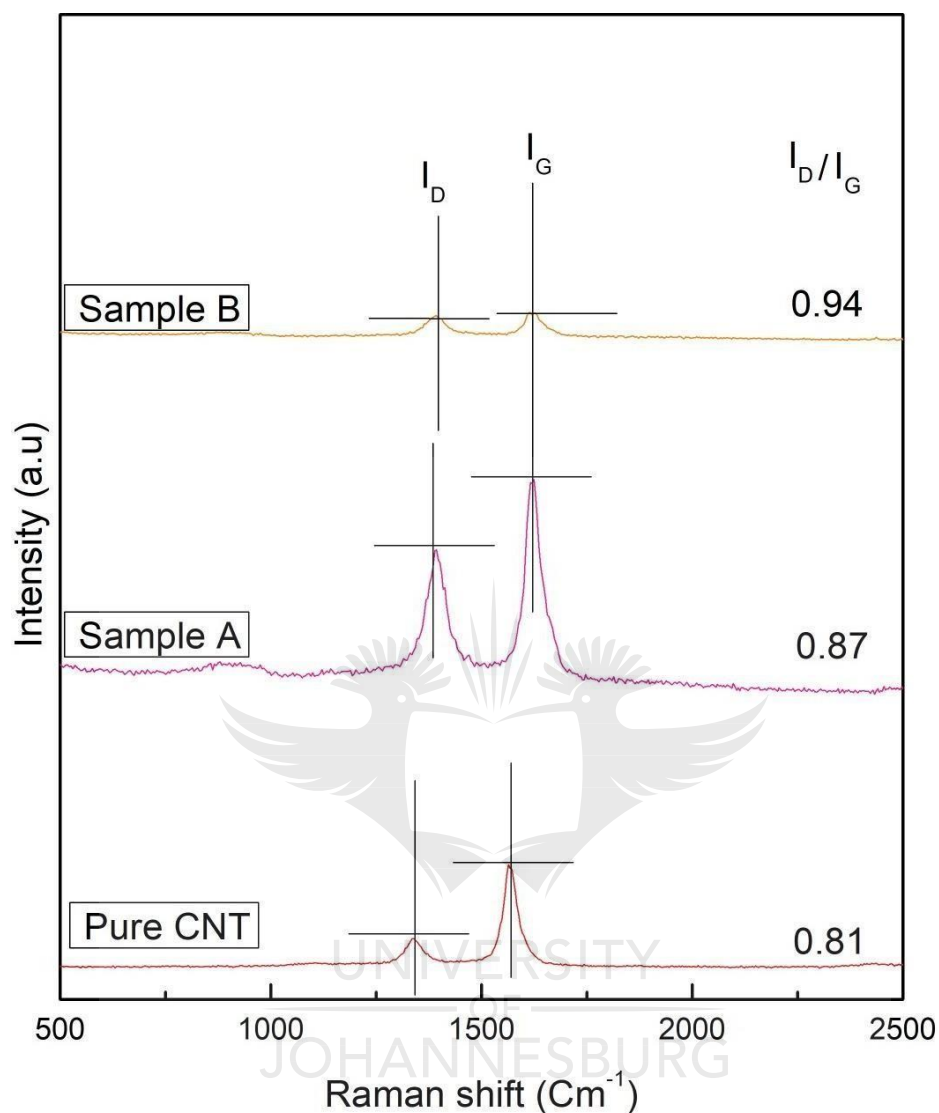
Fig. 8-Showing the Raman ratios of samples A and B including that of the pristine CNTs

It is typical and expected for CNTs to undergo a hybridization pathway during fabrication processes like ball milling [33]. This pathway can be assessed by the characteristic features of the Raman spectra such as the D and G peak intensities via peak broadening/reduction [34]. From Fig. 8, the Raman peak intensity ratios of the milled powder samples experienced a significant shift from 1580 cm^{-1} in the pristine to 1591 cm^{-1}. This indicates that the forces disgorged by the ball milling process may have resulted in some form of structural defects and impaired the crystallinity. This may be due to the infusion of nickel and aluminium atoms into

the CNTs translating to slight distortions in the C-C lattice structure [35]. The Raman peak intensity ratio of the as-received pristine nanotubes was calculated to be 0.81, while that of the Sample A with exclusive LEBM was calculated to be 0.87 revealing a 7.4 % increase in the ratio. This confirms that very slight strain was exerted via this milling regime, amounting to insignificant structural damage which is consistent with LEBM processes. The LEBM process when used exclusively has the unique advantage of preserving the integrity and crystallinity of the nanotubes [36, 37], hence the mild increase in the Raman ratio of this sample. However, sample B which experienced a two stage milling with HEBM as a secondary milling displayed a more significant 16.1 % increase in its peak intensity ratio. This shows that the milling regime experienced by sample B was more severe, translating into a higher level of strain in the walls of the nanotubes. The higher ratio of the characteristic peak intensities also proves that the crystallinity impairment via induced defects in sample B is more substantial than in sample A, and hence, a higher defect concentration in sample B. In addition, the sharp peaks observed in the pristine CNTs and sample A gave way to broadened peaks in sample B due to the severity of the milling regime. This is as a result of the accumulation of defects and disorders in the graphitic structure which may be present as reparations in the walls of the nanotubes [31]. Both results are in complete agreement with the SAED patterns as discussed in the previous section with Sample A reflecting symptoms of slight strain while Sample B depicts a slightly more significant strain on the nanotubes. The combined milling regime was carefully selected to achieve a balance between dispersion and structural integrity so as not to disperse extremely damaged nanotubes in the matrix. Thus, this balance is crucial as the structural integrity in this regime was just slightly impaired. From the statistics displayed in Fig. 8, all the Raman peak intensity ratios are observed to be less than 1, which strongly indicates the supremacy of crystallinity over defects [38], further substantiating that the milling regimes were not harsh on the nanotubes' delicate features. Further evidence buttressing this point are the sharp peaks [30] displayed by the two samples as manifested in their FFT images in Figs. 5d and 6d respectively.

3.4 Microstructural characterization of the spark plasma sintered NiAl-CNTs composites
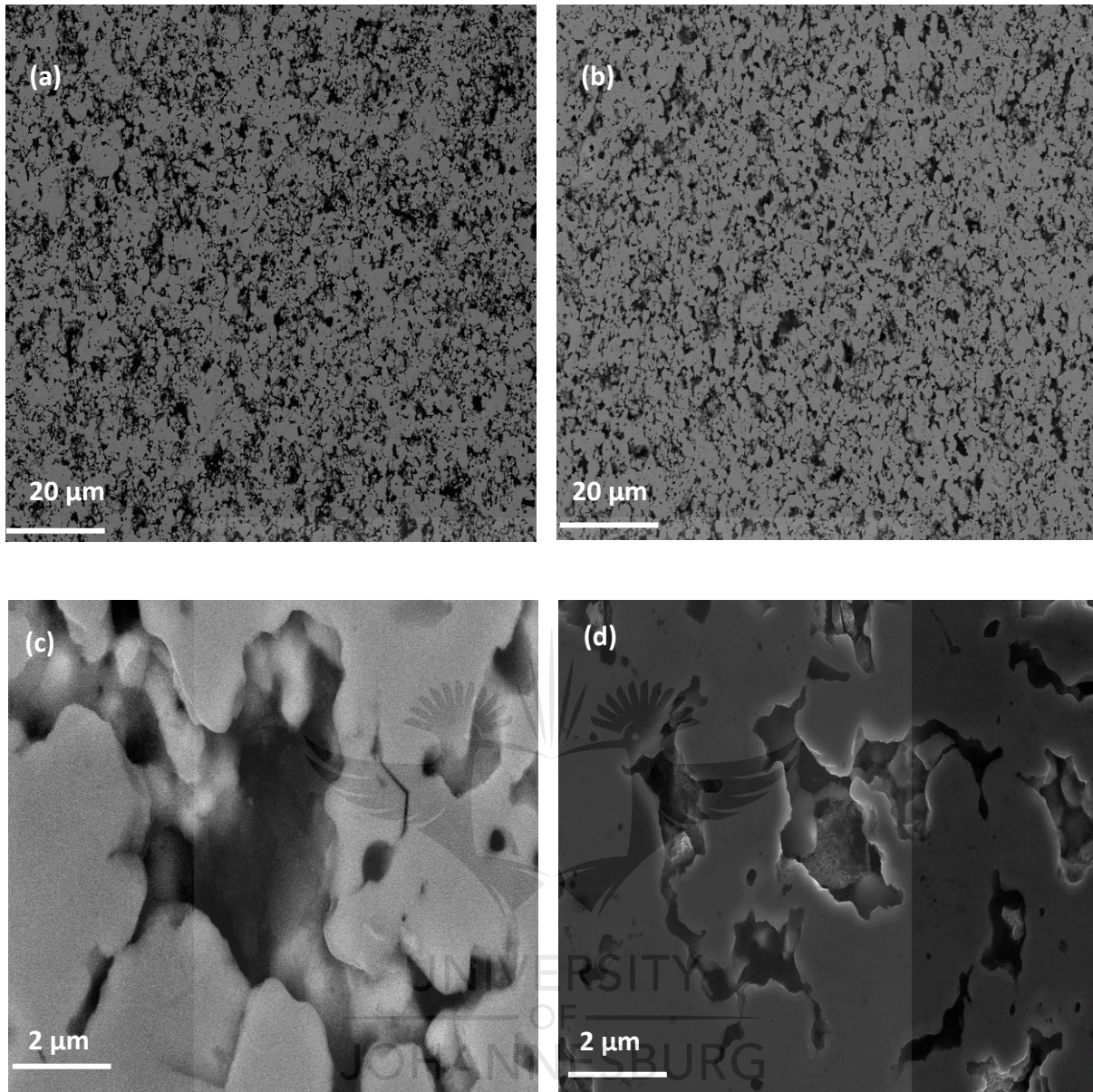
Fig. 9-Illustrating the SEM micrographs of the sintered samples (a) Sample A at lower magnification (b) Sample B at lower magnification (c) Sample A at higher magnification (d) Sample B at higher magnification

Fig. 9 illustrates the SEM images of the sintered NiAl-0.5 wt% CNTs composites after the necessary metallographic preparations revealing slight discrepancies in their porosities. It can be observed that Sample A displayed a slightly more porous microstructure than Sample B. This corroborates the density measurements in Table 1 and can be attributed to the existence of agglomerates still retained in Sample A owing to its process history.

TABLE 1- Mechanical Properties of samples A and B

Sample	Theoretical density (g/cm^3)	Measured density (g/cm^3)	Relative density (%)	Young's modulus (GPa)	Vickers nano-hardness (HV)	Fracture toughness MPam$^{1/2}$
A (no HEBM)	5.068	4.12±0.01	81	7.2	128.07	2.97±0.13
B (with HEBM)	5.068	4.20±0.14	83	50.5	422.79	9.00±1.53

Though the CNTs content dispersed into the samples are the same, the milling process they went through translated to the observed microstructural variations between them. The exclusive LEBM employed for Sample A led to partial detangling and declustering of the CNTs whilst still leaving some CNTs severely clustered within the matrix. These CNTs agglomerations acted as obstacles to diffusion during sintering, thus retarding the kinetics of sintering and consequently preventing the sinterability of Sample A [39]. Since sintering is presumed to be a diffusion dependent phenomenon [40], it led to higher porosities with larger sizes [41] inthe sintered composite as shown in Figs. 9a and c respectively. Sample B shows a slightly higher densification owing to the relatively improved CNTs dispersion in the sample, this is corroborated by the higher density values in Table 1 and further supported by the microstructural images presented in Figs. 9b and d.

Fig. 10a shows the fracture morphology of Sample A with exclusive LEBM. Here, a mixed fracture mode can be observed with intergranular fracture dominating the minor islands of dimpled microstructures. (The circle shows the dimpled structures while the arrows show the intergranular fractures). The plausible explanation for the islands of dimpled microstructures is the presence of CNTs on some minor parts of the matrix due to the in-homogeneous dispersion of the nanotubes in the composite matrix. The intergranular fracture mode is very consistent with the fracture mode observed in pure NiAl from our previous study, as depicted in Fig. 11. In contrast, the relative homogeneous dispersion obtained in Sample B gave rise to a dominantly dimpled microstructure with very few intergranular fracture surfaces as observed in Fig 10b. This is assumed to be as a result of the better dispersion of the CNTs in this sample, solely because of the employed milling regime. With the CNTs well dispersed over larger portions, a more dimpled microstructure was achieved in Sample B. The purely intergranular fracture manifested in the pure NiAl shifted to a mixed fracture mode in the CNTs reinforced NiAl with Sample B revealing a finer distribution of dimples on larger surface areas.
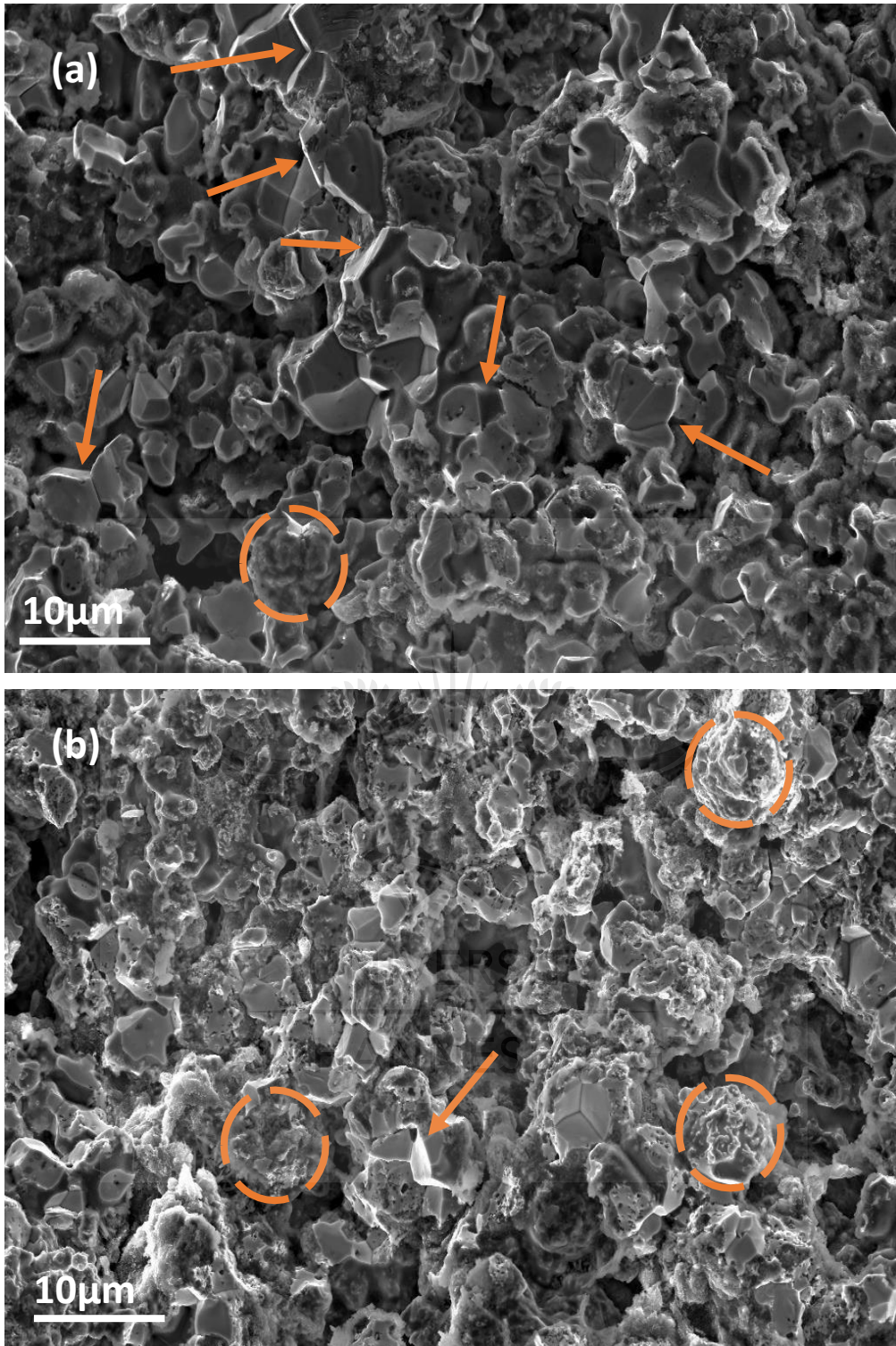
Fig. 10- (a) Fracture morphology of Sample A with no HEBM revealing a dominantly intergranular fracture with very few dimples (b) Fracture morphology of Sample B with HEBM showing a more dimpled microstructure with few intergranular fracture surface. Arrows showing intergranular fracture and circles showing dimpled morphology

3.5 Nanoindentation studies of the spark plasma sintered NiAl-CNTs composites

Nanoindentation is a well-established method for evaluating the mechanical properties of a wide variety of materials especially when a non-destructive methodology is required. The advantage of using nanoindentation techniques which are divergent from the orthodox testing methods includes the capacity for in-situ measurement of material properties without upsetting the microstructure and causing substantial impairment to the material. Additionally, no extraordinary conditions are necessary as regards the size and shape of the test samples [42, 43]. One of the features of this technique, is its ability to provide information such as nano-hardness, Vickers hardness and elastic modulus. Some difficulty has been identified in characterizing the plasticity of brittle intermetallic composites like NiAl, as their brittleness increases their susceptibility to fragmentation [44]. Nanoindentation provides a more feasible approach to characterizing such brittle composites [45, 46].

In this study, nanoindentation was employed to determine the elastic modulus of the different samples, amongst other properties. The samples were individually loaded, held at a maximum load of 100 mN for 100 s and unloaded, giving rise to the curves indicated in Fig. 12.
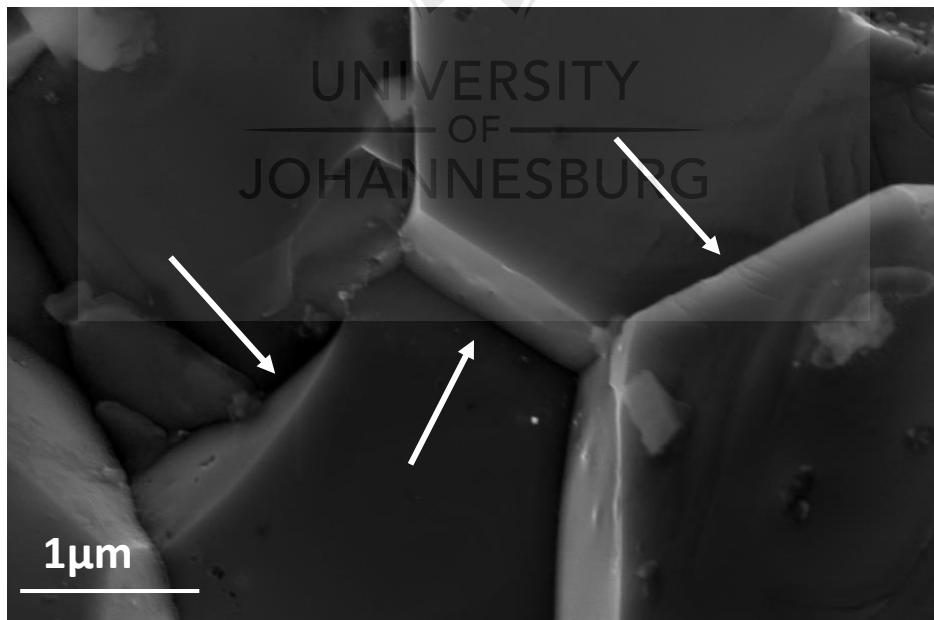
Fig. 11-SEM micrograph showing unreinforced NiAl with pure intergranular fracture surface

Sample B presents a pop-in during the loading phase, which could have been caused by micro-cracking or elastic-plastic deformation shifts [47]. The area sandwiched amongst the loading

and unloading curves represents the dissipated energy by the composites due to plastic deformation [47]. As deduced from Fig. 12, a lower penetration depth is observed for Sample B, demonstrating a lower hardness value than Sample A. The hardness and elastic modulus of the different composites are presented in Table 1 with Sample B showing higher hardness and higher elastic modulus values than Sample A. Remarkably, Sample B displays nano hardness values three times higher than Sample A and elastic modulus even seven times higher respectively. This trend is attributable to the more homogenous dispersion of CNTs through the combined ball milling method utilized in this route [48]. The uniformly distributed nanotubes function as obstacles and hindrances to dislocation movement within the composite, thus imparting strength [49]. Past studies clarified that the elastic moduli of CNTs reinforced composites are contingent on the operative aspect ratios of the dispersed CNTs within the matrix [50]. Figs. 2a and 3a validate this fact as the uniformly dispersed CNTs in Fig. 3a led to higher elastic moduli while the bundled and agglomerated CNTs in Fig. 2a resulted into poor elastic moduli for Sample A.
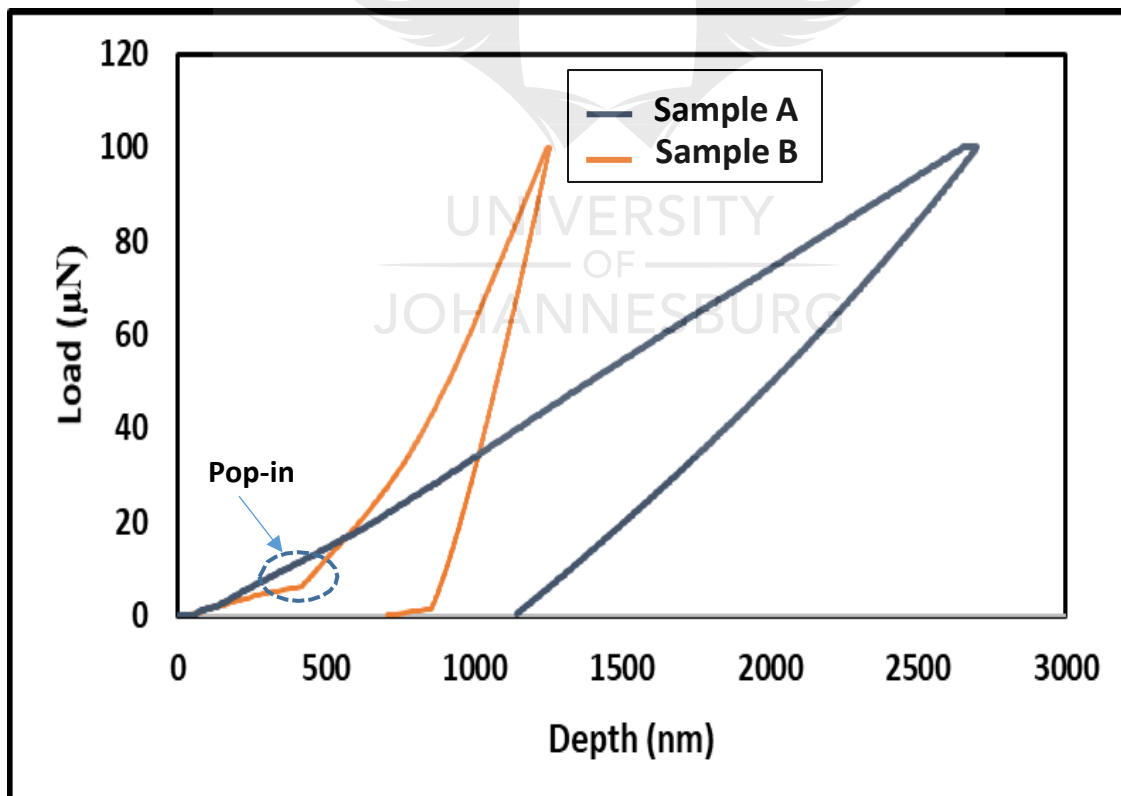
Fig. 12- The load-depth nanoindentation plots for samples A and B.

The hardness and elastic modulus are both obtained by the Oliver and Pharr technique [51] as

follows:

$$H = \frac{Pmax}{Ap} \dots \dots \dots \dots \dots (1)$$

Where Pmax is the maximum indenter load and the A_p is the projected area of indentation.

$$\frac{1}{E} = \frac{1 - v_s^2}{E_s} + \frac{1 - v_i^2}{E_i} \dots \dots \dots \dots \dots (2)$$

Where E_s, v_s and E_i, v_i stand for the Elastic modulus and Poisson's ratio of the nano indenter and sample, respectively.

Though Sample A retained nanotubes with high structural integrity, the mechanical properties of this composite are far lower than that observed in Sample B. The effect of agglomerations in the matrix is most probably responsible for this divergence, as agglomeration effects are often far worse than porosity effects [52]. These agglomerations doubled as fracture initiation points which consequently led to a decline in the mechanical attributes like hardness and elastic modulus of the sample [41, 53].

From the nanoindentation results, the elastic moduli obtained were used to determine the fracture toughness values using the Palmqvist equation. A directly proportional relationship was observed between the elastic moduli and the fracture toughness values obtained. Higher elastic moduli translated to higher fracture toughness values and vice versa. Thus, sample A with elastic modulus of 7.2 GPa displayed fracture toughness values of approximately 3 MPa√m while sample B with elastic modulus of 50.5 GPa displayed a fracture toughness of 9 MPa√m.

4. Conclusion

The aim of this study was to determine which factor weighed more heavily between uniform dispersion and structural integrity of CNTs in nickel aluminide composites. Ball milled powders were consolidated via spark plasma sintering, with different dispersion intensities and defect concentrations and later characterized. The obtained results show that Sample B with a more uniformly dispersed reinforcement exhibited superior mechanical properties despite a slight compromise on the structural integrity of the nanotubes owing to the combined milling regime employed. Conversely, Sample A containing nanotubes with structural integrity almost analogous to the pristine CNTs, exhibited very poor mechanical properties due to the retention of CNTs clusters and agglomerations in its matrix. This indicates that a more uniform dispersion of slightly impaired CNTs translates to better mechanical properties of composites as compared to a non-homogeneous dispersion of CNTs with higher structural integrity. It is observed that the

anticipated strengthening and toughening effect of the dispersed CNTs was dominated by the softening effect of the nanotube agglomerates in Sample A which led to a reduction in the hardness, elastic modulus and fracture toughness as compared to Sample B. This study therefore lends credible the negative effects of CNTs agglomerations on the mechanical properties of NiAl-CNTs intermetallic composites.
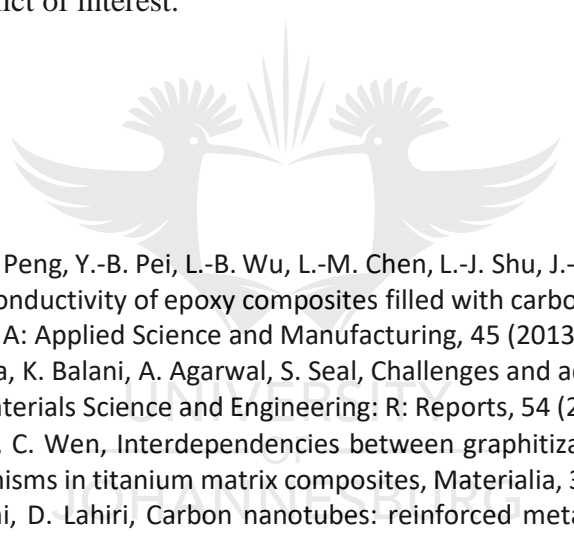
Acknowledgement

Conflict of interest

Authors declare no conflict of interest.

References

[1] L.-C. Tang, Y.-J. Wan, K. Peng, Y.-B. Pei, L.-B. Wu, L.-M. Chen, L.-J. Shu, J.-X. Jiang, G.-Q. Lai, Fracture toughness and electrical conductivity of epoxy composites filled with carbon nanotubes and spherical particles, Composites Part A: Applied Science and Manufacturing, 45 (2013) 95-101.

[2] V. Viswanathan, T. Laha, K. Balani, A. Agarwal, S. Seal, Challenges and advances in nanocomposite processing techniques, Materials Science and Engineering: R: Reports, 54 (2006) 121-285.

[3] K.S. Munir, Y. Li, J. Lin, C. Wen, Interdependencies between graphitization of carbon nanotubes and strengthening mechanisms in titanium matrix composites, Materialia, 3 (2018) 122-138.

[4] A. Agarwal, S.R. Bakshi, D. Lahiri, Carbon nanotubes: reinforced metal matrix composites, CRC press, 2016.

[5] K. Aristizabal, A. Katzensteiner, A. Bachmaier, F. Mücklich, S. Suárez, On the reinforcement homogenization in CNT/metal matrix composites during severe plastic deformation, Materials Characterization, (2018).

[6] Z. Liu, S. Xu, B. Xiao, P. Xue, W. Wang, Z. Ma, Effect of ball-milling time on mechanical properties of carbon nanotubes reinforced aluminum matrix composites, Composites Part A: Applied Science and Manufacturing, 43 (2012) 2161-2168.

[7] A. Esawi, K. Morsi, A. Sayed, M. Taher, S. Lanka, Effect of carbon nanotube (CNT) content on the mechanical properties of CNT-reinforced aluminium composites, Composites Science and Technology, 70 (2010) 2237-2241.

[8] H. Choi, G. Kwon, G. Lee, D. Bae, Reinforcement with carbon nanotubes in aluminum matrix composites, Scripta Materialia, 59 (2008) 360-363.

[9] A. Esawi, K. Morsi, A. Sayed, M. Taher, S. Lanka, The influence of carbon nanotube (CNT) morphology and diameter on the processing and properties of CNT-reinforced aluminium composites, Composites Part A: Applied Science and Manufacturing, 42 (2011) 234-243.

[10] H. Choi, J. Shin, B. Min, J. Park, D. Bae, Reinforcing effects of carbon nanotubes in structural aluminum matrix nanocomposites, Journal of Materials Research, 24 (2009) 2610-2616.

[11] X. Yang, E. Liu, C. Shi, C. He, J. Li, N. Zhao, K. Kondoh, Fabrication of carbon nanotube reinforced Al composites with well-balanced strength and ductility, Journal of Alloys and Compounds, 563 (2013)

216-220.

[12] C. Suryanarayana, Mechanical alloying and milling, Progress in materials science, 46 (2001) 1-184.

[13] F. Rikhtegar, S. Shabestari, H. Saghafian, The homogenizing of carbon nanotube dispersion in aluminium matrix nanocomposite using flake powder metallurgy and ball milling methods, Powder Technology, 280 (2015) 26-34.

[14] R. Xu, Z. Tan, D. Xiong, G. Fan, Q. Guo, J. Zhang, Y. Su, Z. Li, D. Zhang, Balanced strength and ductility in CNT/Al composites achieved by flake powder metallurgy via shift-speed ball milling, Composites Part A: Applied Science and Manufacturing, 96 (2017) 57-66.

[15] R. Haggenmueller, H. Gommans, A. Rinzler, J.E. Fischer, K. Winey, Aligned single-wall carbon nanotubes in composites by melt processing methods, Chemical physics letters, 330 (2000) 219-225.

[16] S. Suarez, F. Lasserre, F. Mücklich, Mechanical properties of MWNT/Ni bulk composites: Influence of the microstructural refinement on the hardness, Materials Science and Engineering: A, 587 (2013) 381-386.

[17] L.-X. Pang, K.-N. Sun, S. Ren, C. Sun, R.-H. Fan, Z.-H. Lu, Fabrication and microstructure of Fe3Al matrix composite reinforced by carbon nanotube, Materials Science and Engineering: A, 447 (2007) 146-149.

[18] P. Jozwik, W. Polkowski, Z. Bojar, Applications of Ni3Al based intermetallic alloys—current stage and potential perceptivities, Materials, 8 (2015) 2537-2568.

[19] M.A. Awotunde, M.A. Okoro, A.O. Adegbenjo, B.M. Shongwe, T.S. Tshephe, P.A. Olubambi, The effect of alloying additions on the mechanical properties of nickel aluminide NiAl—A review, in: Mechanical and Intelligent Manufacturing Technologies (ICMIMT), 2018 IEEE 9th International Conference on, IEEE, 2018, pp. 64-68.

[20] H. Kwon, M. Leparoux, A. Kawasaki, Functionally graded dual-nanoparticulate-reinforced aluminium matrix bulk materials fabricated by spark plasma sintering, Journal of Materials Science & Technology, 30 (2014) 736-742.

[21] C.B. Ponton, R.D. Rawlings, Vickers indentation fracture toughness test Part 1 Review of literature and formulation of standardised indentation toughness equations, Materials Science and Technology, 5 (1989) 865-872.

[22] Z. Li, A. Ghosh, A.S. Kobayashi, R.C. Bradt, Indentation fracture toughness of sintered silicon carbide in the Palmqvist crack regime, Journal of the American Ceramic Society, 72 (1989) 904-911.

[23] K.S. Munir, Y. Zheng, D. Zhang, J. Lin, Y. Li, C. Wen, Microstructure and mechanical properties of carbon nanotubes reinforced titanium matrix composites fabricated via spark plasma sintering, Materials Science and Engineering: A, 688 (2017) 505-523.

[24] E.W. Wong, P.E. Sheehan, C.M. Lieber, Nanobeam mechanics: elasticity, strength, and toughness of nanorods and nanotubes, science, 277 (1997) 1971-1975.

[25] S. Zhao, D. Xiang, A novel route for the synthesis of CNTs/WC composite powders from melamine and metal oxides, Ceramics International, 45 (2019) 4133-4136.

[26] A. Okoro, R. Machaka, S. Lephuthing, M. Awotunde, P. Olubambi, Structural integrity and dispersion characteristics of carbon nanotubes in titanium-based alloy, in: IOP Conference Series: Materials Science and Engineering, IOP Publishing, 2018, pp. 012004.

[27] M.S. El-Eskandarany, Mechanical alloying: nanotechnology, materials science and powder metallurgy, Elsevier, 2015.

[28] M.A. Asadabad, M.J. Eskandari, Electron diffraction, in: Modern Electron Microscopy in Physical and Life Sciences, IntechOpen, 2016.

[29] B. Chen, K. Kondoh, J. Umeda, S. Li, L. Jia, J. Li, Interfacial in-situ Al2O3 nanoparticles enhance load transfer in carbon nanotube (CNT)-reinforced aluminum matrix composites, Journal of Alloys and Compounds, (2019).

[30] A.M. Okoro, R. Machaka, S.S. Lephuthing, M.A. Awotunde, S.R. Oke, O.E. Falodun, P.A. Olubambi, Dispersion characteristics, interfacial bonding and nanostructural evolution of MWCNT in Ti6Al4V powders prepared by shift speed ball milling technique, Journal of Alloys and Compounds, 785 (2019) 356-366.

[31] P. Delhaes, M. Couzi, M. Trinquecoste, J. Dentzer, H. Hamidou, C. Vix-Guterl, A comparison

between Raman spectroscopy and surface characterizations of multiwall carbon nanotubes, Carbon, 44 (2006) 3005-3013.

[32] C. Casiraghi, A. Ferrari, J. Robertson, Raman spectroscopy of hydrogenated amorphous carbons, Physical Review B, 72 (2005) 085401.

[33] S. Suarez, F. Lasserre, O. Prat, F. Mücklich, Processing and interfacial reaction evaluation in MWCNT/Ni composites, physica status solidi (a), 211 (2014) 1555-1561.

[34] K. Aristizabal, A. Katzensteiner, A. Bachmaier, F. Mücklich, S. Suarez, Study of the structural defects on carbon nanotubes in metal matrix composites processed by severe plastic deformation, Carbon, 125 (2017) 156-161.

[35] B. Chen, K. Kondoh, H. Imai, J. Umeda, M. Takahashi, Simultaneously enhancing strength and ductility of carbon nanotube/aluminum composites by improving bonding conditions, Scripta Materialia, 113 (2016) 158-162.

[36] S.R. Bakshi, Plasma and cold sprayed aluminum carbon nanotube composites: Quantification of nanotube distribution and multi-scale mechanical properties, in, Florida International University, 2009.

[37] M.A. Awotunde, A.O. Adegbenjo, B.A. Obadele, M. Okoro, B.M. Shongwe, P.A. Olubambi, Influence of sintering methods on the mechanical properties of aluminium nanocomposites reinforced with carbonaceous compounds: A review, Journal of Materials Research and Technology, (2019).

[38] K.S. Munir, M. Qian, Y. Li, D.T. Oldfield, P. Kingshott, D.M. Zhu, C. Wen, Quantitative Analyses of MWCNT-Ti Powder Mixtures using Raman Spectroscopy: The Influence of Milling Parameters on Nanostructural Evolution, Advanced Engineering Materials, 17 (2015) 1660-1669.

[39] M.H. Wichmann, K. Schulte, H.D. Wagner, On nanocomposite toughness, Composites Science and Technology, 68 (2008) 329-331.

[40] A. Mohammadnejad, A. Bahrami, M. Sajadi, M.Y. Mehr, Spark plasma sintering of Ni3Al-xB-1wt% CNT (0.0< x< 1.5 at%) nanocomposite, Journal of Alloys and Compounds, 788 (2019) 461-467.

[41] B. Duan, Y. Zhou, D. Wang, Y. Zhao, Effect of CNTs content on the microstructures and properties of CNTs/Cu composite by microwave sintering, Journal of Alloys and Compounds, 771 (2019) 498-504.

[42] C. Ng, M. Savalani, M. Lau, H. Man, Microstructure and mechanical properties of selective laser melted magnesium, Applied Surface Science, 257 (2011) 7447-7454.

[43] D. Cáceres, C. Munuera, C. Ocal, J.A. Jiménez, A. Gutiérrez, M. López, Nanomechanical properties of surface-modified titanium alloys for biomedical applications, Acta Biomaterialia, 4 (2008) 1545-1552.

[44] J. Guo, K. Wang, T. Fujita, J. McCauley, J. Singh, M. Chen, Nanoindentation characterization of deformation and failure of aluminum oxynitride, Acta Materialia, 59 (2011) 1671-1679.

[45] Y.-J. Chiu, C.-Y. Shen, S.-R. Jian, H.-W. Chang, J.-Y. Juang, Y.-Y. Liao, C.-L. Fan, Nanoindentation study of FePt thin films deposited by radio frequency magnetron sputtering, Nanoscience and Nanotechnology Letters, 8 (2016) 260-265.

[46] F. Haag, D. Beitelschmidt, J. Eckert, K. Durst, Influences of residual stresses on the serrated flow in bulk metallic glass under elastostatic four-point bending–A nanoindentation and atomic force microscopy study, Acta Materialia, 70 (2014) 188-197.

[47] S.R. Oke, O.O. Ige, O.E. Falodun, P.A. Olubambi, J. Westraadt, Densification and grain boundary nitrides in spark plasma sintered SAF 2205-TiN composite, International Journal of Refractory Metals and Hard Materials, 81 (2019) 78-84.

[48] F. Ogawa, S. Yamamoto, C. Masuda, Strong, ductile, and thermally conductive carbon nanotube-reinforced aluminum matrix composites fabricated by ball-milling and hot extrusion of powders encapsulated in aluminum containers, Materials Science and Engineering: A, 711 (2018) 460-469.

[49] F. Mokdad, D. Chen, Z. Liu, B. Xiao, D. Ni, Z. Ma, Deformation and strengthening mechanisms of a carbon nanotube reinforced aluminum composite, Carbon, 104 (2016) 64-77.

[50] K.S. Munir, Y. Zheng, D. Zhang, J. Lin, Y. Li, C. Wen, Improving the strengthening efficiency of carbon nanotubes in titanium metal matrix composites, Materials Science and Engineering: A, 696 (2017) 10-25.

[51] W.C. Oliver, G.M. Pharr, An improved technique for determining hardness and elastic modulus

using load and displacement sensing indentation experiments, Journal of materials research, 7 (1992) 1564-1583.

[52] S.R. Bakshi, A. Agarwal, An analysis of the factors affecting strengthening in carbon nanotube reinforced aluminum composites, Carbon, 49 (2011) 533-544.

[53] A. Najimi, H. Shahverdi, Effect of milling methods on microstructures and mechanical properties of Al6061-CNT composite fabricated by spark plasma sintering, Materials Science and Engineering: A, 702 (2017) 87-

RESEARCH PAPER 3: REACTIVE SYNTHESIS OF CNTs REINFORCED NICKEL ALUMINIDE COMPOSITES OBTAINED BY SPARK PLASMA SINTERING

Abstract

Nickel aluminide-NiAl holds strong potentials for use as turbine blade applications in aerospace industries, on the condition that the main shortcoming of poor fracture toughness is alleviated. To mitigate this limitation, this work investigated the outcome of carbon nanotubes (CNTs) incorporation into the B2 ordered NiAl lattice structure in varying contents, via a unique two stage milling process with the aim of achieving improved dispersion with negligible damage to the nanotubes. The milled powders were consolidated by spark plasma sintering and the sintered composites were extensively characterized using X-ray diffraction (XRD), scanning electron microscopy (SEM), transmission electron microscopy (TEM), Raman spectroscopy (RS) and nanoindentation techniques. Results show that the NiAl-1.0 wt% CNTs exhibited the best combination of properties with an impressive fracture toughness value of 16.63 MPa√m and microhardness value of 306.37 HV, while the unreinforced showed fracture toughness values of 6.93 MPa√m and microhardness values of 349.49 HV. The enhanced fracture toughness is attributed to the retained lengths of the CNTs in addition to the 'disordering' of the ordered lattice structure of NiAl owing to the introduction of the nanotubes.

Keywords – nickel aluminide, fracture toughness, carbon nanotubes, spark plasma sintering, nanoindentation.

1. Introduction

Nickel aluminide (NiAl) intermetallics have been under research radar as potential high temperature materials to replace nickel-based super-alloys due to a remarkable combination of unique properties. Due to the strong bonding between aluminium and nickel, which persists even at higher temperatures, excellent properties competitive with those of super-alloys are their major strong points. The core leverage NiAl wields over nickel super-alloys is its light weight (5.9 g/cm^3), which translates into enormous weight gains. The approximate 1:1 relationship between weight reduction and fuel savings in aerospace structures [1] makes this a crucial dynamic in aero-engineering applications [2]. In addition, NiAl boasts of a higher thermal conductivity (76 W/mK), quadrupling that of its competition, with good oxidation resistance up to 1400°C [3-7], due to the formation of a stable adhesive layer of Al_2O_3 [8, 9]. These outstanding attributes of NiAl are typically relevant, and therefore highly sought after, especially in the automotive and aerospace industries, where a growing mandate for advanced materials with distinctive properties exists.

However, in spite of these attractive properties, industrial applications of NiAl are still remote, due to its poor fracture toughness and low ductility at ambient temperatures [10]. The exhibition of this poor structural attribute by NiAl is due to the innate lack of the required quantity of independent slip systems [11], thereby disqualifying its current candidacy in aerospace applications. In addition, Stollof [12] and Dey [7] opine that the low grain boundary cohesive energy possessed by this intermetallic is also jointly responsible for its brittleness. Subsequently, the mandate to improve the ductility of polycrystalline NiAl requires the addition of supplementary slip systems in the intermetallic matrix [11, 13]. Some major efforts among researchers towards this obligation have included slip behaviour modification via powder metallurgy [14], grain size refinement [15], mechanical alloying [16], ductile phase incorporation [17], heat treatment [18] and directional solidification [19]. A mutual feature in majority of these aforementioned routes to improving the ductility, is the introduction of an additional element into the B2 ordered intermetallic structure [17].

Consequently, several researchers have incorporated various elements into nickel aluminide matrices with the singular objective of enhancing its properties. From conventional materials like Fe [20], refractory materials like molybdenum [15, 21], rare earth materials like lanthanum and rhenium [8, 17, 22], hard materials like TiN [23] to novel materials like carbon nanotubes (CNTs) [24, 25], an exotic diversity of alloying elements have been explored. Due to the excellent properties and grain refinement attributes of CNTs [26, 27], they have been endorsed as excellent additions to improve the ductility of brittle matrices [28]. Literature has established the supremacy of these nanostructures over their particulate equivalents. This is due to their unconventional tubular morphologies which give rise to their exclusive properties, namely strength of 100 GPa and Young's modulus of 1TPa [29, 30]. This has opened up endless opportunities for their integration in diverse matrices [31-33]. However, in spite of the current aggressive investigation on CNTs as ideal reinforcements, few scholars have been able to successfully incorporate well dispersed CNTs into metal matrices. Traditional and modern routes have been investigated, yet, difficulties such as non-uniform distribution [34] and agglomerations [35] still persist. Needless to say, this is encumbering the full actualization of the potentials of CNTs in revolutionizing the composite world, as better dispersion of CNTs undeniably lead to better mechanical properties of the resulting composites.

Groven and Puszynski [25] incorporated both single walled carbon nanotubes (SWCNTs) and multi-walled carbon nanotubes (MWCNTs) in NiAl matrix using combustion synthesis. Results showed increasing microhardness values up to ~4.6 GPa for 1 wt% SWCNTs, after

which values dropped significantly to less than 2 GPa for 2.5 wt% content. MWCNTs addition on the other hand, showed decreasing microhardness values in comparison with the unreinforced NiAl (3.04 GPa) with increasing MWCNTs content. Authors attributed this reduction to high agglomerations of the nanotubes within the matrix, which yielded poor relative densities and consequently lower microhardness values especially in the MWCNTs reinforced NiAl.

Ameri et al, [24] incorporated CNTs in NiAl through mechanical alloying and achieved strength values up to 5.6 GPa, higher than what was obtained in Groven and Puszynski [25], in addition to an improvement in fracture toughness. Compared with particulate reinforcements however, the strength values obtained were lower. Strength values documented by Gostishchev et al, [21] with borides of molybdenum and tungsten was 8.4 and 9.4 GPa while Enayati et al. [16] achieved strength values of 10.15 GPa by the utilization of mechanical alloying exclusively.

Review of related literature divulges that the most commonly used powder metallurgy technique for the fabrication of this intermetallic is the mechanical alloying (MA) process [36]. Transposing the MA process unto the integration of CNTs in the nickel aluminide matrix however leads to an obliteration of the nanotube properties as it has been observed that the high energy ball milling (HEBM) technique utilized during MA, despite its effectiveness in dispersion [37], adversely affects the structural integrity of CNTs. The unsuitability of the MA technique is hinged on the prolonged HEBM duration [16] characteristic of MA processes which is not suitable for the distribution of these nanostructures. Researchers have reported the flattening, crushing and conversion of CNTs into an amorphous phase during the HEBM processes and these defects tend to minimize the improvement of the composite properties, originally intended by the incorporation of the CNTs [38]. To circumvent the extremedamage done to the delicate unique structures of the nanotubes, a two stage milling was employed in this study, to effectively disperse the MWCNTs in the selected intermetallic matrix. A 7 hlow energy ball milling was used to primarily debundle the MWCNTs uniformly into the matrix powders while a 1 h HEBM was done afterwards to disperse the agglomerations and clusters still retained in the matrix after the low energy ball milling (LEBM). This presents the opportunity of exploiting the advantages of these two milling processes for the ultimate reward of homogenous dispersion with minimal damage. Throughout literature, as far as the authors are concerned, the adapted two stage milling method employed in this study has not been used by any other author to disperse CNTs in a nickel aluminide intermetallic matrix.

It is the intention of the authors to clarify some pertinent issues concerning the fabrication of NiAl-CNTs composites. Some of these issues include: will an in-situ formation of this composite via reactive sintering yield better results than exclusive mechanical alloying? Can ball milling procedures be used exclusively to successfully disperse CNTs in an intermetallic matrix without causing extensive damage to the nanotubes? Will the incorporation of CNTs in the selected intermetallic matrix improve its mechanical properties? What will the effect of a more homogenous dispersion of the nanotubes on the fracture toughness of this intermetallic be? The provision of answers to these questions will irrefutably form a basis for further work to be done towards the perfection of the NiAl-CNTs composites for industrial applications in aerospace and automotive industries.

2. Experimental section

2.1 Raw materials

The two elemental powders, namely powders of nickel (with particle size of 0.5 - 3.0 µm and 99.5 % purity obtained from WearTech Limited) and 99.8% pure aluminium (average particle size of 25µm, supplied by TLS Technik GmbH & Co., Germany), were used as the initial materials for the matrix. Multi-walled carbon nanotubes (MWCNTs) with average diameter of 9.5 nm and l.5 µm average length obtained from Nanocyl Belgium was added as reinforcement.

2.2 Ball milling of nickel, aluminium and CNTs

Powder mixtures of NiAl with atomic weight composition in the ratio 1:1, in addition to pre-determined weight fractions of MWCNTs namely 0, 0.5 and 1.0 wt % were milled together. A modified two stage milling technique was employed, mainly to disperse the CNTs, comprising of a 7 h low energy ball milling (LEBM) at 150 rpm and a short high energy ball milling (HEBM) for 1 h at 75 rpm. The uniqueness of the method used in this study, is the lower speed employed during the second stage HEBM process in the bid to preserve the structural integrity of the nanotubes. Typically from literature, such follow up HEBM processes are conducted at higher milling speeds which have a higher propensity for inducing damage on the nanotubes [39, 40]. Both milling regimes had a ball-to-powder (BPR) weight ratio of 10:1. These milling balls, in addition to the powder mixtures were milled together in a 250 ml stainless steel pot for the durations already mentioned in both milling regimes. The total milling time for the two

stages of milling was intentionally kept at an 8 h lid with a view to preserving the integrity of the CNTs. To prevent excessive over heating of the powders, a 10 min recess was observed after every 10 min of milling throughout the two milling stages.

2.3 Materials characterization

The milled powder samples of the pure and reinforced samples were examined using scanning electron microscopy (SEM) Zeiss Sigma fitted with energy dispersive X-ray spectrometry (EDX). The morphology of the milled MWCNTs was studied using transmission electron microscopy JEOL JEM – 2100 analysed extensively at 150 keV. X-ray diffraction technique was utilized to effectively identify the existing phases in the milled powder samples via X-ray diffractometer (XRD, PANalytical Empyrean model) with Cu-Kα radiation (λ=0.154 nm) at a scanning rate of 1°/ min. The structural integrity of the pure MWCNTs and milled powder samples were assessed using a T6400 Jobin–Yvon, HORIBA, Japan model with a 514.5 nm laser employing a 20x objective lens. Raman scattering was acquired over a spectral range of 200 - 1800 cm^{-1} for all the samples.

2.4 Spark plasma sintering of ball milled powders

The milled powders with 0, 0.5 and 1.0 wt% MWCNTs additions respectively were initially cold compressed in a graphite die which was later placed in the SPS system (model HHPD-25, FCT Germany). 20 mm diameter discs with 5mm height were sintered at 1000 ºC and 32 MPa with holding time of 7 min and heating rate set at 100 ºC per min. Careful choice of sintering parameters was taken to prevent the aluminium from melting out during sintering at a sufficiently high temperature to allow the formation of the desired nickel aluminide phase via reactive sintering.

2.5 Density and hardness measurements

The densities of the sintered discs were carried out using the Archimedes' principle according to ASTM B 962-15 standard. An average value of five repeated measurements taken from each sample and the relative density was calculated as a function of both the theoretical and experimental densities of the sintered samples. Vickers indentation microhardness tests were conducted on sectioned samples that had been previously polished to achieve mirror-like

surfaces. A load of 100 gf and 10 s dwell time was used for the hardness tests. The reported microhardness values are the arithmetic mean of four successive indentations made on the smooth sample surfaces.

2.6 Fractographic examination

Fractographic samples were obtained by cutting the sintered samples three-quarter way through with a precision cutting machine. The incompletely cut discs were worked on to gently knock off the remaining one-quarter portion to completely cut through the sintered disc. Fractographic examinations were performed using a high resolution scanning electron microscope (HR-SEM) to view the morphologies of the fractured samples.

2.7 Nanoindentation techniques

The determination of the nano-mechanical properties of the consolidated composites particularly elastic modulus and nano-hardness was evaluated using an Anton Paar Tritec Nanoindenter with a Berkovich diamond indenter B-T 60. The 20mm by 5 mm sintered samples were sand blasted, grounded and polished to achieve a smooth glass-like surface in mandatory metallurgical preparation for indentations. The samples were linearly loaded up until maximum load of 100 mN at 10 mN per min with dwell time of 100s. The elastic modulus and nano-hardness values for the sintered NiAl-CNTs composites were obtained using the Oliver and Pharr method [41]. This value was then substituted into the Palmqvist equation [42, 43] for the determination of the fracture toughness values.

3.0 Results and discussions

MWCNTs fabricated by chemical vapour deposition (CVD) method as displayed in Fig. 1a, shows the highly tangled web of nanotubes. The existence of strong van der waals forces between the individual strands [44] keep the nanotubes bundled and knotted together. Commercially pure aluminium powders exhibiting spherical morphologies with varying particle sizes and an average particle size of 25μm is presented in Fig. 1b. Fig. 1c shows the characteristically spiky-surfaced morphology of the as-received commercially pure nickel powders. Fig. 1d in agreement with Fig. 1a illustrates the transmission electron microscopy (TEM) image of the highly intertwined and entangled cylindrical tubes of the pristine

nanotubes. Fig. 1e reveals the layered walls of the CNTs with an inset of the fast fourier transform (FFT) image confirming the interlayer spacing between the CNTs walls. The distinctive hexagonal structured lattice of the CNTs is comprised of sp^2 C – C bonds with an interlayer spacing of 0.3507 nm, fitting into the documented range of 0.34–0.38 nm apart [45]. Fig. 1e displays the fully concentric coaxial and halo rings of the selected area diffraction pattern (SAED) in the CNTs.
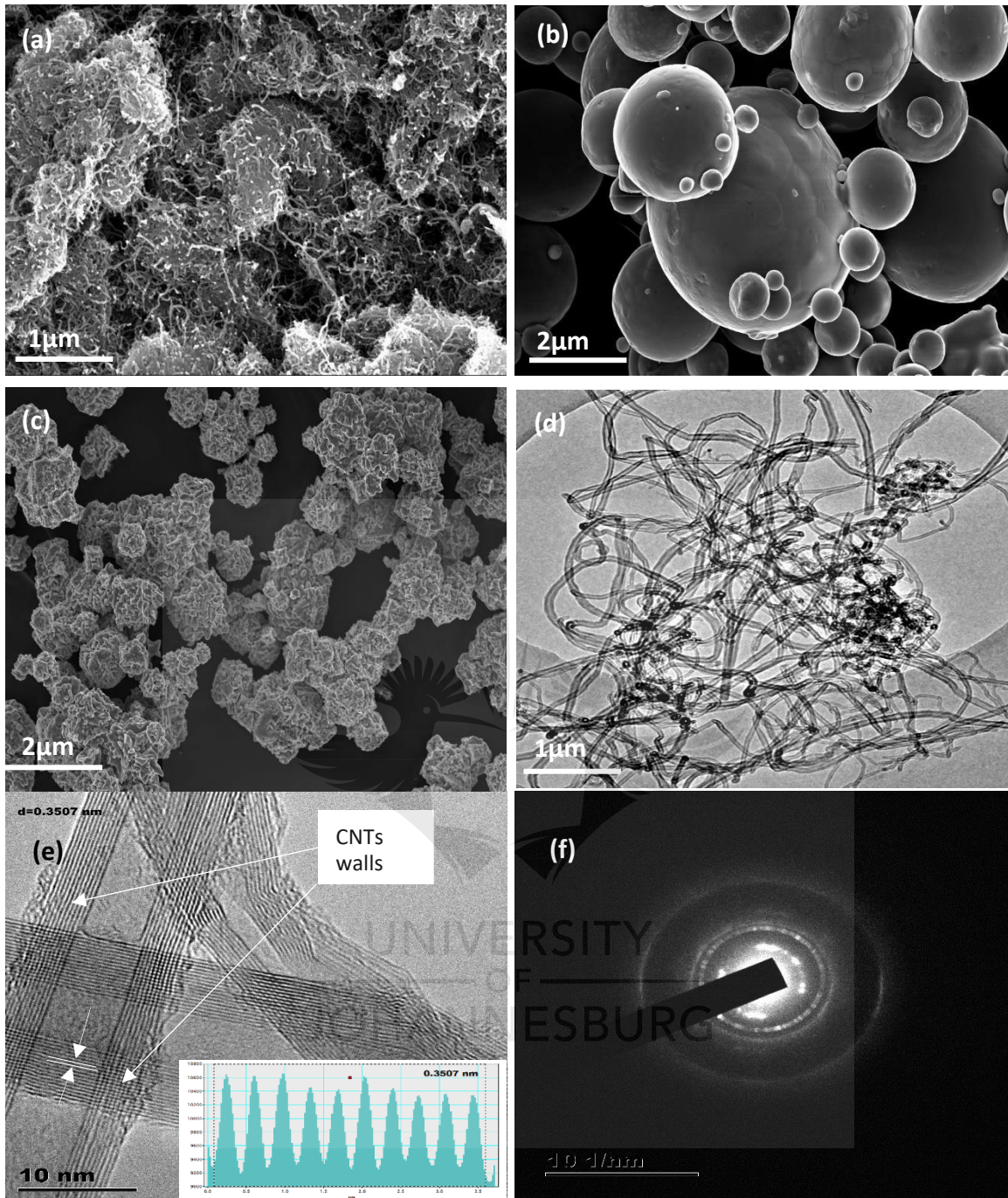
Fig. 1- SEM micrographs of the starting powders (a) MWCNTs, (b) aluminium powders and (c) nickel powders, (d) TEM micrograph of MWCNTs (e) HR-TEM image of CNTs walls with an inset of the FFT image of the pristine CNTs walls and (f) SAED pattern of the pristine CNTs

The nickel aluminide composites in this study were synthesized via reactive sintering of the milled starting powders according to the milling regime previously discussed. The formation of the NiAl-CNTs from the starting powders is due to the proposed reaction expressed in Eq. 1 as follows:

$$(1-\tfrac{x}{2})\,\text{Ni} + (1-\tfrac{x}{2})\,\text{Al} + x\,\text{C*} \rightarrow \text{NiAl-C*} + y\,\text{Al}_4\text{C}_3 \dots\dots\dots\dots\dots\dots\dots\dots\dots\dots\dots. \ (1)$$
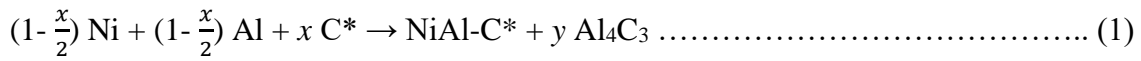
The complete reaction among these powders is facilitated by heating during the sintering process. Thermodynamically, the irreversible sintering process is one in which the total free energy of the system is reduced by reducing the total surface area [46]. In this work, spark plasma sintering (SPS) was employed due to its capacity for property enhancement in consolidated samples. The novelty of the SPS technique is in its utilization of a pulsed direct electrical current which ensures rapid amalgamation and densification of powders [47]. Its superiority over other orthodox sintering methods include rapid heating and cooling rates, lower sintering times, more uniform heating, reduced grain growth and prevention of powder disintegration, amongst others. The universally accepted ideology behind SPS sintering can be summed up in three stages-plasma heating, joule heating and plastic deformation [48]. During plasma heating, electric discharges in the gap between the powder particles lead to very high localized temperatures between them [49] as shown in Fig. 2.
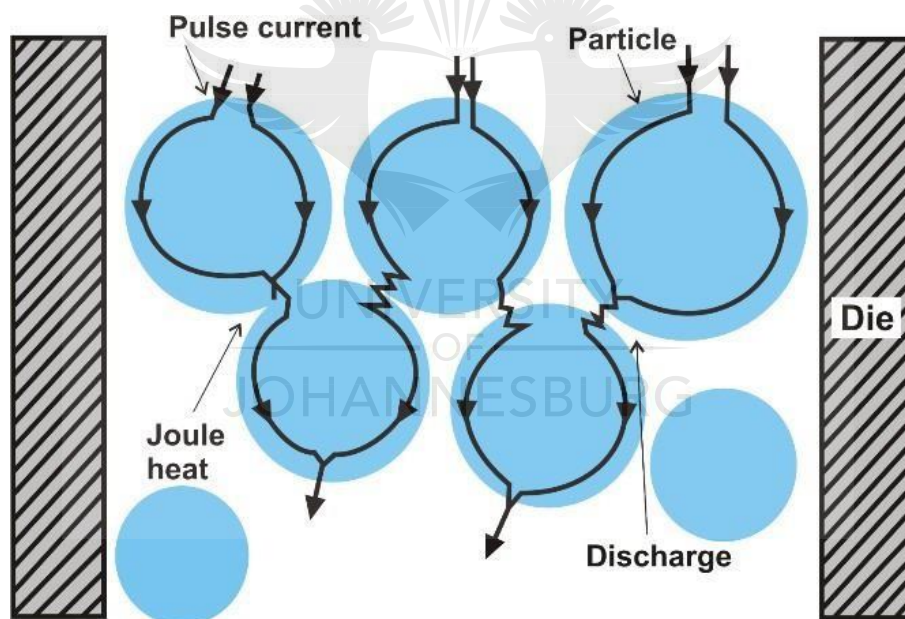
Fig. 2 - A schematic of pulsed current flow through powder particles during spark plasma sintering [47]

This facilitates melting at the particle-particle interface thereby activating the 'necking' phenomenon between the particles. Heating enhances diffusion of atoms between the necks, thereby increasing their growth [50]. Improved diffusion is guaranteed as diffusion mechanisms are promoted at the surface, among grain boundaries, as well as volumetrically thereby giving rise to clean interfaces and good grain to grain bonding [47]. The heated powder particles become softer and deform plastically under uniaxial loading, leading to a dense

compact. Evidence of the necking phenomenon can be seen in Fig. 3 depicting the successful reactive sintering of nickel aluminide composites via SPS.
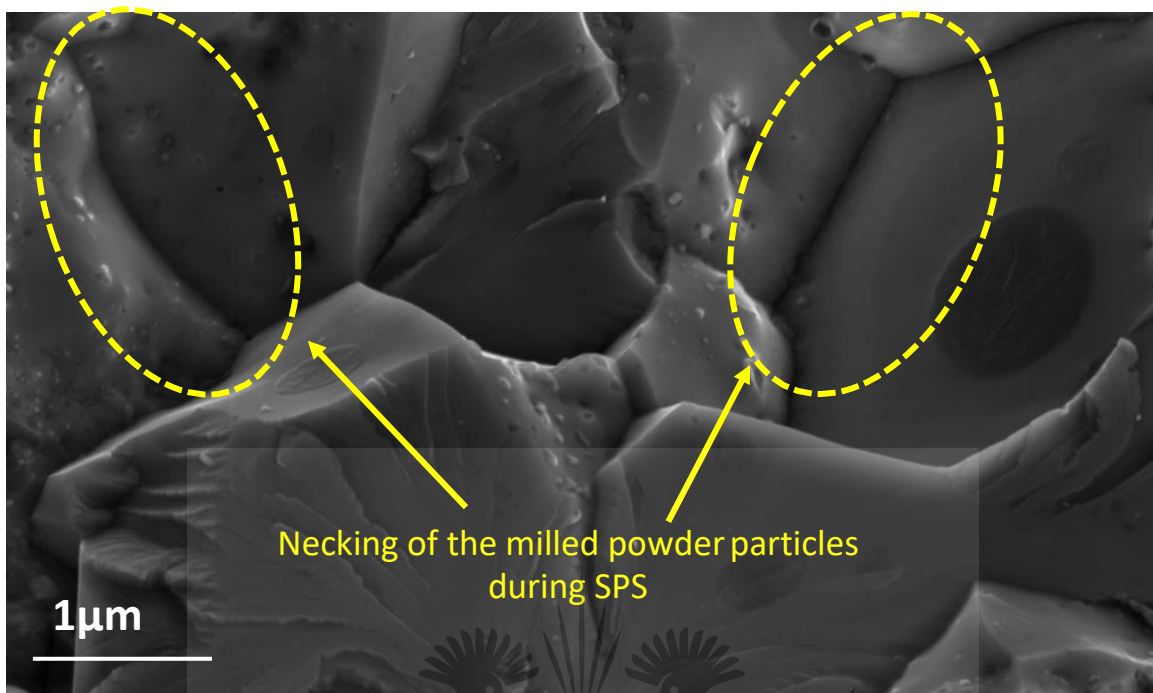
Fig. 3-Showing evidence of necking phenomenon taking place during spark plasma sintering (SPS) of NiAl

3.1.1 X-Ray diffraction of ball milled samples

Some reaction was already triggered during the ball milling due to inter-diffusion between the raw elemental powders. As observed from the XRD spectra of the admixed powders in Fig. 4, distinct peaks of NiAl are apparent. However, peaks of unreacted Ni and Al can also be observed in all the spectrums. A broadening of the initial sharp crystalline peaks of the starting powders can also be observed, indicating induced internal strain and grain size refinement due to the interaction between work hardening and plastic deformation of the powder particles during milling [51]. Though the characteristic long milling duration in mechanical alloying was not employed in this work, and given that diffusion in LEBM is not as high as it is in HEBM due to the low density of defects induced within the lattice [52]. Still, it is not surprising that nickel aluminide peaks were formed, owing to the fact that the 7 h of milling can be regarded as the first phase of mechanical alloying which is sufficient to trigger the initial formation of NiAl. Furthermore, the secondary milling stage which comprised of HEBM acted as a complementary milling stage which sped up the diffusion process, hence the observed NiAl peaks after milling. In addition, the presence of CNTs have been reported to lead to briefer

reaction times between nickel and aluminium for the formation of nickel aluminide [24], hence the observed stronger peaks of NiAl for the reinforced powders. Consequently, a characteristic diffraction peak for NiAl is observed at $2\theta = 44.67$ º corresponding to the (110) plane.
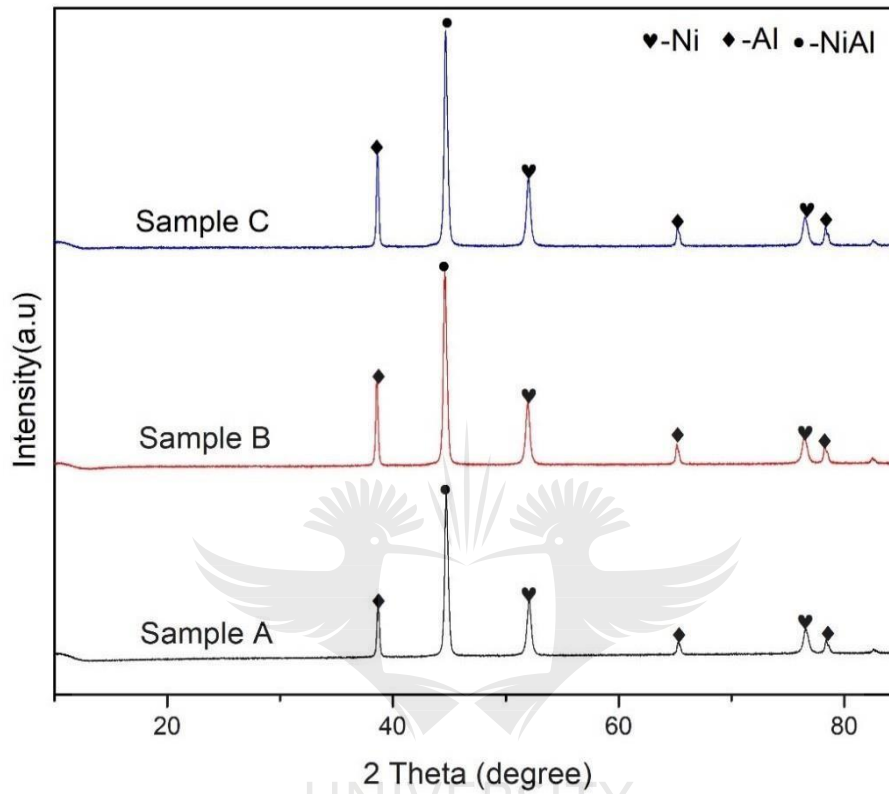
Fig. 4- XRD spectra of samples A (unreinforced NiAl), B (NiAl-0.5 wt% CNTs) and C (NiAl-1.0 wt% CNTs)

The full completion of the NiAl phase was achieved during the reactive sintering via SPS. No peak corresponding to aluminium carbide Al_4C_3 can be observed. The absence of this carbide phase is suggestive of a lack of defective sites in the MWCNTs which would have satisfied the necessary precondition for carbide formations [53, 54]. Such defects usually present as CNTs fragmentation which tends to increase the amount of carbon atoms present at CNTs tips, consequently leading to more reaction sites for the formation of the carbide phase [27]. Past works have established the chemical inertness of pristine CNTs due to the fact that their exposed tubular surfaces comprise of highly stable basal graphitic planes [55]. However, as fabrication progresses, defect sites are triggered and present in the form of sp^3 C atoms expediting preferential sites for carbide phase formations [56]. As the amorphization of the carbon nanotubes occurs, the initial crystalline C-C structure become amorphous due to the

149

generation of sp^3 disorders, thus depleting the carbon atoms in the matrix. Carbon peaks were also not observed in the spectra owing to the fact that the left over carbon after the formation of the NiAl-CNTs composite was seemingly insignificant and hence could not be detected [27, 57] due to the detection limit of the XRD technique [58]. Interestingly, even at higher concentrations of 1.0 wt%, carbon peaks were still not detected, as observed in Fig. 4. Typically, at higher concentrations, dispersibility of CNTs usually declines, and in agreement with Cai et al [59] observed carbon peaks in XRD graphs may also be an indication of in-homogenous dispersion in the matrix. Hence, the absence of carbon peaks in the spectra confirms that the MWCNTs were well dispersed in the matrices in spite of the increasing CNTs content.

3.1.2 SEM analyses of the milled powders

From Fig. 5a it can be observed that the CNTs are well dispersed and embedded within the powder particles substantiating the effectiveness of the dispersion process. Likewise, a similar image is observed in Fig. 5b with a region depicting more evident CNTs tips as indicated by the region within the yellow circle.
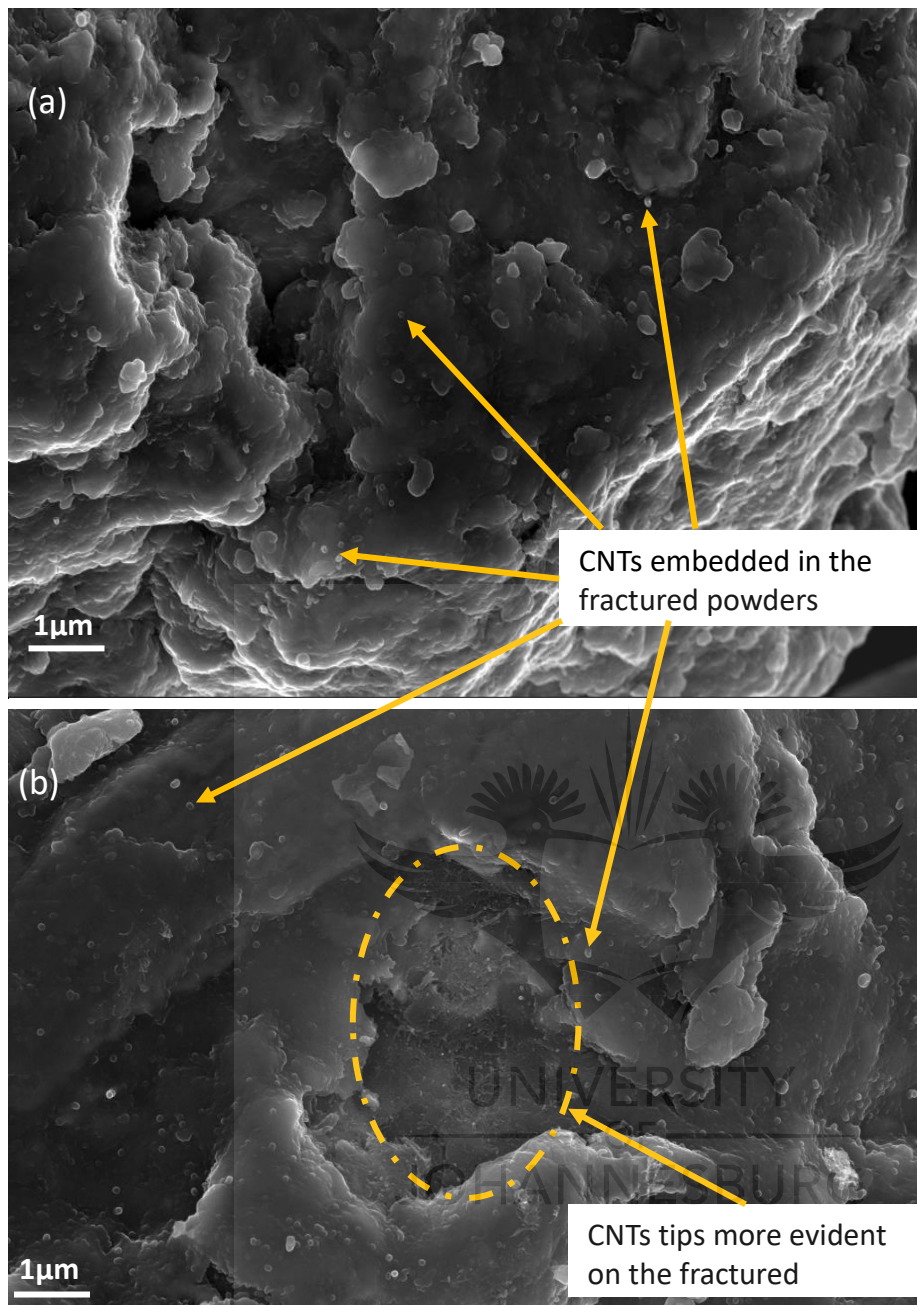
Fig. 5-SEM micrographs of samples with CNTs (a) NiAl-0.5 wt% CNTs (b) NiAl-1.0 wt% CNTs

Generally, the mechanism underlining ball milling processes can be broken down into three discrete stages namely flattening of the powder particles, cold-welding and fracturing [39]. At the initial stages of milling, CNTs are dispersed over the powder particles and then later covered by more powder particles, leading to the entrapment of the CNTs in the cold-welded powders, in response to the repetitive collision forces of the milling balls [60]. The collision forces are made up of two components precisely-the radial and tangential components. The radial component comprises of compressive forces resulting from the impact forces of the milling balls which lead to powder deformation via flattening, cold-welding and fracturing respectively. The tangential components comprise of shearing forces resulting from side motions and rotations in combination with frictional forces [61]. These two components operated in synergy to effectively de-cluster the nanotubes and embed them into the nickel and aluminium powder particles. The relative homogeneity displayed in these figures give credence to the efficacy of the two stage milling process experienced by the samples. The significance of the dispersion route utilized cannot be disregarded as it laid the foundation for the resulting mechanical properties which was exhibited by the consolidated composites. The homogeneous dispersion of undamaged nanotubes within the matrix powders is highly crucial for the achievement of enhanced properties in the composites. The desired mechanical properties in CNTs reinforced composites are not only contingent upon their uniform dispersion, but also on the retention of their tubular morphologies [62].

3.1.3 Raman spectroscopy of Ni-Al-CNTs milled powders

A Raman spectral data reveals the information required to quantitatively and qualitatively evaluate the structural integrity of the carbon nanotubes within the admixed powders. A typical spectrum is displayed in Fig. 6, with the black spectrum depicting the spectrum for the raw or unprocessed MWCNTs used in this study.
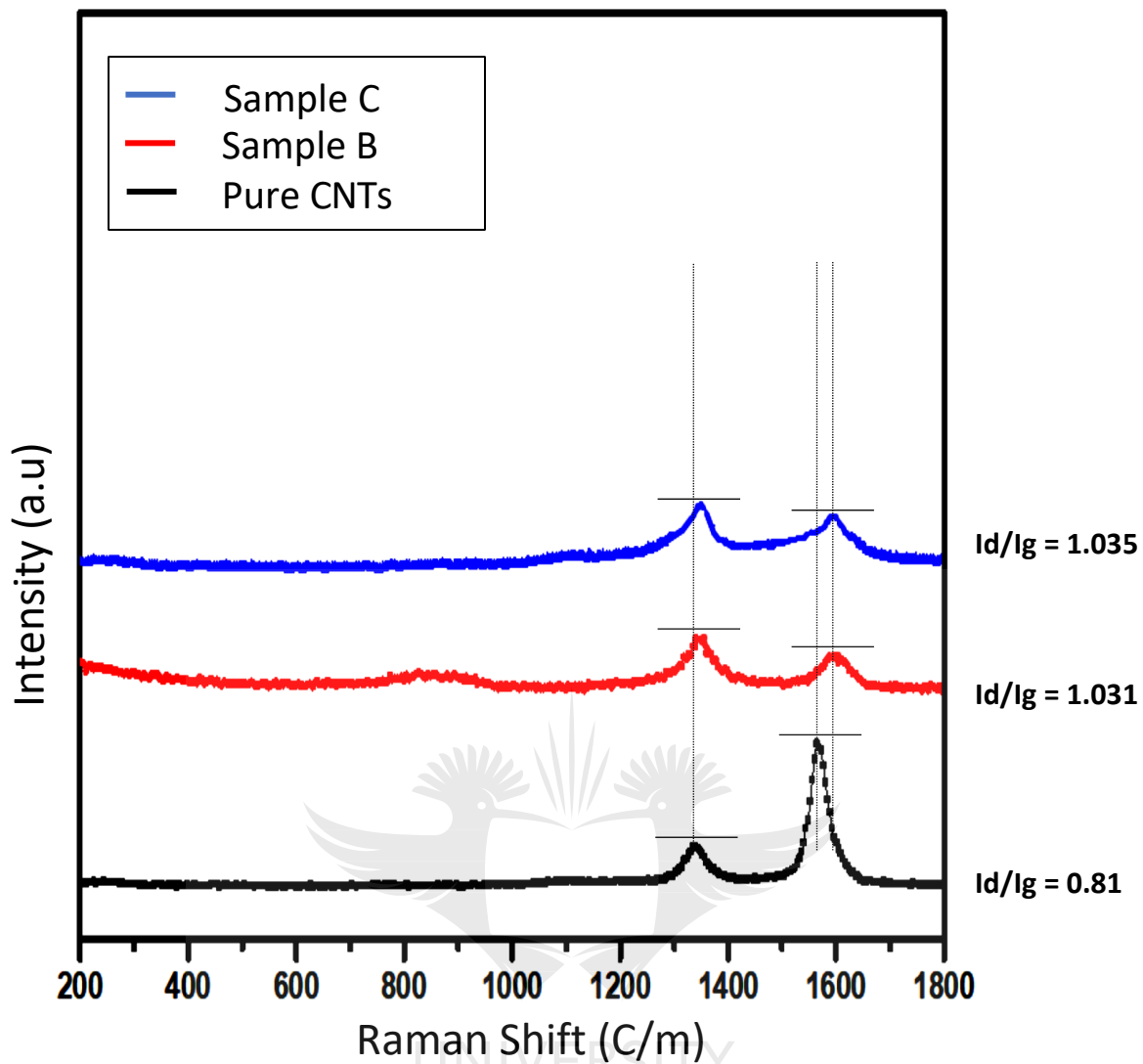
Fig. 6-Raman spectra for pristine MWCNTs and milled powder samples for 0.5 and 1.0 wt% MWCNTs nickel aluminides

The most important features of this spectra are the D and G graphitic peaks as observed in this figure. The D peak typically indicates the magnitude of lattice defects in the nanotubes due to damage done to their unique morphologies as a result of the production or dispersion processes. While the G peak indicates the incidence of protected hexagonal graphitic structure, level of crystallinity or metallicity present in the nanotubes [63]. Thus structural integrity can be assessed using these two characteristic peaks in a ratio I_D/I_G, known as the Raman ratio. It can therefore be inferred that a lower Raman ratio indicates a better protected structure than one with a higher Raman ratio. From Fig. 6 it is observed that the shape of the G peaks for the NiAl-CNTs admixed powders were retained, indicating that the inner walls of the CNTs were not hybridized to sp^3 but rather retained their sp^2 bonding [64]. Usually in sp^2 C-C CNTs structural lattice, three out of every four valence electrons bond covalently with in-plane adjacent

153

electrons [65], forming strong C-C bonds resulting in very high bonding energies (~614 kJ/mol) [66]. It can also be observed from the curves and data that the Raman ratio was very slightly higher with increase in CNTs content, thus sample C showed the highest Raman ratio typically depicting a slight increase in the build-up of defects in the original highly crystalline structure of the CNTs [67, 68].

3.1.4 Transmission Electron Microscopy (TEM) analyses for the Ni-Al-CNTs milled powders

Fig. 7 displays the TEM images of the NiAl-0.5 wt% CNTs milled powders. The carbon nanotubes are seen to be very well dispersed in the nickel aluminide matrix as observed in Figs. 7a and b. These images also depict good interaction between the CNTs and the matrix powders. Fig. 7c shows that the dispersed CNTs retained their cylindrical morphologies. Fig. 7d characterizes the selected area electron diffraction (SAED) pattern of the carbon nanotubes in the NiAl-0.5 wt% CNTs. It can be seen that the coaxial and halo rings [69] are in place and analogous to the diffraction pattern of the pristine CNTs as shown in Fig. 1f. The intact concentric rings are confirmations that the level of strain imbibed by the graphitic planes of the CNTs was quite negligible.
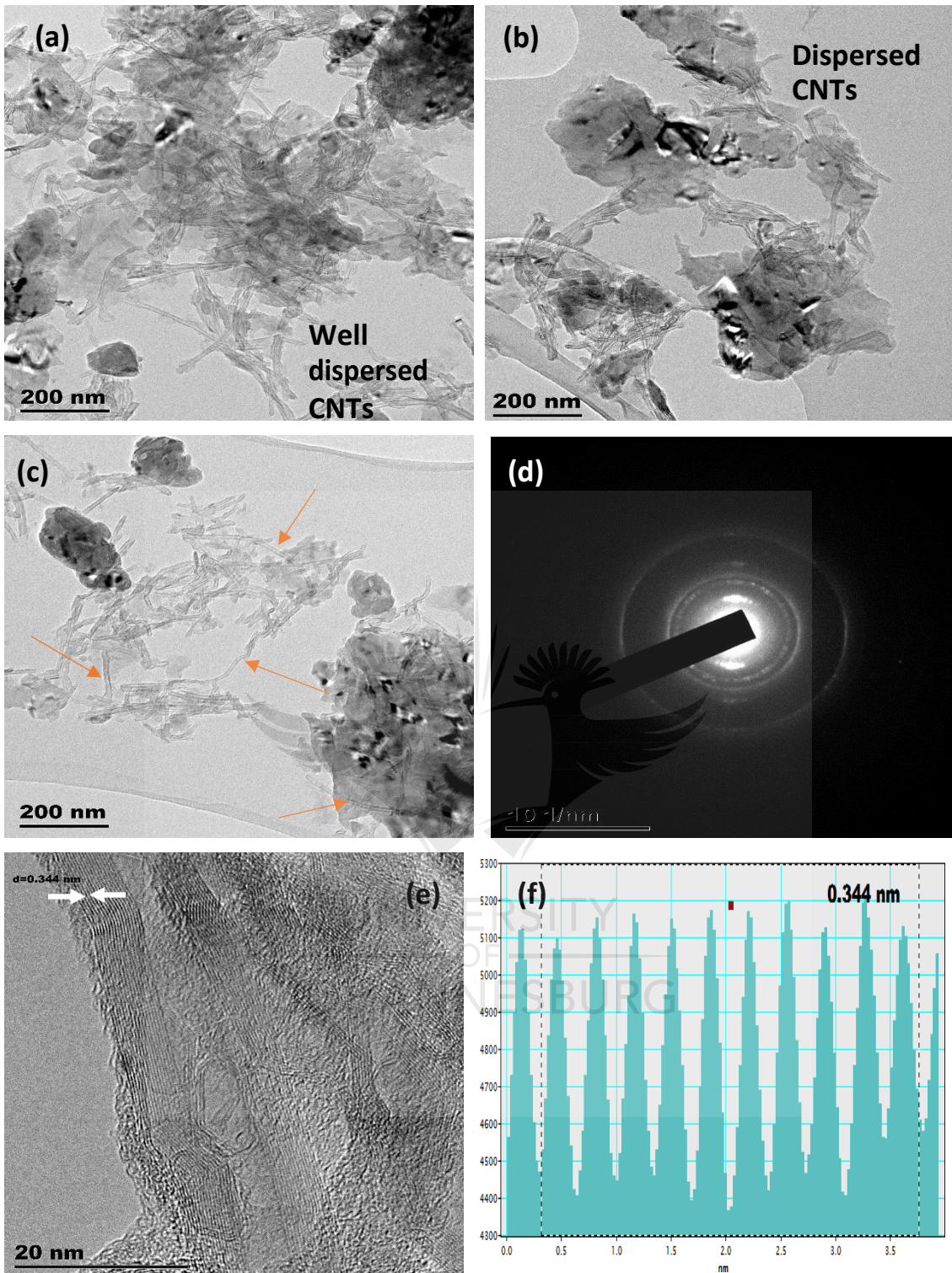
Fig. 7: HR-TEM images showing the evolution of CNTs in NiAl-0.5wt% CNTs milled powders (a-c) dispersed CNTs (d) SAED (e-f) FFT

Fig. 7f is the fast Fourier transform (FFT) revealing the inter wall spacing between the walls (as shown in Fig. 1e) of the pristine CNTs at 0.344 nm within the intermetallic matrix after processing. This is a slight deviation from what was measured as distance apart for the pristine

nanotubes which was 0.3507 nm. This disparity is indicative of a slight strain incurred during the course of milling. The strain pulls apart or collapses the walls of the CNTs leading to an increase or decrease in the interlayer spacing respectively as compared to the pristine. In this case, the walls seem to have been slightly collapsed, as the interlayer spacing reduced slightly indicating that the milling regime imparted some minor strain on the CNTs.

Fig. 8 indicates the TEM images of the NiAl-1.0 wt% MWCNTs powders with (a) revealing the well dispersed nanotubes. Fig. 8b however, reveals some slightly clustered CNTs within the admixed powders indicating that some few incompletely dispersed CNTs may still have persisted even after the secondary HEBM. This may be attributed to the increase in CNTs content of this sample which reduced the dispersibility of the nanotubes within the matrix powders hence favouring some very slight agglomerations. Fig. 8c displays the effectiveness of the milling regime in preserving the tubular structures of the nanotubes as individual cylindrical tubes are seen to be well dispersed in the powder matrix.
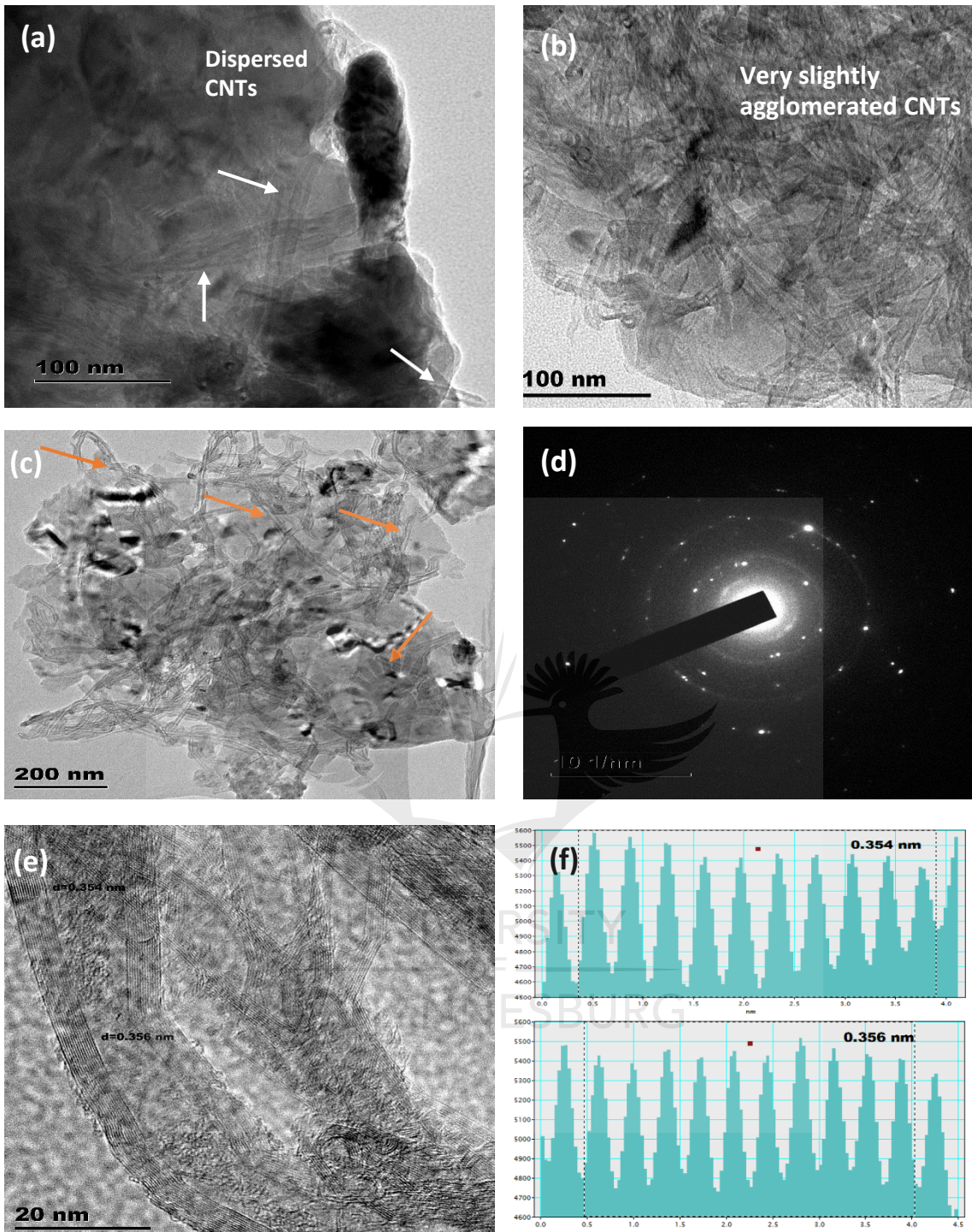
Fig. 8: HR-TEM images showing the evolution of CNTs in NiAl-1.0 wt% CNTs milled powders (a-c) dispersed CNTs (d) SAED (e-f) FFT

Fig. 8d typifies the SAED pattern of the carbon nanotubes in the NiAl-1 wt% CNTs. Here, it can be observed that the coaxial and halo rings are waning out and the image here is quite different from what is observed in Fig. 7d signifying that the strain imparted on this composition was probably higher than in the 0.5 wt% CNTs reinforced NiAl powder. This is as a result of the higher weight fraction present in this composition of admixed powders. Strain

157

is imparted on the CNTs as they are being milled together with the nickel and aluminium powder particles. Furthermore, additional stress is imparted on the discrete nanotubes as they are rubbing and chafing against other neighbouring CNTs. Given the fact that more CNTs are present in this composition, more friction is experienced by individual CNTs from adjacent CNTs present in the mix [58]. In addition, the slight eccentricity observed in the rings here are proofs that the CNTs in this batch endured a more significant form of strain. Nonetheless, the absence of strips and bands indicates that the amount of strain imbibed was not sufficient in inducing crystal defects or generating sp^3 disorders [70].

Fig. 8e and f reveal the distance apart between the walls of the CNTs to be 0.354 and 0.356 nm respectively. The distended walls are purely indicative of strain within the nanotubes. However, though Figs. 7e and f showed a reduction while Figs. 8e and f revealed an increase, both FFT scenarios are indicative of some form of strain as a result of transferred stresses from the impact of the milling balls during dispersion to the CNTs. In this case, the strain from the milling regime caused a pulling apart of the nanotube walls, translating to an increase in the interlayer spacing between the nanotube walls.

3.2 Microstructural analyses of the sintered composites

3.2.1 Densification, hardness and fracture toughness

The densification mechanism in SPS has been discussed in a previous section. Table 1 displays the result of the microstructural analyses of the spark plasma sintered (SPSed) composites. It can be deduced from these values that the densification reduced with increase in CNTs content.

Table 1 - Mechanical Properties of 0, 0.5 and 1.0 wt% CNTs reinforced NiAl composites

Sample	Relative density (%)	Young's modulus (GPa)	Micro-hardness (HV)	Nano-hardness (MPa)	Fracture toughness MPam$^{1/2}$
NiAl (unreinforced)	87.12	109.85	349.49±54.15	7,842.2	6.93±5.47
NiAl-0.5 wt%CNTs	81.24	37.40	191.19±11.65	5,806.8	7.50±2.20
NiAl-1.0 wt%CNTs	77.90	124.64	306.37±48.08	7,069.7	16.63±1.15

This is in good agreement with the SEM images of the polished sample surfaces as shown in Fig. 9 revealing the variation in pore densities as porosity is observed to increase with increase in CNTs content. Subsequently, the unreinforced NiAl composite displayed the highest densification while the NiAl-1.0 wt% CNTs demonstrated the highest porosity. Similar results have been documented in literature for other CNTs reinforced metallic matrices [24, 71, 72].
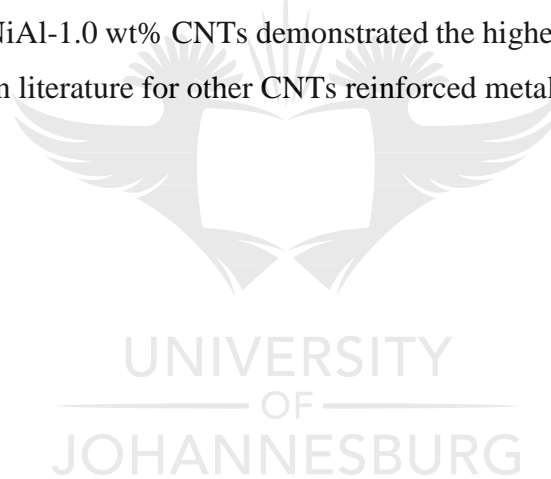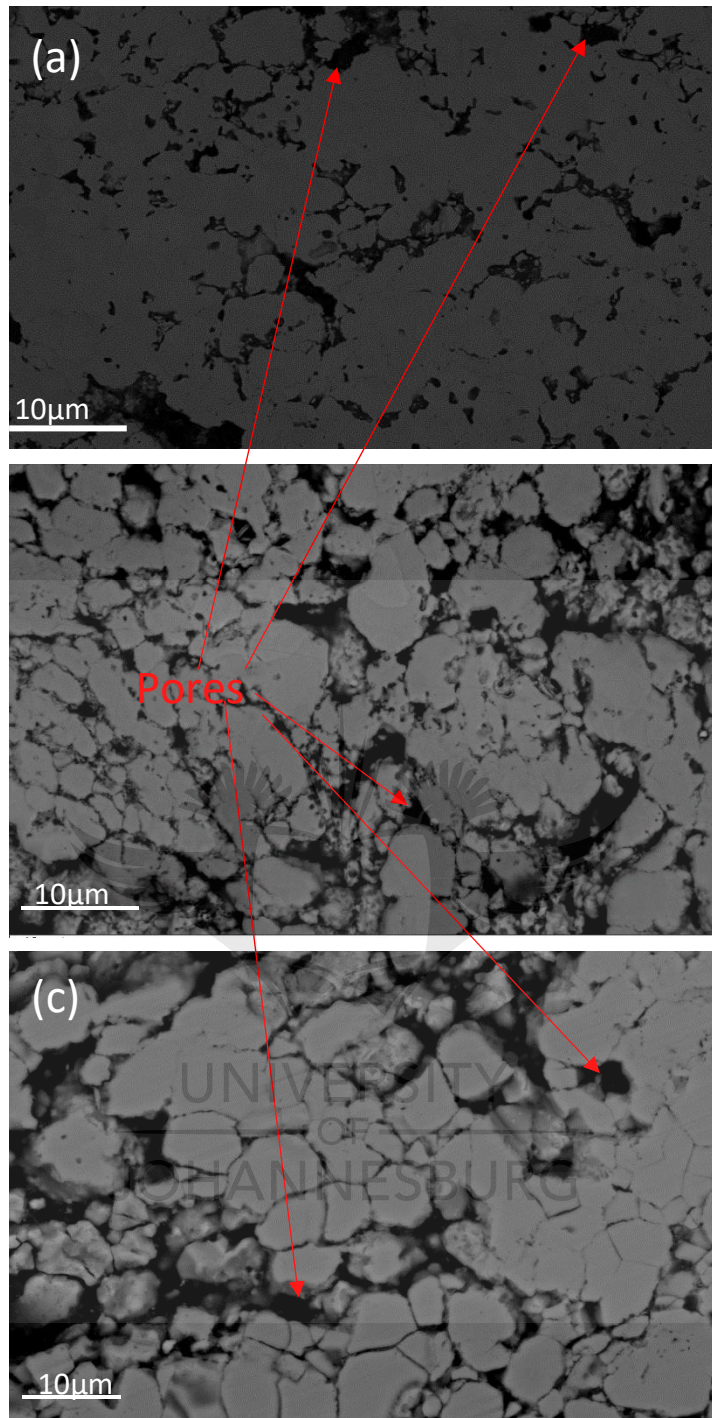
Fig. 9-SEM micrographs revealing the pore distributions in samples (a) A (unreinforced NiAl), (b) B (NiAl-0.5 wt% CNTs) and (c) C (NiAl-1.0 wt% CNTs)

Fig. 10 shows the nanoindentation curves for the pure and reinforced sintered composites obtained during the loading and unloading of the samples. Smooth curves of loading and unloading, devoid of pop-in effects are displayed for each of the samples. This depicts that mechanisms like elastic-plastic deformation shifts, cracking and dislocation bursts did not occur during the nanoindentation testing [73].

160
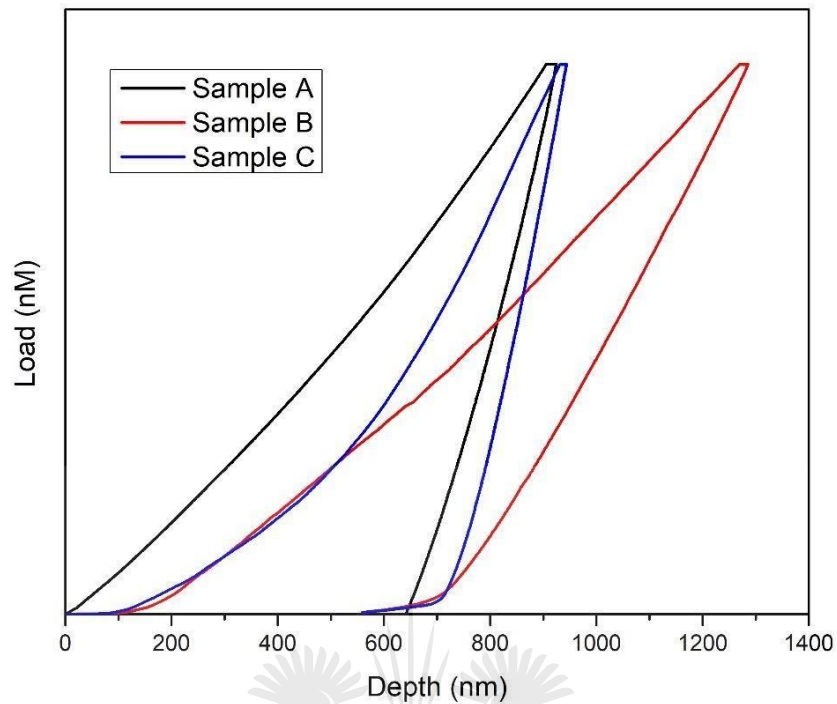
Fig. 10-Nanoindentation curves for samples A (unreinforced NiAl), B (NiAl-0.5 wt% CNTs) and C (NiAl-1.0 wt% CNTs)

The results from the nanoindentation tests are displayed numerically in Table 1 and diagrammatically in Figs. 10 and 11. From Table 1, it is observed that the addition of CNTs to the NiAl composite in this study led to a reduction of hardness values in the reinforced composites. Sample B displayed the least value of hardness and elastic modulus of all the composites. Consequently, a further decrease of mechanical properties was expected in Sample C with 1 wt % CNTs addition due to agglomeration effects as a result of an increase in CNTs content.
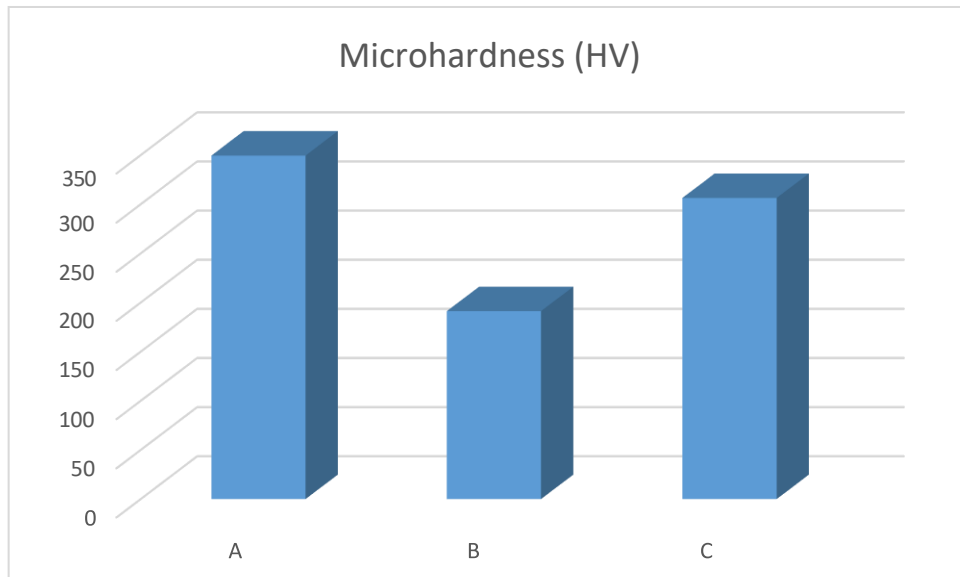
(a)
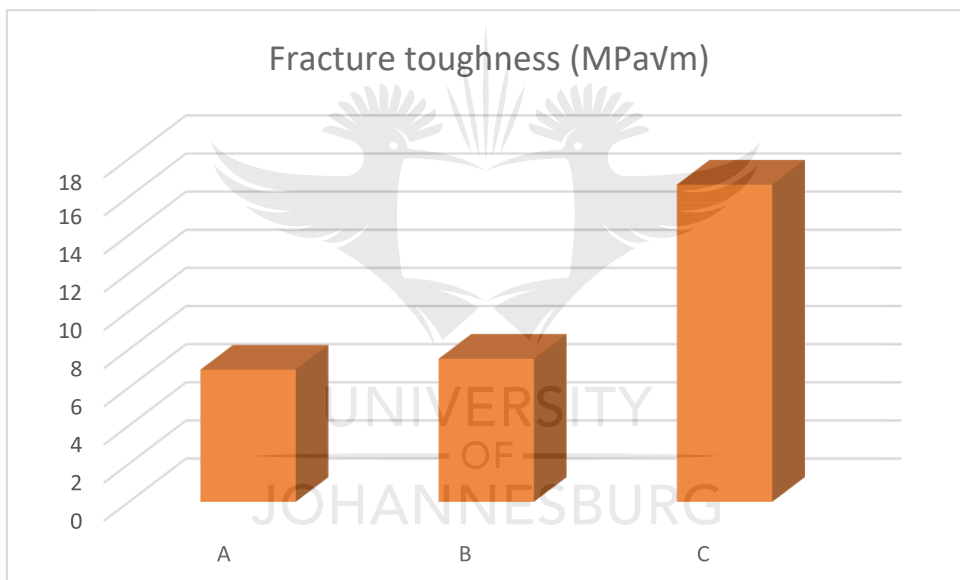
(b)

Fig. 11- Illustrating the relationship between mechanical properties and CNTs content (a) microhardness (b) fracture toughness

This expectation is rooted in the documentation of similar results in literature [25], but interestingly, the mechanical properties were more enhanced than that of the sample with less CNTs content (sample B). The strengthening effects anticipated from the integration of CNTs into metallic matrices are borne out of the intrinsic superlative properties of CNTs [54]. In addition, the grain refinement attributes of CNTs have been known to enhance the mechanical properties, particularly the hardness of composites. However, the reduction in hardness

observed in this study depicts a lack of this trend contrary to other research works. The plausible reason for this is the low densification achieved in this study. As demonstrated in Table 1, the densification values were generally lower than anticipated. However, the homogenous dispersion achieved as displayed by the SEM analysis of the powders, eliminates agglomeration effects as a probable cause. In a related study by Bochenek [8], they observed lower densification values with the spark plasma sintered (SPSed) NiAl-Re composites as compared with the hot pressed samples. This also translated to lower hardness values and other mechanical properties like flexural strength and fracture toughness in the SPSed composites. Though the sintering pressure was higher in the hot pressed samples and the dwell time employed in the SPSed composites was equally half of that which was employed for the hot pressed samples, the superior features of the SPS was expected to compensate for these reductions and still result in more enhanced mechanical properties [74, 75]. Comparing the dwell times between this work and theirs, the 7 min employed in this work was far less than the 30 min used in Bochenek [8]. This translated to very low densification values and subsequently low hardness values as well as displayed in Table 1. The caveat to this, however, is the improvement in mechanical properties of the NiAl-1wt% CNTs over that of the NiAl-0.5 wt% CNTs in spite of the reduced densification. This suggests a lack of dependence of the mechanical properties on the density of the sintered composites. From Table 1, sample C is observed to have the best combination of properties, yet it displays the lowest density of all the samples. The low hardness values recorded for the unreinforced NiAl (as compared to the hardness values of NiAl documented in literature) showed that the observed reduction is not a consequence of CNTs addition but a direct result of low densification.

The most remarkable property displayed by sample C is the fracture toughness of 16.63 MPa√m. Though low fracture toughness values have been anticipated particularly for sintered nickel aluminides [17], this interesting phenomenon however indicates that the improvement in the toughening is vastly dependent on the inherent properties of the CNTs, and possibly its quantity as well. This my throw some light on why the NiAl-0.5 wt% CNTs exhibited the least hardness values of all three samples despite the level of dispersion achieved. Nevertheless, the enhancement of properties recorded in the NiAl-1.0 wt% CNTs goes to show that anoptimum reinforcement content may be crucial. With increasing reinforcement content, mechanical properties such as hardness, elastic modulus and fracture toughness are seen to increase remarkably. Previous works postulate that the toughening attribute of nanotubes is highly dependent on their aspect ratios [76]. Consequently, with increase in CNTs content, more nanotubes are effectively in operation, translating to higher toughening efficiencies. Moreover,

163

the dispersion method employed in this work prevented the shortening of the nanotubes as displayed in Figs. 7 and 8 which reveal the dispersion of nanotubes with their lengths well retained particularly for NiAl-1.0 wt% CNTs. Comparing Fig. 7c to 8c, sample B appears to be dominated by relatively shorter tubes. A plausible explanation for this is that the milling speed employed may have been rigorous for the fewer CNTs present in the NiAl-0.5 wt% CNTs, but optimally adequate for the effective dispersion of the higher CNTs content in NiAl-1.0 wt% CNTs. A stronger evidence supporting this is the larger deviation of the interlayer spacing between the nanotubes in NiAl-0.5 wt% CNTs as compared to that of NiAl-1.0 wt% CNTs as shown in Figs. 7f and 8f respectively. The very slight increase in the Raman ratio in sample C as compared to sample B (though reported otherwise in literature) is also indicative of milder effects of the milling regime on sample C. The chafing experienced by neighbouring CNTs amongst themselves [77] may be responsible for this increase which may not necessarily translate to stretching of the nanotube walls.

The ball milling of CNTs with ceramic or intermetallic powders usually results in the dispersal of the CNTs over the powder particles leading to reduced sinterability and compressibility of the admixed powders [78]. This informed the choice of our milling regime which successfully led to the debundling and embedding of CNTs within the powder particles as observed in Fig. 5. The debundling and embedding took place during the first milling stage which comprised of gentle milling using the LEBM. The second stage was employed to further disperse the CNTs still left clustered within the powders after the LEBM stage via the energetic compressive and shear forces which are characteristically higher in the HEBM than that which the LEBM utilizes and exerts on the powders. This is apparent from the images, as CNTs tips are evident in the SEM micrographs, indicating the embedding of the CNTs within the powder particles. The implanting of the CNTs effectively into the matrix powder particles promotes good interfacial bonding between the nanotubes and the matrix powders [37], which is essential for the composite performance in service. This was made possible due to the combination of the dispersion mechanisms employed using the two milling regimes. The gentle motions of the LEBM instigated the detangling of the CNTs after which the more impactful motions of the HEBM were fleetingly employed to strengthen the interfacial bonding between the CNTs and the matrix and further disperse the CNTs clusters still retained in the matrix after the long term LEBM as illustrated by Fig. 12.
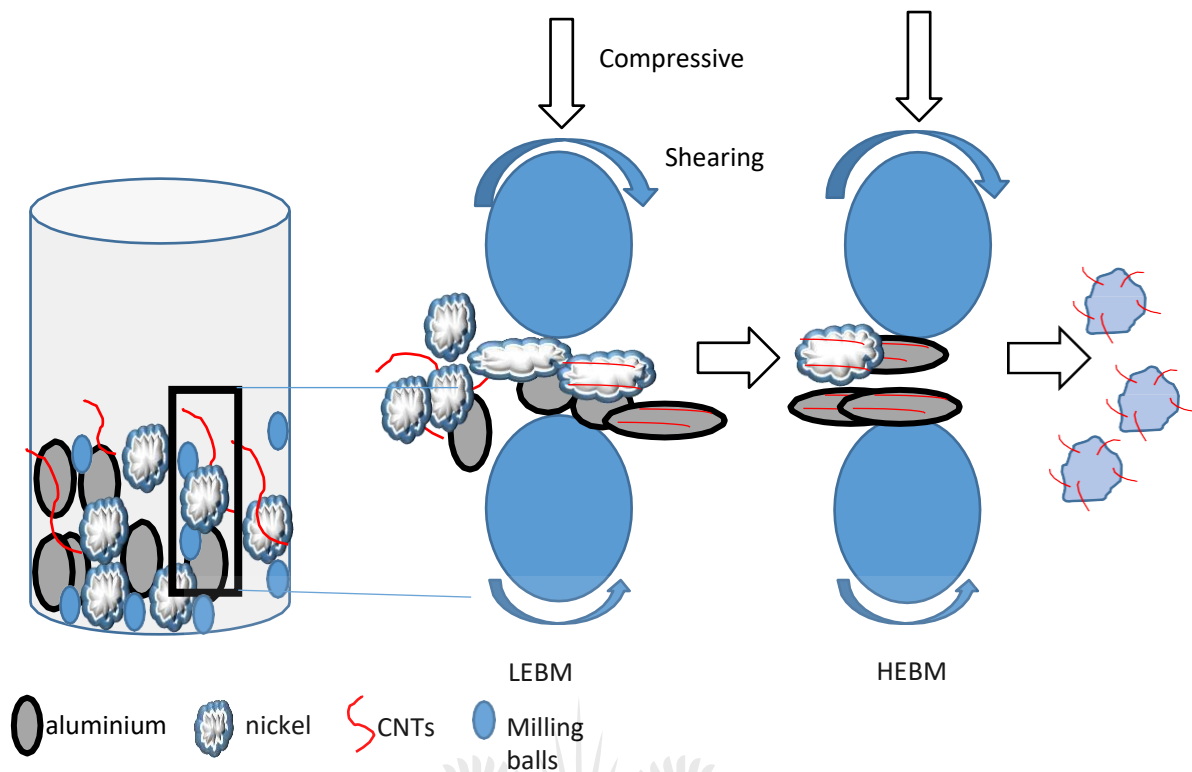
Fig. 12-Schematic of the two stage milling employed in this study

Another interesting feature evident in the TEM micrographs in Figs. 7 and 8 is the good interaction between the matrix powder particles and the nanotubes. There was an absence of isolated CNTs clusters even in the 1.0 wt% CNTs reinforced powders, authenticating the efficacy of the two stage milling method used in this study.

Powder metallurgy (PM) route has been used successfully for other intermetallic compounds like titanium aluminide. A recent breakthrough in the application of TiAl was by means of its production via the PM route-particularly spark plasma sintering technique for its fabrication [79]. The PM technique has the unique advantage of achieving higher densification from shorter sintering times which is desirable for enhanced mechanical properties [80]. Up until then, TiAl had been previously manufactured using the directional solidification (DS) route.

Though this route has produced some outstanding results in the production of NiAl-Cr-Mo alloys as well [81], the novelty of the PM route is that it precludes the additional cost and time of machining due to the near net shaping feature of this technique, thereby consequently eliminating waste. In addition, the success of NiAl-CNTs will yield better rewards particularly in terms of weight reductions as shown in Table 2. Moreover, the intense investigations on NiAl

intermetallic is borne out of the quest to fabricate a balanced composition of NiAl based composite without compromising the core properties of this material, particularly its lightweight, oxidation resistance and excellent thermal properties [17].

Table 2 - Mechanical properties of various NiAl based composites

Composite	Alloying element	Density of alloying element (g/cm^3)	Fabrication method	Hardness (GPa/HV)	Fracture toughness (MPa√m)
NiAl [21]	Mo$_2$B$_5$, W$_2$B$_5$	7.20, 15.3	Self-propagating High temperature Synthesis (SHS)	8.40/ 856.50, 9.40/ 858.50	-
NiAl [15]	Mo$_2$C	8.90	Powder Metallurgy (PM)	6.55/668	-
NiAl-36Cr-6Mo [81]	Cr, Mo	7.19, 10.28	Directional Solidification (DS)	-	26.15
NiAl-20 vol.% SiC [14]	SiC	3.21	Powder Metallurgy (PM)	4.97/507	-
NiAl-40 wt.% (TiB$_2$–TiN) [23]	TiB$_2$, TiN	4.52, 5.40	Combustion synthesis (CS)	8.92/909	-
NiAl-28Cr-5.94Mo-0.05Hf-0.01Ho [19]	Cr, Mo, Hf, Ho	7.19, 10.28, 13.31, 8.80	Directional Solidification (DS)	-	10.2
NiAl-1.25Re [8]	Re	21.02	Powder Metallurgy (PM)	-	12.69
NiAl-1.0wt% MWCNTs [25]	MWCNTs	2.10	Combustion synthesis (CS)	3.04/310	-
NiAl- 0.5wt% MWCNTs [24]	MWCNTs	2.10	Powder Metallurgy (PM)	5.60/571	>5.83
NiAl-1.0wt% MWCNTs (This work)	MWCNTs	2.10	Powder Metallurgy (PM)	3.01/306.37	16.63

3.2.2 Fractography

From SEM fractography results, the fracture morphology can be observed to have transited

from dominantly intergranular in Fig. 13 to a dimpled morphology as indicated in Fig. 14. Given that the brittleness of intermetallics partly originates at grain boundaries, the segregation of CNTs at the grain boundaries altered the grain boundary chemistry and cohesion, which led to the overall toughening of the composites. It can be said that the CNTs within the grain boundaries serve as ductile bridges among the grains thereby enhancing their toughness. The failure mode of the pure nickel aluminide depicts the trajectory of failure as 'respecting' the grain boundaries, hence following the path around the grain boundaries, indicating a dominant intergranular fracture mode. A lack of this morphology can be observed in Fig. 14 which has been replaced by a dominantly dimpled morphology. Evidence of plastic deformation is apparent on the fracture surfaces of the reinforced composites. Due to the texture of the micrograph in Fig. 14, it can be concluded that the integration of CNTs in NiAl intermetallic matrix through the employed route, improved the plasticity of the composites significantly.

Fig. 13-SEM image of the pure NiAl revealing the purely intergranular fracture surface
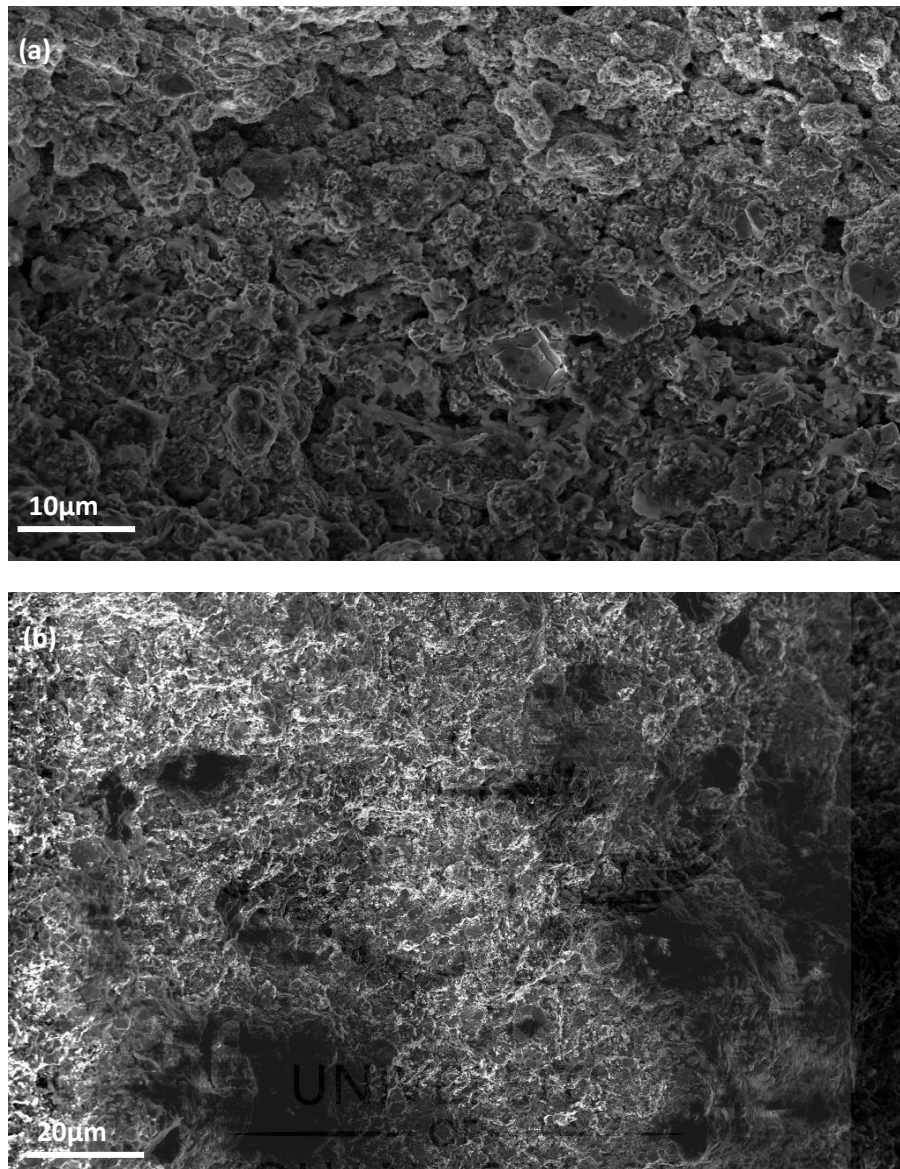
Fig. 14-SEM images showing the fracture surfaces of the reinforced composites (a) sample B (NiAl-0.5 wt% CNTs) and (b) sample C (NiAl-1.0 wt% CNTs)

3.3 Grain size refinement

Another mechanism that has been proposed to not only enhance the strength of this intermetallic but also the ductility via CNTs addition is grain size refinement [17, 82]. It is hypothesized that a finer grain size can help enhance ductility in some systems like NiAl perhaps due to some phenomenon known as slip flexibility. Slip flexibility is facilitated by a finer grain size which initiates uniform plasticity across the whole polycrystalline structure [83]. The incorporation of CNTs during milling helps to significantly refine grain sizes in metallic matrices. Milling, in itself is a means of size reduction to obtain a more homogenized microstructure [71] which leads to an improvement in mechanical properties, particularly

strength [84]. This is in accordance with Hall Petch equation which relays the inverse relationship between grain size and strength.

$$\sigma_y = \sigma_o + k_y\, d^{-1/2}$$ ………………………………………………………….. (2)

Where σ_y is the resulting strength of the refined material, σ_o is the original strength of the material, d is the average grain size of the material and k_y is the strengthening co-efficient. From this equation, it can be inferred that a reduction in grain size will lead to an increase in the strength of the material and vice versa. This is important since it then implies that smaller grains will give rise to a higher density of grain boundaries, due to the variable crystallographic orientations among the grains. Strength is therefore imparted on the material as a result of the interactions between the grain boundaries and the dislocations as the grain boundaries serve as obstacles or impediments blocking the path of dislocation motion [85, 86]. Thus the accumulation of dislocations at grain boundaries tend to increase the flow stress or yield stress of the metal [87]. One of the factors that instigated the choice of CNTs as an addition to NiAl for this work was borne out of its grain refinement properties and the simultaneous improvement on strength and ductility documented by some scholars. Duan et al, 2019 [88] attributed the concurrent increase in both strength and ductility of their copper matrix composite to the grain refining properties of CNTs. It was enthused that though there was an increased resistance to dislocation motion owing to increased grains and grain boundaries, the capacity for plastic deformation also increased, thus improving both strength and plasticity of the composite. Ogawa et al, 2018 [89] documented same phenomenon in an aluminium matrix where an unprecedented ductility of 37.2 % was recorded with an ultimate tensile strength of 450 MPa. Though these results have been recorded for reinforced metallic composites, the evidence presented in this study is strongly reminiscent of the inverse relationship between strength and ductility.

The characteristic strong bond existing in the NiAl intermetallic is due to the hybridization of d-nickel and sp-aluminium band electrons [90]. For plastic deformation to occur in NiAl, the statutory prerequisite of at least five independent slip systems must be satisfied, according to von mises stress criterion theory [91]. However, of the five required slip systems, NiAl can only boast of three, typically - {110} <100>, {110} <110>, and {110} <111> [92]. Literature stipulates that the addition of alloys would be beneficial as it would trigger super dislocations that are present in the interfaces and activate additional slip systems in NiAl for von mises criterion to be fully satisfied.

3.4 Dislocation movement, disordering and plasticity enhancement

Having prior established that the brittleness of NiAl can be ascribed to the absence of adequate number of slip systems [93], the observed improved fracture toughness of the CNTs reinforced nickel aluminide composites over the unreinforced samples can be attributed to the introduction of carbon into the crystal structure by its diffusion into the grain boundaries of the intermetallic matrix [94]. Alloying elements have the propensity to change the bonding and electronic parameters which also affect the stacking faults, bonding energies [95] and consequently, the dislocation mobility, which is a key determinant in ductility and plasticity enhancement. The movement of dislocations in metals is essential for plastic deformation to take place [18]. When materials possess low mobile dislocation densities, their ductility and fracture toughness are dramatically reduced [96]. The disordering triggered in the nickel aluminide sub-lattices due to the introduction of CNTs may have led to an increase in mobile dislocations within the system by freeing up the dislocation paths, resulting in higher ductility and fracture toughness. Though a simultaneous increase in both strength and fracture toughness of the intermetallic was anticipated, yet the fracture toughness may have been enhanced at the expense of strength. Given that dislocation pinning improves strength by restricting the mobility of dislocations [18, 27], the freer movement of these dislocations is essential for an improvement in ductility [97]. This is because strength and ductility are dependent upon one and the same factor – the level of difficulty in dislocation mobility [98]. It therefore appears that an improvement in one property led to a reduction in the other property. Moreover, the high strength generally displayed by NiAl is dependent on the highly ordered B2 structure. It seems that with the disordering of this structure due to the incorporation of the nanotubes, a reduction in strength occurred in favour of an improvement in the fracture toughness. As the disordering triggered more slip systems within the intermetallic structure [99], thereby leading to an improvement in the ductility and fracture toughness of NiAl-CNT composites.

In addition to the Ni and Al content of nickel aluminide, the resulting mechanical properties of the reinforced or alloyed NiAl may be dependent on the preferred site of the alloying or reinforcement elements, that is, the positions they occupy within the lattice structure [95, 100]. Elements like Nb, V and Si show a preference for the aluminium sub-lattice as their preferential sites, while elements like Mn, Co and Fe would rather be located in the nickel sub-lattice of the NiAl structure, while elements like Mo and W do not display any preferences between the two sub-lattices [101, 102]. The preferential site for carbon has not been widely established, as few

170

works have been done on NiAl-CNTs. However, the lattice distortions [93] and disordering that accrued in the sub-lattices of the intermetallic matrix as a result of the introduction of carbon due to impurity-host mismatch by reason of size disparity between the matrix and reinforcement atoms, ultimately led to an improvement in the fracture toughness of the composite.

4. Conclusion

This work successfully investigated the possibility of synthesizing NiAl via reactive sintering using SPS. Focusing on the results herein obtained and discussed, the following conclusions can be deduced:

- The unique two stage milling employed in the dispersal of CNTs within the NiAl matrix led to enhanced dispersion without significant damage to the nanotubes.
- The incorporation of well dispersed and high structural integrity CNTs in the NiAl intermetallic matrix led to a significant improvement of its fracture toughness from 6.93 to 16.63 MPa√m
- The higher fracture toughness obtained is attributed two factors – (a) the retained lengths of the dispersed CNTs and (b) the disordering in the sub-lattices of the highly ordered B2 intermetallic structure which led to the activation of more slip systems and promoted dislocation movement.
- Fracture surfaces of the reinforced composites revealed dominantly dimpled morphologies as compared to the purely intergranular fracture morphology of the unreinforced composite.

These results hold promise that the optimization of key processingparameters will ultimately lead to improved fracture toughness possibly in the range stipulated for engineering structures. Authors are presently working on this, particularly to achieve higher densification values and subsequently better enhancement of mechanical properties. This will facilitate the much awaited use of NiAl composites for turbine blades in aerospace industries.

Acknowledgement

Conflict of interest

None.

References

[1] K.S. Munir, C. Wen, Deterioration of the Strong sp2 Carbon Network in Carbon Nanotubes during the Mechanical Dispersion Processing—A Review, Critical Reviews in Solid State and Materials Sciences, 41 (2016) 347-366.

[2] D.B. Miracle, R. Darolia, NiAl and its alloys, Intermetallic Compounds: Principles and Practice, 2 (2000) 53-72.

[3] V. Sikka, S. Deevi, S. Viswanathan, R. Swindeman, M. Santella, Advances in processing of Ni3Al-based intermetallics and applications, Intermetallics, 8 (2000) 1329-1337.

[4] Y. Terada, K. Ohkubo, K. Nakagawa, T. Mohri, T. Suzuki, Thermal conductivity of B2-type aluminides and titanides, Intermetallics, 3 (1995) 347-355.

[5] F. Scheppe, P. Sahm, W. Hermann, U. Paul, J. Preuhs, Nickel aluminides: a step toward industrial application, Materials Science and Engineering: A, 329 (2002) 596-601.

[6] N. Stoloff, C. Liu, S. Deevi, Emerging applications of intermetallics, Intermetallics, 8 (2000) 1313-1320.

[7] G. Dey, Physical metallurgy of nickel aluminides, Sadhana, 28 (2003) 247-262.

[8] K. Bochenek, W. Węglewski, J. Morgiel, M. Basista, Influence of rhenium addition on microstructure, mechanical properties and oxidation resistance of NiAl obtained by powder metallurgy, Materials Science and Engineering: A, 735 (2018) 121-130.

[9] H. Grabke, Oxidation of NiAl and FeAl, Intermetallics, 7 (1999) 1153-1158.

[10] P. Jozwik, W. Polkowski, Z. Bojar, Applications of Ni3Al based intermetallic alloys—current stage and potential perceptivities, Materials, 8 (2015) 2537-2568.

[11] R. Noebe, R. Bowman, M. Nathal, Physical and mechanical properties of the B2 compound NiAl, International Materials Reviews, 38 (1993) 193-232.

[12] N. Stoloff, Physical and mechanical metallurgy of Ni3Al and its alloys, International Materials Reviews, 34 (1989) 153-184.

[13] P.M. Anderson, J.P. Hirth, J. Lothe, Theory of dislocations, Cambridge University Press 2017.

[14] F. Azarmi, Creep properties of nickel aluminide composite materials reinforced with SiC particulates, Composites Part B: Engineering, 42 (2011) 1779-1785.

[15] E. Liu, Y. Gao, J. Jia, Y. Bai, W. Wang, Microstructure and mechanical properties of in situ NiAl–Mo2C nanocomposites prepared by hot-pressing sintering, Materials Science and Engineering: A, 592 (2014) 201-206.

[16] M. Enayati, F. Karimzadeh, S. Anvari, Synthesis of nanocrystalline NiAl by mechanical alloying, journal of materials processing technology, 200 (2008) 312-315.

[17] K. Bochenek, M. Basista, Advances in processing of NiAl intermetallic alloys and composites for high temperature aerospace applications, Progress in Aerospace Sciences, 79 (2015) 136-146.

[18] J. Hack, J. Brzeski, R. Darolia, Evidence of inherent ductility in single crystals of the ordered intermetallic compound NiAl, Scripta metallurgica et materialia, 27 (1992) 1259-1263.

[19] Y. Liang, J. Guo, Y. Xie, L. Zhou, Z. Hu, High temperature compressive properties and room temperature fracture toughness of directionally solidified NiAl-based eutectic alloy, Materials & Design, 30 (2009) 2181-2185.

[20] A. Albiter, E. Bedolla, R. Perez, Microstructure characterization of the NiAl intermetallic compound with Fe, Ga and Mo additions obtained by mechanical alloying, Materials Science and Engineering: A, 328 (2002) 80-86.

[21] V. Gostishchev, I. Astapov, S. Khimukhin, Fabrication of nickel–aluminum alloys with tungsten and molybdenum borides by the method of self-propagating high-temperature synthesis, Inorganic Materials: Applied Research, 8 (2017) 546-550.

[22] A.I. Kovalev, D.L. Wainstein, A.Y. Rashkovskiy, Influence of Al grain boundaries segregations and La-doping on embrittlement of intermetallic NiAl, Applied Surface Science, 354 (2015) 323-327.

[23] A.A. Shokati, N. Parvin, M. Shokati, Combustion synthesis of NiAl matrix composite powder reinforced by TiB2 and TiN particulates from Ni–Al–Ti–BN reaction system, Journal of Alloys and Compounds, 585 (2014) 637-643.

[24] S. Ameri, Z. Sadeghian, I. Kazeminezhad, Effect of CNT addition approach on the microstructure and properties of NiAl-CNT nanocomposites produced by mechanical alloying and spark plasma sintering, Intermetallics, 76 (2016) 41-48.

[25] L. Groven, J. Puszynski, Combustion synthesis and characterization of nickel aluminide–carbon nanotube composites, Chemical Engineering Journal, 183 (2012) 515-525.

[26] S. Suarez, F. Lasserre, F. Soldera, R. Pippan, F. Mücklich, Microstructural thermal stability of CNT-reinforced composites processed by severe plastic deformation, Materials Science and Engineering: A, 626 (2015) 122-127.

[27] F. Mokdad, D. Chen, Z. Liu, B. Xiao, D. Ni, Z. Ma, Deformation and strengthening mechanisms of a carbon nanotube reinforced aluminum composite, Carbon, 104 (2016) 64-77.

[28] G.-D. Zhan, J.D. Kuntz, J. Wan, A.K. Mukherjee, Single-wall carbon nanotubes as attractive toughening agents in alumina-based nanocomposites, Nature materials, 2 (2003) 38.

[29] A.M. Okoro, S.S. Lephuthing, S.R. Oke, O.E. Falodun, M.A. Awotunde, P.A. Olubambi, A Review of Spark Plasma Sintering of Carbon Nanotubes Reinforced Titanium-Based Nanocomposites: Fabrication, Densification, and Mechanical Properties, JOM, 71 (2019) 567-584.

[30] A.D. Moghadam, E. Omrani, P.L. Menezes, P.K. Rohatgi, Mechanical and tribological properties of self-lubricating metal matrix nanocomposites reinforced by carbon nanotubes (CNTs) and graphene– a review, Composites Part B: Engineering, 77 (2015) 402-420.

[31] M. Bocanegra-Bernal, C. Dominguez-Rios, J. Echeberria, A. Reyes-Rojas, A. Garcia-Reyes, A. Aguilar-Elguezabal, Spark plasma sintering of multi-, single/double-and single-walled carbon nanotube-reinforced alumina composites: Is it justifiable the effort to reinforce them?, Ceramics International, 42 (2016) 2054-2062.

[32] Y. Hou, J. Tang, H. Zhang, C. Qian, Y. Feng, J. Liu, Functionalized few-walled carbon nanotubes for mechanical reinforcement of polymeric composites, ACS nano, 3 (2009) 1057-1062.

[33] S.C. Tjong, Recent progress in the development and properties of novel metal matrix nanocomposites reinforced with carbon nanotubes and graphene nanosheets, Materials Science and Engineering: R: Reports, 74 (2013) 281-350.

[34] A. Esawi, K. Morsi, A. Sayed, M. Taher, S. Lanka, Effect of carbon nanotube (CNT) content on the mechanical properties of CNT-reinforced aluminium composites, Composites Science and Technology, 70 (2010) 2237-2241.

[35] T. Peng, I. Chang, Uniformly dispersion of carbon nanotube in aluminum powders by wet shake-mixing approach, Powder Technology, 284 (2015) 32-39.

[36] T. Peng, I. Chang, Mechanical alloying of multi-walled carbon nanotubes reinforced aluminum composite powder, Powder Technology, 266 (2014) 7-15.

[37] E.I. Salama, A. Abbas, A.M. Esawi, Preparation and properties of dual-matrix carbon nanotube-reinforced aluminum composites, Composites Part A: Applied Science and Manufacturing, 99 (2017) 84-93.

[38] X. Yang, E. Liu, C. Shi, C. He, J. Li, N. Zhao, K. Kondoh, Fabrication of carbon nanotube reinforced Al composites with well-balanced strength and ductility, Journal of Alloys and Compounds, 563 (2013) 216-220.

[39] R. Xu, Z. Tan, D. Xiong, G. Fan, Q. Guo, J. Zhang, Y. Su, Z. Li, D. Zhang, Balanced strength and ductility in CNT/Al composites achieved by flake powder metallurgy via shift-speed ball milling, Composites Part A: Applied Science and Manufacturing, 96 (2017) 57-66.

[40] M.A. Awotunde, A.O. Adegbenjo, B.A. Obadele, M. Okoro, B.M. Shongwe, P.A. Olubambi, Influence of sintering methods on the mechanical properties of aluminium nanocomposites reinforced with carbonaceous compounds: A review, Journal of Materials Research and Technology, (2019).

[41] W.C. Oliver, G.M. Pharr, An improved technique for determining hardness and elastic modulus using load and displacement sensing indentation experiments, Journal of materials research, 7 (1992) 1564-1583.

[42] Z. Li, A. Ghosh, A.S. Kobayashi, R.C. Bradt, Indentation fracture toughness of sintered silicon carbide in the Palmqvist crack regime, Journal of the American Ceramic Society, 72 (1989) 904-911.

[43] J. Lankford, Indentation microfracture in the Palmqvist crack regime: implications for fracture toughness evaluation by the indentation method, Journal of Materials Science Letters, 1 (1982) 493-495.

[44] E.W. Wong, P.E. Sheehan, C.M. Lieber, Nanobeam mechanics: elasticity, strength, and toughness of nanorods and nanotubes, science, 277 (1997) 1971-1975.

[45] K.S. Munir, Y. Li, J. Lin, C. Wen, Interdependencies between graphitization of carbon nanotubes and strengthening mechanisms in titanium matrix composites, Materialia, 3 (2018) 122-138.

[46] F. Delannay, L. Froyen, A. Deruyttere, The wetting of solids by molten metals and its relation to the preparation of metal-matrix composites composites, Journal of materials science, 22 (1987) 1-16.

[47] M. Suárez, A. Fernández, J. Menéndez, R. Torrecillas, H. Kessel, J. Hennicke, R. Kirchner, T. Kessel, Challenges and opportunities for spark plasma sintering: a key technology for a new generation of materials, Sintering Applications, IntechOpen2013.

[48] Z.-H. Zhang, F.-C. Wang, L. Wang, S.-K. Li, Ultrafine-grained copper prepared by spark plasma sintering process, Materials Science and Engineering: A, 476 (2008) 201-205.

[49] X. Song, X. Liu, J. Zhang, Neck formation and self-adjusting mechanism of neck growth of conducting powders in spark plasma sintering, Journal of the American Ceramic Society, 89 (2006) 494-500.

[50] D. Demirskyi, H. Borodianska, D. Agrawal, A. Ragulya, Y. Sakka, O. Vasylkiv, Peculiarities of the neck growth process during initial stage of spark-plasma, microwave and conventional sintering of WC spheres, Journal of Alloys and Compounds, 523 (2012) 1-10.

[51] T. Chen, J. Hampikian, N. Thadhani, Synthesis and characterization of mechanically alloyed and shock-consolidated nanocrystalline NiAl intermetallic, Acta materialia, 47 (1999) 2567-2579.

[52] S. Hashemi, M. Enayati, M. Fathi, Plasma spray coatings of Ni-Al-SiC composite, Journal of thermal spray technology, 18 (2009) 284-291.

[53] Z. Liu, B. Xiao, W. Wang, Z. Ma, Singly dispersed carbon nanotube/aluminum composites fabricated by powder metallurgy combined with friction stir processing, Carbon, 50 (2012) 1843-1852.

[54] B. Chen, K. Kondoh, J. Umeda, S. Li, L. Jia, J. Li, Interfacial in-situ Al2O3 nanoparticles enhance load transfer in carbon nanotube (CNT)-reinforced aluminum matrix composites, Journal of Alloys and Compounds, (2019).

[55] P. Ajayan, T. Ebbesen, T. Ichihashi, S. Iijima, K. Tanigaki, H. Hiura, Opening carbon nanotubes with oxygen and implications for filling, Nature, 362 (1993) 522.

[56] K.S. Munir, D.T. Oldfield, C. Wen, Role of Process Control Agent in the Synthesis of Multi-Walled Carbon Nanotubes Reinforced Titanium Metal Matrix Powder Mixtures, Advanced Engineering Materials, 18 (2016) 294-303.

[57] C. Deng, D. Wang, X. Zhang, A. Li, Processing and properties of carbon nanotubes reinforced aluminum composites, Materials Science and engineering: A, 444 (2007) 138-145.

[58] A.O. Adegbenjo, B.A. Obadele, P.A. Olubambi, Densification, hardness and tribological characteristics of MWCNTs reinforced Ti6Al4V compacts consolidated by spark plasma sintering, Journal of Alloys and Compounds, 749 (2018) 818-833.

[59] W. Cai, X. Feng, J. Sui, Preparation of multi-walled carbon nanotube-reinforced TiNi matrix composites from elemental powders by spark plasma sintering, Rare Metals, 31 (2012) 48-50.

[60] A.M. Esawi, K. Morsi, A. Sayed, A.A. Gawad, P. Borah, Fabrication and properties of dispersed carbon nanotube–aluminum composites, Materials Science and Engineering: A, 508 (2009) 167-173.

[61] R. Andrews, D. Jacques, M. Minot, T. Rantell, Fabrication of carbon multiwall nanotube/polymer composites by shear mixing, Macromolecular Materials and Engineering, 287 (2002) 395-403.

[62] L. Jiang, Z. Li, G. Fan, L. Cao, D. Zhang, The use of flake powder metallurgy to produce carbon nanotube (CNT)/aluminum composites with a homogenous CNT distribution, Carbon, 50 (2012) 1993-1998.

[63] Z. Baig, O. Mamat, M. Mustapha, Recent Progress on the Dispersion and the Strengthening Effect of Carbon Nanotubes and Graphene-Reinforced Metal Nanocomposites: A Review, Critical Reviews in Solid State and Materials Sciences, (2016) 1-46.

[64] J.G. Park, D.H. Keum, Y.H. Lee, Strengthening mechanisms in carbon nanotube-reinforced aluminum composites, Carbon, 95 (2015) 690-698.

[65] M.S. Dresselhaus, G. Dresselhaus, P.C. Eklund, Science of fullerenes and carbon nanotubes: their properties and applications, Elsevier1996.

[66] J. Zhu, S. Wei, J. Ryu, M. Budhathoki, G. Liang, Z. Guo, In situ stabilized carbon nanofiber (CNF) reinforced epoxy nanocomposites, Journal of Materials Chemistry, 20 (2010) 4937-4948.

[67] K. Aristizabal, A. Katzensteiner, A. Bachmaier, F. Mücklich, S. Suarez, Study of the structural defects on carbon nanotubes in metal matrix composites processed by severe plastic deformation, Carbon, 125 (2017) 156-161.

[68] K.P. So, C. Biswas, S.C. Lim, K.H. An, Y.H. Lee, Electroplating formation of Al–C covalent bonds on multiwalled carbon nanotubes, Synthetic Metals, 161 (2011) 208-212.

[69] H.W. Kim, M.A. Kebede, H.S. Kim, M.H. Kong, C. Lee, Effects of annealing on the structure and photoluminescence of ZnO-sputtered coaxial nanowires, Journal of Luminescence, 129 (2009) 1619-1624.

[70] M.A. Asadabad, M.J. Eskandari, Electron diffraction, Modern Electron Microscopy in Physical and Life Sciences, IntechOpen2016.

[71] K. Vasanthakumar, N. Karthiselva, N.M. Chawake, S.R. Bakshi, Formation of TiCx during reactive spark plasma sintering of mechanically milled Ti/carbon nanotube mixtures, Journal of Alloys and Compounds, 709 (2017) 829-841.

[72] A. Adegbenjo, P. Olubambi, J. Potgieter, M. Shongwe, M. Ramakokovhu, Spark plasma sintering of graphitized multi-walled carbon nanotube reinforced Ti6Al4V, Materials & Design, 128 (2017) 119-129.

[73] S.R. Oke, O.O. Ige, O.E. Falodun, P.A. Olubambi, J. Westraadt, Densification and grain boundary nitrides in spark plasma sintered SAF 2205-TiN composite, International Journal of Refractory Metals and Hard Materials, 81 (2019) 78-84.

[74] M. Chmielewski, K. Pietrzak, A. Strojny-Nedza, K. Kaszyca, R. Zybala, P. Bazarnik, M. Lewandowska, S. Nosewicz, Microstructure and thermal properties of Cu-SiC composite materials depending on the sintering technique, Science of Sintering, 49 (2017).

[75] M. Demuynck, J.-P. Erauw, O. Van der Biest, F. Delannay, F. Cambier, Densification of alumina by SPS and HP: A comparative study, Journal of the European Ceramic society, 32 (2012) 1957-1964.

[76] K.S. Munir, Y. Zheng, D. Zhang, J. Lin, Y. Li, C. Wen, Improving the strengthening efficiency of carbon nanotubes in titanium metal matrix composites, Materials Science and Engineering: A, 696 (2017) 10-25.

[77] K.S. Munir, Y. Zheng, D. Zhang, J. Lin, Y. Li, C. Wen, Microstructure and mechanical properties of carbon nanotubes reinforced titanium matrix composites fabricated via spark plasma sintering, Materials Science and Engineering: A, 688 (2017) 505-523.

[78] M. Mazaheri, D. Mari, Z.R. Hesabi, R. Schaller, G. Fantozzi, Multi-walled carbon nanotube/nanostructured zirconia composites: Outstanding mechanical properties in a wide range of temperature, Composites Science and Technology, 71 (2011) 939-945.

[79] T. Voisin, J.P. Monchoux, L. Durand, N. Karnatak, M. Thomas, A. Couret, An Innovative Way to Produce γ-TiAl Blades: Spark Plasma Sintering, Advanced Engineering Materials, 17 (2015) 1408-1413.

[80] O. Guillon, J. Gonzalez-Julian, B. Dargatz, T. Kessel, G. Schierning, J. Räthel, M. Herrmann, Field-assisted sintering technology/spark plasma sintering: mechanisms, materials, and technology developments, Advanced Engineering Materials, 16 (2014) 830-849.

[81] Z. Shang, J. Shen, L. Wang, Y. Du, Y. Xiong, H. Fu, Investigations on the microstructure and room temperature fracture toughness of directionally solidified NiAl–Cr (Mo) eutectic alloy, Intermetallics, 57 (2015) 25-33.

[82] P. Grahle, E. Arzt, Microstructural development in dispersion strengthened NiAl produced by mechanical alloying and secondary recrystallization, Acta materialia, 45 (1997) 201-211.

[83] D. Nagarajan, C. Cáceres, The Friction Stress of the Hall–Petch Relationship of Pure Mg and Solid Solutions of Al, Zn, and Gd, Metallurgical and Materials Transactions A, 49 (2018) 5288-5297.

[84] H. Choi, J. Shin, D. Bae, Grain size effect on the strengthening behavior of aluminum-based composites containing multi-walled carbon nanotubes, Composites Science and Technology, 71 (2011) 1699-1705.

[85] F. Mirza, D. Chen, A unified model for the prediction of yield strength in particulate-reinforced metal matrix nanocomposites, Materials, 8 (2015) 5138-5153.

[86] K. Kim, J. Eckert, S. Menzel, T. Gemming, S.-H. Hong, Grain refinement assisted strengthening of carbon nanotube reinforced copper matrix nanocomposites, Applied Physics Letters, 92 (2008) 121901.

[87] S. Suárez, E. Ramos-Moore, B. Lechthaler, F. Mücklich, Grain growth analysis of multiwalled carbon nanotube-reinforced bulk Ni composites, Carbon, 70 (2014) 173-178.

[88] B. Duan, Y. Zhou, D. Wang, Y. Zhao, Effect of CNTs content on the microstructures and properties of CNTs/Cu composite by microwave sintering, Journal of Alloys and Compounds, 771 (2019) 498-504.

[89] F. Ogawa, S. Yamamoto, C. Masuda, Strong, ductile, and thermally conductive carbon nanotube-reinforced aluminum matrix composites fabricated by ball-milling and hot extrusion of powders encapsulated in aluminum containers, Materials Science and Engineering: A, 711 (2018) 460-469.

[90] R. Saniz, L.-H. Ye, T. Shishidou, A. Freeman, Structural, electronic, and optical properties of NiAl 3: First-principles calculations, Physical Review B, 74 (2006) 014209.

[91] J. Wollmershauser, S. Kabra, S. Agnew, In situ neutron diffraction study of the plastic deformation mechanisms of B2 ordered intermetallic alloys: NiAl, CuZn, and CeAg, Acta Materialia, 57 (2009) 213-223.

[92] J. Cotton, M. Kaufman, R. Noebe, A simplified method for determining the number of independent slip systems in crystals, Scripta metallurgica et materialia, 25 (1991) 2395-2398.

[93] Ş. Talaş, Nickel aluminides, Intermetallic Matrix Composites, Elsevier2018, pp. 37-69.

[94] K. Vedula, High temperature ordered intermetallic alloys III, MRS Sympo. Proc.: Materials Research Society, 133 (1989) 299.

[95] V. Portnoi, A. Blinov, I. Tomilin, T. Kulik, Mechanochemical synthesis of Mo-doped nickel aluminides, Inorganic materials, 38 (2002) 900-904.

[96] A. Najimi, H. Shahverdi, Effect of milling methods on microstructures and mechanical properties of Al6061-CNT composite fabricated by spark plasma sintering, Materials Science and Engineering: A, 702 (2017) 87-95.

[97] R. Valiev, Nanostructuring of metals by severe plastic deformation for advanced properties, Nature materials, 3 (2004) 511.

[98] W. Callister, D. Rethwisch, The structure of crystalline solids, Materials Science and Engineering: An Introduction, (2007) 38-63.

[99] F. Heredia, D. Pope, Effect of boron additions on the ductility and fracture behavior of Ni3Al single crystals, Acta metallurgica et materialia, 39 (1991) 2017-2026.

[100] G. Frommeyer, R. Fischer, J. Deges, R. Rablbauer, A. Schneider, APFIM investigations on site occupancies of the ternary alloying elements Cr, Fe, and Re in NiAl, Ultramicroscopy, 101 (2004) 139-148.

[101] Y. Terada, K. Ohkubo, T. Mohri, T. Suzuki, Site preference in NiAl—determination by thermal conductivity measurement, Materials Science and Engineering: A, 329 (2002) 468-473.

[102] Y. Hao, R. Yang, Q. Hu, D. Li, Y. Song, M. Niinomi, Bonding characteristics of micro-alloyed B2 NiAl in relation to site occupancies and phase stability, Acta materialia, 51 (2003) 5545-5554.

CHAPTER FOUR

DISCUSSIONS ON ISSUES ADRESSED BY THE ARTICLES

4.1 Concept of the dissertation

The motivation for this work is based on evaluating the feasibility of improving the fracture toughness of NiAl composites by incorporating multi-walled carbon nanotubes (MWCNTs). The significance of this is the wide applicability of nickel aluminide composites in the event this feat is accomplished. Nickel aluminide is a strong competitor of nickel base super-alloys which are far more expensive than NiAl. The principle behind this thesis is therefore hinged on presenting solutions to the shortcomings of NiAl that have hitherto prevented their use in service. This lines up with the problem solving context on which scientific researches are based, in proffering solutions through sound and practical scientific findings that impact on our environment. This work carefully navigated the dicey issue of CNTs dispersion in an intermetallic matrix via a thorough understanding of the complexities of dispersion characteristics of the nanotubes. It also investigated the microstructure-property relationship of the reinforced composites and contributed valuable findings to the body of scientific knowledge.

This Chapter comprises of critical discussions focused on the subject matter raised by each article in this work. The motivation behind each article is carefully articulated herein as they each set out to achieve the pre-determined objectives of this work. The novelty of this work and its contributions to the scientific body of knowledge are carefully articulated as well.

4.2 Arguments for originality and contribution to knowledge

In this work, concerted efforts were directed towards improving the major limitation of NiAl without jeopardizing the strong points-particularly its lightweight. This factor, in addition to the superlative properties of CNTs instigated their use as reinforcing agents in the selected nickel aluminide matrix. This work also gives a detailed overview of the dispersion characteristics of the nanotubes in the selected matrix. This included the nano-structural evolution of the nanotubes, dispersion effects and agglomeration effects. A detailed investigation on the effects of agglomeration on the resulting mechanical properties was carried out. The influence of nanotube additions on the sintering characteristics and the densification in the sintered composites were also studied. The effect of CNTs addition on the mechanical properties, particularly the fracture toughness was investigated as well, with the toughening mechanisms discussed. The research thus presents succinctly the influence of CNTs on the densification, microstructure, micro- and nano-hardness, fracture behaviour, elastic modulus and fracture toughness. These scientific findings are carefully articulated in the papers. This section comprises of an abridged version of the critical issues addressed in all the papers.

4.2.1 Issues addressed in the review articles

Article 1 is a comprehensive review on the advances and progress made so far in alleviating the mechanical properties of nickel aluminide. Information deduced from the review showed that the fracture toughness of NiAl composites have not been as aggressively investigated as strength properties, despite low fracture toughness being the major drawback of this compound. As a matter of fact, the strength properties of NiAl are considered one of their major strong points, as they exhibit high structural integrity at elevated temperatures. It was also gathered that the mechanical properties varied with various alloying additions. Additionally, the properties exhibited by the composites were contingent on their processing routes. The MA

process has been the most popular method employed due to its simplicity and economic viability. However, MA processes have proven to be quite incompatible with CNTs integration due to the high energy ball milling processes and prolonged duration of milling. This incapacitates the CNTs from acting optimally as reinforcements owing to the formation of a high concentration of defects in them. Information from the review proved this to be precise, as the expected improvements from CNTs incorporation was not achieved in the very few researches that have investigated NiAl system with CNTs as reinforcements. The authors attributed this to the poor dispersion of CNTs reinforcement in the intermetallic matrix.

The poor dispersion observed in literature prompted the second review article which presents a thorough in-depth review detailing a wide array of dispersion methods for CNTs in one of the constituent elements of the nickel aluminide matrix-aluminium. Literature stipulates that the dispersion characteristics of CNTs vary from matrix to matrix. This made it imperative to study the dispersion behaviour of CNTs within the nickel aluminide matrix. However, information on this was lacking in literature as only very few researchers had investigated this phenomenon. From the brief literature available, mechanical alloying (MA) was the dispersion route employed. Building this study around just one reviewed fabrication method could not provide the solution-based, cutting edge approach on which this project is based. Hence, it was imperative to study and understand the intricacies of nanotube characteristics in metal matrices. Again, regarding the use of MA as the choice route presented two problems – one, the prolonged duration used in combination with the high energy milling during MA stripped the nanotubes of their unique tubular morphologies and by extension, their exceptional mechanical properties. Two, in a bid to prevent the damage to the nanotubes, short term MA is done, which still leaves the nanotubes heavily agglomerated within the matrix. These two scenarios eventually translate to poor mechanical properties of the resulting composites. Some authors have even observed poorer mechanical properties due to in-homogenous dispersion of CNTs in NiAl matrix. Thus the gap remained to investigate the best method of dispersing CNTs within the NiAl matrix to

facilitate the desired enhancement of the mechanical properties in NiAl. This review was embarked upon due to the existing gap in literature reflected in the lack of significant enhancement of mechanical properties in NiAl-CNTs composites. Moreover, the limited literature available on NiAl-CNTs composites prevented the critical evaluation of possible dispersion routes in attaining homogeneous dispersion. The significance of this stage cannot be disregarded, owing to the fact that no meaningful improvement can be achieved in this composite without the uniform dispersion of the nanotubes. Huge effort was therefore concentrated on the dispersion stage of the nanotubes in this work. NiAl consists of two elements namely nickel and aluminium. These two review articles made evident the existing gaps in literature which motivated this study and formed the solid background and framework on which this research was built upon.

4.2.2 Evaluation of dispersion characteristics of CNTs in nickel aluminide matrix

Research Article 1 combined vital information from Review Articles 1 and 2 into three developed methodologies of dispersing CNTs within the intermetallic matrix. Having reviewed the pros and cons of the various dispersion routes in article 2 and the various processing methods in Article 1, these methods were developed to preclude the disadvantages evidenced in each reviewed method. The differently milled powders were characterized extensively using Raman, SEM, XRD and TEM. The nano-structural evolution was studied at every 2 h interval for a detailed examination of the progression of the nanotubes during the milling regimes. The levels of defect concentration induced in the milled powders were assessed to determine the best dispersion route. This selection is contingent on two crucial factors namely the level of dispersion attained and the structural integrity of the nanotubes.

A two-stage milling regime emerged as the best dispersion route exhibiting minimum damage to the nanotubes and good preservation of the structural integrity of the nanotubes. These two features are said to guarantee improved properties of CNTs reinforced composites. This **article** therefore provides a detailed guide for researchers in this field contemplating the delicate issue of dispersing CNTs in intermetallic matrices. This paper thus led to the identification of the best dispersion route for the fabrication of NiAl-CNTs composites.

4.2.3 Evaluation of dispersion and agglomeration effects in SPSed NiAl-CNTs composites

Research Article 2, building on the obtained results from **Research Article 1** fabricated NiAl-CNTs composites with different milling regimes. It presents the metallurgical interactions and microstructural variations that occur as a result of CNTs dispersion or agglomerations. In this **article**, an attempt was made to further preserve the structural integrity of the nanotubes by exploring an exclusive low energy ball milling (LEBM) route. The composite obtained from this route was then compared with the composite obtained from the best dispersion method as deduced from Research Article 1. It was found that though the LEBM process preserves the integrity of the CNTs excellently well, the forces utilized in this process are grossly inadequate in de-clustering the agglomerates present in the CNTs. The enormous attention devoted to the dispersion characteristics of CNTs in this work is due to the significance of this phase. Literature documents that no meaningful improvement can be achieved in CNTs reinforced composites without the successful dispersion of the CNTs. Nanoindentation techniques were employed to determine the mechanical properties of the reinforced composites. Agglomeration effects were studied intensively and found to be a very strong determinant in the resulting mechanical properties. Results showed that the LEBM exclusively milled composite exhibited rather poor mechanical attributes as compared to the two-stage milled composite with higher

182

Vicker's hardness, elastic modulus and fracture toughness. Fracture surfaces and behaviours were also compared. Eventually, the presence of agglomerates in the exclusive LEBM sample led to poor mechanical properties of the sample.

This article therefore validated the results obtained from Research Article 1 by depicting the superior qualities of the two-stage milled composite. In addition, dispersion effects have been widely studied in literature, however, agglomeration effects are very scanty in literature. This article therefore blazed the trail in the detailed analyses of CNTs agglomeration and its influence on mechanical properties of NiAl composites which can be extended to other metallic matrices.

4.2.4 Integrity assessment of SPSed NiAl-CNTs composites

This paper presents the climax of this work in a detailed analysis of the effect of CNTs addition on the mechanical properties of NiAl composites. The dispersion parameters from the previous papers were optimized and the CNTs added in increasing measure to evaluate the influence of CNTs content on the NiAl composites. With dispersion parameters from Research Articles 1 and 2 optimized, higher dispersion was observed in this paper than in the previous papers. The relationship and interactions between the reinforcement and the NiAl ordered lattice was established. NiAl-CNTs composites exhibited superior fracture toughness as compared to the unreinforced composites. Significant effort was devoted to achieving this improvement, some of which include ensuring uniform dispersion of high structural integrity nanotubes and sintering at a sufficiently high temperature to ensure the formation of the NiAl compound. The stipulated range of fracture toughness of materials in service is a minimum of 20 MPa√m. The results documented in this article shows huge promise that CNTs reinforced NiAl composites may attain this requirement with a slight adjustment and optimization of key process parameters. This study therefore endorsed the suitability of CNTs as toughening agents in NiAl

composites.

4.3 Conclusions

This study fabricated NiAl-CNTs composites using a two-stage milling regime in combination with spark plasma sintering. Key parameters were optimized and the CNTs content varied to evaluate its effects on the mechanical properties of the nickel aluminide composites. The following conclusions can be deduced from this work:

1) The optimized ball milling parameters that yielded uniform dispersion of high structural integrity nanotubes were observed to be 150 rpm for 6 h at LEBM in combination with 75 rpm for 1 h at HEBM.

2) The best sintering parameters which led to enhanced mechanical properties were found to be 1000 ˚C, 32 MPa for 7 min at heating rate of 100 ˚C.

3) The optimum reinforcement content which translated to improved fracture toughness was deduced to be 1.0 wt% CNTs.

4) Microhardness reduced initially with lower CNTs content and gradually increased with increase in CNTs content, while the elastic modulus was observed to increase with increasing CNTs content.

5) CNTs additions led to a decline in densification of the composites. However, the intergranular fracture mode of the unreinforced NiAl transited to a predominantly dimpled fracture mode in the CNTs reinforced composites.

6) The fracture toughness increased with increasing CNTs content, with the toughening mechanism being the disordering accrued by the CNTs in the B2 ordered NiAl lattice structure.

4.4 Recommendations

This study endorsed the feasibility of fabricating NiAl composites via reactive sintering using SPS. The toughening role of high aspect ratio CNTs within the NiAl matrix was also established. The significance of uniform dispersion and structural integrity of the nanotubes were evident in this study as well. The developed NiAl composites exhibited high elastic modulus and high fracture toughness, with values in the range of the minimum service requirement for aerospace materials.

Having established the above from this study, it is recommended that the high temperature strength and oxidation resistance of the developed NiAl-CNTs composites be investigated.